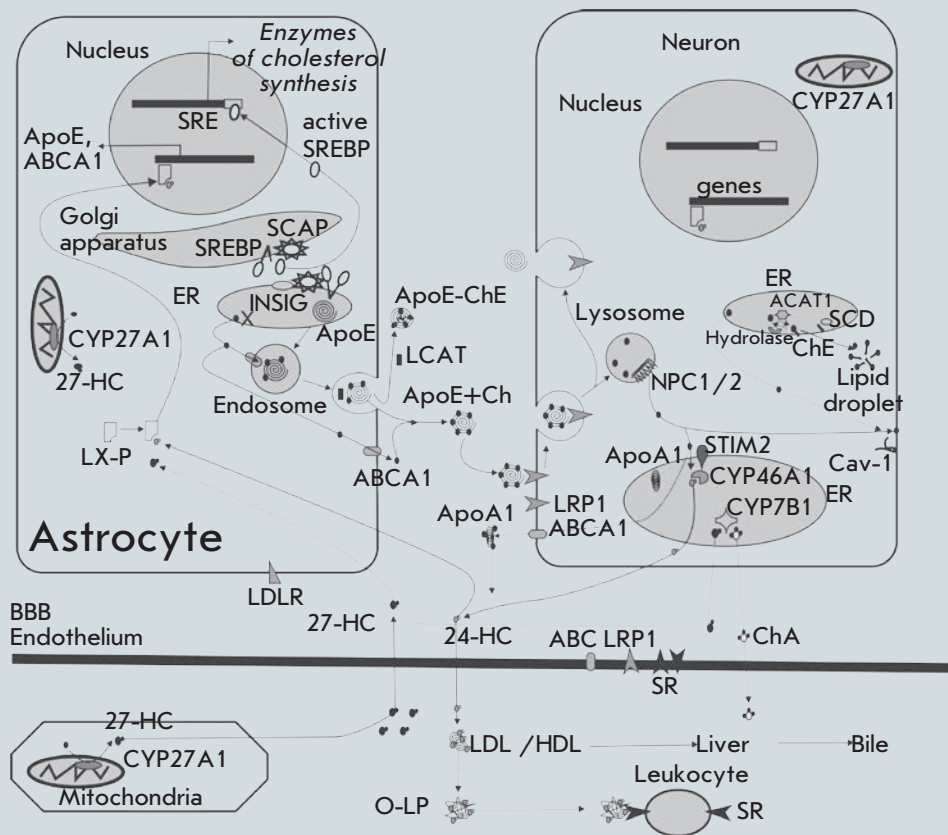


Acta Naturae

Brain cholesterol metabolism and defects: linkage to neurodegenerative diseases and synaptic dysfunction



HOST Ku AND HMGA1 PROTEINS AS PARTICIPANTS OF HIV-1 TRANSMISSION
P. 34

MicroRNAs: THE ROLE IN AUTOIMMUNE INFLAMMATION
P. 21

THE ANALYSIS OF B-CELL EPITOPES OF INFLUENZA VIRUS HEMAGGLUTININ
P. 13

PHAGE PEPTIDE LIBRARIES AS A SOURCE OF TARGETED LIGANDS
P. 48

CHEMRAR Hi-Tech Center is a unique pharma and biotech cluster built in Russian Federation by highly innovative life science R&D organizations, discovering, developing and commercializing novel drugs for partners in Russia and worldwide.


We see **our mission** in bringing novel therapies for unmet needs in treating CNS, oncology, cardiovascular, metabolic and infection diseases through using novel post genomic technology platforms.

CHEMRAR`s companies offer a broad range of services and flexible partnering models in the following areas:

- S**Streamlined drug discovery preclinical and clinical development;
- P**artnering for innovative drug combinations;
- F**ormulation, nano-based delivery technologies for improved pharmacokinetics and efficacy;
- C**o-partnering of innovative molecules from target to market.

CHEMRAR`s companies invite financial and development partners for collaboration on pharmaceutical market in Russia!

Letter from the Editors



Dear readers of *Acta Naturae*,
We are delighted to bring you the 28th
issue of *Acta Naturae*, the first issue
of the year 2016. We would like to introduce
a new section, 'The History of Science' open
with an article by G.P. Georgiev about the
discovery of nuclear DNA-like RNA. Next,
there are five reviews focusing on the rel-
evant problems of life sciences. All the re-
views are to a certain extent related to med-
ical aspects: viral diseases (reviews by D.N.
Shcherbinin et al. and O.A. Shadrina et al.),
autoimmune pathologies (N.M. Baulina et al.),
and neurological disorders (A.M. Petrov et
al.). The fifth review (A.A. Nemudraya et al.)
is to a significant extent methodological and

describes the approach that has proved to be
promising in solving drug delivery problems.
The topics of the reviews are rather diverse,
and we hope that there will be readers inter-
ested in them.

The topics of seven original articles are
also diverse: some articles focus on studies of
the interplay between physiologically active
compounds and various cellular components,
molecular cardiology, and designing new
tools for biological research.

We are looking forward to receiving new
interesting articles from you to be published.
See you in our next issue! ●

The Editorial Board

INNOVATION RUSSIA

Discussion club

We create a dialogue between all socially active groups of people: students, scientists, lecturers, businessmen, managers, innovators, investors, designers, art critics, architects, photographers.

Learn more
at WWW.STRF.RU

Everyone with something to say and
ideas to share is welcome to visit
our events

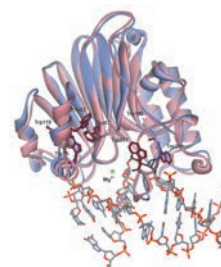


Tel.: +7 (495) 930-87-07, 930-88-50
E-mail: seminar@strf.ru

Thermodynamics of damaged DNA binding and catalysis by human AP endonuclease 1

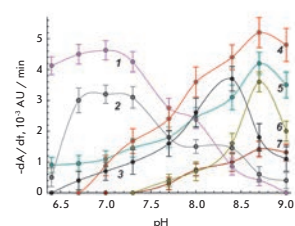
A.D. Miroshnikova, A.A. Kuznetsova, N.A. Kuznetsov, O.S. Fedorova

The thermodynamic parameters of conformational APE1 rearrangements associated with specific recognition of a damaged DNA segment and the catalytic step were obtained. These findings led to the conclusion on the molecular nature of individual steps of the kinetic mechanism describing the enzyme function.



Comparison of the structures of free APE1 and APE1 associated with DNA containing an F site

Screening of human interleukin-2 and hen egg white lysozyme for bacteriolytic activity against various bacterial cells



Dependence of cell lysis rate on pH in the presence of lysozyme

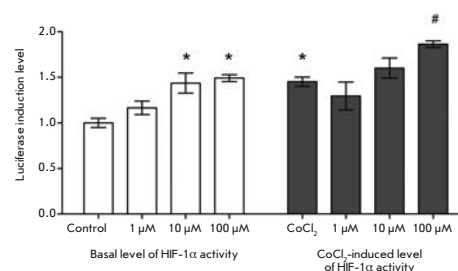
P.A. Levashov, E.D. Ovchinnikova, O.A. Morozova, D.A. Matolygina, H.E. Osipova, T.A. Cherdynseva, S.S. Savin, G.S. Zakharova, A.A. Alekseeva, N.G. Belogurova, S.A. Smirnov, V.I. Tishkov, A.V. Levashov

Bacteriolytic activity of interleukin-2 and hen egg white lysozyme against 34 different species of microorganisms has been studied. Six species of microorganisms belonging to 3 families, Enterobacteriaceae, Bacillaceae and Lactobacillaceae, were found to be lysed in the presence of interleukin-2. It was also found that 12 species of microorganisms are lysed in the presence of lysozyme and 16 species of microorganisms are lysed in the presence of sodium dodecyl sulfate. Bacteriolytic activity of interleukin-2 and lysozyme with respect to various cell substrates was studied at various pH values.

Molecular mechanism underlying the action of Noopept, substituted Pro-Gly dipeptide

Y.V. Vakhitova, S.V. Sadovnikov, S.S. Borisevich, R.U. Ostrovskaya, T.A. Gudasheva, S.B. Seredenin

The ability of Noopept to stimulate the basal DNA-binding activity of transcription factor HIF and activity induced by hypoxia mimetic *in vitro* is demonstrated. The findings on selective increase in DNA-binding activity of HIF with allowance for the functional value of the genes activated by this transcription factor explain the previously revealed nootropic and neuroprotective effects of Noopept. It has been suggested that the HIF-positive effect is the primary mechanism of action of this Pro-Gly-containing dipeptide.



The effect of Noopept on basal and induced activity of HIF-1

Founders

Ministry of Education and
Science of the Russian Federation,
Lomonosov Moscow State University,
Park Media Ltd

Editorial Council

Chairman: A.I. Grigoriev
Editors-in-Chief: A.G. Gabibov, S.N. Kochetkov

V.V. Vlassov, P.G. Georgiev, M.P. Kirpichnikov,
A.A. Makarov, A.I. Miroshnikov, V.A. Tkachuk,
M.V. Ugryumov

Editorial Board

Managing Editor: V.D. Knorre
Publisher: K.V. Kiselev

K.V. Anokhin (Moscow, Russia)
I. Bezprozvanny (Dallas, Texas, USA)
I.P. Bilenkina (Moscow, Russia)
M. Blackburn (Sheffield, England)
S.M. Deyev (Moscow, Russia)
V.M. Govorun (Moscow, Russia)
O.A. Dontsova (Moscow, Russia)
K. Drauz (Hanau-Wolfgang, Germany)
A. Friboulet (Paris, France)
M. Issagouliants (Stockholm, Sweden)
A.L. Konov (Moscow, Russia)
M. Lukic (Abu Dhabi, United Arab Emirates)
P. Masson (La Tronche, France)
K. Nierhaus (Berlin, Germany)
V.O. Popov (Moscow, Russia)
I.A. Tikhonovich (Moscow, Russia)
A. Tramontano (Davis, California, USA)
V.K. Švedas (Moscow, Russia)
J.-R. Wu (Shanghai, China)
N.K. Yankovsky (Moscow, Russia)
M. Zouali (Paris, France)

Project Head: N.V. Soboleva

Editor: N.Yu. Deeva

Designer: K.K. Oparin

Art and Layout: K. Shnaider

Copy Chief: Daniel M. Medjo

Address: 119234 Moscow, Russia, Leninskiye Gory, Nauchny
Park MGU, vlad.1, stroeniye 75G.
Phone/Fax: +7 (495) 727 38 60

E-mail: vera.knorre@gmail.com, actanaturae@gmail.com

Reprinting is by permission only.

© ACTA NATURAE, 2016

Номер подписан в печать 31 марта 2016 г.

Тираж 200 экз. Цена свободная.

Отпечатано в типографии «МИГ ПРИНТ»

CONTENTS

Letter from the Editors.....1

HISTORY OF SCIENCE

G.P. Georgiev

**Discovery of Nuclear DNA-like RNA (dRNA,
hnRNA) and Ribonucleoproteins Particles
Containing hnRNA6**

REVIEWS

D.N. Shcherbinin, S.V. Alekseeva,
M.M. Shmarov, Yu.A. Smirnov,
B.S. Naroditskiy, A.L. Gintsburg

**The Analysis of B-Cell Epitopes
of Influenza Virus Hemagglutinin13**

N. M. Baulina, O. G. Kulakova, O. O. Favorova

**MicroRNAs: Their Role in Autoimmune
Inflammation21**

O. A. Shadrina, E. S. Knyazhanskaya,
S.P. Korolev, M. B. Gottikh

**Host Proteins Ku and HMGA1
As Participants in HIV-1 Transcription34**

A. A. Nemudraya, V. A. Richter, E. V. Kuligina

**Phage Peptide Libraries As a Source
of Targeted Ligands.....48**

A. M. Petrov, M. R. Kasimov, A. L. Zefirov

**Brain Cholesterol Metabolism and its Defects:
Linkage to Neurodegenerative Diseases
and Synaptic Dysfunction58**

RESEARCH ARTICLES

V. L. Andronova, M.V. Jasko,
M.K. Kukhanova, G.A. Galegov,
Yr.S. Skoblov, S.N. Kochetkov

**Study of Antiherpetic Efficiency of Phosphite
of Acycloguanosine Ableto Over come
the Barrier of Resistance to Acyclovir.....74**

Y. V. Vakhitova, S. V. Sadovnikov,
S. S. Borisevich, R. U. Ostrovskaya,
T. A. Gudasheva, S. B. Seredenin

**Molecular Mechanism Underlying
the Action of Substituted Pro-Gly
Dipeptide Noopept82**

E. S. Kotova, S. B. Akopov, D. A. Didych,
N. V. Petrova, O. V. Iarovaia, S. V. Razin,
L. G. Nikolaev

**Binding of Protein Factor CTCF within
Chicken Genome Alpha-Globin Locus90**

P. A. Levashov, E. D. Ovchinnikova,
O. A. Morozova, D. A. Matolygina,
H. E. Osipova, T. A. Cherdyntseva, S. S. Savin,
G. S. Zakharova, A. A. Alekseeva,
N. G. Belogurova, S. A. Smirnov, V. I. Tishkov,
A. V. Levashov

**Human Interleukin-2 and Hen Egg White
Lysozyme: Screening for Bacteriolytic
Activity against Various Bacterial Cells98**

A. D. Miroshnikova, A. A. Kuznetsova,
N. A. Kuznetsov, O. S. Fedorova

**Thermodynamics of Damaged DNA Binding and
Catalysis by Human AP Endonuclease 1103**

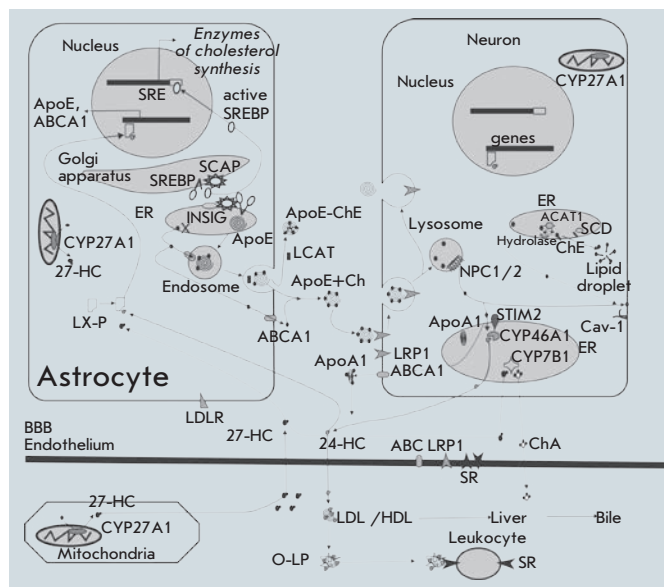
T.R. Nasibullin, L.F. Yagafarova, I.R. Yagafarov,
Y.R. Timasheva, V.V. Erdman, I.A. Tuktarova,
O.E. Mustafina

**Combinations of Polymorphic Markers of
Chemokine Genes, Their Receptors and Acute
Phase Protein Genes As Potential Predictors of
Coronary Heart Diseases111**

V. A. Chernukhin, D. A. Gonchar,
M. A. Abdurashitov, O. A. Belichenko,
V. S. Dedkov, N. A. Mikhnenkova,
E. N. Lomakovskaya, S. G. Udal'yeva,
S. Kh. Degtyarev

**Cloning and Characterization
of a New Site-Specific Methyl-Directed
Elm1 Endonuclease Recognizing and
Cleaving C5-methylated DNA Sequence
5'-G(5mC)^NG(5mC)-3'117**

Guidelines for Authors.....126

**IMAGE ON THE COVER PAGE**

Brain cholesterol metabolism (see the article
by Petrov *et al.*)

Discovery of Nuclear DNA-like RNA (dRNA, hnRNA) and Ribonucleoproteins Particles Containing hnRNA

G.P. Georgiev

Institute of Gene Biology, Russian Academy of Sciences, Vavilova Str., 34/5, Moscow, 119334, Russia

On August 9–11, 2014, Cold Spring Harbor (USA) hosted a special symposium dedicated to the discovery of messenger or informational RNA and the main events in the subsequent studies of its synthesis, regulation of synthesis, maturation, and transport. The existence of mRNA in bacteria was first suggested in 1961 by Jacob and Monod, based on genetic studies [1]. The same year, Brenner *et al.* confirmed the hypothesis [2]. Our laboratory played a key role in the discovery of messenger RNA in eukaryotes, as well as in the discovery of the nuclear ribonucleoproteins that contain it and in the elucidation of their structural organization. Therefore, I was invited to represent Russia at the Symposium and deliver a speech on these topics. However, my visa had only been issued after the end of the Symposium, and, therefore, the presentation was delivered by my former colleague G.N. Yenikolopov, who works at Cold Spring Harbor Laboratory. The transcript of the lecture is presented below.

DISCOVERY OF NUCLEAR DRNA

The research discussed in this paper was initiated in my group at I.B. Zbarsky Laboratory at the A.N. Severtsov Institute of Animal Morphology of the Soviet Academy of Sciences. However, the bulk of the research was conducted in my lab at the Institute of Molecular Biology of the Soviet Academy of Sciences, to which I was invited by its director, V.A. Engelhardt, whose name the Institute now bears.

My main collaborator in the discovery of nuclear dRNA was V.L. Mantieva, who went on to earn a PhD in biology. We were interested in the nature of nuclear RNA [3] and used a newly developed phenol method to isolate RNA from cells [4]. A suspension of mouse Ehrlich ascites carcinoma cells was shaken in 0.14 M NaCl and phenol at pH 6.0 and 4°C, followed by centrifugation. Surprisingly, in addition to the expected aqueous and phenol phases,

the centrifugation produced an intermediate layer that contained cell nuclei that retained their shape [5]. These nuclei contained chromatin and nucleoli, which stored DNA, nuclear RNA, and most of the nuclear proteins (*Fig. 1*). Since phenol inhibits enzyme activity, we believed that “phenolic” nuclei can be a good source of nuclear RNA. Later, it was shown that nuclear RNA can indeed be extracted from “phenolic” nuclei by this procedure if it is performed at 65°C [3]. The isolated nuclear RNA contained components with sedimentation coefficients of 28S and 18S, typical for ribosomal RNA, and heterogeneous material. The nucleotide composition of the nuclear RNA was intermediate between mouse DNA ($G+C/A+T = 0.72$) and ribosomal RNA ($G+C/A+U = 1.65$) (*Fig. 1*). It seemed that nuclear RNA contained ribosomal RNA and a new type of RNA whose nucleotide



Director of the Institute of Molecular Biology, RAS, V.A. Engelhardt with the author

composition was similar to that of DNA: i.e., informational RNA. The first experiments on the fractionation of nuclear RNA, conducted in 1961, confirmed this hypothesis [3].

The best separation was achieved by thermal phenol fractionation, developed in 1962, that included treatment of “phenolic” nuclei with a 0.14 M NaCl–phenol mixture at pH 6.0 and stepwise increase in temperature [6]. At 40°C, the aqueous phase contained pure

Table. Isolation of nuclear DNA-like RNA by phenolic thermal fractionation

RNA (DNA) Fraction	G	C	A	U(T)	G+C / A+U(T)
Mouse DNA	21	21	29	29	0.72
Cytoplasmic, 4°C	32	30	20	18	1.63
Nuclear, 4–40°C	32	29	20	19	1.50
Nuclear, 55–65°C	23	20	28	29	0.76
Nascent nuclear, 55–65°C	21	20	29	30	0.71

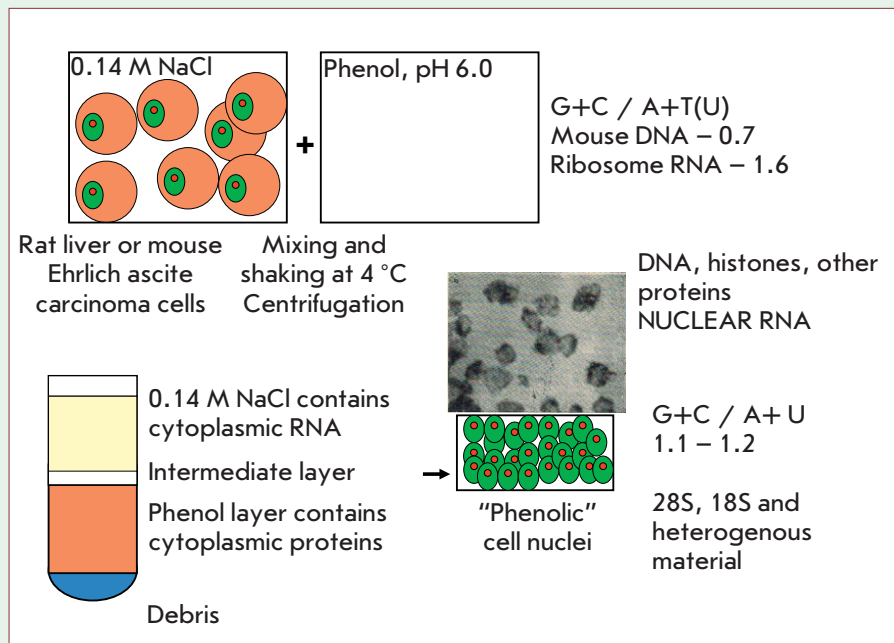


Fig. 1. Isolation and properties of “phenolic” cell nuclei. (left panel) Scheme of cell nuclei isolation by phenol treatment. A photograph of the “phenolic” nuclei of Ehrlich ascites carcinoma cells is presented. (right-hand panel) Composition of the obtained nuclei and properties of their RNA: intermediate nucleotide composition between those of DNA and rRNA; ultracentrifugation data.

RNA whose nucleotide composition corresponded to ribosomal RNA (rRNA) and which contained a precursor of ribosomal RNA. At 55 to 65°C, the aqueous phase contained pure RNA with a nucleotide composition similar to that of DNA ($G+C/A+U = 0.7-0.74$). Notably, ^{32}P -labeled RNA experiments revealed that the nucleotide com-

positions of the total RNA of the isolated fraction and that of the nascent RNA present in it were identical [7, 8] (Table). The discovered and purified DNA-like RNA was named dRNA. Three years later, in 1965, American authors described this type of RNA and called it heterogeneous nuclear RNA (hnRNA) [9–12].

Next, we described the properties of nuclear dRNA. Its molecular mass was highly heterogeneous and reached very high values. The nascent nuclear dRNA had a significantly higher molecular mass than the total nuclear dRNA, which implied its cleavage in the cell nucleus (processing) [7, 8] (Fig. 2).

We also determined the size of dRNA in the cytoplasm, presumably, mature mRNA. We developed a method of partial blocking of RNA synthesis by actinomycin D, which in small doses selectively inhibits rRNA synthesis without affecting dRNA synthesis. The molecular weight of the nascent nuclear dRNA significantly exceeded that of cytoplasmic dRNA [7, 8] (Fig. 2).

Finally, we conducted DNA hybridization-competition experiments with nuclear dRNA and cytoplasmic mRNA. The addition of nuclear dRNA completely inhibited mRNA hybridization with DNA, whereas an excess of mRNA only partially inhibited hybridization of nuclear dRNA with DNA (Fig. 2).

We hypothesized that nuclear dRNA is a high-molecular mass precursor of cytoplasmic mRNA, or pre-mRNA, which is partially destroyed during dRNA processing and mRNA maturation that occurs in the cell nucleus, from which mRNA is exported to the cytoplasm. Definite proof of this hypothesis required several years of research by a number of laboratories, but the initial confirmation of the existence of messenger RNA in eukaryote cells had been presented in the above mentioned papers [6–8].

DISCOVERY OF RIBONUCLEOPROTEIN (RNP) PARTICLES: DRNP (HNRNP)

Our next goal was to elucidate the organization of nuclear dRNA in the cell nucleus. My main collaborator in this work was O.P. Samarina,

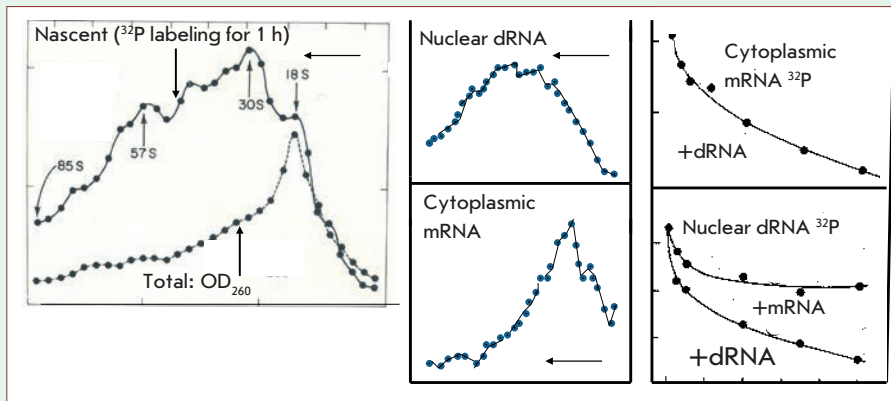


Fig. 2. Characteristics of nuclear dRNA. (left-hand panel) Ultracentrifugation of nuclear dRNA labeled for 1 h with ^{32}P in a sucrose density gradient. Significantly higher molecular weight of the labeled dRNA than that of total dRNA as determined by optical density. Here and later, thin arrows indicate the direction of ultracentrifugation. (central panel) Comparison of the molecular weights of nuclear dRNA and cytoplasmic mRNA labelled in identical conditions (1 h). The former has a much higher molecular weight. (right-hand panel) Hybridization of labeled cytoplasmic mRNA and nuclear dRNA with DNA and competition with unlabeled nuclear dRNA and cytoplasmic mRNA

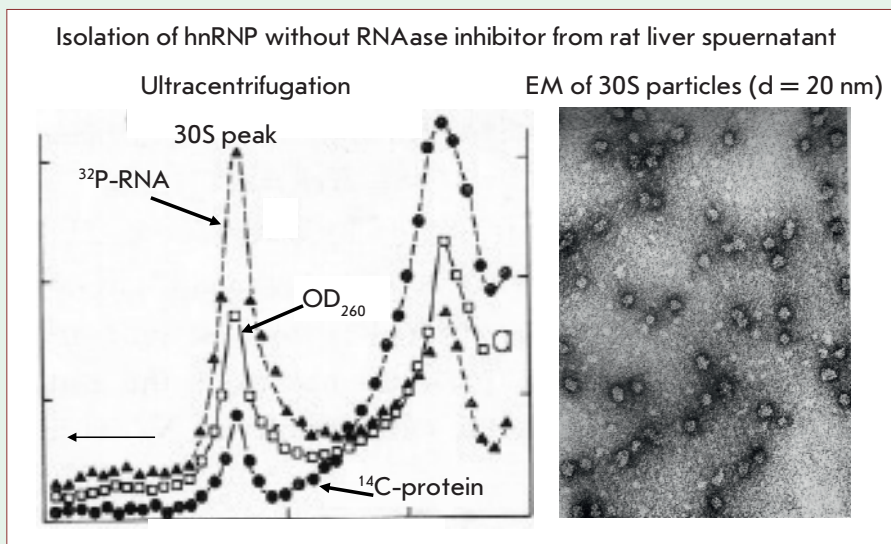


Fig. 3. Properties of the nuclear hnRNP particles obtained at the first stage of the research. (left-hand panel) Sucrose gradient ultracentrifugation of nuclear extracts containing hnRNA. RNA was labeled with ^{32}P -orthophosphate and a protein with a mixture of ^{14}C -amino acids. (right-hand panel) Electron microscopy of 30S particles from the sucrose gradient

who later became doctor of biological sciences, professor, and a Lenin Prize winner.

A mild procedure was used to study hnRNA-containing structures. Rat liver nuclei were treated

with 0.14 M NaCl, 1 mM MgCl_2 , and 10 mM Tris buffer at pH 7.0. A portion of RNA was extracted, and its nucleotide composition was found to be intermediate between rRNA and dRNA. Three subsequent ex-

tractions with the same solution at pH 7.8–8.0 solubilized a significantly higher proportion of RNA that had the same nucleotide composition as pure dRNA. A DNA-like composition was typical of both the total and the nascent RNA in the extract [13].

After ultracentrifugation, most of the hnRNA was detected in a homogeneous 30S peak, which contained particles ca. 20 nm in diameter. The molecular weight of RNA isolated from the 30S peak was low (Fig. 3). It was contrary to the data on the very high molecular mass of hnRNK isolated by phenol fractionation. To resolve this contradiction, we performed extraction in the presence of a RNAase inhibitor from rat liver supernatant. This extraction produced a completely different pattern of ultracentrifugation: a series of peaks ranging from a small 30S peak all the way up to material with sedimentation coefficients of 200S and above (Fig. 4). Obviously, this pattern was much closer to the native one [14].

Notably, both the 30S peak and the peaks with higher molecular masses had the same buoyant density in CsCl (after formaldehyde fixation): ca. 1.4 g/ml, which corresponds to a RNA/protein ratio of about 1:4–1:5.

Next, we characterized the larger particles. Mild ribonuclease A treatment quantitatively transformed them into 30S particles with 20-nm diameter, which were, therefore, monomers of the larger polyparticles. Electron microscopy demonstrated that 30S particles were monomers, 45S particles were dimers, 70S particles were pentamers, and that the 90–100S peak contained polyparticles built up of 9 monomers. The measurement of RNA obtained from various peaks demonstrated that in all cases the monomer was a RNA fragment ca. 700 nucleotides in size. This is consistent with the fact that the buoy-

ant density of all hnRNP peaks was identical (Fig. 4).

Thus, hnRNP are chains built up of similar RNP particles connected by RNA bridges, which are the most sensitive to ribonuclease treatment [15].

To better understand the structure of hnRNP particles, we elucidated the structure of the 30S monomer. Intense ribonuclease treatment completely destroyed the 30S particle RNA, which suggests that it is localized on the particle's surface. The 30S proteins were labeled with ¹²⁵I, and the particles were treated with 2M NaCl to cause dissociation of RNA and the protein. After ultracentrifugation, all of the hnRNA remained in the upper fractions, whereas the protein was detected in the same 30S peak, despite the removal of RNA. The buoyant density of 30S particles dropped to 1.34 g/cm³ [1-6] (Fig. 5).

When protein particles were mixed with hnRNA and 2 M NaCl was removed by dialysis, hnRNP particles were reconstructed and were indistinguishable from the initial ones in a variety of tests. The initial 30S particles, protein particles, and reconstructed hnRNP particles look the same in electron microscopy (Fig. 5). In the presence of hnRNP of about 1.4 kDa in size, dimeric hnRNPs are formed during the reconstruction [15]. The protein 30S particles were called 'informofers' (messenger RNA carriers), but this term failed to gain traction in the literature.

Informofers are protein complexes containing ca. 20 protein molecules with a molecular weight of about 40 kDa, belonging, according to other authors' data, to six different types [16]. It was concluded that nuclear hnRNP particles are long hnRNA chains regularly wrapped on the surface of a series of similar or identical protein globular particles. This structure significantly reduces the size of long

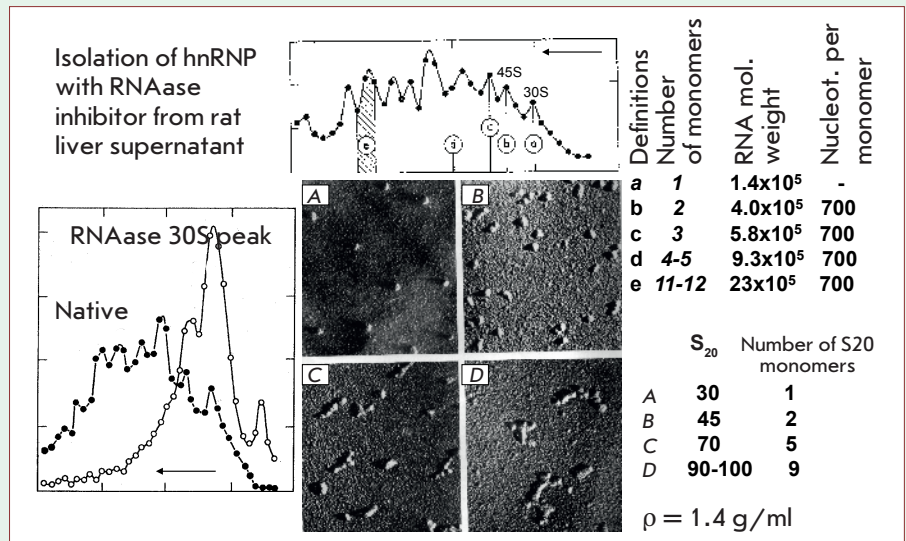


Fig. 4. Properties of nuclear hnRNP polyparticles. (left panel) Distribution of hnRNP particles isolated with a RNAase inhibitor at ultracentrifugation. Conversion of polyparticles into 30S monomers with mild RNAase treatment. (top panel) Polyparticles, molecular weights of RNA extracted from particles with different numbers of monomers, and the number of nucleotide monomers per particle. (bottom right panel) EM of the particles from different areas of the gradient, sedimentation coefficients, and number of monomers. The buoyant density is the same for all particles (1.4)

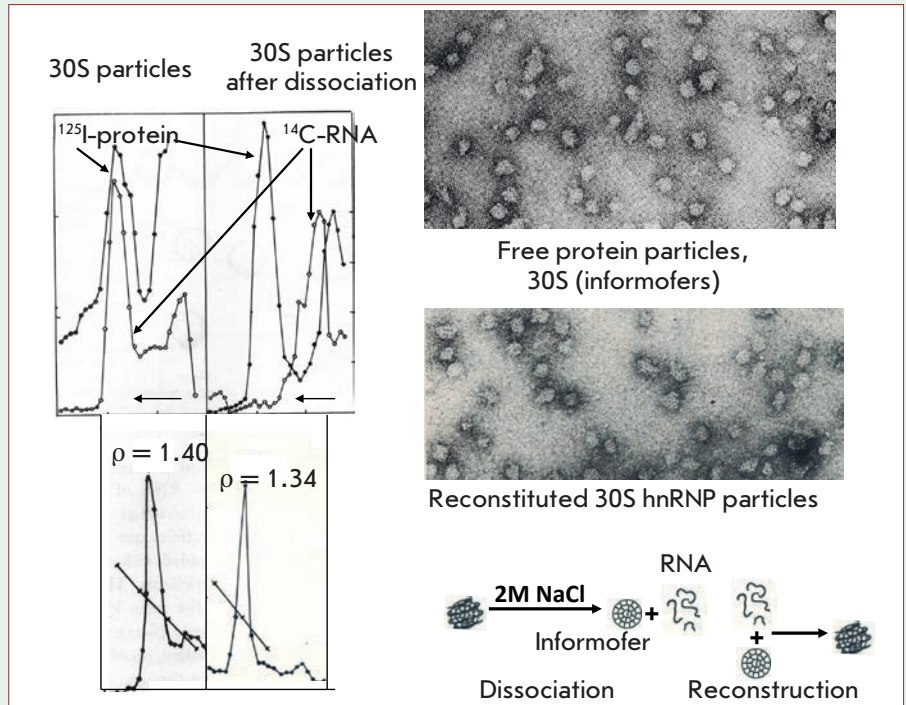


Fig. 5. Structure of hnRNP particles. (right-hand panel) RNA- and protein-labeled 30S particles (the latter labelled with ¹²⁵I) before and after treatment with 2M NaCl. In contrast to the initial particles, those treated with 2M NaCl lost all total RNA, although their sedimentation coefficient and EM dimensions remained unchanged. Buoyant density decreased from 1.4 to 1.34 g/ml. (left-hand panel) EM of dissociated and reconstructed 30S particles. (bottom panel) The scheme of dissociation and reconstruction of hnRNP.

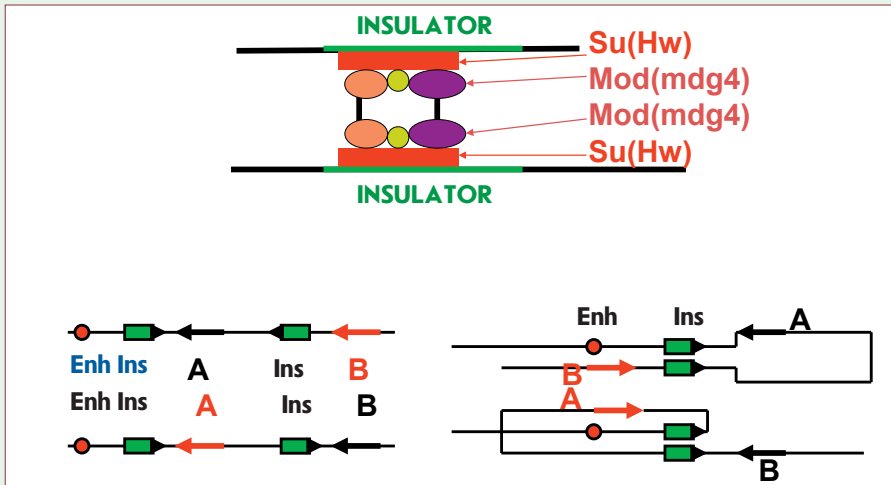


Fig. 6. Insulator interactions. Due to the presence of a series of proteins, multiple contacts are formed in the insulator protein complex and they define strong binding between insulators and the polarity of their interaction. Only similarly aligned insulators can bind to each other, which defined the configuration of the loop and activation of a gene

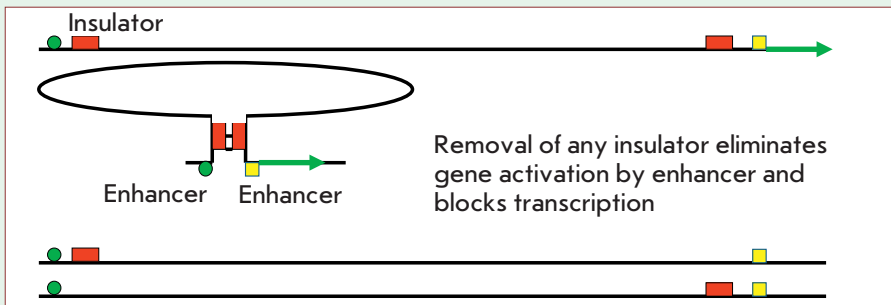


Fig. 7. The super-long-distance interaction in the genome. They are defined by the interaction of insulators and can lead to activation of a promoter by an enhancer. Removal of any one or two insulators prevents this interaction

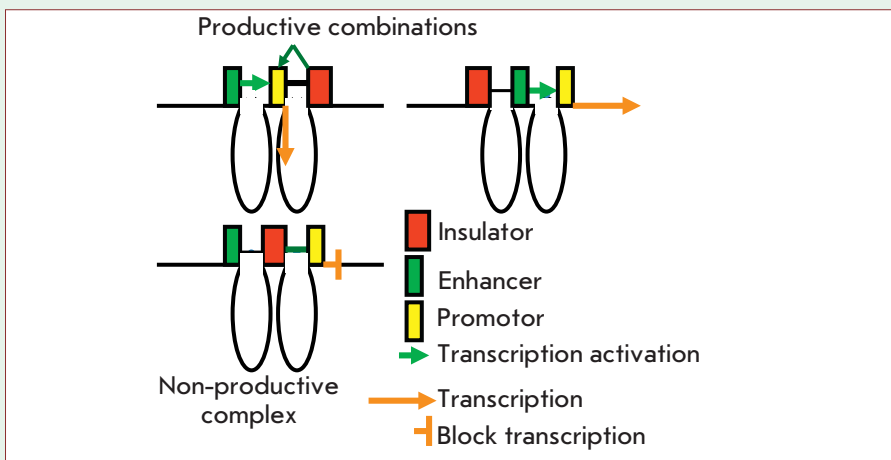


Fig. 8. Interaction of insulators with other elements. Insulators interact with promoters and activate them and with enhancers (more selectively). If an insulator is located between them and there is no other insulators nearby, it may interact with both, forming a non-productive complex

hnRNA, while leaving it available for interaction with more specific factors involved in RNA processing and export.

Interestingly, a similar principle of organization was later discovered for chromatin nucleosomes [17].

FURTHER MRNA STUDIES AT THE INSTITUTE OF GENE BIOLOGY, RAS

This author moved on to other topics related to the organization of genome (discovery and characterization of mobile genetic elements in animal cells) and chromatin. However, regulation of hnRNA synthesis and mRNA export has been actively studied at the Institute of Gene Biology of the Russian Academy of Sciences that was organized 15 years ago and for which it is the main focus of research. Another important area of research at the Institute is new approaches to cancer therapy. This author is now engaged in this research. Some key studies related to mRNA are summarized below.

First of all, new properties belonging to insulators, important *cis*-elements in transcription regulation, have been discovered. Their role has been found to be highly dependent on their ability to bind tightly to each other [18, 19]. This property depends on the dimerization of a number of proteins that make up insulator complexes: e.g., the Mod(mdg4) protein discovered at the Institute [20] (Fig. 6).

In contrast to enhancers, insulators are polar; they only interact with each other if they have the same orientation. This determines conformation of a loop formed as a result of insulators interaction and may define which genes will be activated [21, 22] (Fig. 6).

Super-long-distance interactions have been discovered in the genome [23, 24]. They can reach dozens of millions of base pairs and can occur even between non-homologous chromosomes. They depend

on the interaction between insulators and can lead to activation of a promoter by an enhancer. Removal of one of the insulators results in a complete loss of super-long-distance interaction, which manifests itself as inactivation of the associated transcription (*Fig. 7*).

Finally, it was discovered that insulators can interact with promoters (with low selectivity), activating them, and with enhancers (more selectively). Therefore, an insulator located between an enhancer and a promoter may interact with both, forming a non-productive complex. This may explain the well-known uncoupling effect of an insulator [25, 26] (*Fig. 8*).

Two new proteins, E(y)2/ENY2 and SAMP, have been discovered. They play an important role in the control of hnRNA transcription and subsequent stages of mRNA formation and export [27, 28].

SAMP binds the protein initiating complex TFIID and chromatin remodeling complex SWI/SNF into a single supercomplex. Knockdown SAMP blocks the recruitment of TFIID and SWI/SNF at the promoter and represses the transcription of many genes. It can be assumed that the fusion of the complexes allows TFIID to immediately bind to the promoter as soon as the SWI/SNF-activated movement of nucleosomes along the DNA release it from the nucleosomes [29] (*Fig. 9*).

E(y)2/ENY2 was found to be multifunctional. It is part of the DUB module of the SAGA complex and participates in the activation of transcription initiation [30]. ENY2 is also part of the THO protein complex involved in hnRNA elongation,

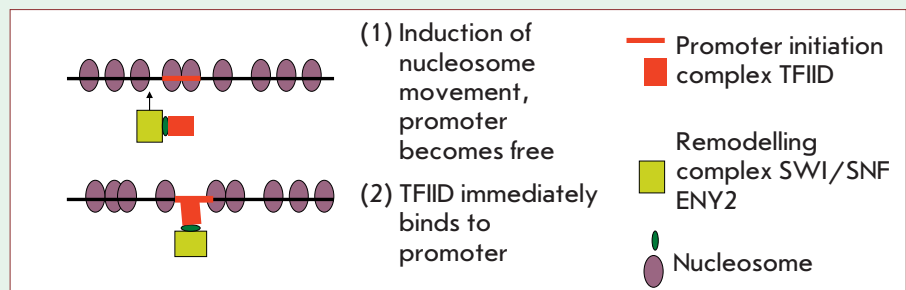


Fig. 9. Scheme of the supercomplex with the SAMP protein. The formation of the supercomplex dramatically increases the efficiency of TFIID binding with a promoter and transcriptional activity

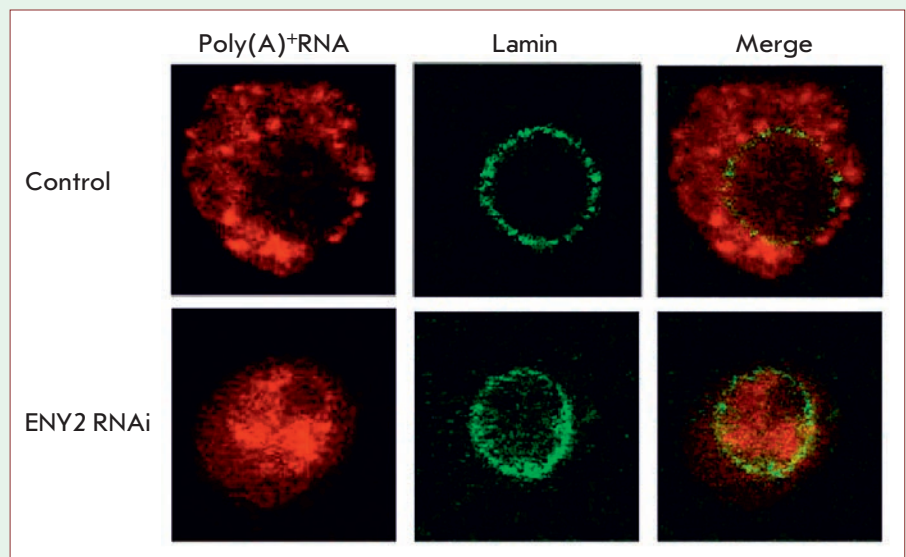


Fig. 10. ENY2 protein knockdown blocks mRNA export from the nucleus to the cytoplasm. Inhibition of protein synthesis is achieved via RNA interference. As a result, almost all of the poly(A)⁺RNA remains in the nucleus

binding to hnRNP and export of some mRNAs. ENY2 is also an important component of the *Drosophila* AMEX protein complex, binding hnRNP and playing a key role in the export of many mRNAs. Knockdown of ENY2 by RNA interference leads to complete blockage of mRNA transport from the nucleus to the cytoplasm. All mRNA accu-

multate in the nucleus [31] (*Fig. 10*). Finally, ENY2 is part of some insulator complexes, performing the barrier function of insulator [32].

This is only part of the Institute's work in the field of regulation of mRNA synthesis and export.

Therefore, early work on the identification of messenger RNA in eukaryotes successfully continues. ●

REFERENCES

- Jacob F., Monod J. // *J. Mol. Biol.* 1961. V. 3. P. 318–356.
- Brenner S., Jacob F., Meselson M. // *Nature* 1961. V. 190. P. 576–581.
- Georgiev G.P. // *Biochemistry (Moscow)*. 1961. V. 26. P. 1095–1126.
- Kirby K.S. // *Biochem. J.* 1956. V. 64. P. 405–408.
- Georgiev G.P., Mantieva V.L. // *Biochemistry (Moscow)*. 1960. V. 25. P. 143–150.
- Georgiev G.P., Mantieva V.L. // *Biochim. Biophys. Acta*. 1962. V. 61. P. 153–154.
- Georgiev G.P., Samarina O.P., Lerman M.I., Smirnov M.N. // *Nature*. 1963. V. 200. P. 1291–1294.
- Samarina O.P., Lerman M.I., Tumanyan V.G., Ananieva

- L.N., Georgiev G.P. // *Biochemistry (Moscow)*. 1965. V. 30. P. 880–893.
9. Scherrer K., Marcaud L., Zajdela F., London I.M., Gros F. // *Proc. Natl. Acad. Sci. USA*. 1966. V. 56. P. 1571–1578.
 10. Warner J.R., Soeiro R., Birnboim H.C., Girard M., Darnell J.E. // *J. Mol. Biol.* 1966. V. 19. P. 349–356.
 11. Penman S. // *J. Mol. Biol.* 1966. V. 17. P. 117–130.
 12. Houssais J.F., Attardi G. // *Proc. Natl. Acad. Sci. USA*. 1966. V. 56. P. 616–623.
 13. Samarina O.P., Krichevskaya A.A., Georgiev G.P. // *Nature*. 1966. V. 210. P. 1319–1322.
 14. Samarina O.P., Lukanidin E.M., Molnar J., Georgiev G.P. // *J. Mol. Biol.* 1968. V. 33. P. 251–263.
 15. Lukanidin E.M., Zalmanzon E.S., Komaromi L., Samarina O.P., Georgiev G.P. // *Nat. New Biol.* 1972. V. 238. P. 193–197.
 16. Dreyfus G., Matenis M.J., Pino-Roma S., Burd C.G. // *Ann. Rev. Biochem.* 1993. V. 62. P. 289–321.
 17. Luger K., Mäder A.W., Richmond R.K., Sargent D.F., Richmond T.J. // *Nature*. 1997. V. 389. P. 251–260.
 18. Gause M., Hovhannisyann H., Kan T., Kuhfittig S., Mogila V., Georgiev P. // *Genetics*. 1998. V. 149. P. 1393–1405.
 19. Muravyova E., Golovnin A., Gracheva E., Parshikov A., Belenkaya T., Pirrotta V., Georgiev P. // *Science*. 2001. V. 291. P. 495–498.
 20. Bonchuk A., Denisov S., Georgiev P., Maksimenko O. // *J. Mol. Biol.* 2011. V. 412. P. 423–436.
 21. Kyrchanova O., Chetverina D., Maksimenko O., Kullyev A., Georgiev P. // *Nucl. Acids Res.* 2008. V. 36. P. 7019–7028.
 22. Kyrchanova O., Ivlieva T., Toshchakov S., Parshikov A., Maksimenko O., Georgiev P. // *Nucl. Acids Res.* 2011. V. 39. P. 3042–3052.
 23. Kyrchanova O., Georgiev P. // *FEBS Lett.* 2014. V. 588. P. 8–14.
 24. Kravchenko E., Savitskaya E., Kravchuk O., Parshikov A., Georgiev P., Savitsky M. // *Mol. Cell Biol.* 2005. V. 25. P. 9283–9291.
 25. Erokhin M., Davydova A., Kyrchanova O., Parshikov A., Georgiev P., Chetverina D. // *Development*. 2011. V. 138. P. 4097–4106.
 26. Kyrchanova O., Maksimenko O., Stakhov V., Ivlieva T., Parshikov A., Studitsky V.M., Georgiev P. // *PLoS Genet.* 2013. V. 9. e1003606.
 27. Shidlovskii Y.V., Krasnov A.N., Nikolenko J.V., Lebedeva L.A., Kopantseva M., Ermolaeva M.A., Ilyin Y.V., Nabirochkina E.N., Georgiev P.G., Georgieva S.G. // *EMBO J.* 2005. V. 24. P. 97–107.
 28. Georgieva S., Nabirochkina E., Dilworth F.J., Eickhoff H., Becker P., Tora L., Georgiev P., Soldatov A. // *Mol. Cell Biol.* 2001. V. 21. P. 5223–5231.
 29. Vorobyeva N.E., Soshnikova N.V., Nikolenko J.V., Kuzmina J.L., Nabirochkina E.N., Georgieva S.G., Shidlovskii Y.V. // *Proc. Natl. Acad. Sci. USA*. 2009. V. 106. P. 11049–11054.
 30. Kurshakova M.M., Krasnov A.N., Kopytova D.V., Shidlovskii Y.V., Nikolenko J.V., Nabirochkina E.N., Spehner D., Schultz P., Tora L., Georgieva S.G. // *EMBO J.* 2007. V. 26. P. 4956–4965.
 31. Kopytova D.V., Orlova A.V., Krasnov A.N., Gurskiy D.Y., Nikolenko J.V., Nabirochkina E.N., Shidlovskii Y.V., Georgieva S.G. // *Genes Dev.* 2010. V. 24. P. 86–96.
 32. Kurshakova M., Maksimenko O., Golovnin A., Pulina M., Georgieva S., Georgiev P., Krasnov A. // *Mol. Cell.* 2007. V. 27. P. 332–338.

The Analysis of B-Cell Epitopes of Influenza Virus Hemagglutinin

D.N. Shcherbinin^{*}, S.V. Alekseeva, M.M. Shmarov, Yu.A. Smirnov, B.S. Naroditskiy, A.L. Gintsburg

Federal State Budgetary Institution "Federal Research Centre for Epidemiology and Microbiology named after the honorary academician N.F. Gamaleya" of the Ministry of Health of the Russian Federation, Gamaleya str. 18, Moscow, Russian Federation, 123098

*E-mail: dim284@inbox.ru

Received: 16.08.2015

Copyright © 2016 Park-media, Ltd. This is an open access article distributed under the Creative Commons Attribution License, which permits unrestricted use, distribution, and reproduction in any medium, provided the original work is properly cited.

ABSTRACT Vaccination has been successfully used to prevent influenza for a long time. Influenza virus hemagglutinin (HA), which induces a humoral immune response in humans and protection against the flu, is the main antigenic component of modern influenza vaccines. However, new seasonal and pandemic influenza virus variants with altered structures of HA occasionally occur. This allows the pathogen to avoid neutralization with antibodies produced in response to previous vaccination. Development of a vaccine with the new variants of HA acting as antigens takes a long time. Therefore, during an epidemic, it is important to have passive immunization agents to prevent and treat influenza, which can be monoclonal or single-domain antibodies with universal specificity (broad-spectrum agents). We considered antibodies to conserved epitopes of influenza virus antigens as universal ones. In this paper, we tried to characterize the main B-cell epitopes of hemagglutinin and analyze our own and literature data on broadly neutralizing antibodies. We conducted a computer analysis of the best known conformational epitopes of influenza virus HAs using materials of different databases. The analysis showed that the core of the HA molecule, whose antibodies demonstrate pronounced heterosubtypic activity, can be used as a target for the search for and development of broad-spectrum antibodies to the influenza virus.

KEYWORDS Influenza virus, hemagglutinin, conformational epitopes, broad-spectrum monoclonal antibodies, broad-spectrum single-domain antibodies.

ABBREVIATIONS HA – influenza virus hemagglutinin, H1–H18 – subtypes of influenza virus hemagglutinin

INTRODUCTION

Hemagglutinin (HA) is the main antigenic component of influenza viruses. It is a homotrimeric mushroom-shaped surface glycoprotein whose monomer consists of two fragments linked by a disulfide bridge: HA1 (330 amino acids), the globular portion distal from the viral membrane, and HA2 (220 amino acids), the stem portion anchored in the viral membrane. Eighteen subtypes of influenza A virus HA were naturally found [1].

Virus-neutralizing antibodies induced by HA form the basis of humoral immunity, which protects the body against influenza infection [2]. The antigenic structure of HA is continuously changing as a result of the selective pressure of the immune system of the host organism, which leads to occurrence and selection of new variants of the virus capable of avoiding the neutralizing effect of available antibodies and overcoming the specific immune defense in humans. This mechanism, known as antigenic drift, reduces the effect of vaccination against influenza [3]. When pan-

demic strains of influenza A virus emerge and a virus with a new antigenic subtype of HA enters the human population (antigenic shift) [2, 4], the existing vaccines are ineffective. These factors explain the need for new approaches to the development of new broad-spectrum influenza drugs [5]. One of these approaches includes a search for and characterization of conserved antigenic determinants in the influenza virus HA molecule and development of broad-spectrum neutralizing antibodies. These antibodies can be used for emergency passive immunization and, therapy, when taking anti-epidemic measures.

Molecular studies of antigenic structures of HA have shown that the sites interacting with antibodies are mainly located in the globular domain of the HA1 subunit [6]. The amino acid sequences of these sites are extremely variable and differ not only in different HA subtypes, but also within the same subtype. Conserved determinants were found in the HA2 subunit [7–10]. These data suggest that conserved antigenic sites in the HA molecule can induce formation of antibodies

with broad cross-neutralizing activity. This assumption was confirmed by Y. Okuno *et al.* [11], who first obtained and characterized a monoclonal antibody to the H2 subtype of HA, having neutralizing activity against influenza A virus strains with H2 and H1 HAs. This monoclonal antibody (C179) recognizes a conformational epitope in the stem region of the HA molecule, which is conserved in the H2 and H1 subtypes of influenza A viruses. It is known that the H5 and H6 subtypes of avian influenza viruses are phylogenetically close to the strains of the H1 and H2 subtypes [12, 13]. Broad-spectrum action of murine antibody S179 was identified at the D.I. Ivanovskiy Research Institute of Virology. It was shown that this antibody interacts with the H1, H2, and H5 subtypes (and even with the H6 subtype of HA in its not-fully-mature form) [14, 15].

Single-domain antibodies are considered to be promising agents for passive immunization against influenza. Single-domain antibodies are small, stable, and easy to produce. It was shown that intranasal administration of llama-derived single-stranded fragments of the variable domains of immunoglobulins, having a neutralizing activity *in vitro* against H5N1 influenza viruses, can control viral replication and reduce the incidence of the disease and mortality in mice infected with the H5N1 influenza virus. Although the study focused on single-domain antibodies recognizing the epitope near the receptor-binding domain, the possibility of selecting molecules of broad-spectrum antibodies that bind to other HA epitopes, including conserved ones, was emphasized [16].

In another study, a single-domain antibody to influenza A virus HA was produced and a recombinant adenovirus expressing this antibody was designed. Administration of this recombinant adenovirus in the period 48 hours to 14 days before the challenge can fully protect mice against influenza A virus [17].

Therefore, there is an obvious need for the search for passive immunization agents with universal specificity, which could allow us to circumvent the antigenic variability of the influenza virus [18].

It is possible that the direction of the search for ways of passive immunization providing protection against a broad spectrum of influenza viruses, which is being conducted in cooperation between Japanese and Russian scientists and is currently underway in several laboratories, will turn out to be the most promising.

ANTIBODIES TO THE GLOBULAR PORTION OF HA MOLECULE

The largest amount of virus-neutralizing antibodies produced in a natural or artificial way bind to the globular portion of HA, resulting in blockage of virion binding to cells. However, since the HA gene rapidly

mutates, new amino acid substitutions occur, leading to formation of new glycosylation sites, which in turn causes changes in the surface structure of the protein. Therefore, these antigenic sites are highly variable and the corresponding antibodies are strain-specific. This partially explains why immunity after natural infection or vaccination is largely limited to the circulating strain. For example, 2D1 antibodies binding to the Sa-antigenic site located in the globular portion of the HA molecule recognize only the pandemic H1N1 viruses of 1918 and 2009, whose epitopes are antigenically similar, although they are separated by almost a century [19]. Other H1 strains, such as PR8, cannot be recognized by these antibodies (*Table 1, Figure*).

However, several antibodies specific to the globular part of HA and having virus-neutralizing activity against several strains of the influenza virus within one subtype have been recently described and characterized. These epitopes are conserved between different viral strains and, therefore, are recognized by the same antibody. It is noteworthy that the epitopes of these antibodies can be located at different antigenic sites. For example, H5M9 antibodies interact with the conserved H5 subtype of the HA epitope, which is located in the rudimentary esterase subdomain in close vicinity to the receptor-binding site and partially overlaps the antigenic site Cb [20]. H5M9 antibodies effectively protect mice against lethal doses of different H5 strains. HC45 and BH151 antibodies also interact with similar antigenic sites (*Figure*), but their ability to interact with different strains was not identified [21, 22]. GC0757 and GC0857 antibodies interact with the same epitope located in the globular portion of HA and recognize various H1 strains [23]. These antibodies interact with a previously unknown epitope which is not located in the known antigenic sites [23].

A number of other antibodies interacting with several strains of the influenza virus recognize the receptor-binding site in the globular part of HA. Since the receptor-binding site is functionally conserved, its amino acid diversity is limited and it is regarded as an attractive target for broad-spectrum antibodies [24].

The receptor-binding site is a wide, shallow pocket localized at the top of the globular domain. The boundaries of the receptor binding site are formed by the loops 130, 150, and 220 and α -helix 190, which indicate positions in the amino acid sequence of HA [25]. Structural characterization of some antibodies bound to the receptor-binding site showed that all antibodies build a variable loop into the receptor-binding site and, thus, directly block the interaction of HA with cellular sialic acids [26-32]. However, most antibodies interact with only one loop due to the compact structure of the site, and only few antibodies interact with two loops. Since

Table 1. Known antibodies to B-cell epitopes of influenza A and B virus HAs

Antigenic site	Antibody	PDB ID	Source of antibodies	Antibody subtype	Source of antigen	Reference
R.b.p.	CH65, CH67	3SM5	H. s.	IgG1	A/Solomon Islands/3/2006(H1N1)	[27,33]
R.b.p.	CH65	3SM5	H. s.	IgG1	A/Solomon Islands/3/2006(H1N1)	[27]
R.b.p.	CH67	4HKX	H. s.	IgG1	A/Solomon Islands/3/2006(H1N1)	[33]
Sasite	2D1	3LZF	H. s.	?	A/South Carolina/1/1918(H1N1)	[19]
R.b.p.	1F1	4GXU	H. s.	?	A/South Carolina/1/1918(H1N1)	[28]
	GC0757	4F15	M. m.	?	A/California/04/2009(H1N1)	[45]
	GC0587	4LVH	M. m.	?	A/California/04/2009(H1N1)	[23]
R.b.p.	5J8	4M5Z	H. s.	?	A/California/07/2009(H1N1)	[26]
R.e.s.	H5M9	4MHH	M. m.	IgG1	A/Viet Nam/1203/2004 (H5N1)	[20]
	H5M9	4MHJ			A/goose/Guangdong/1/1996(H5N1)	[20]
R.b.p.	8F8	4HF5	H. s.	?	A/Japan/305+/1957(H2N2)	[29]
R.b.p.	8M2	4HFU	H. s.	?	A/Japan/305+/1957(H2N2)	[29]
R.b.p.	2G1	4HG4	H. s.	?	A/Japan/305+/1957(H2N2)	[29]
R.e.s.	BH151	1EO8	M. m.	IgG1	A/X-31(H3N2)	[22]
R.e.s.	HC45	1QFU	M. m.	IgG1	A/X-31(H3N2)	[21]
R.b.p.	C05	4FP8 4FQR	H. s.	?	A/Hong Kong/1/1968(H3N2)	[30]
R.b.p.	S139/1	4GMS	M. m.	IgG2a	A/Victoria/3/1975(H3N2)	[31]
R.b.p.	F045-092	4O58	H. s.	?	A/Victoria/3/1975(H3N2)	[32]
R.b.p.	F045-092	4O5I	H. s.	?	A/Singapore/H2011.447/2011(H3N2)	[32]
R.b.p.	HC63	1KEN	M. m.	?	A/X-31(H3N2)	[46]
R.b.p.	HC19	2VIR 2VIS 2VIT	M. m.	IgG1	A/X-31(H3N2)	[47]
	IIB4		M. m.	?	A/Philippines/2/1982(H3N2)	[48]
	Fab 26/9	1FRG	M. m.	IgG2a	A/Victoria/3/1975(H3N2)	[49]
	CR8071	4FQJ	H. s.	IgG1	B/Florida/4/2006	[44]
	CR8059	4FQK	H. s.	IgG1	B/Brisbane/60/2008	[44]
S.p.	FI6v3	3ZTJ	H. s.	?	A/Aichi/2/1968(H3N2)	[42]
	FI6v3	3ZTN	H. s.	?	A/California/04/2009(H1N1)	[42]
	MAb 3.1	4PY8	H. s.	IgG1	A/South Carolina/1/1918(H1N1)	[39]
	CR6261	3GBN	M. m.	IgG1	A/Brevig Mission/1/1918(H1N1)	[37, 50]
	CR6261	3GBM	M. m.	IgG1	A/Viet Nam/1203/2004(H5N1)	[37]
	CR8020	3SDY	H. s.	?	A/Hong Kong/1/1968(H3N2)	[40]
	F10	3FKU	H. s.	IgG1	A/Viet Nam/1203/2004(H5N1)	[38]
	C179	4HLZ	M. m.	IgG2a	A/Japan/305/1957(H2N2)	[11, 15, 36]
	CR8043	4NM8	H. s.	IgG1	A/Hong Kong/1/1968(H3N2)	[41]
	CR9114	4FQI	H. s.	IgG1	A/Viet Nam/1203/2004(H5N1)	[44]
	CR9114	4FQV	-/-/-/-	-/-/-/-	A/Netherlands/219/2003(H7N7)	[44]
	CR9114	4FQY	-/-/-/-	-/-/-/-	A/Hong Kong/1/1968(H3N2)	[44]
	Fab 39.29	4KVN	H. s.	?	A/Perth/16/2009(H3N2)	[43]

Notes. Information on the best known conformational B-cell epitopes of influenza virus HAs was obtained from the database of immunological epitopes (IEDB – Immune Epitope Database and analysis resource www.iedb.org) and the protein database (PDB – Protein Data Bank; www.rcsb.org). The H1 subgroup of influenza viruses (H1, H5, and H2) is colored in blue, the H3 subgroup is colored in green; and antibodies to the stem portion of HAs of different influenza viruses are colored in red. S.p. – stem portion, R.b.p. – receptor binding pocket, R.e.s. – the site localized in a rudimentary esterase subdomain, H. s. – *Homo sapiens*, M. m. – *Mus musculus*.

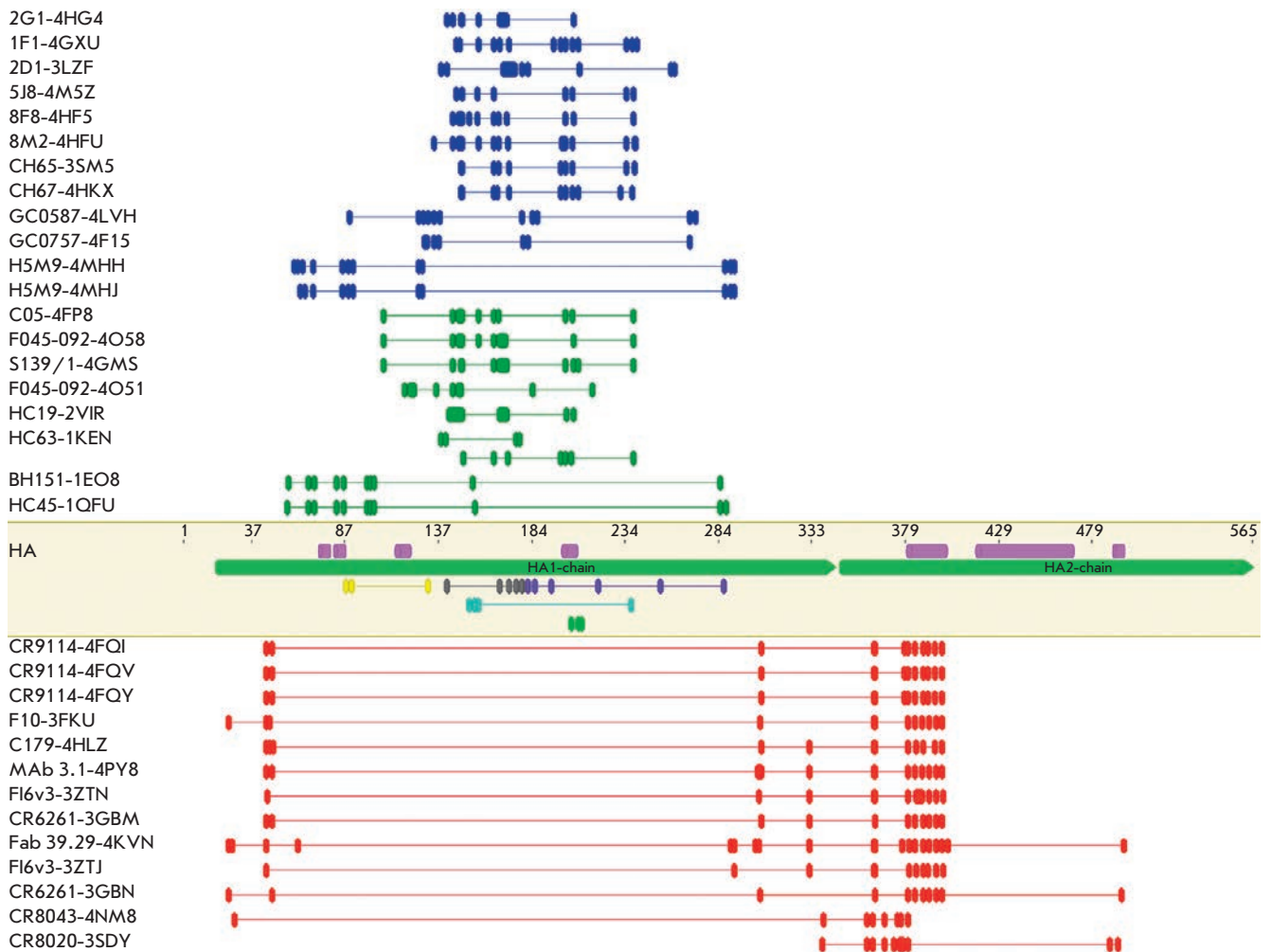


Fig. 1. Schematic arrangement of B-cell epitopes in the amino acid sequence of hemagglutinin (HA). The figure was obtained using the Geneious 9.0.2 software as follows: the amino acid sequences of influenza virus hemagglutinins recognized by the corresponding antibodies (Table 1) were aligned with respect to each other. The epitope recognized by the corresponding antibody was mapped on each sequence. Information on the B-cell epitopes of HAs was obtained from the immunological epitope database. The figure in the middle shows HA with the following elements: HA1 and HA2 chains (green), alpha helices (pink), antigenic sites: Cb (yellow), Ca1 (purple), Ca2 (blue), Sa (gray), and Sb (green). Location of B-cell epitopes of influenza A virus HA is shown above and below the HA (see Table 1). H1 (dark blue) and H3 (dark green) epitopes to the globular portion of HA are shown above; epitopes to the stem portion of HA (dark red) are shown below. Antigenic sites are mapped according to Caton A.J. [50].

the receptor-binding site is located in the globular part of HA, it creates no steric barrier to the formation of antibodies to this antigenic site.

1F1 antibodies were obtained from people who had influenza during the pandemic in 1918. These antibodies can inhibit some strains of the H1 influenza A virus; namely those isolated in 1918, 1943, 1947, and 1977 [28]. The study of the crystal structure of these antibodies in a complex with influenza virus HA from 1918 has shown that they interact with amino acid residues that belong to the antigenic sites Sa, Sb, and Ca₂. The heavy chain of the 1F1 antibody also comes

into contact with the receptor-binding site and interacts with the amino acid residues involved in the binding to sialic acids.

The CH65 and CH67 antibodies bind and neutralize H1 influenza viruses, which have circulated in the human population since 1986 [27, 33]. However, these antibodies are not active against the 2009 H1 pandemic influenza virus. The 5J8 antibodies are active against the H1 subtype of HAs of both the 1918 and 2009 pandemic influenza viruses and seasonal influenza A viruses. The study of the crystal structure of the CH65, CH67, and 5J8 antibodies in a complex with HA revealed that

they recognize epitopes near the receptor-binding site and build their HCDR3 loop into the receptor-binding pocket.

H2N2 viruses circulated in the human population for 11 years, from 1957 to 1968. Since these viruses remained absent for a long time, population immunity decreased significantly. Moreover, it is completely absent in people born after 1968: so, the probability of a reappearance of this subtype of the virus is very high, which undoubtedly raises concern. Antibodies to the H2N2-8F8, 8M2, and 2G1 subtypes, which recognize and neutralize all subtypes of H2 HA from 1957 to 1968, were obtained from donors using hybridoma technology [29]. The analysis of the crystal structures of these antibodies in a complex with HA showed that they recognize the receptor-binding pocket. Antibodies to 8F8 insert their HCDR3 loop into the receptor-binding pocket, whereas antibodies 8M2 and 2G1 insert their HCDR2 loop [29].

The aforementioned antibodies to the receptor-binding pocket of HA indicate that this portion of the globular part of HA is more conserved than the antigenic sites Sa or Sb, but that antibodies to this site are unable to recognize different HA subtypes. Nevertheless, antibodies that recognize the receptor-binding pocket and are capable of heterosubtypic recognition of HA were found.

C05 and S139/1 antibodies have heterosubtypic activity and can bind to many influenza virus subtypes, including H1, H2, and H3 [30, 31]. S139/1 antibodies were obtained from mice immunized with the H3N2 virus. These are the first heterosubtypic antibodies that recognize the receptor-binding pocket by interacting with the H1, H2, H3, H5, and H13 subtypes of HA [34]. The analysis of the crystal structures of these antibodies in a complex with HA has shown that they interact with the receptor-binding pocket through the HCDR2 loop [31]. The study of the binding and neutralization of the virus confirmed that S139/1 antibodies do have heterosubtypic activity, although with narrow specificity within one subtype. Nevertheless, these results suggest that different strains of different subtypes of the influenza A virus may contain a similar epitope within the receptor-binding site.

Other antibodies, C05, were found using a phage library prepared based on cells isolated from individuals infected with the seasonal influenza virus [30]. C05 have neutralizing activity against the H1, H2, H3, and H9 viruses and have a greater breadth of recognition within these subtypes compared to S139/1 antibodies. Unlike other previously described antibodies recognizing the receptor-binding pocket, C05 bind to HA exclusively through the heavy chain. The main interaction is mediated only by a long HCDR3 loop, which penetrates

into the receptor-binding pocket. The epitope for these antibodies on the HA surface is very compact.

Still another group of antibodies with broad heterosubtypic recognition, F045-092, were also obtained using phage libraries based on cells isolated from donors. They are able to recognize and neutralize various strains of the H1, H2, H3, and H5 subtypes of the influenza virus [35]. Analysis of the crystal structure of F045-092 antibodies in a complex with HA showed that they insert the HCDR3 loop into the receptor-binding pocket, wherein the carboxyl group of an aspartate at the apex of the recognition loop mimics the carboxyl group of the sialic acid [32]. Broader recognition of different subtypes of the influenza A virus is probably achieved due to the receptor mimicry.

ANTIBODIES TO THE STEM PART OF THE HA MOLECULE

The originally described antigenic sites were located only in the globular domain of HA, and the viewpoint that the stem region is not accessible for a humoral immune response was wide spread. However, in 1993, S179 antibodies were described which were obtained from mice immunized with the H2N2 influenza virus and were capable of neutralizing the H1, H2, and H5 subtypes of HA [11, 14]. In contrast to the antibodies to the globular part, these antibodies blocked the conformational reorganization of HA at a low pH, thus inhibiting its function. Twenty years after the discovery of the S179 antibodies, their crystal structure in a complex with the H5 subtype of HA was determined. The analysis of this complex showed that the antibodies interact with HA using both heavy and light chains [36].

Fifteen years after the discovery of the S179 of antibodies, several additional antibodies to the stem portion of HA were described. Investigation of the structure of two of these human antibodies, CR6261 [37] and F10 [38], in a complex with HA showed that they interact with a highly conserved epitope in the stem portion, which is similar in all first-group HAs (*Table 2*). Both antibodies interact with HA only through the heavy chain, inserting the HCDR2 loop into the hydrophobic pocket.

Other monoclonal heterosubtypic antibodies (MAb 3.1) were obtained from donors using phage library. MAb 3.1 antibodies are able to neutralize H1a influenza viruses (H1, H2, H5, and H6), but they show weak neutralizing activity against the H1b subgroup (H13, H16, and H11) [39]. Similarly to other heterosubtypic anti-influenza antibodies, CR6261 and F10, MAb 3.1 enters into contact with the stem part of HA, using only the heavy chain. In contrast, the HCDR1 and HCDR3 loops are involved in this interaction in MAb 3.1.

Antibodies that interact exclusively with the second group of HA were also discovered. For example,

Table 2. Interaction between monoclonal antibodies specific to the stem portion of HA and different subtypes of influenza A viruses.

Group classification of influenza viruses		Monoclonal antibody								
		C179	F10	CR6261	MAb 3.1	CR8020	CR8043	Fab 39.29	FI6v3*	CR9114**
	H9	+	+	+	-	-	-	n.t.	n.t.	+
	H8	n.t.	+	+	-	-	-	n.t.	n.t.	+
	H12	-	n.t.	-	-	-	-	n.t.	n.t.	+
	H6	+	+	+	+	-	-	n.t.	n.t.	+
	H1	+	+	+	+	-	-	+	+	+
	H2	+	+	+	+	-	-	+	n.t.	+
	H5	+	+	+	+	-	-	+	+	+
	H11	n.t.	+	-	-	-	-	n.t.	n.t.	n.t.
	H13	-	-	-	-	-	-	n.t.	n.t.	n.t.
	H16	-	-	-	-	-	-	n.t.	n.t.	n.t.
	H3	-	-	-	-	+	n.t.	+	+	+
	H4	-	-	-	-	+	n.t.	n.t.	n.t.	+
	H14	-	-	-	-	n.t.	+	n.t.	n.t.	n.t.
H10	-	-	-	-	+	n.t.	n.t.	n.t.	+	
H7	-	-	-	-	+	+	+	+	+	
H15	-	-	-	-	n.t.	+	n.t.	n.t.	n.t.	

Note. "+"- Neutralization of influenza virus, "-" interaction with HA was not detected, "n.t."- not tested. Group H1 influenza viruses are shown in red, group H3 antibodies are shown in green.

* FI6v3 antibodies interact with other subtypes of HA, but neutralization of the virus has not been investigated.

** CR9114 interacts with the influenza B virus, but it does not neutralize it.

CR8020 antibodies, isolated from a healthy donor, bonded to the highly conserved epitope at the stem portion of HA and exhibited neutralizing activity against the H3, H7, and H10 viruses [39]. Later on, other antibodies were obtained: namely, CR8043, which, unlike CR8020, is encoded by other gene segments [40]. In experiments *in vitro*, CR8043 demonstrated neutralizing activity against the H3 and H10 subtypes of the influenza virus and protected mice against lethal doses of the H3N2 and H7N7 viruses [41]. The CR8020 and CR8043 antibodies bind to similar epitopes, but they interact with HA in different ways. Both antibodies interact with both the light and heavy chains of HA. Similarly to antibodies binding to the first group of HA, CR8020 and CR8043 antibodies also interact with the stem portion of the HA molecule and prevent conformational changes in it at a low pH. These antibodies may also inhibit the HA maturation process, blocking the proteolytic cleavage of immature precursor HA0 into the HA1 and HA2 subunits. Therefore, epitopes of these antibodies, which have been found and structurally characterized, are the second critical area in the stem portion of the HA molecule.

Monoclonal antibodies having heterosubtypic activity against both the first (H1) and second (H3) groups of the influenza A virus were described. Such broad-spectrum heterosubtypic antibodies, FI6v3, were first characterized in 2011. They were isolated from a library consisting of 104,000 plasma cells derived from eight donors using the single-cell culturing method [42]. FI6v3 antibodies show neutralizing activity against both groups of viruses and inhibit the formation of syncytium in a cell culture. Similar Fab-fragments of the monoclonal antibodies Fab 39.29 were obtained using "*in vitro* activation and antigen-specific enrichment" of 840 plasma blasts of vaccinated individuals [43].

Yet other broad-spectrum heterosubtypic antibodies, CR9114, bind to the conserved epitope in the stem portion of HA and demonstrate activity against all tested influenza A virus strains in neutralization tests [44]. Moreover, these antibodies are capable of interacting with the influenza B virus. However, in experiments *in vitro*, neutralization of the influenza B virus was not detected, at least in the tested concentrations. Therefore, at present, CR9114 are antibodies with the broad-

est specificity among all known monoclonal antibodies to influenza A virus HA.

Heterosubtypic antibodies to the influenza B virus were also found. In particular, the CR8059 and CR8071 antibodies can neutralize influenza B viruses in both lines [44].

The possibility of obtaining single-domain antibodies with neutralizing cross-activity was first shown with respect to the H1, H2, H5, and H9 influenza virus subtypes. Four cross-neutralizing antibodies (R2b-E8, R2b-D9, and R1a-B6) were bound to the full-length HA, rather than the HA1 domain, and unbound at low pH. These antibodies can bind to epitopes in the membrane proximal region of the HA stem far from the receptor-binding site. This cross-neutralization mechanism was described for the human monoclonal antibodies F10 and CR6261. One of these antibodies (R2a-G8) binds to a portion of the HA1 domain located in the stem part of HA [18].

Based on the aforementioned data, all antibodies can be classified into four groups according to their breadth of recognition.

1) Antibodies to the globular portion recognizing one or a few strains within one HA subtype (2D1);

2) Antibodies to the globular portion recognizing a large number of strains or all strains within one HA subtype (H5M9, HC45, BH151,8F8, 8M2, 2G1, etc.);

3) Antibodies to the globular portion capable of recognizing several strains of different HA subtypes (C05 and S139/1); and

4) Antibodies to the stem portion reaching pronounced heterosubtypic activity (C179, F10, CR6261, CR8020, FI6v3, MA b 3.1, CR8043, Fab 39.29, and CR9114).

CONCLUSION

The epidemic outbreaks of influenza that occasionally occur in vaccinated populations certainly demonstrate the need for continued search for agents for emergency prevention and treatment of this disease. In this regard, protectors against pandemic influenza strains are of particular importance.

The idea of the development of broad-spectrum agents that can neutralize various subtypes of influenza viruses is the most promising for emergency prevention of influenza caused by the virus, which is volatile against the major antigen hemagglutinin.

In this investigation, we studied the ability of neutralizing broad-spectrum antibodies to recognize various B-cell epitopes of HA, which is very important in view of the evolution of influenza viruses.

The computer analysis of known conformational B-cell epitopes of influenza virus HA has shown that the stem part of the HA molecule, whose antibodies have pronounced heterosubtypic activity, should be the target for the search for and development of broad-spectrum antibodies to the influenza virus. CR9114 antibodies demonstrate the widest cross-neutralizing activity against influenza A virus HA, compared to all the monoclonal antibodies that are currently available and being investigated. The heterosubtypic antibodies CR8059 and CR8071 influenza B virus type have also been found.

These data indicate that it is possible to design broad-spectrum drugs for emergency prevention and treatment of influenza using monoclonal or single-domain antibodies neutralizing certain B-cell epitopes in the stem portion of influenza virus HA. ●

REFERENCES

- Webster R.G., Govorkova E.A. // *Ann. N. Y. Acad. Sci.* 2014. V. 1323. P. 115–139.
- Murphy B.R., Webster R.G. *Orthomyxoviruses*. Virology. 2nd ed. / Eds Fields B.N., Knipe D.M.. N.Y.: Raven Press, 1990. P. 1091–1152.
- Kilbourne E.D. *Influenza*. N.Y.: Plenum Publ. Co., 1987. 4. Webster R.G., Bean W.G., Gorman O.T., Chambers T.M., Kawaoka Y. // *Microbiol. Rev.* 1992. V. 56. P. 152–179.
- Webster R.G., Bean W.G., Gorman O.T., Chambers T.M., Kawaoka Y. // *Microbiol. Rev.* 1992. V. 56. P. 152–179.
- Kilbourne E.D. // *Nat. Medicine*. 1999. V. 5. P. 1119–1120.
- Wiley D.C., Skehel J.J. // *Ann. Rev. Biochem.* 1987. V. 56. P. 365–394.
- Graves P.N., Schulman J.L., Yong J.F., Palese P. // *Virology*. 1983. V. 126. P. 106–116.
- Laver W.G., Air G.M., Dopheide T.A., Ward C.W. // *Nature*. 1980. V. 283. P. 454–457.
- Raymond E.L., Caton A.J., Cox N.J., Kendal A.P., Brownlee G.G. // *Virology*. 1986. V. 148. P. 275–287.
- Verhoeyen M., Fang R., Min Jou W., Devos R., Huylebroeck D., Saman E., Fiers W. // *Nature*. 1980. V. 286. P. 771–776.
- Okuno Y., Isegawa Y., Sasao F., Ueda S. // *J. Virol.* 1993. V. 67. № 5. P. 2552–2558.
- Air G.M. // *Proc. Natl. Acad. Sci. USA*. 1981. V. 78. P. 7639–7643.
- Nobusawa E., Aoyama T., Kato H., Suzuki Y., Tateno Y., Nakajima K. // *Virology*. 1991. V. 182. P. 475–485.
- Smirnov Y.A., Lipatov A.S., Okuno Y., Gitelman A.K. // *Problems of virology*. 1999. V. 44. P. 111–115.
- Smirnov Y.A., Lipatov A.S., Gitelman A.K., Okuno Y., van Beek R., Osterhaus A.D., Claas E.C. // *Acta Virologica*. 1999. V. 43. P. 237–244.
- Ibanez L.I., De Filette M., Hultberg A., Verrips T., Temperton N., Weiss R.A., Vandeveld W., Schepens B., Vanlandschoot P., Saelens X. // *J. Infect. Dis.* 2011. V. 203. № 8. P. 1063–1072.
- Tutykhina I.L., Sedova E.S., Gribova I.Y., Ivanova T.I., Vasilev L.A., Rutovskaya M.V., Lysenko A.A., Shmarov M.M., Logunov D.Y., Naroditsky B.S., et al. // *Antiviral Res.* 2013. V. 97. № 3. P. 318–328.
- Hufton S.E., Risley P., Ball C.R., Major D., Engelhardt O.G., Poole S. // *PLoS One*. 2014. V. 9. № 8. P. e103294.
- Xu R., Ekiert D.C., Krause J.C., Hai R., Crowe J.E.Jr., Wil-

- son I.A. // *Science*. 2010. V. 328. № 5976. P. 357–360.
20. Zhu X., Guo Y.H., Jiang T., Wang Y.D., Chan K.H., Li X.F., Yu W., McBride R., Paulson J.C., Yuen K.Y., et al. // *J. Virol.* 2013. V. 87. № 23. P. 12619–12635.
21. Fleury D., Barrere B., Bizebard T., Daniels R.S., Skehel J.J., Knossow M. // *Nat. Struct. Biol.* 1999. V. 6. № 6. P. 530–534.
22. Fleury D., Daniels R.S., Skehel J.J., Knossow M., Bizebard T. // *Proteins*. 2000. V. 40. № 4. P. 572–578.
23. Cho K.J., Hong K.W., Kim S.H., Seok J.H., Kim S., Lee J.H., Saelens X., Kim K.H. // *PLoS One*. 2014. V. 9. № 2. P. e89803.
24. Martin J., Wharton S.A., Lin Y.P., Takemoto D.K., Skehel J.J., Wiley D.C., Steinhauer D.A. // *Virology*. 1998. V. 241. № 1. P. 101–111.
25. Skehel J.J., Wiley D.C. // *Annu. Rev. Biochem.* 2000. V. 69. P. 531–569.
26. Hong M., Lee P.S., Hoffman R.M., Zhu X., Krause J.C., Laursen N.S., Yoon S.I., Song L., Tussey L., Crowe J.E., et al. // *J. Virol.* 2013. V. 87. № 22. P. 12471–12480.
27. Whittle J.R., Zhang R., Khurana S., King L.R., Manischewitz J., Golding H., Dormitzer P.R., Haynes B.F., Walter E.B., Moody M.A., et al. // *Proc. Natl. Acad. Sci. USA*. 2011. V. 108. № 34. P. 14216–14221.
28. Tsibane T., Ekiert D.C., Krause J.C., Martinez O., Crowe J.E., Wilson I.A., Basler C.F. // *PLoS Pathog.* 2012. V. 8. № 12. P. e1003067.
29. Xu R., Krause J.C., McBride R., Paulson J.C., Crowe J.E. Jr., Wilson I.A. // *Nat. Struct. Mol. Biol.* 2013. V. 20. № 3. P. 363–370.
30. Ekiert D.C., Kashyap A.K., Steel J., Rubrum A., Bhabha G., Khayat R., Lee J.H., Dillon M.A., O’Neil R.E., Faynboym A.M., et al. // *Nature*. 2012. V. 489. № 7417. P. 526–532.
31. Lee P.S., Yoshida R., Ekiert D.C., Sakai N., Suzuki Y., Takada A., Wilson I.A. // *Proc. Natl. Acad. Sci. USA*. 2012. V. 109. № 42. P. 17040–17045.
32. Lee P.S., Ohshima N., Stanfield R.L., Yu W., Iba Y., Okuno Y., Kurosawa Y., Wilson I.A. // *Nat. Commun.* 2014. V. 5. P. 3614.
33. Schmidt A.G., Xu H., Khan A.R., O’Donnell T., Khurana S., King L.R., Manischewitz J., Golding H., Suphaphiphat P., Carfi A., et al. // *Proc. Natl. Acad. Sci. USA*. 2013. V. 110. № 1. P. 264–269.
34. Yoshida R., Igarashi M., Ozaki H., Kishida N., Tomabechei D., Kida H., Ito K., Takada A. // *PLoS Pathog.* 2009. V. 5. № 3. P. e1000350.
35. Ohshima N., Iba Y., Kubota-Koketsu R., Asano Y., Okuno Y., Kurosawa Y. // *J. Virol.* 2011. V. 85. № 21. P. 11048–11057.
36. Dreyfus C., Ekiert D.C., Wilson I.A. // *J. Virol.* 2013. V. 87. № 12. P. 7149–7154.
37. Ekiert D.C., Bhabha G., Elsliger M.A., Friesen R.H., Jongeneelen M., Throsby M., Goudsmit J., Wilson I.A. // *Science*. 2009. V. 324. № 5924. P. 246–251.
38. Sui J., Hwang W.C., Perez S., Wei G., Aird D., Chen L.M., Santelli E., Stec B., Cadwell G., Ali M., et al. // *Nat. Struct. Mol. Biol.* 2009. V. 16. № 3. P. 265–273.
39. Wyrzucki A., Dreyfus C., Kohler I., Steck M., Wilson I.A., Hangartner L. // *J. Virol.* 2014. V. 88. № 12. P. 7083–7092.
40. Ekiert D.C., Friesen R.H., Bhabha G., Kwaks T., Jongeneelen M., Yu W., Ophorst C., Cox F., Korse H.J., Brandenburg B., et al. // *Science*. 2011. V. 333. № 6044. P. 843–850.
41. Friesen R.H., Lee P.S., Stoop E.J., Hoffman R.M., Ekiert D.C., Bhabha G., Yu W., Juraszek J., Koudstaal W., Jongeneelen M., et al. // *Proc. Natl. Acad. Sci. USA*. 2014. V. 111. № 1. P. 445–450.
42. Corti D., Voss J., Gamblin S.J., Codoni G., Macagno A., Jarrossay D., Vachieri S.G., Pinna D., Minola A., Vanzetta F., et al. // *Science*. 2011. V. 333. № 6044. P. 850–856.
43. Nakamura G., Chai N., Park S., Chiang N., Lin Z., Chiu H., Fong R., Yan D., Kim J., Zhang J., et al. // *Cell Host Microbe*. 2013. V. 14. № 1. P. 93–103.
44. Dreyfus C., Laursen N.S., Kwaks T., Zuijdsgeest D., Khayat R., Ekiert D.C., Lee J.H., Metlagel Z., Bujny M.V., Jongeneelen M., et al. // *Science*. 2012. V. 337. № 6100. P. 1343–1348.
45. Cho K.J., Lee J.H., Hong K.W., Kim S.H., Park Y., Lee J.Y., Kang S., Kim S., Yang J.H., Kim E.K., et al. // *J. Gen. Virol.* 2013. V. 94. P. 1712–1722.
46. Barbey-Martin C., Gigant B., Bizebard T., Calder L.J., Wharton S.A., Skehel J.J., Knossow M. // *Virology*. 2002. V. 294. № 1. P. 70–74.
47. Fleury D., Wharton S.A., Skehel J.J., Knossow M., Bizebard T. // *Nat. Struct. Biol.* 1998. V. 5. № 2. P. 119–123.
48. Kostolansky F., Vareckova E., Betakova T., Mucha V., Russ G., Wharton S.A. // *J. Gen. Virol.* 2000. V. 81. P. 1727–1735.
49. Churchill M.E., Stura E.A., Pinilla C., Appel J.R., Houghten R.A., Kono D.H., Balderas R.S., Fieser G.G., Schulze-Gahmen U., Wilson I.A. // *J. Mol. Biol.* 1994. V. 241. № 4. P. 534–556.
50. Throsby M., van den Brink E., Jongeneelen M., Poon L.L., Alard P., Cornelissen L., Bakker A., Cox F., van Deventer E., Guan Y., et al. // *PLoS One*. 2008. V. 3. № 12. P. e3942.
51. Caton A.J., Brownlee G.G., Yewdell J.W., Gerhard W. // *Cell*. 1982. V. 31. P. 417–427.

MicroRNAs: The Role in Autoimmune Inflammation

N. M. Baulina^{1,2*}, O. G. Kulakova^{1,2}, O. O. Favorova^{1,2}

¹Pirogov Russian National Research Medical University, Ostrovityanova St., 1, Moscow, 117997, Russia

²Russian Cardiology Research and Production Complex, 3-rd Cherepkovskay St., 15a, Moscow, 121552, Russia

*E-mail: tati.90@mail.ru

Received: 30.07.2015

Copyright © 2016 Park-media, Ltd. This is an open access article distributed under the Creative Commons Attribution License, which permits unrestricted use, distribution, and reproduction in any medium, provided the original work is properly cited.

ABSTRACT MicroRNAs (miRNAs) are small non-coding RNA molecules that regulate gene expression at the post-transcriptional level through base-pairing predominantly with a 3'-untranslated region of target mRNA, followed by mRNA degradation or translational repression. Totally, miRNAs change, through a complex regulatory network, the expression of more than 60% of human genes. MiRNAs are key regulators of the immune response that affect maturation, proliferation, differentiation, and activation of immune cells, as well as antibody secretion and release of inflammatory mediators. Disruption of this regulation may lead to the development of various pathological conditions, including autoimmune inflammation. This review summarizes the data on biogenesis and the mechanisms of miRNA action. We discuss the role of miRNAs in the development and the action of the immune system, as well as in the development of an autoimmune inflammatory response. Special attention is given to the role of miRNAs in the autoimmune inflammation in multiple sclerosis, which is a serious socially significant disease of the central nervous system. Currently, a lot of research is focused on this problem.

KEYWORDS microRNA, autoimmune inflammation, multiple sclerosis.

ABBREVIATIONS AID – autoimmune disease; APC – antigen-presenting cell; SPMS – secondary progressive multiple sclerosis; DCs – dendritic cells; PBMCs – peripheral blood mononuclear cells; RRMS – relapsing-remitting multiple sclerosis; MS – multiple sclerosis; TF – transcription factor; CNS – central nervous system; EAE – experimental autoimmune encephalomyelitis; NKs – natural killer cells; Th1/2/17 – T-helper 1/2/17 cells; TLR – Toll-like receptor; Treg – regulatory T cells.

INTRODUCTION

Awareness of the fact that more than 80% of the genome has a specific biological function primarily associated with regulation of the expression of protein-coding genes became one of the most important results of the Encyclopedia of DNA Elements (ENCODE) project, which was aimed at deciphering the functional part of the genome. The most commonly identified functional elements were genes encoding various regulatory RNAs, including miRNAs (short, 19 to 24 nucleotide, single-stranded RNA molecules), which are key regulators of various biological processes at the post-transcriptional level [1].

The first miRNA (*lin-4*) was identified in the nematode *Caenorhabditis elegans* as early as in 1993, but only identification of the second miRNA (*let-7*) in *C. elegans* in 2000 provided the impetus for active investigation of miRNAs in vertebrates and invertebrates [2]. To date, miRNAs have been found in animals, plants, protists, and viruses [3]. The miRNA data are stored in

a number of databases, including miRBase, microRNA.org, MicroRNADB, miR2Disease, HMDD, and PhenomiR. According to the latest miRBase version (v21), a total of 35,828 mature miRNAs were identified in 223 species, with 2,588 mature miRNAs being identified in humans [4].

MiRNAs are highly conserved molecules. Evolutionary related miRNAs are combined into 239 different families whose members have highly homologous sequences and some common targets [5]. Recent studies have demonstrated that miRNAs are essential for the normal development of various physiological systems in organisms and maintenance of cell homeostasis, while a change in their expression and/or function is associated with the development of many pathological conditions in humans, including oncological, infectious, neurodegenerative, and autoimmune diseases [4]. In this review, we first discuss briefly the biogenesis and mechanism of action of miRNAs and then consider the involvement of miRNAs in the regulation of

the immune system and the autoimmune inflammatory process, focusing on the participation of miRNAs in the development of multiple sclerosis (MS), which is a chronic autoimmune inflammatory disease of the central nervous system.

BIOGENESIS AND MECHANISM OF ACTION OF miRNAs

Most miRNAs are encoded by genes located in the introns of protein-coding genes; miRNA genes can also be localized in exons, 5'- and 3'-untranslated gene regions, or intergenic regions [6].

MiRNA genes are transcribed in the nucleus, primarily by RNA polymerase II, as a primary miRNA

(pri-miRNA), which is a long transcript (from a few hundred to tens of thousands of nucleotides) (Fig. 1). The primary miRNA is then converted into a miRNA precursor (pre-miRNA) by the Drosha-DGCR8 microprocessor complex (canonical pathway) [6]. There are also several other non-canonical pathways of pre-miRNA production, one of which is the formation of a pre-miRNA during splicing of short hairpin introns (mirtrons), followed by cleaving of pre-miRNA by the Ldbr protein [7]. Then, the miRNA biogenesis pathways merge, and the pre-miRNA is processed in the cytoplasm by the Dicer enzyme (RNase III) to form a miRNA duplex, with one of the duplex chains being in-

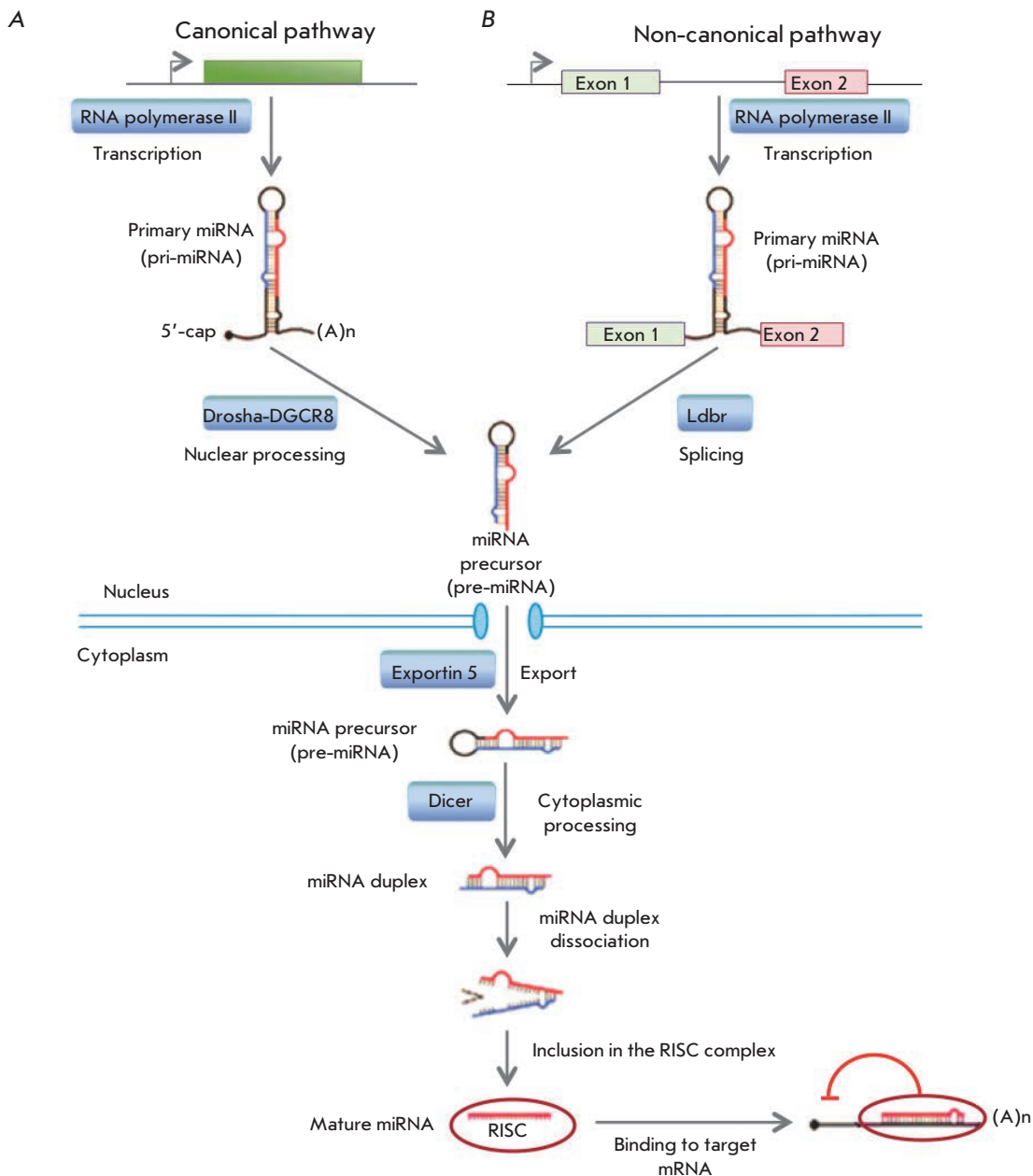


Fig. 1. MiRNA biogenesis. A. The canonical pre-miRNA pathway produces pre-miRNAs through cleavage of pri-miRNA transcripts by the Drosha-DGCR8 microprocessor complex. B. The non-canonical pathway. Mirtrons are spliced and debranched by the Ldbr enzyme, after which they fold into pre-miRNA hairpins. Then, the pathways merge. The green box indicates a miRNA gene; exons 1 and 2 are exons of the host gene encoding intronic miRNA.

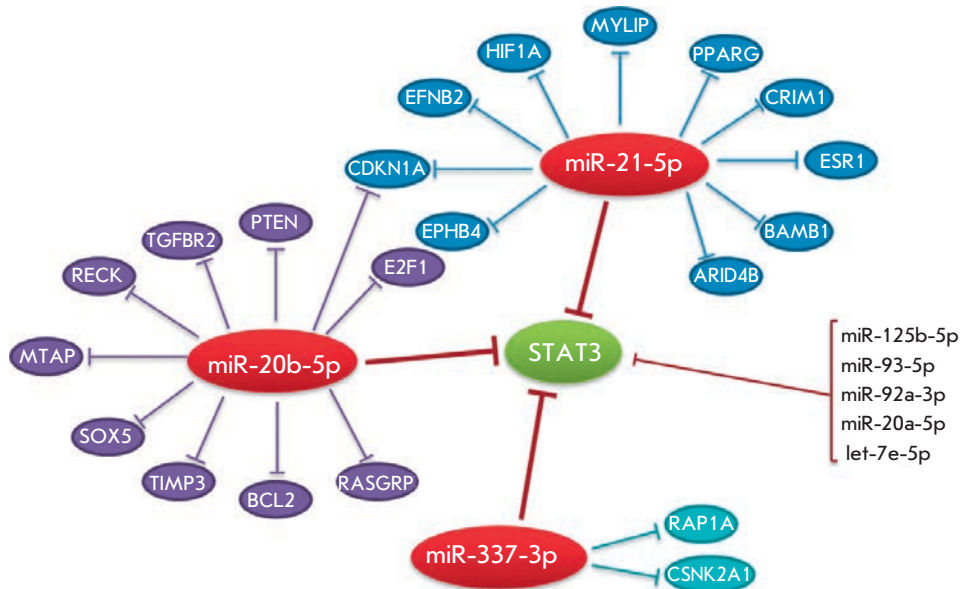


Fig. 2. Redundancy and pleiotropy of the miRNA regulatory system. The *STAT3* gene (green oval) encodes a transcriptional factor. Red ovals are miRNAs downregulating the *STAT3* gene expression. Each of the miRNAs inhibits expression of other target mRNAs (blue, violet, and light blue ovals). Additional miRNAs that may affect the *STAT3* gene expression are listed on the right-hand side. The regulatory network was simulated using the Mirtarbase database (<http://mirtarbase.mbc.nctu.edu.tw/index.php>).

involved in the formation of the RNA-induced silencing complex (RISC) (Fig. 1).

A small, 6–8 nucleotide, miRNA fragment, the seed region, is critical for miRNA binding to the target mRNA within the RISC complex. The degree of complementarity between this miRNA fragment and the target mRNA largely determines the mechanism of gene expression regulation. Complete complementary binding between miRNA and mRNA leads to cleavage and degradation of mRNA. In the case of incomplete complementarity between miRNA and a target mRNA, mRNA translation is inhibited at the stage of initiation or elongation, and the mRNA is destabilized due to cleavage of a polyA sequence and is transferred to processing bodies. MiRNA can act at the transcriptional level through regulation of chromatin reorganization [9]. In most cases, miRNAs reduce the expression level of a target mRNA; but in some cases, binding of miRNAs to certain protein complexes can increase expression of target genes via direct or indirect mechanisms [10].

At present, miRNAs are known to function not only inside the cells, but are also capable of being secreted into the bloodstream and affect other animal cells. In blood, an extracellular mature miRNA (90–99%) primarily associates with proteins of the AGO family [11]. In addition, pre-miRNA can be secreted into the bloodstream within exosomes and/or multivesicular bodies. Exosomes, in turn, can be captured by recipient cells

(including other cell types), and the pre-miRNA in the cytoplasm of recipient cells is processed into a mature miRNA. MiRNA can also be released from cells during apoptosis [12].

To denote the gene encoding miRNA, its precursor, and a mature miRNA molecule, there is a special nomenclature, but it has not yet become conventional. For example, the gene encoding miRNA is denoted by two abbreviations: mir or *MIR*, e.g., mir142 or *MIR142*. The abbreviation “mir” is also used to denote a primary miRNA and pre-miRNA, while a mature miRNA is called “miR”. A certain species of miR origin is designated with a three-letter prefix: “hsa” means a human (*Homo sapiens*) miR, and “rno” means a rat (*Rattus norvegicus*) miR; e.g., hsa-miR-367 or rno-miR-1, respectively. Groups of closely related miRNAs having a similar sequence are combined into families designated by numbers (e.g., miR-33). Within the same family, individual miRNAs are annotated with an additional one-letter suffix; e.g., hsa-miR-451a and hsa-miR-451b. Pre-miRNAs that give rise to identical mature miRNAs but are encoded in different genome regions are denoted with an additional dash-number suffix; e.g., hsa-mir-121-1 and hsa-mir-121-2 precursors give the same mature miRNA hsa-miR-121. The miRNA duplex strand that preferentially binds to the target mRNA (also called the guide strand) is designated as, e.g., miR-56, and the complementary unstable (passenger) chain

is denoted by an asterisk (e.g., miR-56*). If data on the functional activity of miRNA duplex strands are missing, the pre-miRNA end related to the miRNA duplex strand resulting from processing is indicated, e.g., miR-142-5p (5'-end of pre-miRNA) and miR-142-3p (3'-end of pre-miRNA).

Like cytokine action, the miRNA function is characterized by degeneracy (redundancy) and pleiotropy; i.e. the expression level of one mRNA can be regulated by many miRNAs, and one miRNA binds to many target mRNAs, which results in the formation of a complex regulatory network (Fig. 2). Thus, a change in the expression of one miRNA may lead to changes in the expression profile of many target mRNAs: however, this effect for each individual mRNA will also depend on the influence of other miRNAs.

Redundancy of the miRNA system may affect, in total, expression of about 60% of the genes in the organism [13]. It should be noted that the expression level of miRNA genes, like that of protein-coding genes, can be regulated at the epigenetic level, during transcription, processing, and nuclear export, as well as being controlled by the miRNA degradation level [14]. The spectrum of organism miRNAs directly depends on the complexity of the organism structure. In addition, miRNA expression is tissue-specific and ontologically oriented. Thus, as our understanding grows, it becomes increasingly clear that the miRNA network is an essential and evolutionarily ancient component of the system of gene expression regulation.

INVOLVMENT OF miRNAs IN THE DEVELOPMENT AND FUNCTION OF THE IMMUNE SYSTEM

A large number of studies demonstrating the crucial role of miRNAs in the development of immune system elements have been conducted in recent years. The miRNA expression profiles of various hematopoietic organs and cell types were shown to be different, with the expression of specific miRNA sets being changed during differentiation of immune system cells. For example, miR-142a, miR-181a, and miR-223 were found to be preferentially expressed in hematopoietic cells [15]. The importance of miRNAs to immune system development was also shown in transgenic mice. Knock-out of the *Dicer* gene, which is required for normal maturation of miRNAs, leads to serious disruptions in the development and function of mouse immune system cells and death in the early embryonic period [16]. Today, we know that miRNAs are key regulators of the immune response that affect maturation, proliferation, differentiation, and activation of immune system cells, as well as production of antibodies and release of inflammatory mediators. They are necessary for the normal functioning of both innate and adaptive immunity.

MiRNAs and regulation of innate immunity

Innate immunity is the first line of the organism's defense against infectious agents and the initiator of inflammatory response involving monocytes, macrophages, granulocytes, dendritic cells (DCs), and natural killer (NK) cells.

Monocytes and DCs are able to recognize microbial components through Toll-like receptors (TLRs), triggering a cascade of inflammatory reactions. The activity of Langerhans cells, which are one of the DC subtypes, was shown to be strictly dependent on the Dicer enzyme involved in the formation of mature miRNAs. The cell renewal and apoptosis rate increases in the absence of the Dicer enzyme, which leads to a progressive decrease in the number of Langerhans cells *in vivo* [17]. It was also demonstrated that differentiation of granulocytes in humans is regulated by miR-223 [18], and differentiation of monocytes involves miRNAs belonging to the miR-17-92 and miR-106a-92 clusters [19].

Recognition of the conserved structures of various pathogens by TLR receptors on the surface of DCs and monocytes initiates signal transduction into the cell through a cascade involving important specific kinases IRAK-1, -2, or -4 (interleukin-1 (IL-1) associated kinases) and the tumor necrosis factor receptor-associated factor 6 (TRAF6). This stimulates the release of pro-inflammatory and antiviral cytokines, such as interferon IFN- γ , IFN- β , and the tumor necrosis factor (TNF) [17]. All these stages are also regulated by miRNAs. For example, miR-155, whose synthesis is induced by a number of TLR ligands, is involved in the survival and activation of immune cells through binding to its targets: Src homology-2 domain-containing inositol 5-phosphatase 1 (SHIP1) and suppressor of cytokine signaling 1 (SOCS1), which are negative regulators of the immune response [20]. This leads to stimulation of synthesis of proinflammatory cytokines and, as a consequence, to activation of the adaptive immune response. The *MIR146A* gene expression is immediately induced by a lipopolysaccharide, which is a cell-wall component of Gram-negative bacteria, while miR-146a itself is capable of complementarily binding to 3'-UTR mRNAs of IRAK-1 and TRAF6, inhibiting production of these key signaling proteins, which inhibits activation of the NF- κ B factor and reduces production of proinflammatory cytokines IL-6 and TNF [21].

In response to lipopolysaccharides, monocytic cell lines and macrophages also significantly increase expression of miR-132, -125b, -21, and -9, which indicates involvement of miRNAs in controlling the Toll signaling pathway, with some miRNAs (according to the effect pattern) acting at the stage when the organism returns to normal homeostasis after a response to an infection. This feedback regulation is very important, because not

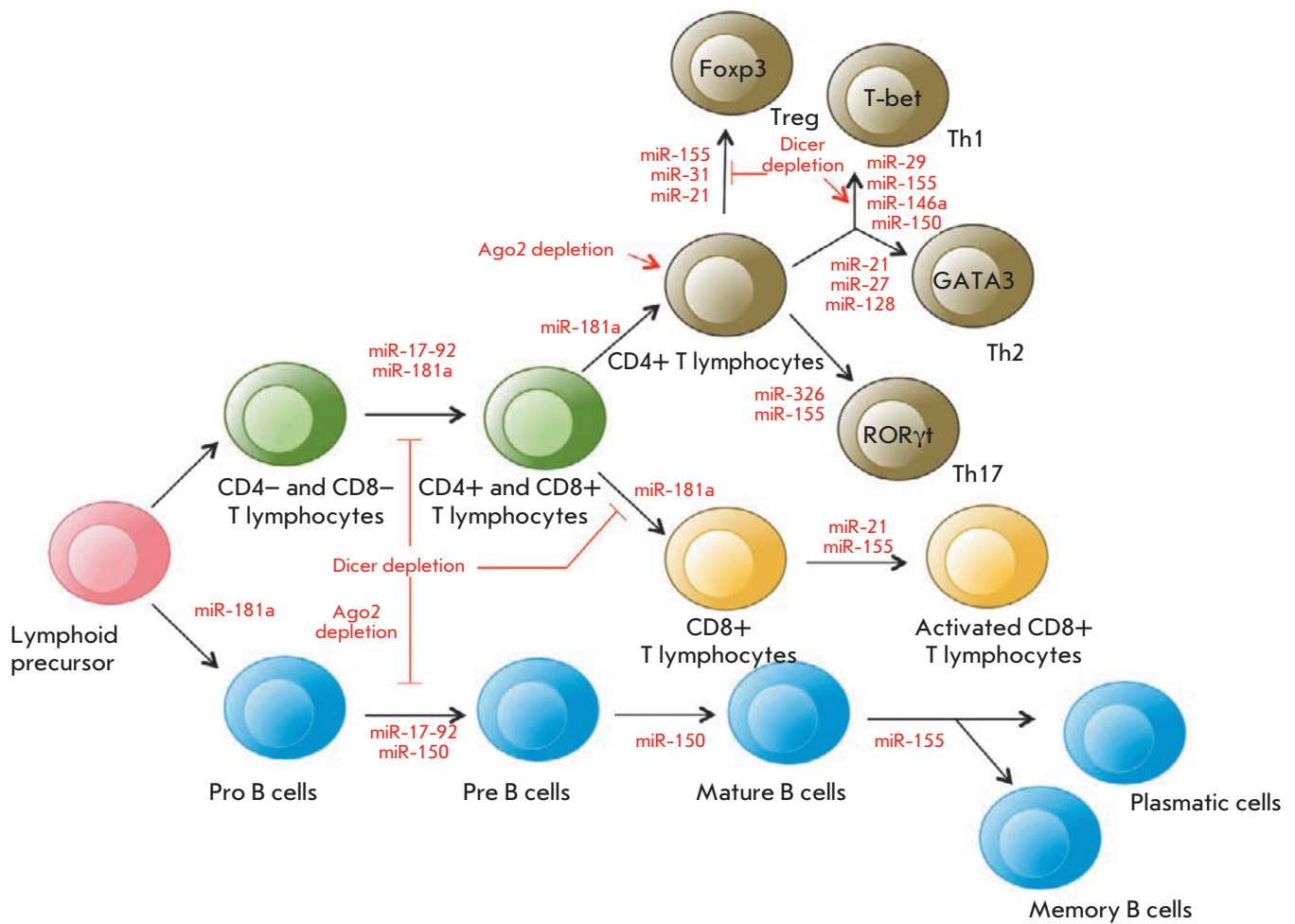


Fig. 3. The role of miRNAs in the differentiation of T and B cells (modified from [28]). Th1, Th2, and Th17 are T helper cells; Treg are regulatory T cells; Foxp3, T-bet, GATA3, and ROR γ t are transcription factors required for the normal development of various T helper cell subsets. See the text for details.

only reduced, but also increased activation of the TLR signaling pathway may harm the organism [22].

NK cells provide early protection through disruption of transformed cells and also affect the development of many immune cells, producing various cytokines. Peripheral NK cells not expressing miRNA biogenesis' genes Dicer or Pasha (*Dgcr8*) had functional disturbances of cellular receptor activation [17], which emphasizes the significance of the miRNA system for the function of NK cells.

All these studies strongly indicate that miRNAs are actively involved in the regulation of the innate immune response.

MiRNAs and regulation of adaptive immune response

The adaptive immune response is characterized by specific recognition of foreign antigens by T and B lymphocytes, followed by selection and proliferation of the antigen-specific clones of these cells. This results in

both a dramatic increase in the number of T and B lymphocytes responding to an antigen and production of memory cells providing a secondary immune response.

MiRNAs are actively involved in the regulation of the development and differentiation of T and B cells (Fig. 3). For example, disruption of miRNA processing in T cells caused by a deletion of the *Dicer* gene reduces the amount of thymocytes and increases their apoptosis at an early developmental stage [23]. The lack of Dicer or AGO2 proteins disrupts differentiation of B cells at different stages and changes the spectrum of secreted antibodies [24, 25]. Furthermore, Dicer deficiency is supposed to affect the program of V(D)J-recombination in developing B cells [25]. At the same time, naive T cells with reduced miRNA expression and production of the AGO2 protein differentiate more rapidly into effector T cells [26].

Many studies have focused on exploring individual miRNAs whose expression is specific at each stage of

the differentiation of B and T cells. According to [27], more than 100 miRNAs were identified that may potentially affect the molecular pathways controlling the differentiation and function of innate and adaptive immunity cells. MiR-181a is differentially expressed in hematopoietic cells and is involved in the regulation of differentiation of B and T cells at early developmental stages. Inhibition of miR-181a in immature T cells disrupts both positive and negative selection of T cells, despite the fact that increased expression of this miRNA in mature T cells enhances the sensitivity of their response to an antigen [28]. Along with miR-181a, miR-17-92 expression is increased in B and T cells precursors and reduced in mature cells, and miR-155 is required for the differentiation of naive T cells into effector cells (Treg, Th1/2, Th17) [29].

A reduction in the amount of Dicer or Drosha in regulatory T cells (Treg) leads to the early development of autoimmune diseases. CD4⁺ T cells not expressing miRNAs were shown not to be capable of differentiating into Treg cells in the thymus. *MIR155* knockout mice have a reduced amount of Treg cells [30]. At the same time, miR-21 and miR-31 regulate Treg cell differentiation by changing the expression of the basic transcription factor Foxp3 required for the normal development of this subset of CD4⁺ cells [31]. Unlike Treg cell, a *Dicer* deletion leads to activation of differentiation of naive CD4⁺ T-cells towards Th1 cells. Increased expression of miR-29 in naive CD4⁺ T cells inhibits differentiation of Th1 cells and production of IFN- γ . MiR-146a has been demonstrated to be involved in the regulation of differentiation of Th1 cells targeting *Traf1* and *Irak1* (as previously discussed), as well as *Stat1* mRNAs. Furthermore, miR-146a expression is increased in Th1 cells, whereas this expression is reduced in Th2 cells. An increased expression of miR-21 in T cells promotes *in vitro* differentiation of Th2 cells, while increased expression of miR-27 and miR-128 reduces production of IL-4 and IL-5 in activated CD4⁺ T cells. The subset of Th17 cells is regulated by miR-326 that binds to the target *Ets1* gene and enhances differentiation of these cells and production of IL-17 [31]. At the later stages of differentiation, increased expression of miR-155 and miR-21 in CD8⁺ cells was observed [32]. MiR-150 prevents the development of mature B cells but promotes activation of T cells through binding to specific transcription factors, including c-Myb and T-bet [33]. *MIR155* knockout mice were detected with disruptions of antibody secretion and switching of the production of antibody isotypes in B cells [34].

Therefore, increasingly growing evidence indicates that miRNAs are involved in the regulation of the immune response. Disruption of this regulation may lead

to various pathological conditions, including autoimmune inflammatory processes.

MI RNAs AND DEVELOPMENT OF AUTOIMMUNE INFLAMMATION

Autoimmune inflammation underlies the pathogenesis of many systemic and organ-specific autoimmune diseases (AIDs), such as systemic lupus erythematosus, MS, rheumatoid arthritis, type 1 diabetes mellitus, autoimmune thyroiditis, Crohn's disease, etc. The cause of these diseases is considered to be a negative reaction of the immune system to self-tissues that leads to the formation of autoreactive cells and autoantibodies, production of a wide range of pro-inflammatory cytokines and mediators, and eventually to damage and destruction of normal tissues. Now, it is believed that the initial impetus for the development of many AIDs is chronic inflammation that, due to mediators constantly produced by autoimmune cells, exacerbates the negative reaction of the immune system to the self antigens and prevents, through a negative feedback mechanism, immune response completion.

Analysis of the miRNA profile in AID patients revealed numerous disruptions of miRNA expression [35–37], with the most frequent changes in some miRNAs (e.g., miR-155, -146a, -326, -21, and -181). Specific miRNAs expressed by cells of the immune system and resident cells of tissues can repress the synthesis of key proteins, thereby contributing to the development of the autoimmune inflammatory response at different stages (*Fig. 4*). These stages include an inflammatory reaction; activation of antigen-presenting cells (APCs); recognition of an antigen by specific lymphocyte receptors; differentiation of CD4⁺ T cells into different subsets; functioning of Treg cells; production of various cytokines; transduction of the signal into resident cells of various tissues in response to inflammatory cytokines; additional recruitment of inflammatory cells by chemokines and cytokines; formation of germinal centers of B cells and switching of immunoglobulin isotypes; as well as some mechanisms of tissue damage not mediated by immune cells.

As mentioned above, sequential activation of certain miRNAs can control the strength level and duration of the inflammatory response induced by activation of TLR receptors. For example, induction of miR-155 and repression of miR-125b and let-7i caused by activation of TLR receptors were shown to lead to synthesis of various pro-inflammatory cytokines and activation of an adaptive immune response. Induction of expression of miR-146a, -132, and -9, which are negative regulators of inflammation, promotes inhibition of TLR signaling. MiR-21 and miR-147, which are induced later, are involved in the activation of the inflammatory re-

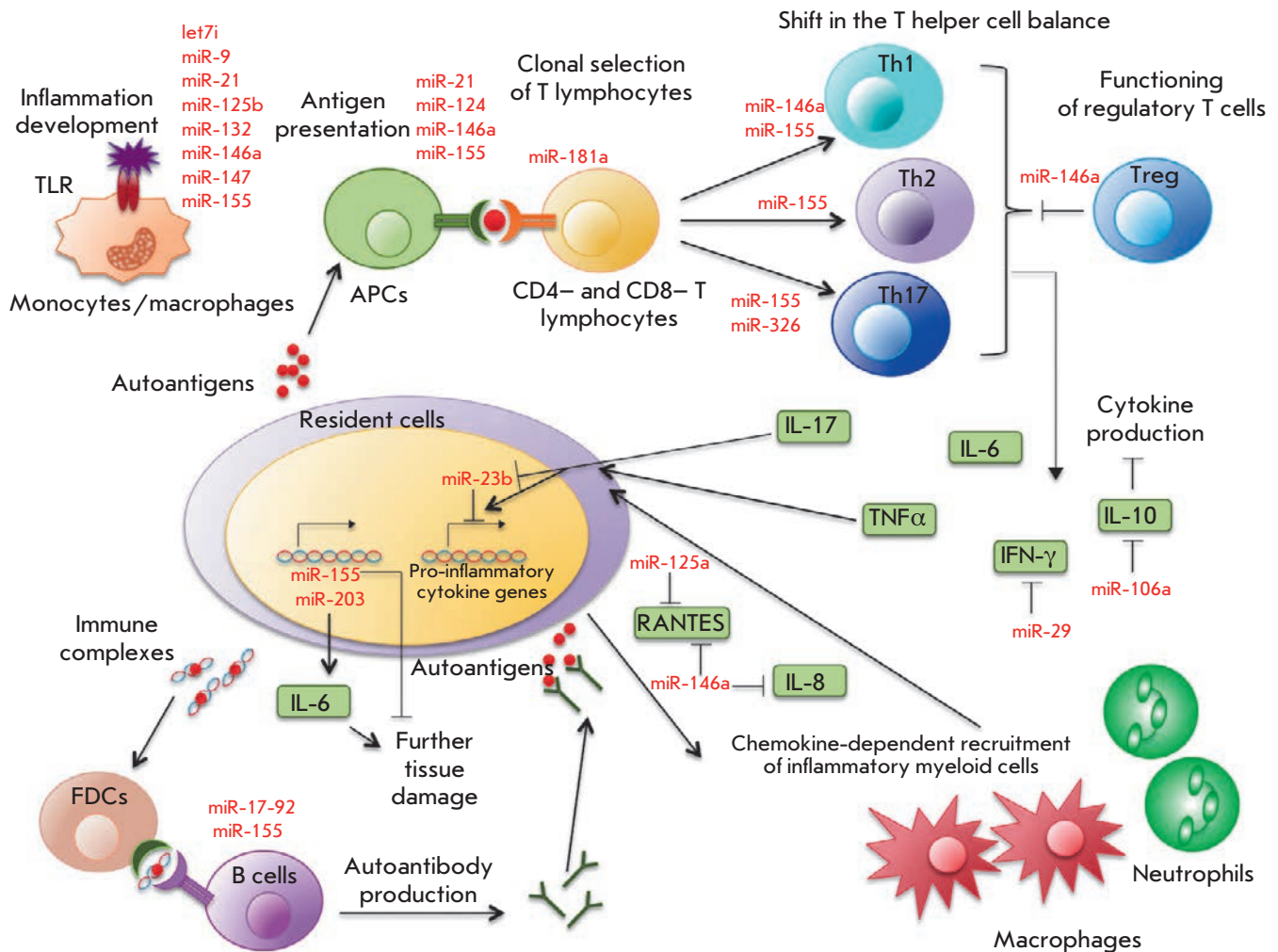


Fig. 4. The role of miRNAs in autoimmune inflammation (modified from [35]). APCs are antigen-presenting cells; Th1, Th2, and Th17 are T helper cells; Treg are regulatory T cells; FDCs are follicular dendritic cells. See text for more details.

response, inhibiting the synthesis of miR-155 and pro-inflammatory cytokines [22].

The role of certain miRNAs in the function of APCs and differentiation of CD4+ T cells was described above. Production of several cytokines is directly regulated by miRNAs. For example, miR-29 in T lymphocytes can bind to mRNA of IFN- γ and inhibit its production [30], while miR-23b expressed in resident fibroblast-like synoviocytes can inhibit NF- κ B activation by binding to target mRNAs of the *TAB2*, *TAB3*, and *IKK- α* genes in response to inflammatory cytokines [38]. Thus, miRNAs can regulate crosstalk between cytokines produced by immune cells and signal transduction from cytokine receptors to resident cells of various tissues during AID development. MiRNAs can be involved in the recruitment of additional inflammatory cells with participation of chemokines. It was demon-

strated that miRNA-125a is involved in the negative regulation of chemokine RANTES (CCL5) production in activated T cells upon development of systemic lupus erythematosus [39], and increased miRNA-146a expression inhibits secretion of chemokines CCL5 and IL-8 in epithelial cells of the human lung [40]. Immunoglobulin isotype switching can also be disrupted in the absence of some miRNAs; e.g., miR-155 [34]. Finally, activation of certain matrix metalloproteinases promoting penetration of immune cells into the inflammatory lesion was shown to be also regulated by miRNAs [41].

A screening comparative study of miRNA expression in resident cells in inflammatory lesions in patients with rheumatoid arthritis, systemic lupus erythematosus, and also in animal models of these diseases and MS revealed miRNA expression disturbances common to these autoimmune diseases: expression of miR-23b and

miR-30a-5p was enhanced, and expression of miR-214 and miR-146a was reduced [38].

The accumulated data suggest a significant role of miRNAs in the development of AIDs. Let us consider this role in more details using the example of multiple sclerosis, which is one of the most studied AIDs.

THE ROLE OF miRNAs IN THE DEVELOPMENT OF MULTIPLE SCLEROSIS

MS is a severe chronic autoimmune inflammatory CNS disease associated with a complex of immune-mediated pathological reactions that destruct the myelin sheath of neurons, which eventually leads to irreversible loss of neurological functions and severe disability.

Currently, the etiology and pathogenesis of MS are not fully elucidated; however, numerous studies suggest the triggering role of the autoimmune process causing damage to the myelin sheath of nerve cells in the CNS. Activation of anergic T and B lymphocytes in the periphery (outside the CNS) is the first stage in MS immunopathogenesis. MS is associated with disturbance of both cellular and humoral immunity. The development of MS is characterized by shifting of the balance of CD4+ T helper cells towards Th1 and Th17 subsets and also by dysfunction of Treg cells. Disruption of the blood-brain barrier permeability promotes penetration of autoreactive cells into the CNS, where they are reactivated by proteins and lipids of the neuron myelin sheath. Then, myelin-specific cells are involved in the development of pathologic demyelinating lesions (plaques). Activated resident CNS cells (microglia and astrocytes) also participate in the formation of the plaques. They produce cytokines and chemokines, mainly proinflammatory, that additionally recruit both autoreactive T and B lymphocytes and monocytes/macrophages to demyelinating plaques; these cells, in turn, secrete a variety of the active molecules (cytokines, antibodies, oxygen and nitrogen radicals, proteases) involved in further damage to the myelin sheath and oligodendrocytes. Long-term and severe demyelination causes axonal death that leads to the development of symptoms of a persistent neurological deficit. Damage to oligodendrocytes and myelin is accompanied by the release of a large number of autoantigens providing impetus to the further development of the autoimmune process.

MiRNAs and the autoimmune inflammatory process in experimental autoimmune encephalomyelitis

The relationship between immunopathological and neurodegenerative processes enables use of experimental autoimmune encephalomyelitis (EAE) as the primary animal model for studying the role of miRNAs in MS development.

One of the first studies demonstrated that *MIR155* knockout mice are resistant to EAE due to reduced differentiation of Th1 and Th17 cells upon autoimmune inflammation [42]. Screening studies revealed changes in the expression of many miRNAs upon EAE. For example, 43 miRNAs were identified whose expression in the lymph nodes of EAE rats was higher than that in rats resistant to EAE [43]; 33 of these miRNAs were previously associated with the development of MS and other AIDs. In oligodendrocytes of EAE mice, expression of 56 miRNAs was lower than that in oligodendrocytes of normal mice; the lowest expression level was that of miR-15a-5p, -15b-5p, -20b-5p, -106b-5p, -181a-5p, -181c-5p, -181d-5p, -320-3p, -328-3p, and -338-3p [44].

Studying the role of miRNAs in the EAE development helped identify specific target genes of some miRNAs and evaluate their involvement in the pathogenesis of the disease (Table 1). The main method to induce EAE in C57Bl/6 [38, 42, 47–57] and SJL [45] mice or Dark Agouti and PVG rats was immunization with the myelin oligodendrocyte glycoprotein, proteolipid protein, or their immunogenic peptides in a complete Freund's adjuvant in combination with the pertussis toxin [43]. The studies were performed mainly in cells of the immune system (in particular, CD4+ T lymphocytes) and also in various cells of the nervous tissue. An increase in the expression level of miRNA genes (except miR-20b and miR-132/212) was mostly observed in CD4+ T cells; in nervous system cells, expression of the three miRNAs was reduced, and that of two miRNAs was enhanced. The main targets of miRNAs both in CD4+ T lymphocytes and in nervous system cells were mRNAs of genes of transcription factors and modulators of transcription factor activity and genes of signaling pathway elements and cytokines. It is important to note that targets of miR-29b and miR-20b are mRNAs of the *TBX21* and *RORC* genes encoding T-bet and ROR γ t, which are the main transcription factors involved in the differentiation of Th0 cells to Th1 and Th17 cells, respectively. The target of miR-326 is the *ETS1* gene encoding a transcription factor that directly controls the expression of cytokine and chemokine genes and is involved in the regulation of differentiation and proliferation of lymphoid cells.

Targets of other miRNAs include genes of members of various signaling pathways, in particular the NF- κ B (*TNFAIP3* and *CHUK*) and JAK/STAT (*STAT3*, *SMAD7*, *SOCS1*, and *PIAS3*) pathways, as well as genes encoding phosphatases (*INPP5D* and *PTEN*). Genes of some cytokines (*IL-10*, *IL-6*, and *IFNG*) and signaling pathways of IL-1 and IL-17 cytokines (*TAB2* and *TAB3*) are also targets of miRNAs, whose expression varies upon EAE.

Table 1. Targets and the possible mechanisms of the effect of certain miRNAs whose expression was disrupted during the development of experimental autoimmune encephalomyelitis in mice.

miRNA	Cell type	Change in expression*	Target genes	Effect of changed miRNA expression	Reference
let-7e	CD4+ T lymphocytes	↑	<i>IL10</i>	Stimulation of development of Th1 and Th17 cells	[48]
miR-17	CD4+ T lymphocytes	↑	<i>IKZF4</i>	Increased polarization of Th17 cells	[49]
miR-19b	CD4+ T lymphocytes	↑	<i>PTEN</i>	Activation of Th17 cell differentiation	[49]
miR-20b	CD4+ T lymphocytes	↓	<i>RORC, STAT3</i>	Activation of Th17 cell differentiation	[50]
mir-21	CD4+ T lymphocytes	↑	<i>SMAD7</i>	Activation of Th17 cell differentiation	[51]
miR-23b	Spinal cord cells	↓	<i>TAB2, TAB3, CHUK</i>	Stimulation of IL-17-mediated autoimmune inflammation	[38]
miR-26a	Brain cells	↓	<i>IL6</i>	Increased expression of Th17-mediated cytokines	[52]
miR-29b	CD4+ T lymphocytes	↑	<i>TBX21, IFNG</i>	Regulation of Th1 cell differentiation	[53]
miR-124	Bone marrow macrophages	↓	<i>CEBPA, SPI1</i>	Activation of phagocytic activity, inhibition of microglia differentiation	[47]
miR-132/212	CD4+ T lymphocytes	↓	<i>ACHE</i>	Stimulation of T cell proliferation and production of IL-17 and IFN- γ ; increased catalytic activity of acetylcholinesterase	[54]
miR-146a	Bone marrow stem cells	↑	<i>PTGES2</i>	Inhibition of prostaglandin E2 synthesis	[45]
miR-155	CD4+ T lymphocytes	↑	<i>SOCS1</i>	Stimulation of development of Th1 and Th17 cells	[42]
		↑	<i>INPP5D</i>	Disturbance of myelin proliferation	[42]
miR-301a	CD4+ T lymphocytes	↑	<i>PIAS3</i>	Regulation of Th17 cell differentiation	[55]
miR-326	CD4+ T lymphocytes	↑	<i>ETS1</i>	Stimulation of development and proliferation of Th17 cells	[56]
miR-873	Primary astrocyte culture	↑	<i>TNFAIP3</i>	Stimulation of production of inflammatory cytokines and increased demyelination of nerve fibers	[57]

*Hereinafter: an increase (↑) or decrease (↓) in miRNA expression upon experimental autoimmune encephalomyelitis.

The action of miRNAs (such as let-7e, miR-155, -17-92, -20b, -21, -29b, -301a, and -326) on the target is mainly observed in the disruption of differentiation and proliferation of Th1 and Th17 cells, which are believed to play a major role in the EAE development. MiR-26a and miR-873 stimulate production of pro-inflammatory cytokines, affecting the neuroinflammatory process and severity of EAE. In addition, miR-155 is involved in the disruption of myelin proliferation, which may also contribute to the development of neurodegenerative processes. An increased level of miR-146a in neuronally-differentiated bone-marrow-derived mesenchymal stem cells (BMSCs) during EAE inhibits the synthesis of prostaglandin E2, which may lead to increased production of TNF and IFN- γ by activated DC and T cells [45, 46]. Reduced miR-124 expression promotes activation of the phagocytic activity and inhibition of

microglial differentiation, which leads to worsening of EAE in animals [47].

Thus, EAE proved to be an adequate experimental model suitable for studying the differential expression of miRNAs in autoimmune inflammation and for identifying the role of individual miRNAs in regulation of differentiation of Th1 and Th17 cells and synthesis of pro- and anti-inflammatory cytokines.

MiRNAs and the development of autoimmune inflammation in MS

Table 2 presents the results of a study of miRNA expression in MS patients. Various tissues and cells were used to isolate miRNAs: blood components, cerebrospinal fluid, and demyelinating plaques. miRNA expression levels were compared between a control group of healthy people and patients with various MS forms.

Table 2. MiRNAs whose expression is altered in multiple sclerosis.

miRNA source	Multiple sclerosis form	miRNAs differentially expressed in MS patients compared to a control	Change in expression	Reference
Whole blood	RRMS	miR-142-3p, -145, -186, -223, -442a, -491-5p, -584, -664, -1275	↑	[58]
		miR-20b	↓	
	RRMS, CIS	miR-16-2-3p, -574-5p	↑	[59]
		miR-7-1-3p, -20a-5p, -20b , -146b-5p, -3653	↓	
RRMS, PPMS, SPMS	miR-17, -20	↓	[60]	
MNCs	RRMS	miR-326	↑	[56]
		miR-18b, -193a, -328, -599	↑	[61]
		let-7d, miR-145, -744	↑	[62]
		miR-142-3p, -146a, -155, -326	↑	[63]
	RRMS, PPMS, SPMS	let-7g, miR-150	↓	[64]
RRMS, CIS	miR-29a-3p, -29c-3p , -532-5p	↓	[65]	
CD4+ T lymphocytes	RRMS	miR-326	↑	[56]
		miR-17-5p , -193a, -376a, -485-3p	↑	[66]
		miR-34a, -126, -497	↓	
	RRMS, PPMS, SPMS	miR-27b, -128, -340	↑	[67]
		miR-29b	↑	[53]
CD4+ CD25+ T regulatory lymphocytes	RRMS	miR-19a, -19b , -25, -93, -106b	↑	[68]
B lymphocytes	RRMS	miR-19b , -106b, -191, -551a	↑	[69]
Plasma	N/A	miR-22, -422a, -572, -614, -648, -1826	↑	[70]
		miR-1979	↓	
CSF*	RRMS, PPMS, SPMS	miR-181c, -633	↑	[71]
		miR-922	↓	
Demyelinating plaque**	RRMS, PPMS, SPMS	miR-21, -23a , -27a, -34a, -142-3p, -146a, -155 , -199a, -326 , -346, -650	↑	[72]

*The cerebrospinal fluid of patients with other neurological diseases was used as a control.

**Postmortem sections of brain white matter obtained from patients without a neurologic disease were used as a control.

Note. SPMS – secondary progressive multiple sclerosis (MS); CIS – clinically isolated syndrome; MNCs – mononuclear cells; PPMS – primary progressive MS; RRMS – relapsing remitting MS; CSF – cerebrospinal fluid. MiRNAs whose expression is changed both in multiple sclerosis and in experimental autoimmune encephalomyelitis are shown in bold.

The group of MS patients consisted mostly of patients with relapsing-remitting MS (RRMS), clinically isolated syndrome, primary progressive MS, and secondary progressive MS. *Table 2* shows that the spectrum of expressed miRNAs is very broad and probably depends on the source of their isolation and/or the MS form.

Changes in the expression of certain miRNAs were observed in various cells. For example, expression of miR-142-3p, -155, and -326 was increased both in demyelinating plaques and in the whole blood of MS patients; expression of miR-19b and miR-106b was increased in Treg and B cells; and expression of miR-145 was increased in the whole blood and peripheral blood mononuclear cells. Opposite effects, depending on the cell type, were observed for certain miRNAs (miR-17,

miR-34a): expression of miR-17 was increased in the whole blood and reduced in CD4+ T cells; expression of miR-34a was increased in plaques and decreased in CD4+ T cells. A number of changes (shown in bold in *Table 2*) in the expression of miRNAs (miR-17, -19, -20, -21, -23, -29, -146, -155, -326) coincided with the data obtained in EAE models. However, different miRNA expression patterns were observed in many cases that may be explained by various causes, including experimental conditions. It should be noted that the data on miRNA expression levels presented in *Table 2* are not correlated with a MS stage and the approach to the treatment of MS patients.

Target genes of some miRNAs, whose expression is changed during MS development, were identified in

Table 3. Target mRNAs and the possible mechanisms of the effect of certain miRNAs whose expression is changed during the development of multiple sclerosis in humans.

miRNA	Tested cells	Change in expression	Target genes	Putative functions	Reference
miR-17	CD4+ T lymphocytes	↑	TGFBR2, PTEN, BCL2L11, CDKN1A	Proliferation and activation of T cells	[73]
miR-34a miR-155 miR-346	Demyelinating plaques	↑	CD47	Stimulation of myelin phagocytosis	[72]
miR-132	B lymphocytes	↑	SIRT1	Increased production of pro-inflammatory cytokines	[74]
miR-320a	B lymphocytes	↓	MMP9	Disturbance of HEB permeability	[75]
miR-340	CD4+ T lymphocytes	↑	IL4	Shift of the balance of Th2/Th1 cytokines towards Th1 cytokines	[67]

B and CD4+ T cells. These genes and their putative functions are shown in *Table 3*. The gene encoding the cell adhesion molecule SD47 is the target of miR-34a, miR-155, and miR-346. Other targets are genes encoding regulators of apoptosis (BIM) and transcription (SIRT1), cell proliferation inhibitor (p21), matrix metalloprotease 9 (MMP9), and cytokine IL-4. The action of miRNAs on these targets causes stimulation of myelin phagocytosis, changes in the blood brain barrier permeability, and disturbance of proliferation and activation of T cells and secretion of pro- and anti-inflammatory cytokines.

The analysis of the data presented in *Tables 2* and *3* indicates a variety of miRNA differential expression profiles in MS, depending on the type of analyzed cells. Given the complex nature of MS, it may be assumed that miRNA expression determines the stages of the clinical course of MS; however, the available data are

not sufficient to draw final conclusions. Further investigation of miRNA differential expression may help to identify potential MS biomarkers and clinical MS patterns, as well as shed light on the mechanisms of miRNA action. Of particular interest are the trigger mechanisms underlying the processes that control the transition of patients from remission to relapse and from relapse to remission upon a RRMS clinical course.

In general, investigation of the role of miRNA in the epigenetic regulation of autoimmune inflammation in various inflammatory AIDs may not only facilitate the understanding of the processes that maintain the stability and plasticity of the immune system, but also affect the development of strategies for the prevention and treatment of these serious social diseases. ●

This work was supported by the Russian Science Foundation (Project No. 14-14-00605).

REFERENCES

1. Rebane A., Akdis C.A. // *J. Allergy Clin. Immunol.* 2013. V. 132. P. 15–26.
2. Reinhart B.J., Slack F.J., Basson M., Pasquinelli A.E., Bettinger J.C., Rougvié A.E., Horvitz H.R., Ruvkun G. // *Nature.* 2000. V. 403. P. 901–906.
3. Kamanu T.K., Radovanovic A., Archer J.A., Bajic V.B. // *Sci. Rep.* 2013. V. 3. P. 2940.
4. Eulalio A., Mano M. // *J. Biomol. Screen.* 2015. V. 20. P. 1003–1017.
5. Meunier J., Lemoine F., Soumillon M., Liechti A., Weier M., Guschanski K., Hu H., Khaitovich P., Kaessmann H. // *Genome Res.* 2013. V. 23. P. 34–45.
6. Zhuo Y., Gao G., Shi J.A., Zhou X., Wang X. // *Cell Physiol. Biochem.* 2013. V. 32. P. 499–510.
7. Westholm J.O., Lai E.C. // *Biochimie.* 2011. V. 93. P. 1897–1904.
8. Okamura K., Hagen J., Duan H., Tyler D., Lai E. // *Cell.* 2007. V. 130. P. 89–100.
9. Valinezhad Orang A., Safaralizadeh R., Kazemzadeh-Bavili M. // *Int. J. Genomics.* 2014. V. 2014. P. 970607.
10. Vasudevan S. // *WIREs RNA.* 2012. V. 3. P. 311–330.
11. Turchinovich A., Cho W.C. // *Front. Genet.* 2014. V. 5. P. 30.
12. Vickers K.C., Palmisano B.T., Shoucri B.M., Shamburek R.D., Remaley A.T. // *Nat. Cell Biol.* 2011. V. 13. P. 423–433.
13. Diao L., Marcais A., Norton S., Chen K.C. // *Nucl. Acids Res.* 2014. V. 42. P. e135.
14. Ainiding G., Kawano Y., Sato S., Isobe N., Matsushita T., Yoshimura S., Yonekawa T., Yamasaki R., Murai H., Kira J., et al. // *J. Neurol. Sci.* 2014. V. 337. P. 147–150.
15. Shivdasani R.A. // *Blood.* 2006. V. 108. P. 3646–3653.
16. Belver L., de Yebenes V.G., Ramiro A.R. // *Immunity.* 2010. V. 33. P. 713–722.
17. Jia S., Zhai H., Zhao M. // *Discov. Med.* 2014. V. 18. P. 237–247.
18. Fazi F., Rosa A., Fatica A., Gelmetti V., De Marchis M.L., Nervi C., Bozzoni I. // *Cell.* 2005. V. 123. P. 819–831.

19. Fontana L., Pelosi E., Greco P., Racanicchi S., Testa U., Liuzzi F., Croce C.M., Brunetti E., Grignani F., Peschle C. // *Nat. Cell. Biol.* 2007. V. 9. P. 775–787.
20. O'Connell R.M., Chaudhuri A.A., Rao D.S., Baltimore D. // *Proc. Natl. Acad. Sci. USA.* 2009. V. 106. P. 7113–7118.
21. Taganov K.D., Boldin M.P., Chang K.J., Baltimore D. // *Proc. Natl. Acad. Sci. USA.* 2006. V. 103. P. 12481–12486.
22. O'Neill L.A., Sheedy F.J., McCoy C.E. // *Nat. Rev. Immunol.* 2011. V. 11. P. 163–175.
23. Zhang N., Bevan M.J. // *Proc. Natl. Acad. Sci. USA.* 2010. V. 107. P. 21629–21634.
24. Korolov S.B., Muljo S.A., Galler G.R., Krek A., Chakraborty T., Kanellopoulou C., Jensen K., Cobb B.S., Merkschlager M., Rajewsky N., et al. // *Cell.* 2008. V. 132. P. 860–874.
25. O'Carroll D., Mecklenbrauker I., Das P.P., Santana A., Koenig U., Enright A.J., Miska E.A., Tarakhovsky A. // *Genes Dev.* 2007. V. 21. P. 1999–2004.
26. Bronevetsky Y., Villarino A.V., Eisley C.J., Barbeau R., Barczak A.J., Heinz G.A., Kremmer E., Heissmeyer V., McManus M.T., Erle D.J., et al. // *J. Exp. Med.* 2013. V. 210. P. 417–432.
27. Zhu S., Pan W., Qian Y. // *J. Mol. Med. (Berl.)*. 2013. V. 91. P. 1039–1050.
28. Dai R., Ahmed S.A. // *Transl. Res.* 2011. V. 157. P. 163–179.
29. Sethi A., Kulkarni N., Sonar S., Lal G. // *Front. Genet.* 2013. V. 4. P. 8.
30. Baumjohann D., Ansel K.M. // *Nat. Rev. Immunol.* 2013. V. 13. P. 666–678.
31. Rouas R., Fayyad-Kazan H., El Zein N., Lewalle P., Rothe F., Simion A., Akl H., Mourtada M., El Rifai M., Burny A., et al. // *Eur. J. Immunol.* 2009. V. 39. P. 1608–1618.
32. Salaun B., Yamamoto T., Badran B., Tsunetsugu-Yokota Y., Roux A., Baitsch L., Rouas R., Fayyad-Kazan H., Baumgaertner P., Devevre E., et al. // *J. Transl. Med.* 2011. V. 9. P. 44.
33. Xiao C., Calado D.P., Galler G., Thai T.H., Patterson H.C., Wang J., Rajewsky N., Bender T.P., Rajewsky K. // *Cell.* 2007. V. 131. P. 146–159.
34. Thai T.H., Calado D.P., Casola S., Ansel K.M., Xiao C., Xue Y., Murphy A., Friendewey D., Valenzuela D., Kutok J.L., et al. // *Science.* 2007. V. 316. P. 604–608.
35. Hu R., O'Connell R.M. // *Arthritis Res. Ther.* 2013. V. 15. P. 202.
36. Qu Z., Li W., Fu B. // *Biomed. Res. Int.* 2014. V. 2014. P. 527895.
37. Singh R.P., Massachi I., Manickavel S., Singh S., Rao N.P., Hasan S., Mc Curdy D.K., Sharma S., Wong D., Hahn B.H., et al. // *Autoimmun. Rev.* 2013. V. 12. P. 1160–1165.
38. Zhu S., Pan W., Song X., Liu Y., Shao X., Tang Y., Liang D., He D., Wang H., Liu W., et al. // *Nat. Med.* 2012. V. 18. P. 1077–1086.
39. Zhao X., Tang Y., Qu B., Cui H., Wang S., Wang L., Luo X., Huang X., Li J., Chen S., et al. // *Arthritis Rheum.* 2010. V. 62. P. 3425–3435.
40. Perry M.M., Moschos S.A., Williams A.E., Shepherd N.J., Larner-Svensson H.M., Lindsay M.A. // *J. Immunol.* 2008. V. 180. P. 5689–5698.
41. Stanczyk J., Ospelt C., Karouzakis E., Filer A., Raza K., Kolling C., Gay R., Buckley C.D., Tak P.P., Gay S., et al. // *Arthritis Rheum.* 2011. V. 63. P. 373–381.
42. O'Connell R.M., Kahn D., Gibson W.S., Round J.L., Scholz R.L., Chaudhuri A.A., Kahn M.E., Rao D.S., Baltimore D. // *Immunity.* 2010. V. 33. P. 607–619.
43. Bergman P., James T., Kular L., Ruhrmann S., Kramarova T., Kvist A., Supic G., Gillett A., Pivarecsi A., Jagodic M. // *J. Immunol.* 2013. V. 190. P. 4066–4075.
44. Lewkowicz P., Cwiklinska H., Mycko M.P., Cichalewska M., Domowicz M., Lewkowicz N., Jurewicz A., Selmaj K.W. // *J. Neurosci.* 2015. V. 35. P. 7521–7537.
45. Matysiak M., Fortak-Michalska M., Szymanska B., Orłowski W., Jurewicz A., Selmaj K. // *J. Immunol.* 2013. V. 190. P. 5102–5109.
46. Aggarwal S., Pittenger M.F. // *Blood.* 2005. V. 105. P. 1815–1822.
47. Ponomarev E.D., Veremeyko T., Barteneva N., Krichevsky A.M., Weiner H.L. // *Nat. Med.* 2011. V. 17. P. 64–70.
48. Guan H., Fan D., Mrelashvili D., Hao H., Singh N.P., Singh U.P., Nagarkatti P.S., Nagarkatti M. // *Eur. J. Immunol.* 2013. V. 43. P. 104–114.
49. Liu S.Q., Jiang S., Li C., Zhang B., Li Q.J. // *J. Biol. Chem.* 2014. V. 289. P. 12446–12456.
50. Zhu E., Wang X., Zheng B., Wang Q., Hao J., Chen S., Zhao Q., Zhao L., Wu Z., Yin Z. // *J. Immunol.* 2014. V. 192. P. 5599–5609.
51. Murugaiyan G., da Cunha A.P., Ajay A.K., Joller N., Garo L.P., Kumaradevan S., Yosef N., Vaidya V.S., Weiner H.L. // *J. Clin. Invest.* 2015. V. 125. P. 1069–1080.
52. Zhang R., Tian A., Wang J., Shen X., Qi G., Tang Y. // *Neuromol. Med.* 2015. V. 17. P. 24–34.
53. Smith K.M., Guerau-de-Arellano M., Costinean S., Williams J.L., Bottoni A., Mavrikis Cox G., Satoskar A.R., Croce C.M., Racke M.K., Lovett-Racke A.E., et al. // *J. Immunol.* 2012. V. 189. P. 1567–1576.
54. Hanieh H., Alzahrani A. // *Eur. J. Immunol.* 2013. V. 43. P. 2771–2782.
55. Mycko M.P., Cichalewska M., Machlanska A., Cwiklinska H., Mariasiewicz M., Selmaj K.W. // *Proc. Natl. Acad. Sci. USA.* 2012. V. 109. P. E1248–1257.
56. Du C., Liu C., Kang J., Zhao G., Ye Z., Huang S., Li Z., Wu Z., Pei G. // *Nat. Immunol.* 2009. V. 10. P. 1252–1259.
57. Liu X., He F., Pang R., Zhao D., Qiu W., Shan K., Zhang J., Lu Y., Li Y., Wang Y. // *J. Biol. Chem.* 2014. V. 289. P. 28971–28986.
58. Keller A., Leidinger P., Lange J., Borries A., Schroers H., Scheffler M., Lenhof H.P., Ruprecht K., Meese E. // *PLoS One.* 2009. V. 4. P. e7440.
59. Keller A., Leidinger P., Steinmeyer F., Stahler C., Franke A., Hemmrich-Stanisak G., Kappel A., Wright I., Dorr J., Paul F., et al. // *Mult. Scler.* 2014. V. 20. P. 295–303.
60. Cox M.B., Cairns M.J., Gandhi K.S., Carroll A.P., Moscovis S., Stewart G.J., Broadley S., Scott R.J., Booth D.R., Lechner-Scott J., et al. // *PLoS One.* 2010. V. 5. P. e12132.
61. Otaegui D., Baranzini S.E., Armananzas R., Calvo B., Munoz-Culla M., Khankhanian P., Inza I., Lozano J.A., Castillo-Trivino T., Asensio A., et al. // *PLoS One.* 2009. V. 4. P. e6309.
62. Sondergaard H.B., Hesse D., Krakauer M., Sorensen P.S., Sellebjerg F. // *Mult. Scler.* 2013. V. 19. P. 1849–1857.
63. Waschbisch A., Atiya M., Linker R.A., Potapov S., Schwab S., Deraus T. // *PLoS One.* 2011. V. 6. P. e24604.
64. Martinelli-Boneschi F., Fenoglio C., Brambilla P., Sorosina M., Giacalone G., Esposito F., Serpente M., Cantoni C., Ridolfi E., Rodegher M., et al. // *Neurosci. Lett.* 2012. V. 508. P. 4–8.
65. Hecker M., Thamilarasan M., Koczan D., Schroder I., Flechtner K., Frieseleben S., Fullen G., Thiesen H.J., Zettl U.K. // *Int. J. Mol. Sci.* 2013. V. 14. P. 16087–16110.
66. Lindberg R.L., Hoffmann F., Mehling M., Kuhle J., Kappos L. // *Eur. J. Immunol.* 2010. V. 40. P. 888–898.

67. Guerau-de-Arellano M., Smith K.M., Godlewski J., Liu Y., Winger R., Lawler S.E., Whitacre C.C., Racke M.K., Lovett-Racke A.E. // *Brain*. 2011. V. 134. P. 3578–3589.
68. De Santis G., Ferracin M., Biondani A., Caniatti L., Rosaria Tola M., Castellazzi M., Zagatti B., Battistini L., Borsellino G., Fainardi E., et al. // *J. Neuroimmunol.* 2010. V. 226. P. 165–171.
69. Sievers C., Meira M., Hoffmann F., Fontoura P., Kappos L., Lindberg R.L. // *Clin. Immunol.* 2012. V. 144. P. 70–79.
70. Siegel S.R., Mackenzie J., Chaplin G., Jablonski N.G., Griffiths L. // *Mol. Biol. Rep.* 2012. V. 39. P. 6219–6225.
71. Haghikia A., Haghikia A., Hellwig K., Baraniskin A., Holzmann A., Decard B.F., Thum T., Gold R. // *Neurology*. 2012. V. 79. P. 2166–2170.
72. Junker A., Krumbholz M., Eisele S., Mohan H., Augstein F., Bittner R., Lassmann H., Wekerle H., Hohlfeld R., Meinl E. // *Brain*. 2009. V. 132. P. 3342–3352.
73. Meira M., Sievers C., Hoffmann F., Rasenack M., Kuhle J., Derfuss T., Kappos L., Lindberg R.L. // *J. Immunol. Res.* 2014. V. 2014. P. 897249.
74. Miyazaki Y., Li R., Rezk A., Misirliyan H., Moore C., Farooqi N., Solis M., Goiry L.G., de Faria Junior O., Dang V.D., et al. // *PLoS One*. 2014. V. 9. P. e105421.
75. Aung L.L., Mouradian M.M., Dhib-Jalbut S., Balashov K.E. // *J. Neuroimmunol.* 2015. V. 278. P. 185–189.

Host Proteins Ku and HMGA1 As Participants of HIV-1 Transcription

O. A. Shadrina¹, E. S. Knyazhanskaya², S.P. Korolev², M. B. Gottikh^{3*}

¹Faculty of Bioengineering and Bioinformatics, Lomonosov Moscow State University, Leninskie Gory, Moscow, 119991, Russia

²Chemistry Department, Lomonosov Moscow State University, Leninskie Gory, Moscow, 119991, Russia

³Belozersky Institute of Physical-Chemical Biology, Lomonosov Moscow State University, Leninskie Gory, Moscow, Russia; 119991

*E-mail: gottikh@belozersky.msu.ru

Received: 17.07.2015

Copyright © 2016 Park-media, Ltd. This is an open access article distributed under the Creative Commons Attribution License, which permits unrestricted use, distribution, and reproduction in any medium, provided the original work is properly cited.

ABSTRACT Human immunodeficiency virus type 1 is known to use the transcriptional machinery of the host cell for viral gene transcription, and the only viral protein that partakes in this process is Tat, the viral trans-activator of transcription. During acute infection, the binding of Tat to the hairpin at the beginning of the transcribed viral RNA recruits the PTEFb complex, which in turn hyperphosphorylates RNA-polymerase II and stimulates transcription elongation. Along with acute infection, HIV-1 can also lead to latent infection that is characterized by a low level of viral transcription. During the maintenance and reversal of latency, there are no detectable amounts of Tat protein in the cell and the mechanism of transcription activation in the absence of Tat protein remains unclear. The latency maintenance is also a problematic question. It seems evident that cellular proteins with a yet unknown nature or role regulate both transcriptional repression in the latent phase and its activation during transition into the lytic phase. The present review discusses the role of cellular proteins Ku and HMGA1 in the initiation of transcription elongation of the HIV-1 provirus. The review presents data regarding Ku-mediated HIV-1 transcription and its dependence on the promoter structure and the shape of viral DNA. We also describe the differential influence of the HMGA1 protein on the induced and basal transcription of HIV-1. Finally, we offer possible mechanisms for Ku and HMGA1 proteins in the proviral transcription regulation.

KEYWORDS cellular transcription factors, latent phase, HIV-1 transcription, elongation.

ABBREVIATIONS HIV-1 – human immunodeficiency virus type I; AIDS – acquired immune deficiency syndrome; TAR – trans-activation response element; Tat – trans-activator of transcription; HMGA1 – high-mobility group protein A1; DNA-RK – DNA-dependent protein kinase; DNA-PKcs – DNA-PK catalytic subunit; LTR – long terminal repeat; RNAP II – DNA-dependent RNA polymerase II; CTD RNAP II – C-terminal domain of RNAP II; P-TEFb – positive transcription elongation factor b; HTLV-1 – human T-lymphotropic virus; MMTV – mouse mammary tumor virus; NRE-1 – negative regulatory element 1; TF – transcription factor.

INTRODUCTION

Although the human immunodeficiency virus (HIV-1) was discovered over 30 years ago, the fight against the HIV infection still has not been won. Highly active antiretroviral therapy that is used to manage the HIV infection has significantly reduced mortality among patients with AIDS; however, interruption of treatment inevitably results in viral reproduction and increases the viral titer. One of the reasons for this phenomenon is the presence of cells in the human organism with the transcriptionally silent provirus integrated in their genome. The silent state, which is typical for the latent phase of the viral infection, is characterized by the absence of full-fledged transcription from the viral promoter. How-

ever, without treatment, the silent provirus can be activated and cause the development of AIDS [1].

The hairpin structure located at the 5'-end of the synthesized mRNA and known as TAR (trans-activation response) plays a key role in active transcription from the HIV-1 promoter. Elongation of transcription of the integrated viral genome takes place only when TAR is bound by the viral regulatory protein Tat (trans-activator of transcription) [2]. Formation of the TAR-Tat complex ensures phosphorylation of RNA polymerase II that is required for the elimination of transcription block and transition into the elongation stage [3]. However, Tat protein is not detected in the latently infected cells; hence, the mechanism of tran-

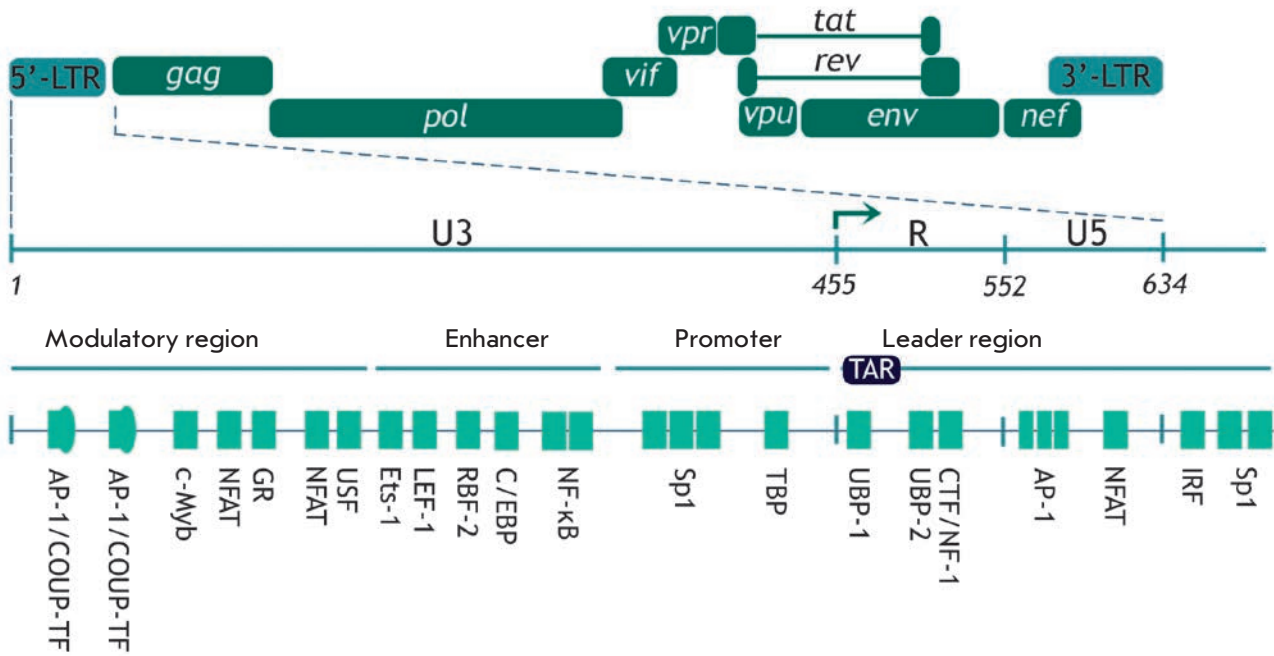


Fig. 1. Binding sites of transcription factors in HIV-1 5'-LTR. Schematic representation of HIV-1 provirus and the major binding sites of transcription factors. Positions of the 5'-LTR regions are specified: U3 (nucleotides 1–455), R (456–552), and U5 (553–634). The transcription initiation site is shown with an arrow and corresponds to the border between the U3 and R regions [13].

scription activation of the silent integrated provirus upon transition from the latent into the lytic phase of the HIV-1 life cycle remains unclear. This is highly relevant to study the proteins partaking in the activation of transcription from the HIV-1 promoter via the Tat-independent mechanism, since in the long run it could allow one to understand the mechanism of transition of the virus from the latent to the lytic phase and to develop approaches to regulate this process.

It has recently been shown that cellular protein HMGA1 can be recruited in the regulation of transcription from HIV-1 promoter during the latent phase (basal transcription) [4, 5]. DNA-binding protein Ku, a component of DNA-dependent protein kinase (DNA-PK), can also be involved in transcription regulation [6–10]. In this review, we summarize the data on the effect of the Ku and HMGA1 proteins on HIV-1 transcription and present the putative schemes for a possible involvement of these proteins in the regulation of transcription.

REGULATION OF TRANSCRIPTION FROM THE HIV-1 PROMOTER

Human immunodeficiency virus type I is a member of the genus Lentivirus, part of the family Retroviridae. It affects the human immune system and causes the acquired immune deficiency syndrome (AIDS). Like

the genome of other lentiviruses, the HIV-1 genome is an RNA molecule, which serves as a template for the synthesis of a DNA copy by viral enzyme reverse transcriptase. The DNA copy is then integrated into the cellular genome forming proviral DNA. However, most of the viral DNA remains non-integrated [11]. This DNA mainly exists in the circular form. Transcription can be carried out from the circular viral DNA, but it is the integrated provirus that serves as the main template for synthesizing viral proteins [12].

Being integrated into the chromosome of an infected cell, viral DNA can either stay silent or be actively transcribed. In other words, the transcription level can be low thus resulting in a small number of transcripts without rapid progression of the infection and is generally referred to as basal (not activated) transcription. Alternatively, transcription can be active and yield a large amount of RNA and new viral particles. Regulation of the HIV-1 genome transcription, which precludes the fate of the provirus, depends on a large number of factors: cis-acting elements of viral DNA, cellular transcription factors, viral trans-activator Tat, and the degree of chromatin condensation.

Viral DNA integrated into the cellular genome carries long terminal repeats (LTRs) at its ends. Each of them consists of U3, R, and U5 regions (*Fig. 1*). Transcription starts at the border between the U3 and R re-

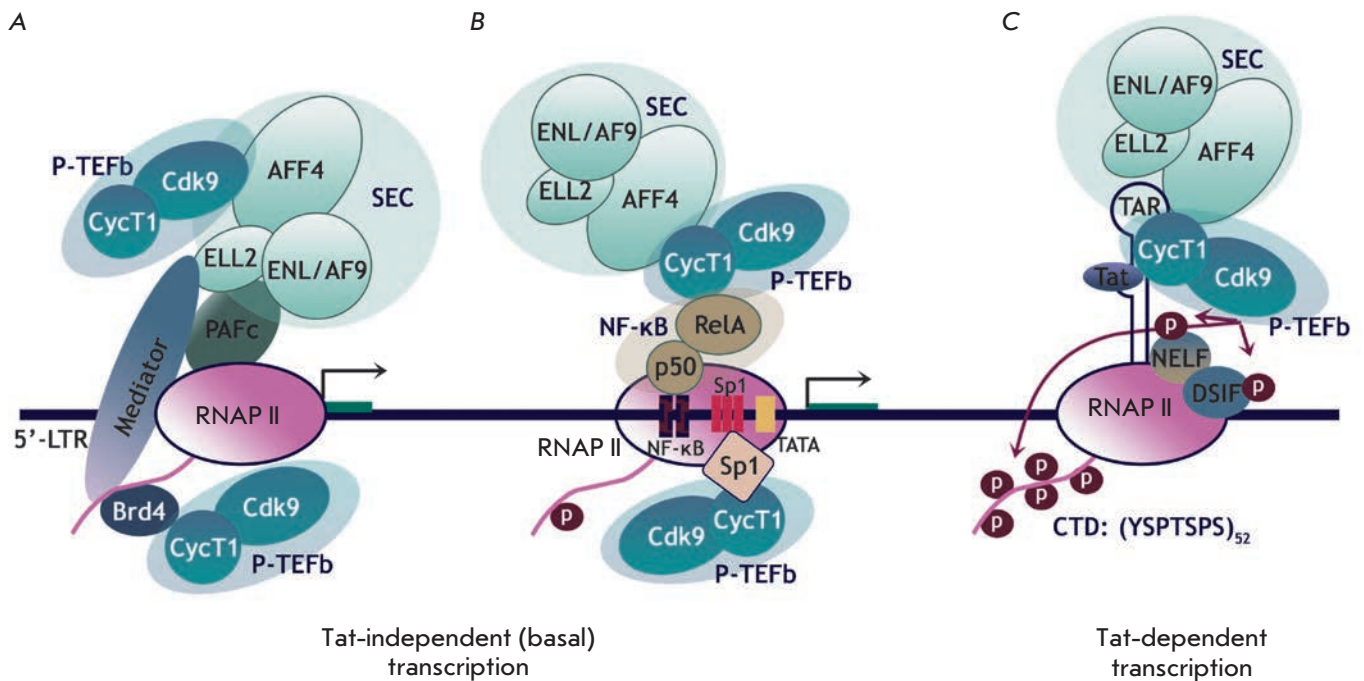


Fig. 2. Possible mechanisms for recruitment of P-TEFb to the HIV-1 promoter. *A, B* – Tat-independent transcription when P-TEFb stimulates basal transcription from the HIV-1 promoter in the absence of Tat. P-TEFb can be recruited by cellular proteins Brd4, SEC (*A*) or NF-κB, Sp1 (*B*). *C* – Tat-dependent transcription. Tat is bound to TAR RNA, thus facilitating the release of P-TEFb from 7SK snRNP and its recruitment to the paused elongation complex [14].

gions in the 5'-LTR, since the viral promoter recognized by RNA polymerase II (RNAP II) and some other regulatory elements are located in the U3 region. 5'-LTR contains four functional regions partaking in the regulation of the HIV-1 genome transcription: the modulatory region, the enhancer, the promoter, and the leader regions (*Fig. 1*) [13]. They contain many binding sites for the cellular transcription factors, including the ones that play a crucial role in the transcriptional regulation: NF-κB, NFAT, Sp1, and AP-1 (*Fig. 1*). These factors are involved in the initiation of transcription [1, 13].

Transition of the provirus from a silent to an active state starts with the transcription initiation. Short abortive transcripts ~60–80 nucleotides long are synthesized [14]; they form a stable hairpin called TAR at the 5'-end. Just after the TAR RNA synthesis RNAP II stops, since it is associated with the factors that repress elongation: NELF (negative elongation factor) and DSIF (5,6-dichloro-1-β-D-ribofuranosylbenzimidazole sensitivity-inducing factor) [15]. To continue transcription and proceed to the active elongation stage, the C-terminal domain (CTD) of RNAP II needs to be hyperphosphorylated at Ser2 residues in heptapeptide repeats YSPTSPS. Hyperphosphorylation is ensured by the transcription elongation factor P-TEFb (positive transcription elongation factor b), which consists of cy-

clin-dependent kinase 9 (Cdk9) and cyclin T1 (CycT1). The level of accessible P-TEFb is regulated by its binding to 7SK small nuclear ribonucleoprotein (7SK snRNP), which inhibits the kinase activity of the P-TEFb factor and impedes transcription elongation [16].

The viral protein Tat is the key regulator at the elongation stage: it enhances efficiency of RNA synthesis by several orders of magnitude [2]. Binding of Tat to the synthesized TAR RNA facilitates dissociation of P-TEFb from the complex with 7SK snRNP and recruits it to the viral promoter. As a result, P-TEFb ensures hyperphosphorylation of RNAP II, as well as the NELF and DSIF factors [17]. Phosphorylation of DSIF converts it to the activating elongation factor, while phosphorylated NELF dissociates from the transcription complex, thus allowing RNAP II to perform effective elongation and synthesize full-size mRNA (*Fig. 2*) [3].

However, Tat is not detected in cells at the latent stage of infection. Neither is it found when the provirus starts exiting from dormancy. In some cases, the TAR-Tat-P-TEFb complex cannot be formed due to mutations disrupting the interplay between its components [18]. Nevertheless, transcription from the HIV-1 promoter may still occur. Several mechanisms of Tat-independent activation of transcription are known. First, it has been assumed that P-TEFb can perform phosphor-

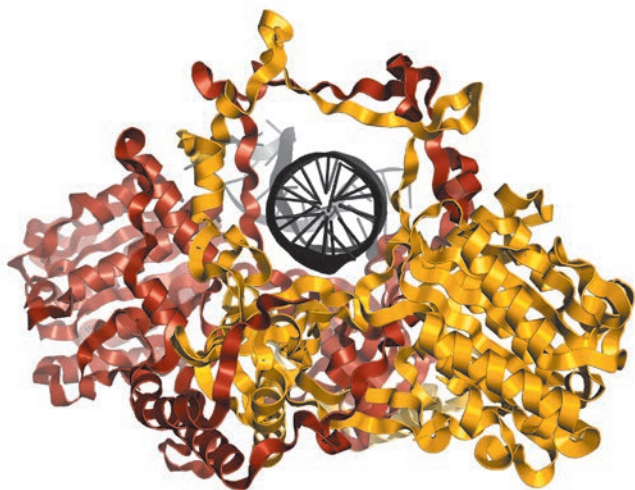


Fig. 3. Structure of the Ku heterodimer in a complex with DNA according to [26]. DNA (shown in black) resides in the channel formed by Ku70 (shown in yellow) and Ku80 (shown in brown). PDBID 1JEY

ylation of the CTD RNAP II required for transcription elongation in the absence of Tat [19]. Some cellular factors (Sp1 [20], SEC [14], Brd4 [21, 22], and NF- κ B [14]) probably participate in the recruitment of P-TEFb to the viral promoter (*Fig. 2A,B*). Alternatively, a cellular protein different from P-TEFb but capable of the phosphorylation of CTD RNAP II (as well as the NELF and DSIF repressive factors) may bind to the HIV-1 promoter.

Although a significant amount of data on the regulation of HIV-1 transcription and involvement of various cellular factors in it has been accumulated, many aspects have not been completely elucidated yet. In particular, the role of two cellular proteins involved in HIV-1 transcription (Ku and HMG1) remains unclear. Some available data attest to the positive role of these proteins in the regulation of transcription, while other studies demonstrate that their role is negative. Nevertheless, the accurate mechanisms of involvement of these proteins in HIV-1 transcription are still to be determined.

ROLE OF KU PROTEIN IN HIV-1 TRANSCRIPTION

Human Ku protein is a heterodimer consisting of two subunits with masses of ~70 and 80 kDa, which are known as Ku70 (p70) and Ku80 (Ku86, p80). These proteins are encoded by the *xrcc6* (Ku70) and *xrcc5* (Ku80) genes. Ku protein mainly functions in the cell in the form of a very stable heterodimer [23]. However, some research demonstrates that isolated Ku70 and Ku80 subunits can be involved in certain processes [24].

The Ku70/Ku80 heterodimer is a DNA-binding protein that mostly interacts with the free ends of double-stranded DNA, and its biological function is mainly related to this feature. The interaction between the Ku heterodimer and DNA is rather strong: the K_d value varies within a range of $1.5\text{--}4.0 \times 10^{-10}$ M [25]. According to X-ray data [26], Ku70 and Ku80 within a heterodimer form an asymmetric ring with a wide base and a thin bridge; the resulting channel is big enough to encircle DNA (*Fig. 3*). The channel predominantly consists of positively charged amino acid residues that interact with the negatively charged sugar-phosphate backbone of the DNA molecule, which explains why Ku can bind DNA in a sequence-independent manner. After binding to the DNA end, Ku can migrate (slide) along DNA and pause at certain sequences [25, 27].

The most well-known and the best studied biological function of Ku is its involvement in double-strand DNA break repair by nonhomologous end joining (NHEJ). Ku also participates in such cellular processes as V(D)J-recombination, mobile element-induced genomic rearrangement, telomere length maintenance, apoptosis, and transcription [28, 29]. One key function of Ku is binding to the DNA-PKcs catalytic subunit to form DNA-dependent protein kinase DNA-PK. It is worth mentioning that the catalytic function of DNA-PK is activated after its binding to DNA, which is provided by the Ku heterodimer [25].

The possible mechanisms of Ku-mediated regulation of transcription

Participation in transcriptional regulation is one of the numerous functions of Ku. Several mechanisms of transcriptional activation or suppression by Ku have been described. The first mechanism is a direct sequence-specific interaction between Ku and the promoter region of genes. It has been hypothesized that transcription of the cellular genes *c-Myc*, *Hsp70* [30], U1 snRNA [31], as well as retroviruses HTLV-1 (human T-lymphotropic virus) [32] and MMTV (mouse mammary tumor virus) [33], is regulated via this mechanism. The mechanism of Ku binding to the promoter region that does not involve interactions with DNA ends is yet unclear; however, there is data attesting to a possible sequence-specific interaction between the heterodimer and a certain Ku-binding motif in DNA [34].

A sequence whose binding to Ku is considered to be truly sequence-specific and more preferable compared to Ku binding to DNA ends has been identified in the NRE-1 region (negative regulatory element 1) in the LTR of MMTV retrovirus (*Fig. 4*) [34]. The interaction between Ku and this sequence reduces the efficiency of transcription from viral LTR. The catalytic subunit DNA-PKcs is believed to be involved in this regulation

-396	-	CTGAGAAAGAGAAAGACGACA	-	-376	GR MMTV LTR
-396	-	CTcAagAAGaaAAAGACGACA	-	-376	C3H MMTV LTR
-292	-	tacAGAAAGgGAAAGgggacta	-	-268	c-myc PRE
292	-	gaatGAAAGgGAAAGggGtgG	-	269	U5 HTLV LTR

Fig. 4. Putative Ku-binding sites in gene promoters. Ku-binding sites homologous to the NRE-1 sequence in the LTR of the GR strain of MMTV. Direct repeat is shown in color. Mismatches are denoted by lowercase letters [34].

[33, 35]. It has been demonstrated that GR (glucocorticoid receptor) [34] and Oct-1 [36], the two transcription factors binding to 5'-LTR MMTV and activating its transcription, can be *in vitro* phosphorylated by DNA-PK. Specific recruitment of DNA-PK to the promoter and subsequent phosphorylation of transcription factors is probably one of the transcriptional regulatory mechanisms.

All the Ku-binding sites in promoters homologous to the NRE-1 sequence in the promoter of the GR strain of MMTV and known up to the publication date are reported in [34] (Fig. 4). Only these sequences were shown to be capable of direct and specific interaction with the Ku heterodimer in the absence of free DNA ends.

The *second mechanism* via which Ku affects the transcription is its direct interaction with transcription factors, including Oct-1, Oct-2 [36], NF45/NF90 [37], AP-1 [38], E2F-1 [39], YY1 [40], and p53 [41]. Some of these factors are involved in the regulation of HIV-1 transcription. In addition, as mentioned above, some transcription factors can act as a DNA-PK substrate *in vitro*. The ability of DNA-PK to interact both with transcription factors and a number of nuclear receptors (AR [42], GR [34], PR [43], and ER- α [44]) probably suggests that there is a shared mechanism via which Ku participates in cell signaling and transcription regulation.

Ku can indirectly regulate gene transcription by influencing the expression of other transcription factors. Thus, in the AGS cell line, Ku positively regulates the expression of the gene of the NF- κ B p50 subunit [45]. Ku80 also stimulates the expression of the *c-jun* gene, the AP-1 transcription factor component [38]. It should be mentioned that NF- κ B and AP-1 are the key regulators of the transcription of HIV-1 genes.

The Ku70 and Ku80 subunits may have a different effect on transcription. It has been demonstrated that the subunits of the Ku heterodimer dynamically bind to the promoter of the interleukin 2 (IL-2) gene and interact with the NF45/NF90 factor in response to T-cell activation [37]. This activation increases the amount of the Ku80/NF90 complex bound to the antigen receptor

response element (ARRE) sequence in the *IL-2* gene promoter, while the amount of the Ku70 subunit bound to this region decreases [37]. In another work [30], the repressive role of Ku in the transcription of the *Hsp70* gene was attributed to the Ku70 subunit rather than to Ku80.

The *third mechanism* of transcriptional regulation is the direct interaction between Ku heterodimer or its Ku80 subunit and RNAP II holoenzyme. Ku80 was found to be colocalized with the elongational form of RNAP II and transcription factors specific for the elongation stage (in particular, DSIF) in the nucleus. The C-terminal domain of Ku80 was also found to play a key role in the interplay with these proteins [48]. Let us mention that DNA-PK can phosphorylate RNAP II *in vitro* [49]; however, the role of this phosphorylation in transcriptional regulation still needs to be ascertained.

The *fourth mechanism* of Ku involvement in transcriptional regulation is related to its role in the repair of double-strand DNA breaks [50]. Double-strand breaks need to be introduced by DNA topoisomerase II β to successfully initiate transcription from a number of promoters regulated by binding to AP-1 and nuclear receptors (including those interacting with Ku). In this case, the break repair and local alterations in the chromatin structure occur in the presence of the complex of the proteins PARP-1 (poly[adenosinediphosphate (ADP)-ribose]polymerase-1), DNA-PKcs, and Ku70/Ku80.

Hence, the isolated heterodimer subunits, the heterodimer as a whole, or its complex with the DNA-PKcs catalytic subunit can be involved in the regulation of transcription. No common mechanism of action of Ku has been revealed. It is most likely that there is a specific mechanism of Ku-dependent regulation for each particular gene. It should be mentioned once again that Ku may act both as an activator and as a suppressor; its effect usually depends on subunits, which are involved in the regulation. It seems that the catalytic subunit of DNA-PK is not necessarily involved in the Ku-dependent regulation of transcription; however, in certain cases its capability of DNA-dependent phosphorylation of transcription factors and RNAP II can be the key element of regulation.

Role of Ku in HIV-1 transcription

The significance of Ku for maintaining the HIV-1 life cycle has been demonstrated in numerous studies. The Ku70 subunit is a part of the pre-integration complex and interacts with HIV-1 integrase [51, 52]. The Ku80 subunit was detected within the virion [53], where it can be incorporated at the stage when a new viral particle is formed in a previously infected cell. Repair of single-strand breaks formed when viral DNA is integrated

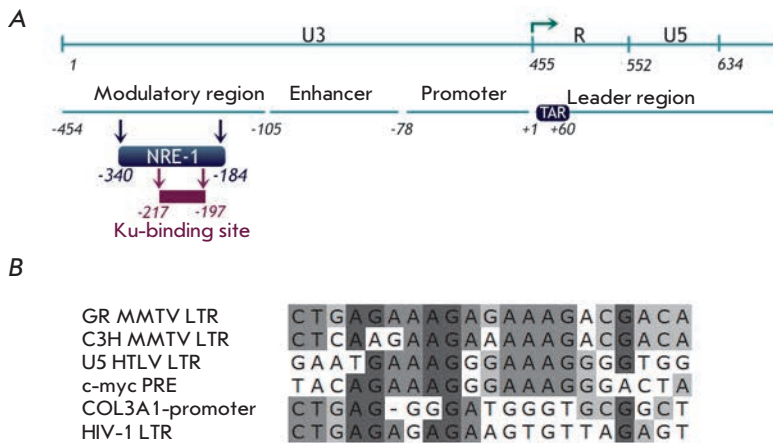


Fig. 5. Scheme of the HIV-1 genome and position of the Ku-binding site in 5'-LTR. A – positions of the 5'-LTR regions are specified: U3 (nucleotides 1–455), R (456–552), and U5 (553–638) (counting from the beginning of the genome). The major regulatory regions of 5'-LTR are shown. +1 – counting from the transcription initiation site denoted by an arrow. The Ku-binding site predicted in [6] is shown. B – alignment between the putative Ku-binding sites in the NRE-1 region of HIV-1 and MMTV, as well as some other sequences similar to MMTV NRE-1 [6].

into the cellular genome is required for successful integration of viral cDNA into the host cell genome. It is believed that proteins from the NHEJ system, and the Ku70/Ku80 heterodimer in particular, can be involved in this process [54]. Thus, lentiviral vector transduction efficiency is significantly decreased in cells defective in Ku80, DNA-PKcs, Xrcc4 (X-ray repair cross-complementing protein 4), and DNA ligase IV [55, 56]. Ku is also involved in the formation of the circular form of viral DNA from non-integrated linear DNA [57–59].

Involvement of Ku in the transcriptional regulation of HIV-1 was first reported in the early 2000s. However, the role of Ku in this regulation is still to be clarified. Data attesting both to the positive and negative effects of Ku on transcription of the HIV-1 genome have been obtained.

The role of Ku in transcription from viral 5'-LTR was first studied using the xrs-6 cell line, a variant of CHO-K1 (Chinese hamster ovary) cells lacking *Ku80* gene expression. These cells supported enhanced expression from the plasmid carrying the *CAT* (chloroamphenicol acetyltransferase) gene under the control of the viral promoter from 5'-LTR [6]. Stable transfection of xrs-6 cells with the vector carrying the human *Ku80* gene reduced *CAT* expression. Hence, Ku80 has a negative effect on transcription from the HIV-1 5'-LTR promoter. The negative role of Ku80 has been confirmed using a human U1 cell line whose genome contained the integrated provirus; this cell line is used as a model of the latent state of HIV-1. It turned out that a decreased amount of endogenous Ku80 in the cells increases the level of transcription of the HIV-1 genes, both for basal and TNF α -induced transcription.

Taking into account that Ku has a negative effect on transcription from other retroviral promoters (MMTV, HTLV-1) [32, 33], L. Jeanson and J.F. Mouscadet [6] searched for the Ku-binding site in the HIV-1 LTR and

detected a motif (-217/-197) in the NRE-1 region that was rather similar to the Ku-binding site in MMTV NRE-1 (Fig. 5) [6]. Several variants of Ku-mediated repression of HIV-1 transcription were proposed. Considering the fact that Ku can bind to the Oct-1 and Oct-2 transcription factors [36], which repress both the basal and Tat-activated transcription of HIV-1, it was hypothesized that binding of Ku in the modulatory region (Fig. 5A) facilitates recruitment of these factors to the HIV-1 promoter [6]. It is also possible that Ku can be involved in the regulation of the chromatin structure. NRE-1 contains a nuclear matrix binding site [60] overlapping with the predicted Ku-binding site. The interplay between Ku and the nuclear matrix in this region presumably impedes NF- κ B-activated transcription.

In their next study [7], this group of authors reported that Ku80 negatively influences transcription from retroviral vectors. It turned out that regardless of the promoter used in the lentiviral system, transcription was more active in the absence of Ku80. In other words, the effect of Ku80 on retroviral vector expression was found to be not sequence-specific; hence, the Ku-binding site suggested in [6] could not completely explain the mechanism of negative transcriptional regulation. It has also been reported that Ku80 has no effect on the efficiency of transduction and integration of lentiviral vectors. Meanwhile, no Ku-dependent regulation was observed when plasmid vectors carrying the same promoters were used as a template instead of the pseudotyped virus [7]. Ku80 is believed to guide integration of lentiviral vectors into transcriptionally inactive regions instead of directly influencing transcription.

As opposed to the aforementioned findings, Ku plays a positive role in the regulation of transcription from the HIV-1 promoter in human MAGI and CEM-T4 cell lines [8]. Furthermore, insertion of siRNAs targeting Ku80 reduced the efficiency of integration of the viral

genome into the infected cell DNA and disrupted Tat-TAR trans-activation.

The positive influence of the Ku heterodimer on transcription of the HIV-1 genome was also mentioned in [9], where wild-type HCT 116 human cells and their *Ku80*^{+/-} variant, which were transduced with HIV-1-based lentiviral vectors, were used. It has been preliminarily shown that in the HCT 116 *Ku80*^{+/-} cells with a twofold reduced level of Ku80 the level of Ku70 is equally lowered. It turned out that a twofold decrease in the amount of endogenous Ku in cells reduces the efficiency of viral transcription. It should be mentioned that, as opposed to data [7], this effect was specific for viral LTR, since changes in the Ku heterodimer level had no effect on transcription from other promoters. Moreover, viral proteins were not involved in Ku-mediated transcriptional regulation and the influence of Ku was independent of Tat-trans-activation. The effect of Ku on transcription was also noticeable in the presence of Tat; however, its effect was most significant at the basal level of transcription from the nonactivated provirus, when Tat is not detected in the cell. Interestingly, Ku influences the basal HIV-1 transcription only at the initial stage after integration of the viral genome and reduction of the Ku level in cells contributes to the emergence and maintenance of viral latency.

It is known that Ku80 is incorporated into the virion during its assembly [53]. Hence, both endogenous Ku80 and Ku80 from the virion can influence provirus transcription in the infected cell. In order to eliminate the effect of the latter, the lentivirus was harvested in the cell line with a decreased level of Ku heterodimer [9]. It turned out that it is endogenous Ku that affects transcription in the target cell.

It should be mentioned that the involvement of the previously predicted Ku-binding site in HIV-1 LTR in Ku-mediated regulation of the provirus transcription was also refuted in [9]. Replacement of this site with a random sequence had no effect on Ku-dependent transcriptional regulation.

Another important aspect of this study is that Ku does not affect transcription from the circular forms of viral DNA. Taking into account that, according to [7], Ku had no effect on transcription from the HIV-1 promoter within a plasmid vector, it can be concluded that Ku stimulates transcription only from the provirus integrated into the genome.

We would like to draw special attention to study [10] by S. Tyagi *et al.* who investigated the possible involvement of both the Ku70/Ku80 and the entire DNA-dependent protein kinase DNA-PK in the transcriptional regulation of HIV-1. Experiments were carried out using Jurkat-E4 cells whose DNA carried the integrated HIV-1 genome. Thus, this cell line was used as a model

of T cells in the latency period of infection. DNA-PK was found on the HIV-1 promoter, and its location correlates with that of RNAP II. It was also determined that transcription activation significantly increases the DNA-PK and RNAP II levels not only on the promoter, but also on the transcribed region of the genome.

It has also been demonstrated [10] that DNA-PK can phosphorylate the C-terminal domain of RNAP II. Furthermore, *in vitro* experiments showed that DNA-PK predominantly phosphorylates Ser2 rather than Ser5 or Ser7 in the heptapeptide repeats YSPTSPS. Considering the fact that phosphorylation of Ser2 is required to activate elongation, it has been hypothesized that involvement of DNA-PK can be important, mostly at the elongation phase of transcription. DNA-PK presumably directly interacts with RNAP II at the HIV-1 promoter, and DNA-PK can act as a factor phosphorylating polymerase and eliminating elongation block. At any rate, parallel distribution of DNA-PK and RNAP II along the provirus and their simultaneous recruitment in response to transcription activation allow one to suggest that DNA-PK (and Ku as its component) is an element of a large transcriptional complex that is involved in HIV-1 gene expression.

Furthermore, it has been demonstrated that DNA-PK has a positive effect on transcription from HIV-1 5'-LTR and lentiviral vectors [10]. Knockdown of the catalytic subunit DNA-PKcs in Jurkat cells significantly reduces expression of LTR-regulated genes and has a minor effect on expression from another promoter (CMV). Hence, knockdown of both DNA-PKcs [10] and Ku80 [9] reduces the level of transcription from the LTR promoter.

Summarizing the role of the Ku protein in the regulation of HIV-1 transcription, it should be mentioned that the currently available data are rather controversial. The possible reason is that different cell lines and different viral systems were used. Thus, most data attesting to negative regulation have been obtained using rodent cells, which obviously cannot be an adequate model for processes occurring in HIV-1-infected human cells. Nevertheless, the data obtained using human cells provide ground for drawing some reliable conclusions.

The first general conclusion is that Ku-mediated regulation of transcription depends on viral LTR. The regulation mechanism remains unclear, but one should not rule out the possibility of direct binding of the heterodimer to LTR, although the putative Ku-binding site within LTR probably is not the key element in Ku-dependent regulation of HIV-1 transcription, as opposed to MMTV and HTLV-1.

Second, the integrated provirus is crucial for Ku-mediated transcriptional regulation of HIV-1 and HIV-

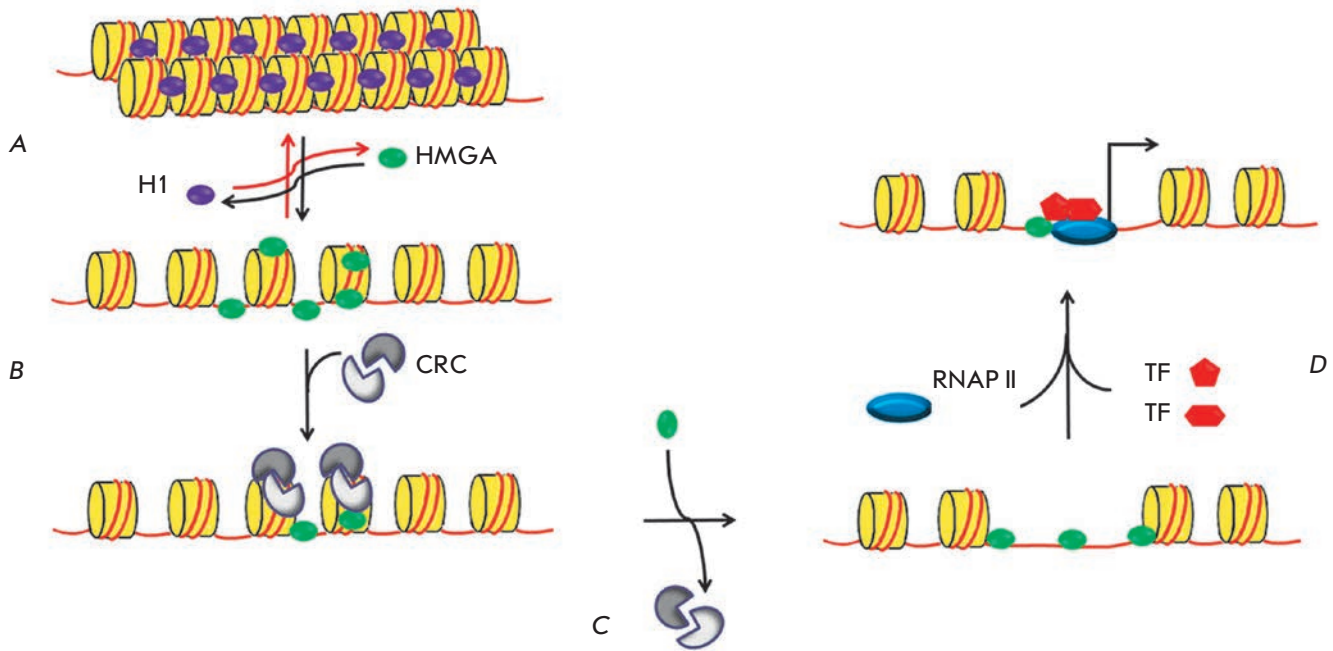


Fig. 6. The putative model of HMGA1-mediated activation of transcription. The putative mechanism of transcriptional regulation by HMGA1: HMGA1 promotes chromatin reorganization by exposing DNA sites for transcription initiation factors. *A* – HMGA1 competes with histone H1 by replacing it. *B* – chromatin decompaction using chromatin-remodeling complexes (CRCs). Binding of CRC to chromatin increases when it interacts with HMGA1. *C* – release of DNA for binding to transcription factors. *D* – initiation of transcription: HMGA1 can interact with transcription factors (TFs) by recruiting them to the promoter [62].

1-based lentiviral vectors. Although HIV-1 transcription can occur from circular DNA, it is clear that Ku is not involved in its regulation. This can be explained by the fact that the heterodimer is recruited to the provirus either during integration or immediately after it.

Let us mention once again that there remain many questions concerning the mechanism of involvement of Ku in the transcriptional regulation of HIV-1. Even if the incorporation of the Ku70/Ku80 heterodimer or the entire DNA-PK into the transcription complex is considered to be an established fact, the mechanism through which they influence HIV-1 gene expression has not been elucidated yet and it is important to clarify their role in HIV-1 transcription.

Role of HMGA1 in HIV-1 transcription

HMGA1 (high-mobility group protein A1, previously known as HMG I[Y]), the DNA-binding non-histone chromatin protein, is another cellular protein whose role in the HIV-1 life cycle has not been studied sufficiently. HMGA1 carries three DNA-binding motifs that preferentially bind to the DNA minor groove in AT-rich regions (A/T hook) [61]. However, HMGA1 is more likely to recognize the spatial structure of DNA than the nucleotide sequence: it prefers to interact with bent

and supercoiled DNA, with DNA that has a structure different from the classical B-form. The free protein has an unordered spatial structure. When interacting with DNA, it undergoes conformational changes, thus facilitating ATP-independent DNA unwinding, supercoiling, and bending [62, 63]. This ability to change the chromatin structure determines the broad range of functions performed by HMGA1 in the cell nucleus.

Actually, all the high-mobility group proteins are capable of binding both DNA and proteins, which allows them to get involved in a large number of processes [64]. Alteration in the chromatin structure induced by HMGA binding either stimulates or represses such DNA-dependent processes as transcription, replication, and DNA-repair. HMGA1 is considered to be an architectural transcription factor, and this emphasizes its role in the organization of multiprotein complexes bound to the promoter [62–64]. The ability of HMGA1 to interact with core histones and displace the linker histone H1 from DNA results in chromatin reorganization and exposure of transcription factor binding sites (Fig. 6). HMGA1 plays a crucial role in the regulation of enhanceosome assembly or disassembly, thus affecting transcription. It has been repeatedly demonstrated that HMGA1 directly interacts with other chromatin-re-

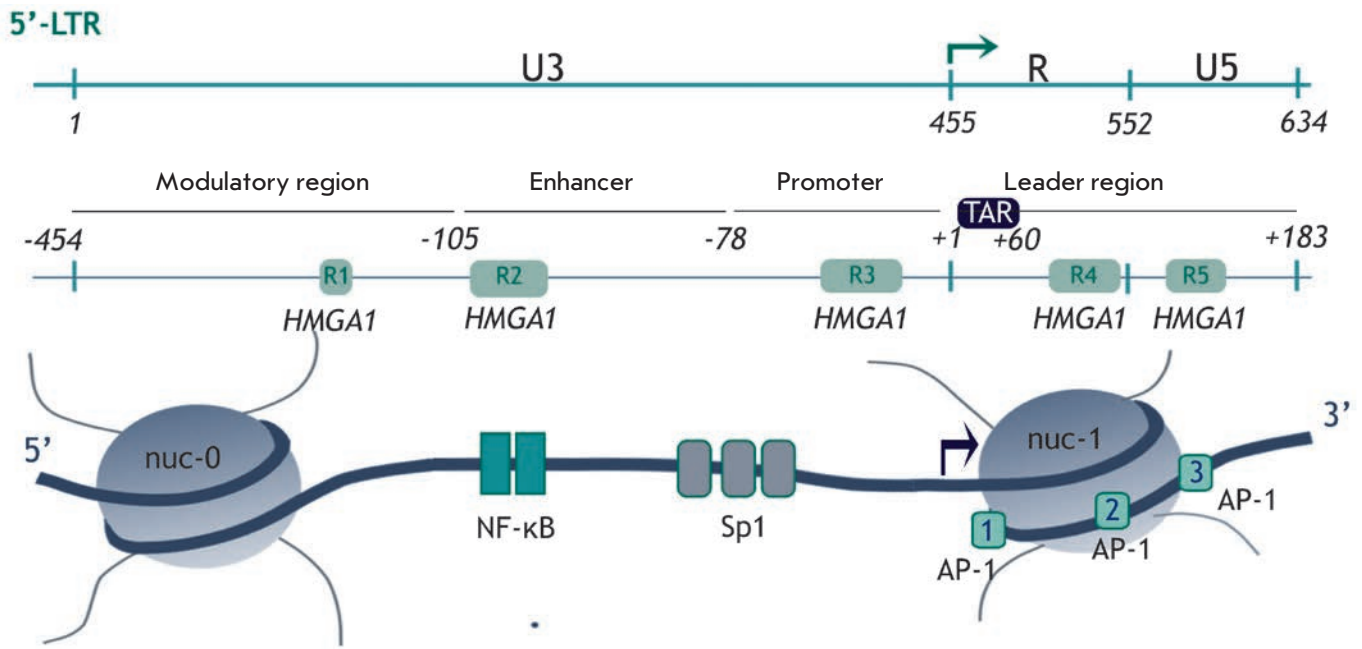


Fig. 7. Positions of the predicted HMGA1 binding sites at HIV-1 5'-LTR. Positions of the 5'-LTR regions are specified: U3 (nucleotides 1–455), R (456–552), and U5 (553–634). Nucleotides are counted from the beginning of the genome. The major regulatory regions of 5'-LTR are shown. +1 – counting from the transcription initiation site denoted by an arrow. HMGA1 binding sites determined in [69] are shown. The positions of nucleosomes on the HIV-1 promoter are shown below; three sites of binding to the AP-1 transcription factor are specified.

modeling proteins and transcription factors (Sp1, TFIID, NF-κB, ATF-2, SRF, Oct2, and c-Rel) [62, 63]. The ability of HMGA1 to bend DNA upon binding probably facilitates spatial proximity of the enhancer and promoter regions of the genes.

Involvement of HMGA1 in the life cycle of HIV-1 has been demonstrated in many studies. This protein was detected within the pre-integration complex [65]. HMGA1 was found to stimulate the integration of HIV-1 DNA into the cellular genome [66, 67]. It is assumed that HMGA1 binds to and bends viral DNA, pulling the ends together and facilitating their binding to integrase. Meanwhile, no direct interaction between HMGA1 and HIV-1 integrase has been observed. However, other authors have been critical of the idea that HMGA1 is involved in retroviral integration, since the absence of HMGA1 in infected cells had no effect on the integration of the viral genome [68].

Some rather ambiguous evidence in support of the involvement of HMGA1 in HIV-1 transcription has been obtained to date.

Putative HMGA1 binding sites have been detected by DNase I footprinting in the -187/+230 region within HIV-1 LTR (R1–R5 in Fig. 7) [69]. The interplay between HMGA1 and the transcription factor AP-1 has also been studied: they were found to share a binding

site (R5 in Fig. 7). This site resides at the border of the repressive nucleosome nuc-1, which exists in the provirus near the transcription initiation site in the latent phase and degrades after transcription of the viral genome is activated (Fig. 7). HMGA1 was found to facilitate binding of AP-1, an important inducible HIV-1 transcription activator, to viral DNA in response to external stimuli activating viral expression. HMGA1 is possibly involved in the reorganization of nuc-1 by competing for this site and making it free for AP-1. Hence, it has been suggested that HMGA1 can positively regulate HIV-1 transcription [69].

The role of HMGA1 as an architectural transcription factor involved in the reorganization of nucleosome nuc-1 has been confirmed [70]. HMGA1 was found to facilitate binding of the ATF-3 subunit of the transcription factor AP-1 to site R3 at the border of nuc-1 in response to induction of viral transcription by PMA (phorbol myristate acetate – NF-κB activator) (Fig. 7). This makes it possible to recruit the ATP-dependent chromatin-remodeling complex SWI/SNF to the repressive nucleosome: a process required for efficient activation of viral transcription.

Another possible mechanism via which HMGA1 can be involved in transcription regulation has recently been proposed [71]. It turns out that HMGA1 binds

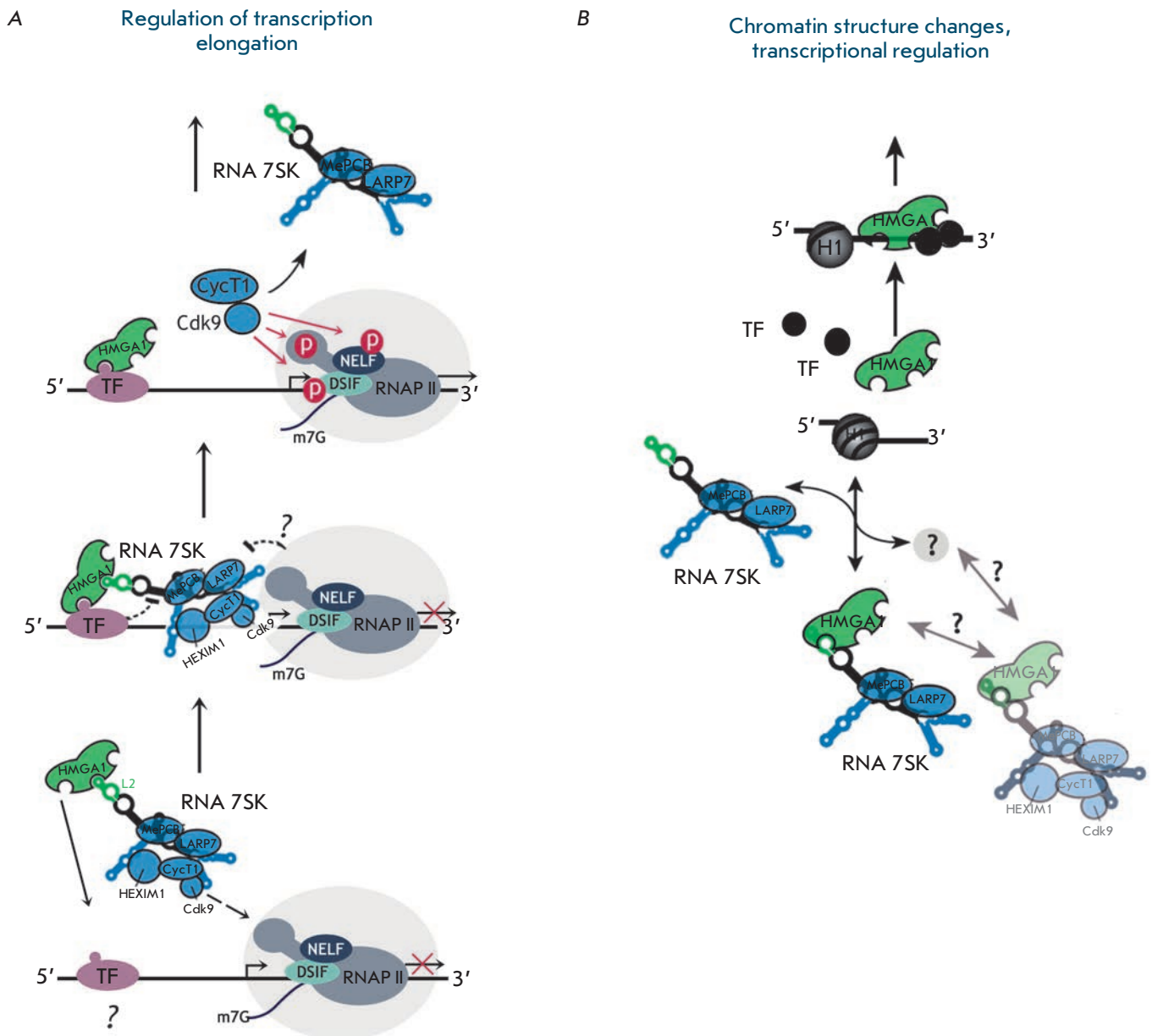


Fig. 8. Mechanism of transcriptional regulation by the HMGA1–7SK–P-TEFb complex. **A** – HMGA1 can recruit P-TEFb/7SK snRNP complex to the paused transcription complex by interacting with DNA or a certain transcription factor. **B** – the level of free HMGA1 in the nucleus is regulated by its binding to 7SK snRNP. Dissociation of HMGA1 from its complex with 7SK snRNP can be caused by a factor that has not been identified yet [4, 72].

to loop 2 of RNA in 7SK snRNP (7SK L2 RNA). As mentioned above, the key function of 7SK RNA is to regulate the level of the free P-TEFb factor activating transcription elongation [17]. This factor interacts with loop 1 and the HEXIM1 protein within 7SK snRNP. As a result, the HMGA1 complex with 7SK snRNP and P-TEFb can be formed. The role of this complex in transcription regulation can be a dual one (Fig. 8) [72].

First, HMGA1 can bind directly to DNA or a transcription factor located on the promoter region and recruit P-TEFb to the paused RNAP II elongation complex (Fig. 8A). Secondly, binding of 7SK to HMGA1 regulates the amount of free HMGA1 that can interact with DNA and functions in various processes (Fig. 8B). The mechanism is believed to depend on the nature of the particular gene.

In the case of HIV-1 transcription regulation, Sp1 can be a factor that interacts with HMGA1 and, thus, is recruited to the elongation complex. On one hand, this factor is known to be involved in HIV-1 transcription [1, 13], while on the other hand it directly interacts with HMGA1 [62]. Hence, upon transcription from HIV-1 LTR, HMGA1 may be involved in P-TEFb-dependent activation of elongation via the scheme shown in *Fig. 8A* [72] and, therefore, have a stimulating effect.

Another mechanism via which HMGA1 influences HIV-1 transcription was uncovered while studying the expression of a reporter gene under the control of viral 5'-LTR from a plasmid [4]. In this case, HMGA1 had a repressive effect. A detailed study of the mechanism of HMGA1 action has shown that it can bind to TAR RNA due to the similarity between its structure and 7SK L2 RNA (*Fig. 9*); HMGA1 may compete with viral protein Tat for binding to TAR RNA. This results in a negative effect of HMGA1 on HIV-1 transcription both in the presence and absence of Tat. The influence of overexpression and knockdown of the *HMGA1* gene and 7SK L2 RNA on transcription from the HIV-1 promoter was studied in the presence and absence of Tat. HMGA1 was found to reduce both the basal and Tat-activated transcription from the HIV-1 promoter, which is partially recovered upon 7SK L2 RNA overexpression. Based on this experiment, the model of HMGA1-mediated repression has been proposed (*Fig. 10*) [4]. According to this model, HMGA1 impedes binding of TAR RNA with Tat, or, in the absence of Tat, with a cellular cofactor of viral transcription that has not been described yet. 7SK L2 RNA competes with TAR for HMGA1, destroys their complex, and takes away the HMGA1 protein from the HIV-1 promoter. This facilitates transcription activation. However, the existence and nature of the putative cellular cofactor involved in this process still remains open.

A different model of the repressive effect of HMGA1 on transcription from the HIV-1 promoter has also been proposed [5]. Factors associated with chromatin reorganization play a crucial role in the regulation of HIV-1 transcription; the CTIP2 protein is among these factors. The presence of CTIP2 at the promoter represses transcription of the integrated HIV-1 genome and is typical for the latent state of the virus. CTIP2 recruits histone deacetylases and histone methyltransferases, thus being involved in chromatin condensation [73]. In addition, CTIP2 interacts with the Sp1 and COUP-TF factors by repressing the initial stages of HIV-1 transcription [74] and is involved in delocalization of Tat and its binding to heterochromatin-associated protein HP1 [75]. CTIP2 has recently been shown to interact with 7SK snRNP by binding to loop L2 and the HEX-IM1 protein. Within this complex, CTIP2 participates

in the repression of Cdk9 kinase that is a component of P-TEFb [76]. It has been discovered that HMGA1 can bind to CTIP2 [5]. Moreover, transcription of a number of cellular genes is negatively regulated by both proteins; some of these genes are transcribed via the P-TEFb/7SK-dependent mechanism [5]. A model of joint transcriptional regulation of these genes by the HMGA1 and CTIP2 proteins has been proposed. It is assumed that HMGA1 can recruit either CTIP2 or the CTIP2/P-TEFb/7SK snRNP complex to the promoters of regulated genes (*Fig. 11*) [5].

It has been demonstrated that when interacting with the HIV-1 promoter, HMGA1 and CTIP2 synergistically repress basal transcription [5]. Knockdown of the *HMGA1* gene significantly reduces the levels of CTIP2 and P-TEFb/7SK snRNP recruited to the viral promoter and consequently recovers the level of transcription from it. Hence, it is assumed that a mechanism of HMGA1-mediated negative transcriptional regulation similar to that shown in *Fig. 11* may be realized on the viral LTR. Nevertheless, in the case of HIV-1 it remains unclear which DNA region or the LTR-bound factor is involved in recruitment of the HMGA1/CTIP2/7SK snRNP complex. The role of HMGA1 binding to TAR in the HMGA1/CTIP2-mediated repression of basal transcription is also unclear. Neither has it been studied whether HMGA1 has a direct effect on the binding of CTIP2 to viral DNA, similar to what happens with the transcription activator AP-1 [69].

Hence, HMGA1 can both activate and repress HIV-1 transcription. Its positive effect was seen in induced transcription, while a negative influence was shown for basal transcription. Possibly, some external factors trigger the switch of protein partners of HMGA1 and subsequent alteration in the mechanism of HMGA1-mediated transcriptional regulation.

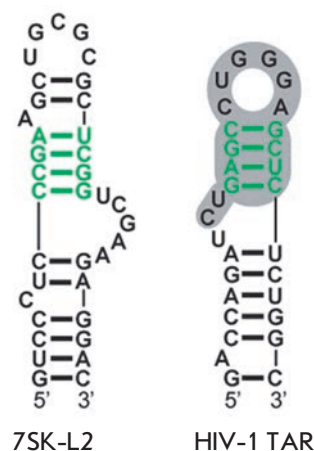


Fig. 9. Structures of the 7SK L2 and TAR RNA regions interacting with HMGA1. The HMGA1 binding site in both RNAs is shown in green. The TAR region responsible for the interaction with Tat and CycT1 is shown in gray [4].

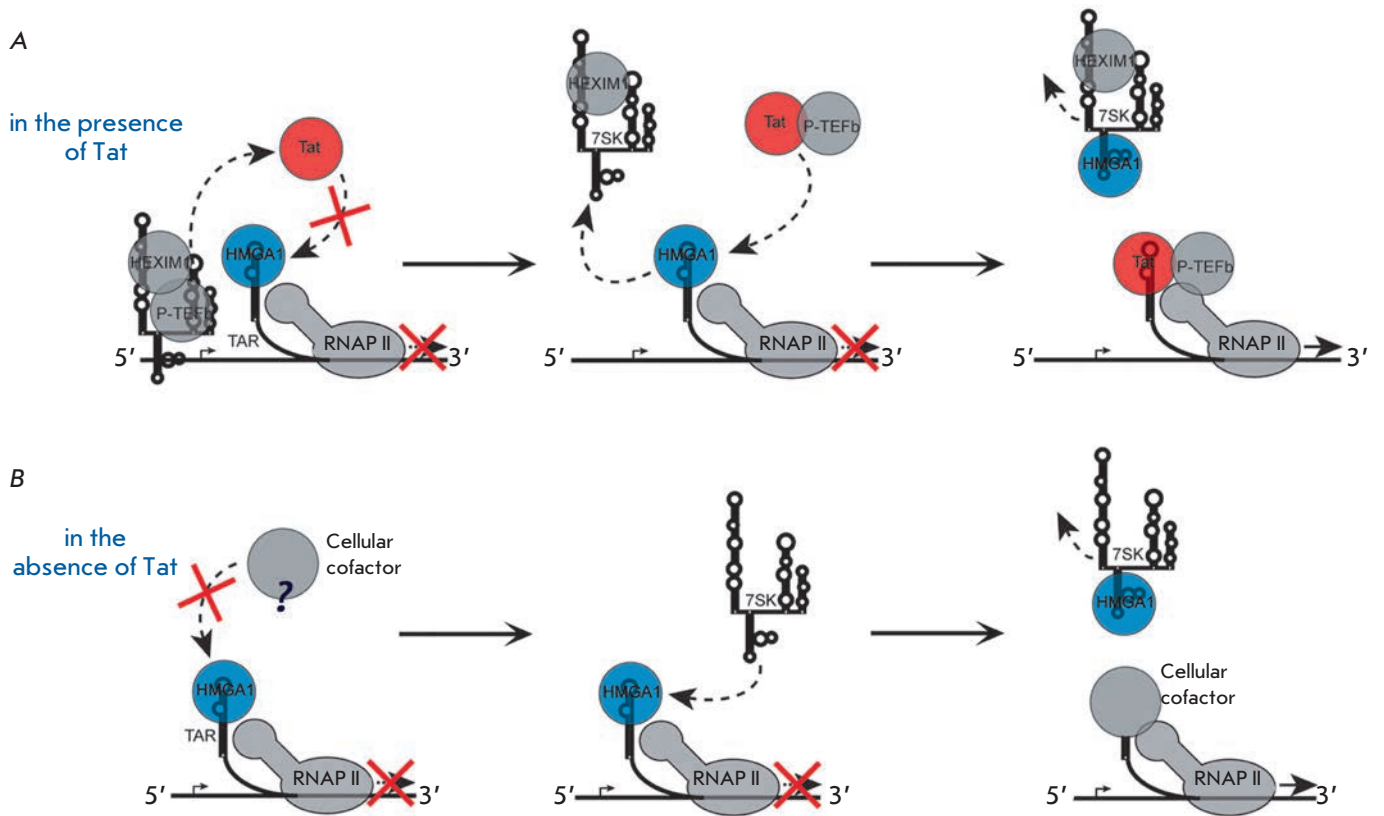


Fig. 10. Model of HMGA-1-mediated repression of HIV-1 transcription. **A** – competition between HMGA1 and Tat for TAR reduces the activity of the viral promoter. Tat releases 7SK from its complex with P-TEFb bound to the promoter. 7SK binds to HMGA1 to release TAR for subsequent interaction with Tat-P-TEFb. **B** – in the absence of Tat, HMGA1 impedes binding of a certain cellular cofactor, which is required for TAR-mediated HIV-1 transcription, to TAR RNA. 7SK binds to HMGA1, thus releasing TAR for subsequent interaction with this cofactor [4].

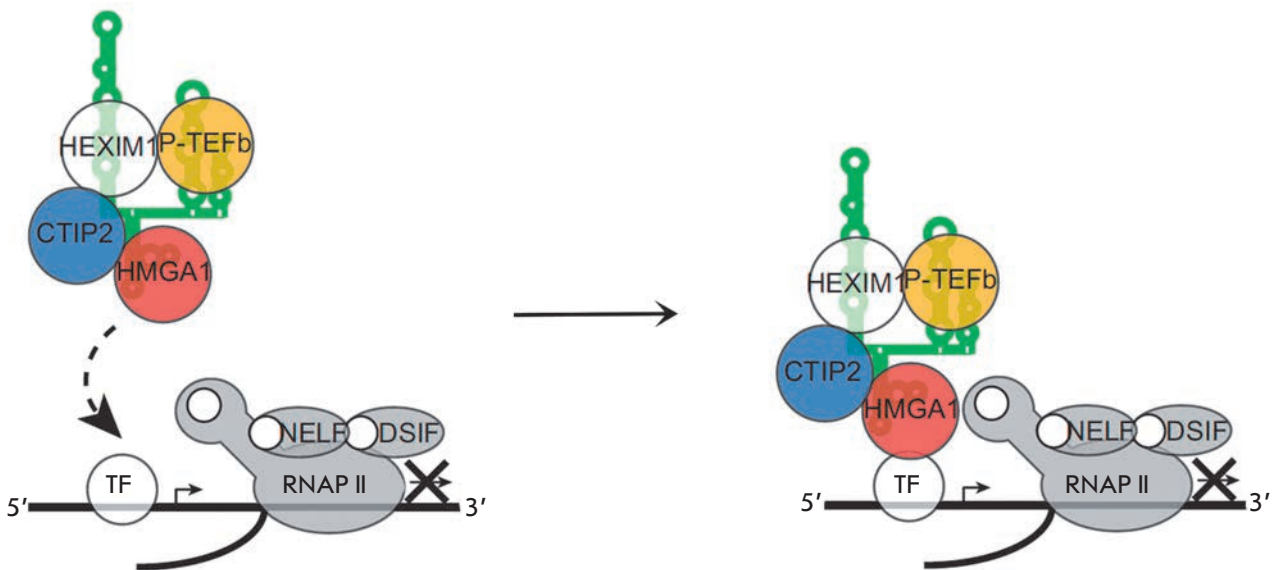


Fig. 11. The model of cooperative transcription regulation by HMGA1 and CTIP2. The CTIP2-repressed 7SK/P-TEFb complex is recruited to the promoter through 7SK L2 bound HMGA1 via its interaction with DNA, or with a transcription factor residing in the promoter region [5].

CONCLUSIONS

Although the features of HIV-1 transcription have been extensively studied, many aspects still have not been fully elucidated. It is well known that elongation of transcription of the viral genome takes place after the viral regulatory protein Tat binds to TAR RNA, which interacts with the multiprotein transcription elongation factor P-TEFb for its recruitment to the viral promoter. Cyclin-dependent kinase Cdk9 within P-TEFb performs phosphorylation of RNAP II that is required for elongation. However, a question arises: how is the transcription of the latent provirus activated in the absence of Tat protein? It was assumed that the phosphorylation of RNAP II, which is required for eliminating transcription block and transition to the elongation stage, can be activated by cellular factors. Some cellular factors may recruit P-TEFb to the promoter.

Regulation of HIV-1 transcription is a process that involves many cellular proteins; however, the role of some of them is not fully clear. Two cellular proteins described in this review, Ku and HMGA1, are among these “unclear factors.” Data attesting to both the stimulative and repressive effects of these proteins on the expression of HIV-1 genes has been obtained. Their role is often particularly prominent upon basal transcription.

The majority of studies performed on human cells demonstrate that the Ku heterodimer activates tran-

scription from the HIV-1 promoter. The importance of the DNA-PK catalytic subunit for the activation of transcription has been reported in a number of studies. A hypothesis has been put forward that DNA-PK is involved in the transcription elongation stage [10]. Let us mention that the ability of DNA-PK to phosphorylate RNAP II makes this kinase a promising candidate for a protein factor that activates elongation of transcription of viral genes in the absence of Tat.

The architectural factor HMGA1 may influence the chromatin composition upon HIV-1 transcription regulation. In this case, HMGA1 has a positive effect. On the other hand, the interplay between HMGA1 and TAR demonstrated *in vitro* seems to suppress the basal transcription of the HIV-1 genes and is important for maintaining latency [4]. Recruitment of a repressive transcription factor within 7SK snRNP, which HMGA1 can bind to, may be another mechanism of HMGA1-mediated suppression of transcription. There probably is no single mechanism for the involvement of HMGA1 in the regulation of HIV-1 genes transcription; the role of this protein depends on the phase of infection and activity of other cellular proteins. Elucidation of the mechanisms of the influence of Ku and HMGA1 on HIV-1 transcription may result in new approaches for the regulation of the replication of this dangerous virus. ●

This work was supported by the Russian Science Foundation (grant № 14-24-00061).

REFERENCES

- van Lint C., Bouchat S., Marcello A. // *Retrovirology*. 2013. V. 10. P. 67.
- Ruelas D.S., Greene W.C. // *Cell*. 2013. V. 155. № 3. P. 519–529.
- Zhou M., Halanski M.A., Radonovich M.F., Kashanchi F., Peng J., Price D.H., Brady J.N. // *Mol. Cell. Biol.* 2000. V. 20. № 14. P. 5077–5086.
- Eilebrecht S., Wilhelm E., Benecke B.-J., Bell B., Benecke A.G. // *RNA Biol.* 2013. V. 10. № 3. P. 436–444.
- Eilebrecht S., Le Douce V., Riclet R., Targat B., Hallay H., van Driessche B., Schwartz C., Robette G., van Lint C., Rohr O., et al. // *Nucl. Acids Res.* 2014. V. 42. № 8. P. 4962–4971.
- Jeanson L., Mouscadet J.F. // *J. Biol. Chem.* 2002. V. 277. № 7. P. 4918–4924.
- Masson C., Bury-Moné S., Guiot E., Saez-Cirion A., Schoëvaert-Brossault D., Brachet-Ducos C., Delelis O., Subra F., Jeanson-Leh L., Mouscadet J.F. // *J. Virol.* 2007. V. 81. № 15. P. 7924–7932.
- Waninger S., Kuhen K., Hu X., Chatterton J.E., Wong-Staal F., Tang H. // *J. Virol.* 2004. V. 78. № 23. P. 12829–12837.
- Manic G., Maurin-Marlin A., Laurent F., Vitale I., Thierry S., Delelis O., Dessen P., Vincendeau M., Leib-Mösch C., Hazan U., et al. // *PLoS One*. 2013. V. 8. № 7. P. 69691.
- Tyagi S., Ochem A., Tyagi M. // *J. Gen. Virol.* 2011. V. 92. № 7. P. 1710–1720.
- Meyerhans A., Breinig T., Vartanian J.-P., Wain-Hobson S. HIV Sequence Compendium 2003. Los Alamos National Laboratory: Theoretical Biology and Biophysics Group, 2003. 420 p.
- Sloan R.D., Wainberg M.A. // *Retrovirology*. 2011. V. 8. P. 52.
- Colin L., Verdin E., van Lint C. // *Meth. Mol. Biol.* 2014. V. 1087. P. 85–101.
- Taube R., Peterlin M. // *Viruses*. 2013. V. 5. № 3. P. 902–927.
- Kwak H., Lis J.T. // *Annu. Rev. Genet.* 2013. V. 47. P. 483–508.
- Nguyen V.T., Kiss T., Michels A.A., Bensaude O. // *Nature*. 2001. V. 414. № 6861. P. 322–325.
- Peterlin B.M., Price D.H. // *Mol. Cell*. 2006. V. 23. № 3. P. 297–305.
- Emiliani S., van Lint C., Fischle W., Paras P. Jr., Ott M., Brady J., Verdin E. // *Proc. Natl. Acad. Sci. USA*. 1996. V. 93. № 13. P. 6377–6381.
- Bieniasz P.D., Grdina T.A., Bogerd H.P., Cullen B.R. // *Proc. Natl. Acad. Sci. USA*. 1999. V. 96. № 14. P. 7791–7796.
- Yedavalli V.S., Benkirane M., Jeang K.T. // *J. Biol. Chem.* 2003. V. 278. № 8. P. 6404–6410.
- Itzen F., Greifenberg A.K., Böskén C.A., Geyer M. // *Nucl. Acids Res.* 2014. V. 42. № 12. P. 7577–7590.
- Patel M.C., Debrosse M., Smith M., Dey A., Huynh W., Sarai N., Heightman T.D., Tamura T., Ozato K. // *Mol. Cell. Biol.* 2013. V. 33. № 12. P. 2497–2507.
- Jin S., Weaver D.T. // *EMBO J*. 1997. V. 16. № 22. P. 6874–6885.

24. Ochem A.E., Skopac D., Costa M., Rabilloud T., Vuillard L., Simoncsits A., Giacca M., Falaschi A. // *J. Biol. Chem.* 1997. V. 272. № 47. P. 29919–29926.
25. Dynan W.S., Yoo S. // *Nucl. Acids Res.* 1998. V. 26. № 7. P. 1551–1559.
26. Walker J.R., Corpina R.A., Goldberg J. // *Nature.* 2001. V. 412. № 6847. P. 607–614.
27. Postow L. // *FEBS Lett.* 2011. V. 585. № 18. P. 2876–2882.
28. Hill R., Lee P.W. // *Cell Cycle.* 2010. V. 9. № 17. P. 3460–3469.
29. Fell V.L., Schild-Poulter C. // *Mutat. Res. Rev. Mutat. Res.* 2015. V. 763. P. 15–29.
30. Yang S.H., Nussenzweig A., Li L., Kim D., Ouyang H., Burgman P., Li G.C. // *Mol. Cell. Biol.* 1996. V. 16. № 7. P. 3799–3806.
31. Knuth M.W., Gunderson S.I., Thompson N.E., Strasheim L.A., Burgess R.R. // *J. Biol. Chem.* 1990. V. 265. № 29. P. 17911–17920.
32. Okumura K., Takagi S., Sakaguchi G., Naito K., Minoura-Tada N., Kobayashi H., Mimori T., Hinuma Y., Igarashi H. // *FEBS Lett.* 1994. V. 356. № 1. P. 94–100.
33. Giffin W., Torrance H., Rodda D.J., Préfontaine G.G., Pope L., Hache R.J. // *Nature.* 1996. V. 380. № 6571. P. 265–268.
34. Giffin W., Kwast-Welfeld J., Rodda D.J., Préfontaine G.G., Traykova-Andonova M., Zhang Y., Weigel N.L., Lefebvre Y.A., Haché R.J. // *J. Biol. Chem.* 1997. V. 272. № 9. P. 5647–5658.
35. Giffin W., Gong W., Schild-Poulter C., Haché R.J. // *Mol. Cell. Biol.* 1999. V. 19. № 6. P. 4065–4078.
36. Shi L., Qiu D., Zhao G., Corthesy B., Lees-Miller S., Reeves W.H., Kao P.N. // *Nucl. Acids Res.* 2007. V. 35. № 7. P. 2302–2310.
37. Schild-Poulter C., Shih A., Yarymowich N.C., Haché R.J. // *Cancer Res.* 2003. V. 63. № 21. P. 7197–7205.
38. Jiang D., Zhou Y., Moxley R.A., Jarrett H.W. // *Biochemistry.* 2008. V. 47. № 35. P. 9318–9334.
39. Wang H., Fang R., Cho J.Y., Libermann T.A., Oettgen P. // *J. Biol. Chem.* 2004. V. 279. № 24. P. 25241–25250.
40. Sucharov C.C., Helmke S.M., Langer S.J., Perryman M.B., Bristow M., Leinwand L. // *Mol. Cell. Biol.* 2004. V. 24. № 19. P. 8705–8715.
41. Hill R., Madureira P.A., Waisman D.M., Lee P.W. // *Oncotarget.* 2011. V. 2. № 12. P. 1094–1108.
42. Mayeur G.L., Kung W.J., Martinez A., Izumiya C., Chen D.J., Kung H.J. // *J. Biol. Chem.* 2005. V. 280. № 11. P. 10827–10833.
43. Sartorius C.A., Takimoto G.S., Richer J.K., Tung L., Horwitz K.B. // *J. Mol. Endocrinol.* 2000. V. 24. № 2. P. 165–182.
44. Medunjanin S., Weinert S., Schmeisser A., Mayer D., Braun-Dullaeus R.C. // *Mol. Biol. Cell.* 2010. V. 21. № 9. P. 1620–1628.
45. Lim J.W., Kim H., Kim K.H. // *J. Biol. Chem.* 2004. V. 279. № 1. P. 231–237.
46. Dvir A., Stein L.Y., Calore B.L., Dynan W.S. // *J. Biol. Chem.* 1993. V. 268. № 14. P. 10440–10447.
47. Maldonado E., Shiekhattar R., Sheldon M., Cho H., Drapkin R., Rickert P., Lees E., Anderson C.W., Linn S., Reinberg D. // *Nature.* 1996. V. 381. № 6577. P. 86–89.
48. Mo X., Dynan W.S. // *Mol. Cell. Biol.* 2002. V. 22. № 22. P. 8088–8099.
49. Peterson S.R., Dvir A., Anderson C.W., Dynan W.S. // *Genes Dev.* 1992. V. 6. № 3. P. 426–438.
50. Ju B.G., Lunyak V.V., Perissi V., Garcia-Bassets I., Rose D.W., Glass C.K., Rosenfeld M.G. // *Science.* 2006. V. 312. № 5781. P. 1798–1802.
51. Studamire B., Goff S.P. // *Retrovirology.* 2008. V. 5. P. 48.
52. Zheng Y., Ao Z., Wang B., Jayappa K.D., Yao X. // *J. Biol. Chem.* 2011. V. 286. № 20. P. 17722–17735.
53. Santos S., Obukhov Y., Nekhai S., Bukrinsky M., Iordanskiy S. // *Retrovirology.* 2012. V. 9. P. 65.
54. Skalka A.M., Katz R.A. // *Cell Death Differ.* 2005. V. 12. P. 971–978.
55. Daniel R., Greger J.G., Katz R.A., Taganov K.D., Wu X., Kappes J.C., Skalka A.M. // *J. Virol.* 2004. V. 78. № 16. P. 8573–8581.
56. Daniel R., Katz R.A., Merkel G., Hittle J.C., Yen T.J., Skalka A.M. // *Mol. Cell. Biol.* 2001. V. 21. № 4. P. 1164–1172.
57. Jeanson L., Subra F., Vaganay S., Hervy M., Marangoni E., Bourhis J., Mouscadet J.F. // *Virology.* 2002. V. 300. № 1. P. 100–108.
58. Li L., Olvera J.M., Yoder K.E., Mitchell R.S., Butler S.L., Lieber M., Martin S.L., Bushman F.D. // *EMBO J.* 2001. V. 20. № 12. P. 3272–3281.
59. Kilzer J.M., Stracker T., Beitzel B., Meek K., Weitzman M., Bushman F.D. // *Virology.* 2003. V. 314. № 1. P. 460–467.
60. Hoover T., Mikovits J., Court D., Liu Y.L., Kung H.F., Raziuddin // *Nucl. Acids Res.* 1996. V. 24. № 10. P. 1895–1900.
61. Reeves R., Nissen M.S. // *J. Biol. Chem.* 1990. V. 265. № 15. P. 8573–8582.
62. Ozturk N., Singh I., Mehta A., Braun T., Barreto G. // *Front. Cell. Dev. Biol.* 2014. V. 2. P. 5.
63. Reeves R. // *Meth. Enzymol.* 2004. V. 375. P. 297–322.
64. Cleyne I., van de Ven W.J. // *Int. J. Oncol.* 2008. V. 32. № 2. P. 289–305.
65. Farnet C.M., Bushman F.D. // *Cell.* 1997. V. 88. № 4. P. 483–492.
66. Hindmarsh P., Ridky T., Reeves R., Andrade M., Skalka A.M., Leis J. // *J. Virol.* 1999. V. 73. № 4. P. 2994–3003.
67. Li L., Yoder K., Hansen M.S., Olvera J., Miller M.D., Bushman F.D. // *J. Virol.* 2000. V. 74. № 23. P. 10965–10974.
68. Beitzel B., Bushman F. // *Nucl. Acids Res.* 2003. V. 31. № 17. P. 5025–5032.
69. Henderson A., Bunce M., Siddon N., Reeves R., Tremethick D.J. // *J. Virol.* 2000. V. 74. № 22. P. 10523–10534.
70. Henderson A., Holloway A., Reeves R., Tremethick D.J. // *Mol. Cell. Biol.* 2004. V. 24. № 1. P. 389–397.
71. Eilebrecht S., Brysbaert G., Wegert T., Urlaub H., Benecke B.-J., Benecke A. // *Nucl. Acids Res.* 2011. V. 39. № 6. P. 2057–2072.
72. Eilebrecht S., Benecke B.J., Benecke A. // *RNA Biol.* 2011. V. 8. № 6. P. 1084–1093.
73. Marban C., Suzanne S., Dequiedt F., de Walque S., Redel L., van Lint C., Aunis D., Rohr O. // *EMBO J.* 2007. V. 26. № 2. P. 412–423.
74. Marban C., Redel L., Suzanne S., van Lint C., Lecestre D., Chasserot-Golaz S., Leid M., Aunis D., Schaeffer E., Rohr O. // *Nucl. Acids Res.* 2005. V. 33. № 7. P. 2318–2331.
75. Rohr O., Lecestre D., Chasserot-Golaz S., Marban C., Avram D., Aunis D., Leid M., Schaeffer E. // *J. Virol.* 2003. V. 77. № 9. P. 5415–5427.
76. Cherrier T., Le Douce V., Eilebrecht S., Riclet R., Marban C., Dequiedt F., Goumon Y., Paillart J.C., Mericskay M., Parlakian A., et al. // *Proc. Natl. Acad. Sci. USA.* 2013. V. 110. № 31. P. 12655–12660.

Phage Peptide Libraries As a Source of Targeted Ligands

A. A. Nemudraya, V. A. Richter, E. V. Kuligina*

Institute of Chemical Biology and Fundamental Medicine, Siberian Branch of the Russian Academy of Sciences, Lavrentiev Ave., 8, 630090, Novosibirsk, Russia

*E-mail: kuligina@niboch.nsc.ru

Received 15.03.2015

Copyright © 2016 Park-media, Ltd. This is an open access article distributed under the Creative Commons Attribution License, which permits unrestricted use, distribution, and reproduction in any medium, provided the original work is properly cited.

ABSTRACT One of the dominant trends in modern pharmacology is the creation of drugs that act directly on the lesion focus and have minimal toxicity on healthy tissues and organs. This problem is particularly acute in relation to oncologic diseases. Short tissue- and organ-specific peptides capable of delivering drugs to the affected organ or tissue are considered promising targeted agents that can be used in the diagnosis and therapy of diseases, including cancer. The review discusses in detail the technology of phage display as a method for obtaining specific targeted peptide agents and offers examples of their use in diagnostic and clinical practice.

KEYWORDS targeted peptides, drug delivery, phage display, phage peptide libraries.

INTRODUCTION

Drug delivery directly to the lesion focus is one of the main challenges in modern pharmacology. This problem is particularly acute in relation to oncologic diseases. Generally, anticancer drugs exhibit significant toxicity, affecting healthy cells and tissues alongside malignant ones. Therefore, the development of principally new antitumor agents, the effectiveness of which is provided by a selective effect on the tumor, is considered as one of the key areas in antitumor therapy. The appearance of such tumor-targeted drugs would allow us to reduce the effective therapeutic dose and minimize side effects.

Cancer cells are known to have many quantitative and/or qualitative characteristics that distinguish them from normal cells. For instance, the expression of growth factor receptors, such as epidermal growth factor receptors (EGFR), transferrin or folate receptors, is often higher in tumor cells, which allows for their uncontrolled proliferation and promotes metastatic processes [1]. Tumor growth is also known to be accompanied by active processes of angiogenesis, which are mainly activated in an adult organism during the regeneration of damaged tissues. The processes of angiogenesis can be activated, for example, upon overexpression of vascular endothelial growth factors (VEGF) [2]. Finally, there are physical differences between tumor and normal tissues: temperature change, low oxygen concentration (hypoxia), and reduced pH [3].

The unique properties of cancer cells allow one to find specific ligands that interact directly with the tumor and to conduct targeted therapy of malignant tumors.

Phage display technology is one of the promising approaches in the search for tissue- and/or organ-specific molecules. Combinatorial phage peptide libraries allow one to obtain highly specific peptides, including peptides specific to various types of tumors. The search for tumor-specific peptides using combinatorial phage peptide libraries can be carried out *in vitro* and *in vivo*. Currently, such tumor-specific peptides are considered as targeting vehicles for the delivery of therapeutic genes, cytokines, agents for imaging, proapoptotic peptides, and cytotoxic drugs.

This article reviews in detail phage display technology as a method for obtaining a targeted agent capable of ensuring specificity of interaction between a drug and the target organ or tissue. Examples of the use of organ- and tissue-specific peptides in biomedicine are given.

PHAGE DISPLAY TECHNOLOGY

Phage display technology, first proposed by G.P. Smith in 1985, played an important role in the development of fundamentally new approaches in molecular biology and opened up new opportunities for the development of the pharmaceutical industry. The concept of phage display lies in the cloning of a foreign DNA sequence into a specific site of a bacteriophage surface protein gene so that this sequence shares the reading frame with the protein. The result is a chimeric protein containing a foreign amino acid sequence formed (displayed) on the surface of the bacteriophage (*Fig. 1*). Furthermore, the physiological properties and viability of the viral particle are preserved [4, 5].

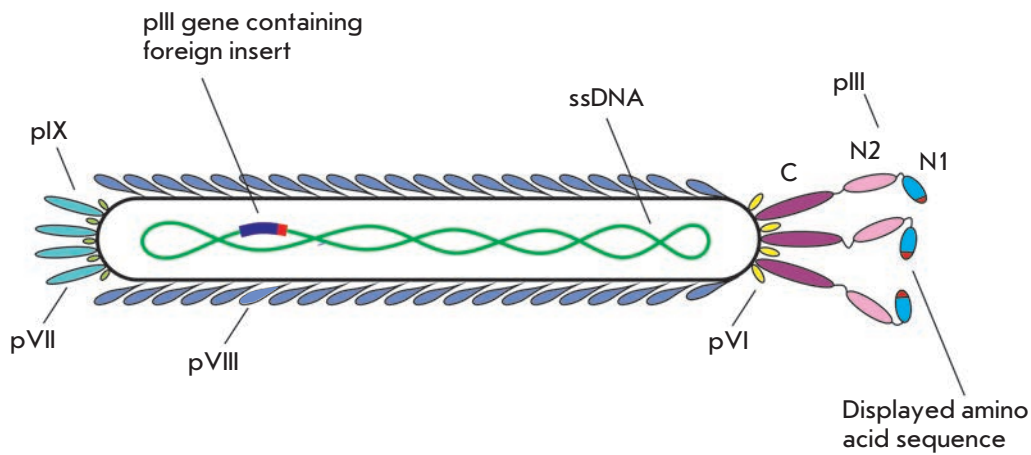


Fig. 1. The structure of a bacteriophage with a displayed foreign amino acid sequence in a pIII surface protein (indicated in red). N1, N2 and C – domains of the pIII surface protein

The technology of phage display has been developed for various bacteriophages; for example, λ , T4 and T7 [6–8]. The most widely used in phage display construction are filamentous bacteriophages [9], the virions of which resemble a long, thin thread. Filamentous phages are small and have a simply arranged genome [10]. The most studied filamentous phages – M13, f1, and fd – are under the genus *Inovirus*, family *Inoviridae* and combined into the Ff group since they infect *Escherichia coli* carrying F-pili [11]. Ff strain phages contain circular single-stranded DNA, which is 98.5% identical among various strains in the group [10]. The genome of Ff phages consists of 11 genes, the products of which can be grouped according to their functional purpose: capsid proteins – pIII, pVI, pVII, pVIII, pIX; proteins involved in DNA replication – pII, pV, pX; and proteins responsible for the assembly of phage particle – pI, pIV, pXI (Fig. 1) [12].

Typically, filamentous phages infect Gram-negative bacteria (*Escherichia*, *Salmonella*, *Pseudomonas*, *Xanthomonas*, *Vibrio*, *Thermus* and *Neisseria*). A bacterial cell infected with the phage releases new viral particles but does not undergo lysis.

Depending on which surface protein gene the foreign DNA is cloned into, there are several types of phage display (Table).

The proteins pIII and pVIII (406 and 50 amino acid residues, respectively), which are also called the minor and major proteins, are the most applied in the technology of phage display for the introduction of a foreign amino acid sequence. Both proteins have N-terminal signaling sequences, which are cleaved by a signal peptidase during protein maturation after transfer to the internal side of the bacterial membrane. Mature proteins incorporate into the phage envelope during its assembly. Thus, in order for the foreign peptide to be displayed on the phage particle surface, its encod-

ing nucleotide sequence should be cloned between the sequence of the surface protein and signaling sequence in the same translation frame [13].

Bacteriophage contains three to five copies of the pIII protein. Together with pVI, they form a distal cover of the virion and are necessary for its stabilization and the termination of phage particle assembly during the release from the bacterial cell. Moreover, pIII plays an important role in infection by attaching to the bacterial cell via F-pili [14]. Protein pIII contains three domains: N1, N2, and C separated by glycine spacers (Fig. 1). Domain C is responsible for virion assembly, while N1 and N2 are required for the infection of bacterial cells [15]. If a short nucleotide sequence is embedded in the *pIII* gene, the foreign insert will be carried

Types of phage display depending on the surface protein used

Type of phage display	Used surface protein (whether all copies of the protein represent foreign sequence)	Number and localization of surface protein gene copies
3	pIII (all)	1 in bacteriophage genome
8	pVIII (all)	1 in bacteriophage genome
33	pIII (partially)	2 in bacteriophage genome
88	pVIII (partially)	2 in bacteriophage genome
3+3	pIII (partially)	2 in bacteriophage genome and phagemid vector
8+8	pVIII (partially)	2 in bacteriophage genome and phagemid vector

by every molecule of the pIII protein. The phage display in this case is called type 3 display (*Table*).

One phage particle contains about 2,700 copies of the pVIII protein that forms the bacteriophage envelope and has a spiral structure. Four positively charged lysine residues, which interact with the negatively charged phosphate groups of viral ssDNA inside the phage, are located at the C-terminus of the protein. N-termini are located on the outside of the viral particle [16, 17]. The maximum length of the foreign insert that does not lead to significant aberrations of the phage particle assembly and is displayed on each pVIII protein is 6–7 amino acid residues (type 8 phage display) [18, 19].

The loss of chimeric protein function takes place upon display of long heterologous amino acid sequences, which should be replenished with wild-type pIII or the pVIII protein. There are systems with a phage genome containing *pIII* (*pVIII*) genes of two types: recombinant and wild. As a result, only a portion of pIII (pVIII) proteins carries heterologous sequences, while the other part preserves native functions (type 33 (88) phage display) [20]. Replenishment of the lost function of the protein can occur in systems using phagemid vectors and helper phages [21, 22]. The Phagemid vector in such a case contains a plasmid and phage origins of the replication, the sequence encoding an antibiotic resistance gene, and the sequence encoding the chimeric protein. The helper phage encodes a wild-type protein necessary for the proper assembly of viral particles. Upon infection, the wild-type gene enters the *E. coli* cell, along with the helper phage, with the recombinant gene in the plasmid. As a result, mature particles of the released bacteriophage are arranged in a mosaic pattern; i.e., they contain wild-type and recombinant proteins (type 3+3 or 8+8 phage display) [20].

The first studies of phage display technology application were aimed at obtaining peptides and proteins capable of specifically binding to antibodies. In his pilot work, Smith G.P. obtained a phage clone (fECO1) that contained the pIII protein with an inserted fragment of EcoRI restrictase. This clone was effectively neutralized by antibodies against restrictase [4]. Further development of this work yielded numerous other experiments in which phage particles with a displayed antigen served as immunogens capable of eliciting an immune response [23–25].

In the second part of his work, Smith investigated the possibility of enriching a mixed population of bacteriophages with specific fECO1 phages by affinity binding with antibodies against EcoRI. A mixture of phage fECO1 and a considerable excess in the wild-type M13mp8 phage were added to the absorbed antibodies against EcoRI. Unbound phages were washed away

with the medium, while absorbed phages were eluted with an acidic buffer, neutralized, and titrated. As a result of three consecutive experiments, a population enriched with fECO1 phage 1,500–7,200 times more than in the case of the wild-type phage was obtained [4]. At this stage, an idea appeared of using antibodies for the selection of specific clones from a population of bacteriophages (combinatorial phage library) where each individual phage particle displays a random amino acid sequence on its surface. Since 1988, the procedure of affinity enrichment of a phage population with a specific bacteriophage has become known as biopanning [26].

A typical biopanning round comprises the following steps: 1) incubation of a combinatorial phage library with the target (protein, cell culture, tumor tissue, etc); 2) washing-off of unbound phages; 3) elution of bound phages; and 4) amplification of the eluted phage for the next rounds (*Fig. 2*).

After several rounds of biopanning, the rate of population enrichment with the bacteriophage is determined by titration and/or immunoenzyme techniques. Then, individual phage clones are isolated and the sequence of the foreign insert is determined. It is important to note that a simple physical bond between the

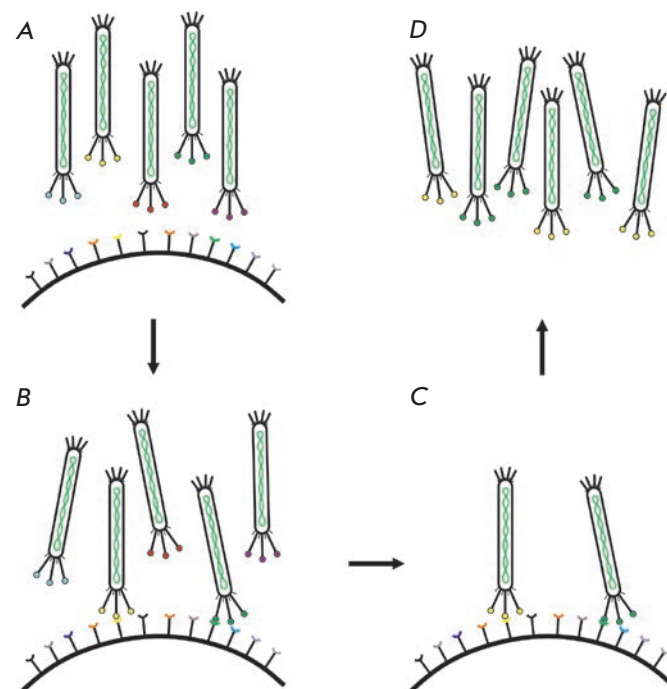


Fig. 2. Schematic representation of a typical biopanning of a phage library. *A, B* – incubation of a combinatorial phage library with a target; *C* – washing-off of the unbound phages; *D* – elution of bound phages and their amplification for the next rounds

displayed peptide and a sequence cloned into the phage genome allows for an easy analysis of the insert primary structure. Due to the small size of filamentous bacteriophages (5 nm diameter, 1 μm length), the concentration of phage particles can be as high as 10^{14} particles/ml, which allows for the screening of a large number of variants. The representativeness of the peptide phage library reaches 10^9 different insertion variants [27].

Nowadays, combinatorial phage libraries are widely used as a tool that allows one to solve various tasks in molecular biology, biochemistry, and biomedicine. Libraries can be performed based on random combinations of oligopeptides, antibodies, enzymes, fragments of genomic DNA, cDNA, open reading frames, or other functional genomic regions [28–30]. Library screening allows one to select molecules with specific properties, study protein-protein interactions, investigate markers of specific tissues, organs and biochemical processes, search for the substrates of various enzymes, epitopes of antigens and paratopes of antibodies and, finally, obtain highly specific molecules with the desired properties [31, 32].

SELECTION OF SPECIFIC PEPTIDES FROM PHAGE LIBRARIES

Construction of a peptide library is one of the key moments in successful screening, since the probability of a ligand selection that specifically binds to a certain target depends considerably on the library diversity and insert length. One of the most common strategies for constructing a combinatorial library of peptides is based on the triplet rule and degeneracy of the genetic code. The strategy is to generate various combinations based on a $(\text{NNK})_n$ codon, where N is the equimolar ratio of all four nucleotides, and K stands for the mixture of guanine and thymine only (1 : 1). Due to the use of the codon $(\text{NNK})_n$ instead of $(\text{NNN})_n$, the number of possible stop codons is reduced from three (TAA, TGA, TAG) to one (TAG) and the probability of coding different amino acids is aligned. Thus, 32 possible $(\text{NNK})_n$ codon variants encode 20 canonical amino acids and one stop codon [13]. The number of possible variants of amino acid sequence of length n is equal to 20^n . However, other factors such as the presence of a stop codon in the peptide sequence and transformation efficiency of *E. coli* cells with phage constructs affect the representativeness of the library in practice. Typically, the representativeness of a commercial phage peptide library is about 10^9 phage particles [33]. Furthermore, the peptide insertion may be both linear and circular due to the formation of disulfide bridges between the cysteine residues flanking the insert.

As mentioned above, a heterologous insert can be displayed either by the pIII or pVIII protein. Librar-

ies based on pIII, which is represented by only three to five copies at one of the ends of the viral particle, are used for the generation of highly specific ligands with high affinity for the target. Ligands with a dissociation constant in the range of 1–10 μM are obtained using such libraries [34]. Such specific peptides are most commonly used for the delivery of various substances to a target or imaging of specific structures and biochemical processes.

The major protein pVIII covering the capsid provides multivalent binding and high avidity, which adversely affects the affinity of interaction between peptide and target. Using pVIII-protein-based libraries, ligands with lower individual affinity are selected; the dissociation constants of such ligands are in the range of 10–100 μM [34]. However, these libraries are also widely used since the selected phage particles show a high affinity for the target, stability and they can be easily produced in large amounts. For example, Lang Q. et al. applied enzyme immunoassay in the detection of a prostate-specific antigen (PSA) using a phage clone selected from the pVIII library [35]. The possibility of targeted delivery of GAPDH siRNA to cancer cells using the ability of phage proteins to self-assemble in the presence of any nucleic acid is shown [36]. A phage peptide library based on the pVIII major protein was used for the selection of clones specific to human breast adenocarcinoma cells MCF-7. Recombinant pVIII proteins of this clone were generated by conventional amplification of the phage clone separated from the phage particle and incubated with GAPDH siRNA to form so-called nanophages. The resulting particles (nanophages) protected GAPDH siRNA from degradation by plasma nucleases, provided their specific delivery to MCF-7 cells, and internalization into the cell but did not affect the functionality of GAPDH siRNA.

Screening of phage peptide libraries can be carried out both *in vitro* and *in vivo*. *In vitro* screening is conducted using a variety of objects: inactivated viruses and bacteria, purified protein fractions, enzymes, receptors, functional domains, and cell cultures [37, 38]. *In vitro* screening also includes selection using inorganic molecules (e.g., metals) and synthetic materials [39].

The most simple and direct method of *in vitro* selection of specific peptides is the selection on a purified substance of the target protein. For example, using screening of a phage peptide library displaying a seven-residue peptide with a fibroblast growth factor 8 (FGF8b), a HSQAAVP (P12) peptide was obtained that specifically binds to the receptor of this factor. FGF8b is a major isoform that is produced by prostate cancer cells. The selected P12 peptide inhibits cell proliferation induced by FGF8b, causes cell cycle arrest in the G0/G1 phase by suppression of cyclin D1 and PCNA,

and block activation of the Erk1/2 and Akt cascades in both prostate cancer cells and vascular endothelial cells. Thus, P12 acting as an antagonist of FGF8b is a potential therapeutic tool in prostate cancer [40].

The disadvantage, or rather limitation of such a selection method, is that the peptides obtained after screening on the substance of purified proteins may not have the targeted properties *in vivo*. One of the reasons for this can be the specific post-translational modification of proteins that occur during various processes, including malignant cell transformation. Moreover, obtaining a soluble substance of a purified protein while maintaining its native structure and function is not always a trivial task [41].

In vitro screening on cell cultures allows one to successfully select peptides to various cell surface structures and also peptides capable of internalization into cells both through receptor-mediated and non-receptor-mediated ways: so-called cell-penetrating peptides (CPP) peptides. The advantages of a selection on cell cultures include the ability to obtain peptides specific to a particular cell type without knowledge of the particular target the peptides bind to.

Phage peptide libraries with additional properties are constructed on the basis of the vast data obtained. Thus, for example, a new class of peptide phage libraries (iPhage libraries) exists in which the displayed peptide is able to internalize a phage particle into the cell and provide specific binding to the cellular organelles and functional domains of intracellular proteins. The peptides selected from such a library allow one to study intracellular signaling and metabolic pathways [42].

A less common means for screening a phage peptide library is different biological fluids. Thus, a large amount of fibrin is found in the extracellular matrix of a tumor, which is caused by a constant penetration of fibrinogen into the tumor stroma and its cleavage. Pilch J. *et al.* performed biopanning with coagulated plasma and selected two cyclic decapeptides (CLT1 and CLT2) capable of specifically binding to fibrin-fibronectin complexes. Intravenous administration of fluorescently labeled CLT1 and CLT2 in mice with different grafted tumors led to their accumulation in the extracellular space of the tumor. The selected peptides also specifically bound to lesion sites in tissues. Thus, such peptides can be useful for the development of targeted drugs for the diagnosis and therapy of tumors and damaged tissues [43].

The possibility of selecting specific peptides by *in vivo* screening of a phage peptide library was shown by Pasqualini and Ruoslahti in 1996 [44]. There are several ways to introduce a phage peptide library into experimental animals in *in vivo* screening. The most common is intravenous administration, which allows almost im-

mediate introduction of the library into blood vessel receptors, organs, and tissues. During circulation of a phage peptide library in the bloodstream, part of the phage population binds to plasma proteins and other non-target organs and tissues. This part of the library does not get involved in further rounds of selection, because only the associated-with-the-target-organ part of the library is amplified.

However, intravenous administration complicates the selection of peptides specific to brain structures, because penetration of phage particles is limited by the blood-brain barrier. Intranasal administration of a peptide phage library was developed for this purpose. It has been established that the bulk of the substance is absorbed into the blood upon intranasal administration, while a smaller part enters the brain directly from the neurons of the olfactory tract with the help of perineural transport in sensory nerves and spreads through brain structures through mechanisms not associated with the blood flow [45, 46]. Nevertheless, the intravenous way of administration of a phage peptide library allows one to select peptides specific to the blood-brain barrier only [47]. These peptides have the potential to translocate to the inside of the blood-brain barrier and provide delivery of associated molecules to the brain structures.

An alternative to the intravenous and intranasal administration methods is introduction directly into the target (orthotopic). For example, intraperitoneal administration of a phage peptide library in mice with gastric cancer allowed one to select peptides that specifically bind to gastric cancer metastasis [48]. Orthotopic administration allows one to introduce all possible target library variants into the target and reduces the probability of phage particle capture by other organs. On the other hand, target properties of the peptides selected orthotopically are significantly reduced upon intravenous administration.

Finally, there is a transdermal way of administration, which allows one to select peptides capable of penetrating through intact skin [49, 50].

The main limitations of *in vivo* screening are non-specific distribution of phage particles in organs and tissues and half-life of the introduced phage. It is shown that phage accumulates in considerable amounts in the liver and spleen upon circulation in the organism. Maximum concentration of the wild-type M13 phage is observed in the blood 5 and 15 minutes after intravenous administration in mice with an intact immune system (line CF-1) and mice with immunodeficiency, respectively. Then, the concentration of phage particles in the bloodstream decreases rather rapidly. It is important to note that the concentration of phage particles in the spleen of mice with immunodeficiency is much lower than in healthy ones, which indicates the

involvement of the immune system, particularly the reticuloendothelial system, in phage capture [51]. The half-life of the wild-type M13 phage in a mouse bloodstream is about 4.5 hours, while various modifications of phage particles (e.g., glycosylation or succinylation) dramatically reduce the half-life (up to several minutes). Reduction of the half-life in the bloodstream and rapid degradation of modified phages are apparently associated with their interaction with the corresponding receptors and internalization in a cell [52]. These nuances must be considered in the construction and analysis of *in vivo* experiments.

In 2002, the results of the first screening of a phage peptide library carried out *in vivo* in a patient in coma were published [53]. After intravenous administration of such a library (one round of screening), biopsies of several organs were analyzed. It was shown that the distribution of 47,160 phage clones between organs was not coincidental. The experiment was the first step in the development of a molecular map of the distribution of human receptors. One of the selected phage-displayed peptides had a high affinity for prostate tissue and accumulated in it in considerable amounts. It was demonstrated later that this peptide is a ligand of interleukin-11 [54].

Subsequently, phage particles selected from the biopsies of various organs after the first round of selection were combined into a new library. Two consecutive rounds of selection in two patients with prostate cancer were conducted using this library. A bioinformatic analysis of clones selected from various organs identified 15 peptides that could potentially serve as ligands of specific receptors. Bioinformatics methods (high-throughput analysis by similarity search, protein arrays) and affinity chromatography demonstrated that four of these 15 peptides are ligands of annexins A2 and A4, apolipoprotein E3, and leukocyte proteinase 3 [55].

Thus, one of the main advantages of using an *in vivo* system is that the targets for which the specific peptides are selected are presented in the natural microenvironment of the living organism.

APPLICATION OF ORGAN- AND TISSUE-SPECIFIC PEPTIDES

Development of the technology for obtaining organ- and tissue-specific peptides using phage libraries and the discovery of new properties of these peptides has allowed researchers to consider them as promising diagnostic and therapeutic agents.

Peptides with antitumor activity

In most cases, the screening of phage peptide libraries is carried out in order to identify peptides that bind specifically to the receptor structures of the target or-

gan or tissue and can subsequently serve as targeted agents for the delivery of different substances. On the other hand, organ- and tissue-specific peptides themselves have specific biological properties. In particular, some peptides exhibit antitumor activity.

For example, peptide LyP-1 that specifically binds to the lymphatic vessels of certain tumors inhibits the growth of human breast cancer MDA-MB-435 in model mice with severe combined immunodeficiency (SCID) upon regular intravenous administration. LyP-1 is shown to induce apoptosis of only the cells it binds to [56].

Cyclic peptide CIGB-300 blocks phosphorylation of serine-threonine protein kinase CK2, the synthesis of which is significantly elevated in various cancers. Impaired function of this enzyme leads to growth inhibition and induction of apoptosis of cancer cells in culture. CIGB-300 is also known to exhibit significant antitumor effect both upon local and systemic administration in mice with syngeneic tumors and human tumors and can serve as the basis for the development of anticancer drugs [57].

Peptide SMSIASPYIALE (peptide pIII) specific to GC9811-P endothelial cells of gastric cancer accumulating in the metastasis of this tumor was selected from a phage peptide library after four rounds of selection. A synthetic pIII analogue significantly inhibited the ability of GC9811-P cells for adhesion and invasion, impeded the development of metastasis and increased the lifespan of mice inoculated with a gastric cancer graft [58]. Afterwards, a GMBP1 peptide was obtained that specifically binds to the receptors of gastric cancer cells exhibiting multidrug resistance, and it contributed to cell phenotype alteration and restoration of drug sensitivity [59].

The acidic fibroblast growth factor (aFGF) is known to be produced by breast cancer cells and to promote tumor progression by interacting with the FGF receptor (FGFR). Peptide AP8 obtained from a phage peptide library is capable of specifically binding aFGF and inhibiting the proliferation of tumor cells and newly formed tumor vessels by arresting the cell cycle [60]. Such bifunctional peptides specific to tumor cells and tumor vascular cells can serve both as independent antitumor agents and vehicles for other drugs, enhancing their effect by their own anti-tumor action.

Wang H. *et al.* developed the strategy of joint application of the AVPI apoptotic peptide and DNA of the gene encoding the p53 protein for adjuvant therapy of breast cancer. The AVPI peptide was modified by addition of eight arginine residues. Due to the positively charged tail of arginine residues, AVPIR8 acquired the ability to effectively penetrate into cancer cells and serve as a vector for gene delivery due to the formation

of nanocomplexes with the nucleic acid. Application of the AVPIR8/p53 DNA combination significantly increased the sensitivity of cancer cells to doxorubicin in experiments *in vitro*, as well as in breast cancer mouse models with a multidrug resistance phenotype [61].

A series of promising anticancer drugs was developed on the basis of tumor-targeted peptides. Several examples of anti-tumor peptides, which are at various stages of clinical trials (www.clinicaltrials.gov), can be noted. For example, a cyclic peptide [Arg-Gly-Asp-Dphe-(NMeVal)] containing an RGD motif serves as the basis for the Cilengitide antitumor agent. Cilengitide, a highly selective integrin inhibitor that arrests angiogenesis, is considered as the drug for central nervous system tumors, particularly glioblastoma, also small cell lung cancer, prostate cancer, and metastatic and/or squamous cell carcinoma of the head and neck. Clinical trials of cilengitide (phase I/II) in combination with standard radiotherapy and temozolomide conducted in patients with newly diagnosed glioblastoma showed attainment of a primary endpoint (69% survival rate without progression for 6 months) [62, 63].

Clinical trials of the anticancer drug NGR-hTNF consisting of the human tumor necrosis factor (hTNF) and the NGR amino acid motif, the target of which is aminopeptidase N (CD13), began after the obtaining of encouraging results in antitumor therapy in animal models [64]. To date, there have been clinical trials conducted (phase I/II) for NGR-hTNF as a monotherapy drug for pleural mesothelioma and liver cancer. Clinical trials (phase I/II) of a combination of NGR-hTNF with such drugs as doxorubicin, oxaliplatin, capecitabine, gemcitabine, etc. in recurrent ovarian cancer, colorectal cancer, and small-cell lung cancer are at various stages of completion [5, 63]. According to the results of the clinical trials, NGR-hTNF is most effective in combination with conventional chemotherapy.

There are clinical trials (phase II/III) of oncolytic adenovirus Ad5- Δ 24-RGD, a modified RGD capable of replicating in cells lacking a Rb/p16 signal pathway, as a drug for ovarian cancer and glioblastoma recurrence [5].

Encouraging results in completed and ongoing clinical trials inspire hope that soon there will be drugs based on tumor-specific peptides.

Application of peptides in gene therapy

Tumor-specific peptides are actively used as targeted components in the development of gene therapy drugs. For example, liposomes integrated into a membrane and peptides loaded with nucleic acid provide additional targeting of delivery structures. In the work by Yang *Z. et al.*, two receptor-specific peptides were included in

liposomes: angiopep and tLyP-1. Angiopep is specific to the receptor of low-density lipoproteins, the expression of which is enhanced in the blood-brain barrier structures. Peptide tLyP-1 is specific to the receptor of neuropilin-1, it effectively penetrates into tumor parenchyma. These modified liposomes loaded with siRNA suppressing gene expression of the vascular endothelial growth factor (VEGF siRNA) were efficiently transfected into U87MG human glioblastoma cells *in vitro* and reduced the expression of a target gene. The antitumor activity of the created modified liposomes was shown in a U87MG glioblastoma xenograft model *in vivo* [65].

A vector based on the adeno-associated virus (AAV), the capsid of which has an integrated peptide selected from the phage peptide library and containing an NGR-motif, was capable of targeted delivery of genetic information to CD13+ target cells. The CD13 receptor is expressed on endothelial cells of newly formed vessels and many cancer cells, which indicates that peptides containing a NGR-motif can be used as tumor-targeted agents [66].

Genetically modified bacteriophages displaying targeted peptides within one of their surface proteins can also be used as agents for targeted gene therapy. Among the important advantages of bacteriophages are their safety for humans, high stability of phage particles, and plasticity of the genome for construction [67, 68].

One of the first works that proved the possibility of targeted gene therapy with a modified bacteriophage was performed using a filamentous bacteriophage, a minor part of the pIII protein of which had an incorporated fibroblast growth factor (FGF2). The green fluorescent protein (GFP) gene under the cytomegalovirus (CMV) early promoter was used as a reporter gene. The modified bacteriophages specifically penetrated only into cells expressing the FGF2 receptor on the surface and internalized into the cell interior. Expression of the reporter gene and synthesis of GFP were observed [69]. Thus, bacteriophage, despite the lack of tropism for human cells, can be modified so that it acquires specificity to a particular cell type and the capacity to deliver foreign genetic material.

Bacteriophage M13 expressing the tumor-specific peptide RGD4C was used for the delivery of a transgene cassette regulated by the CMV promoter and flanked by AAV2 inverted terminal repeats. Phage particles were modified with cationic polymers in order to improve transfection properties. The modified phage particles possessed a higher antitumor activity compared to unmodified phages [70].

Finally, a tumor-specific peptide can be covalently attached to a therapeutic nucleic acid for its delivery

to the target. For example, the possibility of delivery of VEGFR2 siRNA covalently linked to the targeted peptide cRGD was studied. Peptide cRGD specifically binds to $\alpha\beta 3$ -receptors that are expressed at a high density on the endothelium of tumor vessels and in tumor cells. A covalent complex of cRGD-siRNA was shown to specifically enter $\alpha\beta 3$ -positive HUVEC cells and turn off the target gene. The specific antitumor effect of the considered structures was identified in *in vivo* experiments in mice with immunodeficiency and inoculated A549 lung cancer tumor [71].

The obtained positive results allow one to consider tumor-specific peptides as a promising platform for the development of gene therapy agents.

Targeted peptides in the diagnosis of diseases

Peptides that specifically bind to certain tumor organs, tissues, cells, or vessels can be used for characterization of a cell culture, visualization of certain structures (including tumors) *in vivo*, and disease diagnostics [72].

For example, the RGD peptide conjugated with FITC is used in *in vitro* experiments to evaluate the expression level of $\alpha\beta 3$ integrins on the surface of various cancer cells in culture. Staining of human tumor biopsies embedded in paraffin using FITC-RGD allows one to evaluate the $\alpha\beta 3$ profile of the tumor tissue. This method of staining is much easier and cheaper than staining with antibodies to $\alpha\beta 3$ receptors [73].

Positron emission tomography (PET) is a radionuclide tomographic method of diagnostic study. The method is based on the detection of the distribution of compounds (radioligands) labeled with positron-emitting radioisotopes in an organism. Natural peptides (bombesin, somatostatin) are for the most part used as protein markers in PET [74]. Tumor-specific peptides can also be used as targeted agents for the delivery of radionuclide labels in the diagnosis of malignant neoplasms. Novel radioligands based on the RGD peptide are currently under clinical trials [75].

Another radioligand for PET imaging is based on a ^{64}Cu -labeled NGR-containing peptide specific to the CD13 receptor. This compound bound to CD13⁺ HT-1080 cells and showed no tropism for CD13⁻ MCF-7 cells in experiments *in vitro*. Results of *in vitro* experiments were confirmed *in vivo* using HT-1080 and MCF-7 tumor xenografts [76].

Tumor-specific peptides can conjugate not only with radionuclides, but also with other diagnostic agents, such as paramagnetic substances for MRT (magnetic resonance tomography), SPECT (single photon emission computed tomography), or fluorescent dyes in case of FOT (fluorescence optical imaging) [74]. These conjugates selectively accumulate in tumor at concentrations greatly exceeding their con-

centration in other organs, thereby amplifying the signal detected by the device.

Thus, tumor-specific peptides have significant potential for improving existing technologies of diagnostics and imaging of tumor structures.

Peptides: agents for targeted drug delivery

An example of using tumor-specific peptides for the delivery of pro-apoptotic proteins is a protein that combines the pro-apoptotic peptide KLAK and targeted peptide RGD. The RGD motif of the peptide recognizes integrin receptors, which are expressed in a large number on newly formed vessels and cancer cells [77]. The obtained bifunctional protein specifically binds to target cells (tumor endothelial cells), penetrates into the cells, and induces their apoptosis through the mitochondrial pathway [78].

Peptide M2pep, which specifically binds to tumor-associated macrophages and mouse M2 macrophages, was proposed as an agent for the targeted delivery of the KLA pro-apoptotic protein [79]. Tumor-associated macrophages play an important role in tumor progression by stimulating tumor cell growth, angiogenesis and metastasis, and promote drug resistance [80]. The resulting recombinant protein M2pepKLA inhibited tumor growth and reduced the population of tumor-associated macrophages [79].

Peptide **CRGDKGPDC** (iRGD) combining the properties of two motives, RGD (integrin-binding) and R/KXXR/K (neuropilin (NRP)-binding), was selected based on the T7 phage peptide using a phage peptide library [81, 82]. RGD guides the peptide to the tumor, while R/KXXR/K increases the permeability of tumor vessels and improves the efficiency of drug delivery to tumor parenchyma through the vascular barrier. Furthermore, iRGD inhibits spontaneous metastasis in mice. The antimetastatic activity is provided by neuropilin-binding RXXK but not the integrin-binding RGD motif [83]. Such peptides that have targeting properties and at the same time are able to deeply penetrate into tumor parenchyma form a separate class of peptides, CPHP (cell-penetrating homing peptides) [84].

A conjugate of iRGD with the anticancer agent abraxane (albumin-stabilized paclitaxel) is known to increase the effectiveness of abraxane and significantly reduce the overall toxicity of the drug [85, 82]. Furthermore, it was found that co-administration of the iRGD peptide with various drugs (doxorubicin, abraxane, liposomes with doxorubicin, trastuzumab) improves the effectiveness of drug penetration into tumor parenchyma and their therapeutic index [86].

Thus, short targeted peptides selected from phage libraries are increasingly being used both in diagnostic and clinical practice.

CONCLUSION

Screening of phage peptide libraries is a fast and convenient method of obtaining organ-, tissue- and tumor-specific peptides. The safe nature of the bacteriophages for humans and simplicity of manipulations with them allowed us to obtain a wide variety of targeted peptide ligands. Some of them are in clinical trials, both as individual therapeutic agents and as vehicles for drug delivery to target organs and tissues.

The possibility of a tumor-targeted peptide application in the diagnosis and therapy of malignant neoplasms is of great interest. The small size of the targeted peptides allows them to penetrate deeply into tumor parenchyma, which is important in targeted therapy [87, 88]. Short peptides are virtually non-immunogenic, which makes them safe for clinical use [89]. Peptides can be easily modified, for example, by protection of the N- and C-termini from proteolytic degradation [87]. Chemical synthesis of short peptides is much cheaper than the production of monoclonal antibodies and re-

combinant proteins, while the final product does not require additional purification from bacterial cell wall components or the eukaryotic plasma membrane [90].

Tumor-specific peptides are the keys to the bulk of information about the changes that occur in cell during carcinogenesis, the mechanisms responsible for survival, proliferation, and metastasis of cancer cells. Identification of targets for such peptides is very important, but often rather not a trivial task. A tumor-specific ligand can be used for targeted delivery of diagnostic and therapeutic agents even in the absence of information on the target.

This work was supported by the Ministry of Education of Russia (Federal Target Program “Researches and Development in the Priority Directions of Development of a Scientific and Technological Complex of Russia for 2014–2020”, agreement № 14.607.21.0063, unique identifier for the project RFMEFI60714X0063).

REFERENCES

- Wicki A., Witzigmann D., Balasubramanian V., Huwyler J. // *J. Control Release*. 2015. V. 200. P. 138–157.
- Ruoslahti E. // *Nat. Rev. Cancer*. 2002. V. 2. № 2. P. 83–90.
- Arachchige M.C., Reshetnyak Y.K., Andreev O.A. // *J. Biotechnol.* 2015. doi: 10.1016/j.jbiotec.2015.01.009.
- Smith G.P. // *Science*. 1985. V. 228. № 4705. P. 1315–1317.
- Bábíčková J., Tóthová L., Boor P., Celec P. // *Biotechnol. Adv.* 2013. V. 31. № 8. P. 1247–1259.
- Nicastro J., Sheldon K., Slaveev R.A. // *Appl. Microbiol. Biotechnol.* 2014. V. 98. № 7. P. 2853–2866.
- Gamkrelidze M., Dąbrowska K. // *Arch. Microbiol.* 2014. V. 196. № 7. P. 473–479.
- Teesalu T., Sugahara K.N., Ruoslahti E. // *Meth. Enzymol.* 2012. V. 503. P. 35–56.
- Ebrahimizadeh W., Rajabibazi M. // *Curr. Microbiol.* 2014. V. 69. № 2. P. 109–120.
- Rakonjac J., Bennett N.J., Spagnuolo J., Gagic D., Russel M. // *Curr. Issues Mol. Biol.* 2011. V. 13. № 2. P. 51–76.
- King A.M.Q., Adams M.J., Lefkowitz E.J. *Virus Taxonomy: Ninth Report of the International Committee on Taxonomy of Viruses*. San Diego:Elsevier, 2012.
- Marvin D.A., Symmons M.F., Straus S.K. // *Prog. Biophys. Mol. Biol.* 2014. V. 114. № 2. P. 80–122.
- Fagerlund A., Myrset A.H., Kulseth M.A. // *Meth. Mol. Biol.* 2014. V. 1088. P. 19–33.
- Rakonjac J., Feng Jn., Model P. // *J. Mol. Biol.* 1999. V. 289. № 5. P. 1253–1265.
- Hoffmann-Thoms S., Weininger U., Eckert B., Jakob R.P., Koch J.R., Balbach J., Schmid F.X. // *J. Biol. Chem.* 2013. V. 288. № 18. P. 12979–12991.
- Zeri A.C., Mesleh M.F., Nevzorov A.A., Opella S.J. // *Proc. Natl. Acad. Sci. USA*. 2003. V. 100. № 11. P. 6458–6463.
- Marvin D.A., Welsh L.C., Symmons M.F., Scott W.R., Straus S.K. // *J. Mol. Biol.* 2006. V. 355. № 2. P. 294–309.
- Iannolo G., Minenkova O., Petruzzelli R., Cesareni G. // *J. Mol. Biol.* 1995. V. 248. № 4. P. 835–844.
- Kay B.K., Kasanov J., Yamabhai M. // *Methods*. 2001. V. 24. № 3. P. 240–246.
- Bratkovic T. // *Cell Mol. Life Sci.* 2010. V. 67. № 5. P. 749–767.
- Gupta A., Shrivastava N., Grover P., Singh A., Mathur K., Verma V., Kaur C., Chaudhary V.K. // *PLoS One*. 2013. V. 8. № 9. e75212.
- Qi H., Lu H., Qiu H.J., Petrenko V., Liu A. // *J. Mol. Biol.* 2012. V. 417. № 3. P. 29–43.
- Prisco A., De Berardinis P. // *Int. J. Mol. Sci.* 2012. V. 13. № 4. P. 5179–5194.
- Sartorius R., Bettua C., D’Apice L., Caivano A., Trovato M., Russo D., Zanoni I., Granucci F., Mascolo D., Barba P., et al. // *Eur. J. Immunol.* 2011. V. 41. № 9. P. 2573–2584.
- Samoylova T.I., Norris M.D., Samoylov A.M., Cochran A.M., Wolfe K.G., Petrenko V.A., Cox N.R. // *J. Virol. Meth.* 2012. V. 183. № 1. P. 63–68.
- Parmley S., Smith G. // *Gene*. 1988. V. 73. P. 305–318.
- Hamzeh-Mivehroud M., Alizadeh A.A., Morris M.B., Church W.B., Dastmalchi S. // *Drug Discov. Today*. 2013. V. 18. № 23–24. P. 1144–1157.
- Ayat H., Burrone O.R., Sadghizadeh M., Jahanzad E., Rastgou N., Moghadasi S., Arbabi M. // *Biologicals*. 2013. V. 41. № 6. P. 345–354.
- Brunet E., Chauvin C. Choumet V., Jestin J.L. // *Nucl. Acids Res.* 2002. V. 30. № 9. e40.
- Sundell G.N., Ivarsson Y. // *Biomed. Res. Int.* 2014. 2014:176172.
- Azzazy H.M., Highsmith W.E. Jr. // *Clin. Biochem.* 2002. V. 35. № 6. P. 425–445.
- Pande J., Szweczyk M.M., Grover A.K. // *Biotechnol. Adv.* 2010. V. 28. № 6. P. 849–858.
- Derda R., Tang S.K., Li S.C., Ng S., Matochko W., Jafari M.R. // *Molecules*. 2011. V. 16. № 2. P. 1776–1803.
- Noren K.A., Noren C.J. // *Methods*. 2001. V. 23. № 2. P. 169–178.
- Lang Q., Wang F., Yin L., Liu M., Petrenko V.A., Liu A. // *Anal. Chem.* 2014. V. 86. № 5. P. 2767–2774.
- Bedi D., Gillespie J.W., Petrenko V.A. // *Protein Eng. Des. Sel.* 2014. V. 27. № 7. P. 235–243.
- Guo Z., Wang X., Li H., Gao Y. // *PLoS One*. 2013. V. 8. № 10. e76622.

38. Kuramoto K., Yamasaki R., Shimizu Y., Tatsukawa H., Hitomi K. // *Arch. Biochem. Biophys.* 2013. V. 537. № 1. P. 138–143.
39. Frascione N., Codina-Barrrios A., Bassindale A.R., Taylor P.G. // *Dalton Trans.* 2013. V. 42. № 28. P. 10337–10346.
40. Wang W., Chen X., Li T., Li Y., Wang R., He D., Luo W., Li X., Wu X. // *Exp. Cell Res.* 2013. V. 319. № 8. P. 1156–1164.
41. Krumpel L.R., Mori T. // *Int. J. Pept. Res. Ther.* 2006. V. 12. № 1. P. 79–91.
42. Rangel R., Dobroff A.S., Guzman-Rojas L., Salmeron C.C., Gelovani J.G., Sidman R.L., Pasqualini R., Arap W. // *Nat. Protoc.* 2013. V. 8. № 10. P. 1916–1939.
43. Pilch J., Brown D.M., Komatsu M., Järvinen T.A., Yang M., Peters D., Hoffman R.M., Ruoslahti E. // *Proc. Natl. Acad. Sci. USA.* 2006. V. 103. № 8. P. 2800–2804.
44. Pasqualini R., Ruoslahti E. // *Nature.* 1996. V. 380. № 6572. P. 364–636.
45. Wan X.M., Chen Y.P., Xu W.R., Yang W.J., Wen L.P. // *Peptides.* 2009. V. 30. № 2. P. 343–350.
46. Chen H., Chen C.C., Acosta C., Wu S.Y., Sun T., Konofagou E.E. // *PLoS One.* 2014. V. 9. № 10. e108880.
47. Smith M.W., Al-Jayyousi G., Gumbleton M. // *Peptides.* 2012. V. 38. № 1. P. 172–180.
48. Akita N., Maruta F., Seymour L.W., Kerr D.J., Parker A.L., Asai T., Oku N., Nakayama J., Miyagawa S. // *Cancer Sci.* 2006. V. 97. № 10. P. 1075–1081.
49. Chen Y., Shen Y., Guo X., Zhang C., Yang W., Ma M., Liu S., Zhang M., Wen L.P. // *Nat. Biotechnol.* 2006. V. 24. № 4. P. 455–460.
50. Lee N.K., Kim H.S., Kim K.H., Kim E.B., Cho C.S., Kang S.K., Choi Y.J. // *J. Drug Target.* 2011. V. 19. № 9. P. 805–813.
51. Zou J., Dickerson M.T., Owen N.K., Landon L.A., Deutscher S.L. // *Mol. Biol. Rep.* 2004. V. 31. № 2. P. 121–129.
52. Molenaar T.J., Michon I., de Haas S.A., van Berkel T.J., Kuiper J., Biessen E.A. // *Virology.* 2002. V. 293. № 1. P. 182–191.
53. Arap W., Kolonin M.G., Trepel M., Lahdenranta J., Cardó-Vila M., Giordano R.J., Mintz P.J., Ardelt P.U., Yao V.J., Vidal C.I., et al. // *Nat. Med.* 2002. V. 8. № 2. P. 121–127.
54. Zurita A.J., Troncoso P., Cardó-Vila M., Logothetis C.J., Pasqualini R., Arap W. // *Cancer Res.* 2004. V. 64. № 2. P. 435–439.
55. Staquicini F.I., Cardó-Vila M., Kolonin M.G., Trepel M., Edwards J.K., Nunes D.N., Sergeeva A., Efsthathiou E., Sun J., Almeida N.F., et al. // *Proc. Natl. Acad. Sci. USA.* 2011. V. 108. № 46. P. 18637–18642.
56. Laakkonen P., Porkka K., Hoffman J.A., Ruoslahti E.A. // *Nat. Med.* 2002. V. 8. № 7. P. 751–755.
57. Perea S.E., Reyes O., Baladron I., Perera Y., Farina H., Gil J., Rodriguez A., Bacardi D., Marcelo J.L., Cosme K., et al. // *Mol. Cell Biochem.* 2008. V. 316. № 1–2. P. 163–167.
58. Bai F., Liang J., Wang J., Shi Y., Zhang K., Liang S., Hong L., Zhai H., Lu Y., Han Y. // *J. Mol. Med. (Berl.)* 2007. V. 2. P. 169–180.
59. Kang J., Zhao G., Lin T., Tang S., Xu G., Hu S., Bi Q., Guo C., Sun L., Han S., et al. // *Cancer Lett.* 2013. V. 339. № 2. P. 247–259.
60. Dai X., Cai C., Xiao F., Xiong Y., Huang Y., Zhang Q., Xiang Q., Lou G., Lian M., Su Z., et al. // *Biochem. Biophys. Res. Commun.* 2014. V. 445. № 4. P. 795–801.
61. Wang H., Wang H., Liang J., Jiang Y., Guo Q., Peng H., Xu Q., Huang Y. // *Mol. Pharm.* 2014. V. 11. № 10. P. 3352–3360.
62. Stupp R., Weller M. // *Curr. Opin. Neurol.* 2010. V. 23. № 6. P. 553–555.
63. D'Onofrio N., Caraglia M., Grimaldi A., Marfella R., Servillo L., Paolisso G., Balestrieri M.L. // *Biochim. Biophys. Acta.* 2014. V. 1846. № 1. P. 1–12.
64. Corti A., Ponzoni M. // *Ann. N.Y. Acad. Sci.* 2004. V. 1028. P. 104–112.
65. Yang Z., Xiang B., Dong D., Wang Z., Li J., Qi X. // *Curr. Gene Ther.* 2014. V. 14. № 4. P. 289–299.
66. Grifman M., Trepel M., Speece P., Gilbert L.B., Arap W., Pasqualini R., Weitzman M.D. // *Mol. Ther.* 2001. V. 3. № 6. P. 964–975.
67. Larocca D., Burg M.A., Jensen-Pergakes K., Ravey E.P., Gonzalez A.M., Baird A. // *Curr. Pharm. Biotechnol.* 2002. V. 3. № 1. P. 45–57.
68. Shoaee-Hassani A., Keyhanvar P., Seifalian A.M., Mortazavi-Tabatabaei S.A., Ghaderi N., Issazadeh K., Amir-mozafari N., Verdi J. // *PLoS One.* 2013. V. 8. № 11. e79907.
69. Larocca D., Kassner P.D., Witte A., Ladner R.C., Pierce G.F., Baird A. // *FASEB J.* 1999. V. 13. № 6. P. 727–734.
70. Yata T., Lee K.Y., Dharakul T., Songsivilai S., Bismarck A., Mintz P.J., Hajitou A. // *Mol. Ther. Nucl. Acids.* 2014. V. 3. e185.
71. Liu X., Wang W., Samarsky D., Liu L., Xu Q., Zhang W., Zhu G., Wu P., Zuo X., Deng H., et al. // *Nucl. Acids Res.* 2015. V. 42. № 18. P. 11805–11817.
72. Bakhshinejad B., Sadeghizadeh M. // *Exp. Opin. Drug Deliv.* 2014. V. 11. № 10. P. 1561–1574.
73. Ji S., Zheng Y., Czerwinski A., Valenzuela F., Pennington M., Liu S. // *Bioconjug. Chem.* 2014. V. 25. № 11. P. 1925–1941.
74. Reubi J.C., Maecke H.R. // *J. Nucl. Med.* 2008. V. 49. № 11. P. 1735–1738.
75. Haubner R., Maschauer S., Prante O. // *Biomed. Res. Int.* 2014. 2014:871609.
76. Li G., Wang X., Zong S., Wang J., Conti P.S., Chen K. // *Mol. Pharm.* 2014. V. 11. P. 3938–3946.
77. Li Z.J., Cho C.H. // *J. Transl. Med.* 2012. V. 10. Suppl 1. S1.
78. Ellerby H.M., Arap W., Ellerby L.M., Kain R., Andrusiak R., Rio G.D., Krajewski S., Lombardo C.R., Rao R., Ruoslahti E., et al. // *Nat. Med.* 1999. V. 5. № 9. P. 1032–1038.
79. Cieslewicz M., Tang J., Yu J.L., Cao H., Zavaljevski M., Motoyama K., Lieber A., Raines E.W., Pun S.H. // *Proc. Natl. Acad. Sci. USA.* 2013. V. 110. № 40. P. 15919–15924.
80. Mantovani A., Allavena P., Sica A., Balkwill F. // *Nature.* 2008. V. 454. № 7203. P. 436–444.
81. Teesalu T., Sugahara K.N., Kotamraju V.R., Ruoslahti E. // *Proc. Natl. Acad. Sci. USA.* 2009. V. 106. № 38. P. 16157–16162.
82. Sugahara K.N., Teesalu T., Karmali P.P. // *Cancer Cell.* 2009. V. 16. № 6. P. 510–520.
83. Sugahara K.N., Braun G.B., de Mendoza T.H., Kotamraju V.R., French R.P., Lowy A.M., Teesalu T., Ruoslahti E. // *Mol. Cancer Ther.* 2015. V. 14. № 1. P. 120–128.
84. Svensen N., Walton J.G., Bradley M. // *Trends Pharmacol. Sci.* 2012. V. 33. № 4. P. 186–192.
85. Wang X., Li S., Shi Y., Chuan X., Li J., Zhong T., Zhang H., Dai W., He B., Zhang Q. // *J. Control. Release.* 2014. V. 193. P. 139–153.
86. Sugahara K.N., Teesalu T., Karmali P.P., Kotamraju V.R., Agency L., Greenwald D.R., Ruoslahti E. // *Science.* 2010. V. 328. P. 1031–1035.
87. Aina O.H., Sroka T.C., Chen M.L., Lam K.S. // *Biopolymers.* 2002. V. 66. № 3. P. 184–199.
88. Gao H., Xiong Y., Zhang S., Yang Z., Cao S., Jiang X. // *Mol. Pharm.* 2014. V. 11. № 3. P. 1042–1052.
89. Brown K.C. // *Curr. Pharm. Des.* 2010. V. 16. № 9. P. 1040–1054.
90. Laakkonen P., Vuorinen K. // *Integr. Biol. (Camb.)* 2010. V. 2. № 7–8. P. 326–337.

Brain Cholesterol Metabolism and Its Defects: Linkage to Neurodegenerative Diseases and Synaptic Dysfunction

A. M. Petrov*, M. R. Kasimov, A. L. Zefirov

Kazan Medical University, Department of Normal Physiology, Butlerova str. 49, Kazan, Russia, 420012

*Email: Fysio@rambler.ru

Received: 11.09.2015

Copyright © 2016 Park-media, Ltd. This is an open access article distributed under the Creative Commons Attribution License, which permits unrestricted use, distribution, and reproduction in any medium, provided the original work is properly cited.

ABSTRACT Cholesterol is an important constituent of cell membranes and plays a crucial role in the compartmentalization of the plasma membrane and signaling. Brain cholesterol accounts for a large proportion of the body's total cholesterol, existing in two pools: the plasma membranes of neurons and glial cells and the myelin membranes. Cholesterol has been recently shown to be important for synaptic transmission, and a link between cholesterol metabolism defects and neurodegenerative disorders is now recognized. Many neurodegenerative diseases are characterized by impaired cholesterol turnover in the brain. However, at which stage the cholesterol biosynthetic pathway is perturbed and how this contributes to pathogenesis remains unknown. Cognitive deficits and neurodegeneration may be associated with impaired synaptic transduction. Defects in cholesterol biosynthesis can trigger dysfunction of synaptic transmission. In this review, an overview of cholesterol turnover under physiological and pathological conditions is presented (Huntington's, Niemann-Pick type C diseases, Smith-Lemli-Opitz syndrome). We will discuss possible mechanisms by which cholesterol content in the plasma membrane influences synaptic processes. Changes in cholesterol metabolism in Alzheimer's disease, Parkinson's disease, and autistic disorders are beyond the scope of this review and will be summarized in our next paper.

KEYWORDS lipid rafts, neurodegenerative disease, oxysterols, synaptic transmission, cholesterol.

ABBREVIATIONS ABC -ATP-binding cassette transporters; ACAT1 -acetyl coenzyme A cholesterol acyltransferase; ApoE - apolipoprotein E; BDNF - brain derived neurotrophic factor; HMGCoA -3-hydroxy-3-methylglutaryl-coenzyme A; HC - hydroxycholesterol; BBB - blood-brain barrier; Dhcr7 -7-dehydrocholesterol reductase; LDL-receptor - low-density lipoprotein receptor; LRP -LDL-receptor related protein; LX-receptor - Liver X receptor; MCD - methyl- β -cyclodextrin; CYP46A1 - cholesterol 24-hydroxylase; CYP27A1 -cholesterol 27-hydroxylase; CYP7B1 - oxysterol 7 α -hydrolase; ER - endoplasmic reticulum

CHOLESTEROL RECYCLING IN THE BRAIN

The pools of cholesterol in the brain

Cholesterol is a major lipid component of brain cell membranes, accounting for 23–25% of the body's total cholesterol content. The brain has cholesterol content at 15–30 mg/g tissue, whereas the average in other tissues is at 2–3 mg/g tissue [1]. In the central nervous system (CNS), cholesterol has a number of essential functions. Cholesterol-enriched myelin sheaths serve as an insulation layer increasing nerve conduction velocity. Cholesterol is abundantly present in the synaptic membranes to aid in nerve signal transmission. Cholesterol deficiency has been shown to inhibit dendrite growth [2, 3].

A total of over 30 enzymes catalyze the synthesis of cholesterol in mammals. Outside the CNS, cholesterol can be synthesized *de novo* (about 50–60%), or it can be

obtained from the diet (lipoprotein-bound). However, the blood brain barrier (BBB) prevents the uptake of lipoprotein-bound cholesterol from the circulation. Most brain cholesterol (over 95%) comes from *in situ* synthesis mainly in glial cells [1]. Increased permeability of BBB to sterol molecules is related to BBB impairment [4]. Partial disruption of BBB may be a result of aging. In addition, the function of the BBB can be significantly affected in neurodegenerative disorders, which can ultimately lead to pathological conditions [5, 6]. Using pericyte-deficient mice, which are critical to BBB functioning, an age-related progressive neurodegenerative disease was observed [4, 6].

Brain cholesterol is found in two major stores. The smaller one is subject to relatively fast turnover rates (half-life of 5–10 months, 8 mg/g) and made up by the plasma membranes of neurons (10%) and glial cells (20%). The larger pool of CNS cholesterol (70%) is in

myelin (40 mg/g) with very slow turnover (half-life of approximately 5 years) [7]. The rate of cholesterol synthesis is highest during the period of active myelination by oligodendrocytes (the first few weeks/months after birth). Oligodendrocytes use ketone bodies as precursors for lipid synthesis (ketone-metabolizing enzymes), whose plasma levels are 10-fold increased during myelin sheath formation. Cholesterol-deficient oligodendrocytes show dependence on the local supply of extracellular cholesterol, dramatically reducing CNS myelination [8]. Following myelination the production of cholesterol drops by 90%, and in the mature brain it only occurs in astrocytes and neurons, albeit at a 5-fold slower rate than in astrocytes [1]. Neuronal cholesterol biosynthesis plays a crucial role in the survival and differentiation of axons and dendrites, and formation of non-efficient synapses. The *de novo* synthesis of cholesterol in neurons can be upregulated by the brain-derived neurotrophic factor (BDNF) [9]. This period of extensive synapse formation (particularly, presynaptic terminals away from the soma) requires astrocyte-derived cholesterol. Cultured neurons elicit a 10-fold increase in excitatory synaptic transmission and generate 5–7 fold greater synapses in the presence of astrocytes, suggesting a role for astrocyte-derived cholesterol in neuronal function. Overall, the synthesis of cholesterol by neurons is essential to the developing brain, whereas in the adult brain neurons rely on external sources of cholesterol [1, 7].

Regulation of cholesterol synthesis

De novo cholesterol synthesis begins with the transformation of acetyl-CoA into 3-hydroxy-3-methylglutaryl-coenzyme A (HMG-CoA) via a reaction catalyzed by HMG-CoA synthetase and then by HMG-CoA reductase into mevalonate. The HMG-CoA reductase-catalyzed formation of mevalonate is an irreversible and rate-limiting step in the cholesterol biosynthesis, targeted by statin drugs. There are two cholesterologenic pathways in the brain (*Fig. 1*). Neurons mainly contain sterols synthesized via the Kandutsch-Russel cholesterol synthetic pathway (7-dehydrocholesterol, lanosterol), and astrocytes contain precursors of the Bloch pathway (desmosterol) [10]. The machinery of cholesterol synthesis resides in the endoplasmic reticulum (ER). The cholesterol content in the ER shows greater variations than in plasma membranes. Indeed, the cholesterol environment in the ER influences the total cholesterol levels in the cell. One of the key players in cholesterol regulation is SREBP-2 (sterol-regulatory element-binding protein), an inactive transcription factor anchored to the ER membrane and capable of binding to SCAP (SREBP cleavage-activating protein), which functions as a detector of cholesterol due to a

sterol-sensing domain. During high cholesterol concentrations, the SREBP-2/SCAP complex is retained in the membranes of the ER by the retention proteins INSIG-1 and -2 (insulin-induced protein 1 and 2). In sterol-depleted cells, the interaction between the INSIG retention complex and SREBP-2/SCAP is lost, allowing SCAP to escort SREBP-2 to the Golgi compartment. Within this organelle, SCAP releases the N-terminal domain of SREBP-2, which translocates to the nucleus to bind sterol regulatory elements (SRE) in the promoter regions of over 30 target genes encoding enzymes of cholesterol biosynthesis (*Fig. 2*) [1, 10–12].

SCAP knockout mice show a 30–40% reduction in brain cholesterol synthesis, leading to defects in synaptic transmission [13]. Disruption of the SCAP gene in astrocytes results in microcephaly, motor deficits and behavioral dysfunctions, which could be partially rescued by the uptake of dietary lipids [14]. Schwann cell SCAP mutant mice exhibit congenital hypomyelination and neuropathy-related behavior, tremor, and abnormal gait [15]. The inhibition of cholesterol synthesis reduces the expression of cholesterol-binding proteins, such as myelin proteins [8].

Newly synthesized cholesterol leaves the ER by vesicular and non-vesicular mechanisms (by means of carrier proteins) and is targeted to the plasma membrane, thus maintaining a low ER cholesterol content. The trafficking between membranes through direct contact sites seems to be the easiest way to make cholesterol available to extracellular acceptors [11, 16].

Deposition and cholesterol esters

A surplus of cholesterol in neurons and other cell types is stored in the form of esters. Cholesterol esters constitute ~1% of the total cholesterol pool in the adult brain and exist as lipid droplets. A transient increase in esterified cholesterol concentrations, which accounts for over 5% of total cholesterol, is detected in a specific region of the brain at the onset of myelination. Cholesterol esters are a reserve pool of cholesterol and fatty acids which is utilized for the formation of myelin sheaths and synaptic contacts. The accumulation of cholesterol esters as cytoplasmic lipid droplets can result from increased Acyl-CoA cholesterol acyltransferase 1 gene expression (ACAT1, also named SOAT1), upregulated in response to high cholesterol levels in the ER. ACAT1 ablation leads to a decreased (by 86%) level of cholesterol esters. Conversely, neurotoxic agents and oxidative stress enhance ACAT1 activity [17]. ACAT1 is more abundantly expressed in neurons as compared to glial cells. Importantly, in astrocytes, ACAT1 is activated following impaired cholesterol efflux or in the presence of an excess of exogenous cholesterol [18]. Substrates for cholesterol esterification are provided

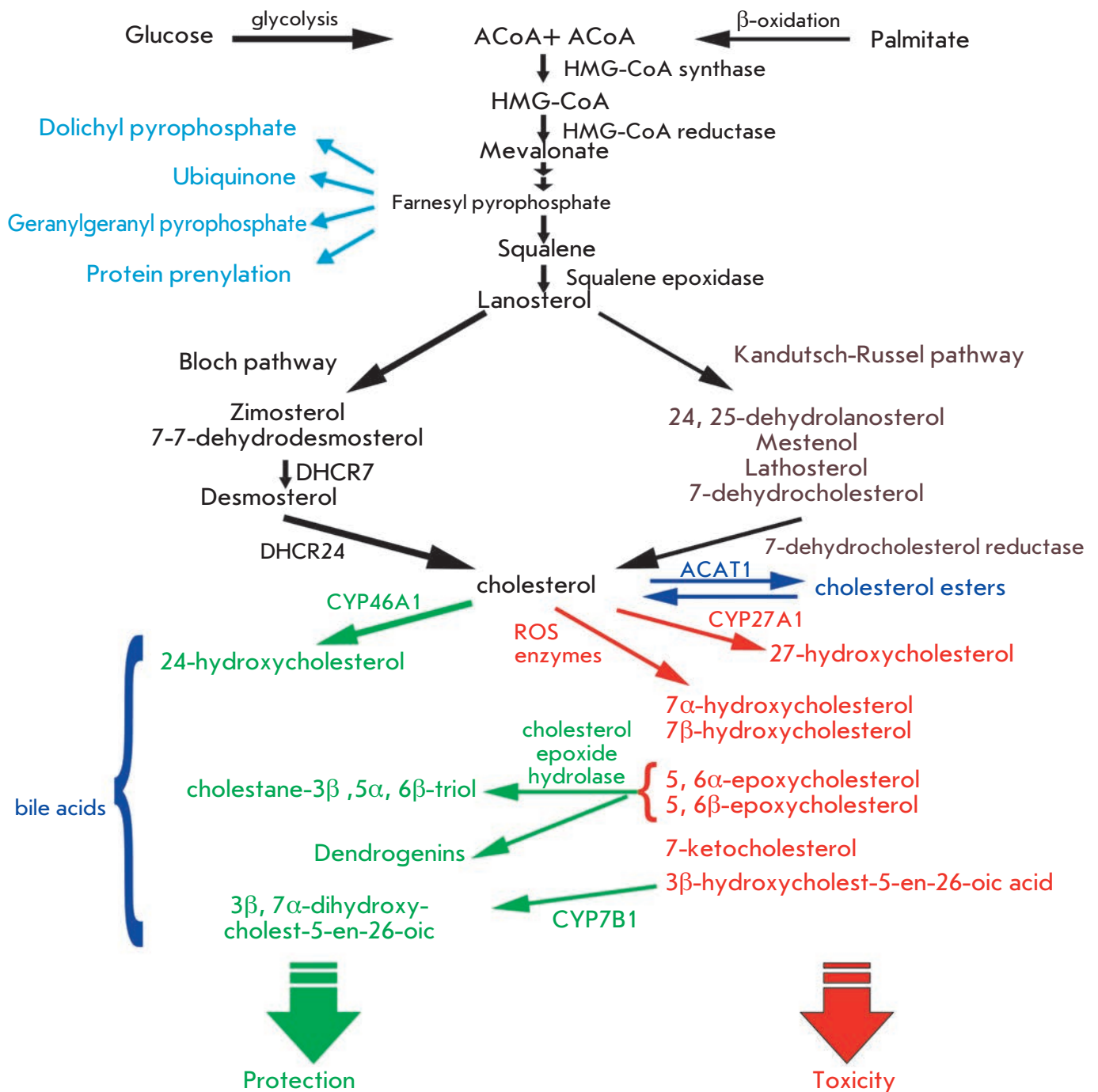


Fig. 1. Cholesterol synthesis and oxysterol formation. Cholesterol is produced from acetyl-coenzyme A in a multistage enzymatic process. There are two pathways for cholesterol synthesis; the Bloch and Kandutsch-Russel pathways. *De novo* synthesized cholesterol can accumulate as cholesterol esters or be modified by enzymic or non-enzymic oxidation into oxysterols. A wide array of oxysterols have been described, each of which may have a specific effect on cellular functions. See text for a detailed explanation.

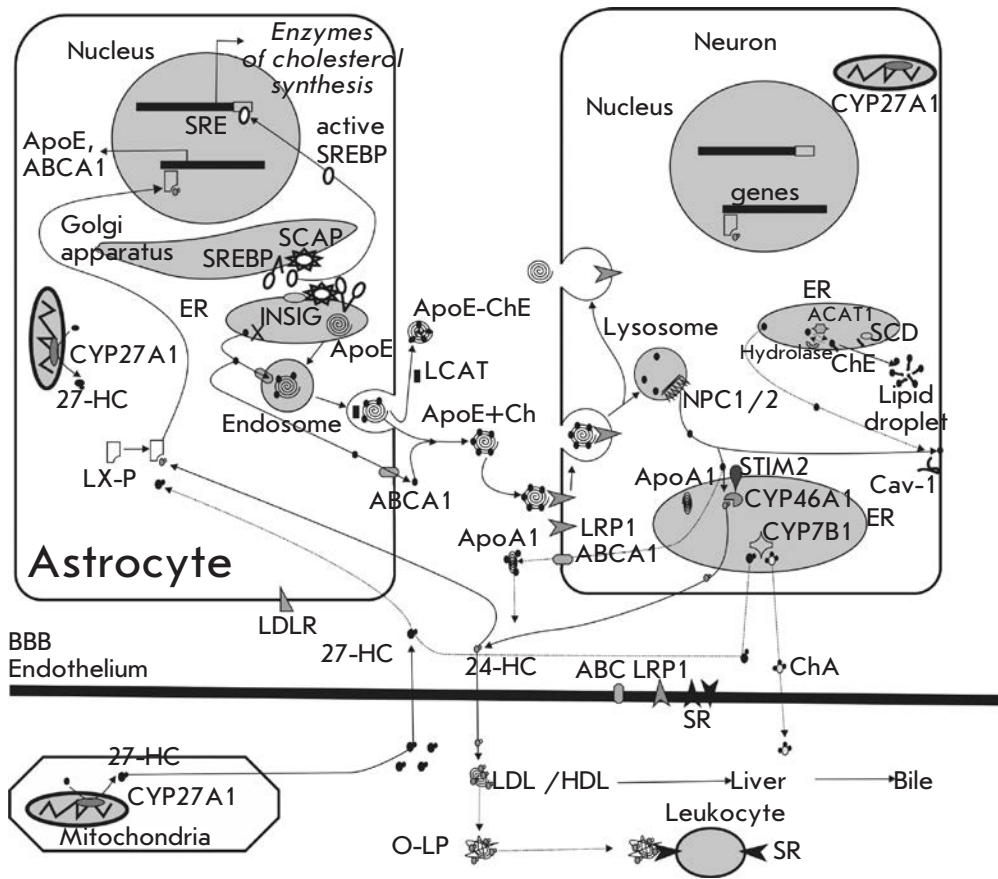


Fig. 2. Brain cholesterol metabolism: neuron–glial interplay. The major input of cholesterol into the brain comes from *in situ* synthesis in the endoplasmic reticulum (ER) of astrocytes. The proteins INSIG, SREBP, and SCAP regulate the cholesterol biosynthetic machinery. These proteins are tightly associated and retained in the ER at high levels of sterols. When sterol levels drop below a threshold, the complex dissociates, allowing SREBP and SCAP to translocate to the Golgi apparatus. Within this organelle, SCAP cleaves SREBP, releasing the active transcription factor, which then migrates to the nucleus to activate the genes involved in cholesterol synthesis and trafficking. Lipoprotein particles, including apolipoproteins E (ApoE), assembled in the ER are targeted to endosomes for secretion into the extracellular space. Newly synthesized cholesterol is transported from the ER to endosomes or extracellular space by non-vesicular mechanisms via ATP-binding cassette transporters (ABCA1). Cholesterol-rich ApoE-particles interact with the neuronal receptors (LRP1), undergo internalization by receptor-mediated endocytosis, and are routed to late endosomes/lysosomes. Once there, NPC1 /2 proteins promote trafficking of cholesterol to the plasma membrane or the ER. The supply of the plasma membrane with cholesterol requires caveolin-1 (Cav-1). Membrane cholesterol could be processed by CYP46A1 to 24-hydroxycholesterol (24-HC), which passes through the blood-brain barrier (BBB) and binds to light or high density lipoproteins (LDL or HDL). Increased plasma levels of 24-HC can oxidize the plasma lipoproteins (O-LP) that are then accumulated in leukocytes via scavenger receptor (SR) mediated endocytosis. Binding of 24HC to the cytoplasmic LX-receptors of astrocytes (or neurons) triggers expression of the genes (ApoE and ABCA1) involved in cholesterol trafficking from astrocytes to neurons. A certain amount of cholesterol can exit the brain through the BBB in the form of ApoA1-particles. Elevated cholesterol content in the ER upregulates an ACAT1-dependent generation of cholesterol esters, which build up in the cytoplasm as lipid drops. SCD (stearoyl-CoA desaturase) supplies the mono-unsaturated fatty acids required for cholesterol esterification. Accumulation of cholesterol esters (as ApoE-particles, ApoE-ChE) in the extracellular space is associated with LCAT (lecithin–cholesterol acyltransferase) activity secreted by astrocytes. Mitochondria of many cells (in particular, macrophages) have the enzyme CYP27A1 that catalyzes the conversion of cholesterol to 27-hydroxycholesterol (27-HC) that could transverse the BBB and less effectively (as compared to 24-HC) activate LX-receptors. The neuronal enzyme CYP7B1 can convert 27-HC to 7 α -hydroxy-3-oxo-4-cholestenoic acid (ChA) cleared from the brain into the circulation. Although the BBB is not permeable to plasma cholesterol, BBB endothelial cells make possible cholesterol flux across the BBB via ABC transporters and LRP1 and SR.

by stearoyl-CoA desaturase, an ER enzyme that catalyzes the biosynthesis of monounsaturated fatty acids from saturated fatty acids [11].

Cytosolic cholesterol esters undergo degradation by hydrolyses. The concentration of cholesterol esters in the brain is maintained at a low level, and cholesterol hydrolase can convert the esters back to unesterified cholesterol. When cholesterol ester levels are dramatically raised, the enzyme fails to keep up with the cholesterol influx, allowing cholesterol ester droplets to build up in neuronal cytoplasm [1].

Intercellular cholesterol trafficking

The CNS cholesterol is transported to neurons via particles containing apolipoproteins (mainly ApoE, 39 kDa) and lipids. Astrocytes are the major source of cholesterol and apolipoprotein E (ApoE), which together with phospholipids forms lipoprotein complexes (ApoE-particles) (*Fig. 2*). The core of ApoE-particles is assembled in the ER, and the lipidation and secretion of ApoE are mediated by one or several ATP-binding cassette transporters (ABC), such as ABCA1, ABCG1, and ABCG4 [19–21]. ABCA1 catalyzes the transfer of cellular lipid to lipid-free apolipoproteins to generate nascent particles that undergo further lipidation, followed by ABCG1/ABCA1-mediated export from the cell [22]. Lipid-poor particles (for example, in the case of ABCA1 deficiency) show higher degradation rates, which leads to reduced ApoE levels in the brain. Mice in which ABCA1 has been specifically knocked out in the brain demonstrate cortical astrogliosis, increased inflammatory gene expression, as well as altered synaptic transmission and sensorimotor behavior [23].

Lipoproteins are mainly targeted at neurons that are taken up by receptors belonging to the family of low-density lipoproteins (LDL): LDL-receptors and LDL-receptor-like proteins (LRP, LRP1B, LRP2/megalin, LRP4, LRP5/6, LRP8/APOER2, LRP11/SORL1). These receptors also bind the proteins involved in brain development (Sonic hedgehog, Wnt, reelin), including proteases, protease inhibitors (α_2 -macroglobulin), vitamin transporters, chaperones, and proinflammatory molecules [21]. LRP1 is an important receptor for ApoE-particles. It has a high transport capacity for ApoE due to the elevated rates of endocytic recycling (*Fig. 2*). LRP1 is primarily expressed in neurons; and the LDL-receptor – in glial cells [24]. Ablation of LRP1 function in neurons leads to global impairment of cholesterol homeostasis and neurodegeneration [25]. Following receptor-mediated endocytosis, vesicles deliver lipid particles to late endosomes/lysosomes. Immediately after endocytosis, ApoE is detached from lipid components and is not targeted at lysosomes but recycles back to the plasma membrane (*Fig. 2*) [26]. The

liberated cholesterol exits late endosomes/lysosomes via NPC1- and NPC2-mediated pathways to reach the plasma membrane or the membrane of the ER, whereby the cholesterol content regulates the genes involved in cholesterol homeostasis via negative feedback (the SREBP-2/SCAP/INSIG-1 pathway) [16]. Within the endolysosome, cholesterol seems to be bound first by NPC2 (transmembrane protein), and then by NPC1 (intraluminal protein). In the bound state, cholesterol is shielded from the aqueous environment, followed by intracellular trafficking to the plasma membrane or the ER [27].

The interaction between ApoE-particles and receptors triggers multiple signaling networks essential to neuron survival and function [20, 21]. For example, ApoE upregulation in glial cells can accelerate nerve repair by 150-fold [28].

Cholesterol excretion from the brain. Oxysterols

Cholesterol is eliminated at a rate of 1g/day as bile acids (0.5 g) and cholesterol (0.5 g), as such, or coprostanol, a bacterially modified form. The brain lacks pathways for cholesterol degradation. However, cholesterol is exported from the brain at a rate of 6–12 mg/day (0.02–0.04% of total cholesterol turnover) [1] in the form of the brain-specific 24(S)-hydroxycholesterol (24-HC, 6–8 mg/day). The flux of 24-HC (in brain homogenate, 30 μ M) out of the brain takes place by passing through the BBB (via diffusion or the anion transporting polypeptide 2, oatp2). Once in the circulation, it binds to LDL, is taken up by hepatocytes, and excreted in bile salts [7]. A small portion of cholesterol is removed from the brain as ApoE/A-particles via the BBB. Neuronal ABCA1 effluxes excess cholesterol to lipid-poor ApoA1, which are then transported through the BBB via LRP1 and scavenger receptor class B type 1 (SR1B) [29]. The upregulation or downregulation of neuronal ABCA1 expression can increase or reduce the cholesterol efflux, respectively [20].

The 24-HC production occurs by the action of cholesterol-24-hydroxylase (CYP46A1), which is normally expressed in cell bodies and dendrites of nerve cells (large pyramidal cells of cortical areas, hippocampal cells, amygdale cells, putamen cells, thalamic cells, Purkinje cells) (*Fig. 2*) [7]. In disease or after trauma, CYP46A1 can be detected in non-nerve cells (astrocytes, microglia, macrophages) [11]. The brain-derived cholesterol metabolite 24-HC (as other oxysterols) stimulates the nuclear liver X receptor in astrocytes and neuron, inducing the expression of the proteins required for cholesterol biosynthesis and transport (ABCA1, ApoE). Following on from this, increased cholesterol excretion from the brain activates the mechanisms of *de novo* cholesterol synthesis and supply to

neurons. When cholesterol levels in the ER membrane rise above a threshold, the expression of CYP46A1 is enhanced [1]. Overall, the brain engages in a rhythmic process of synthesis and export of cholesterol. However, using mice negative for CYP46A1 in the brain (CYP46A1 $-/-$ mice, in which 24-HC levels were reduced by 95% when compared to 24-HC levels in wild-type mice), it was found that cholesterol levels remained fairly stable due to a 40–50% reduction in cholesterol production [7]. Overexpressing CYP46A1, which produces larger amounts of 24-HC, left cholesterol levels unaffected due to increased cholesterol synthesis [30]. The conversion of cholesterol into 24(S)-hydroxycholesterol in neurons is regulated by cholesterol etherification: therefore, ACAT1 gene ablation that reduces total brain cholesterol content by 13% increases 24-HC levels by 32% [17].

CYP46A1 can be activated by increased synaptic transmission. As early as 30 min after synaptic activity, the membrane cholesterol content in the glutamatergic synapse declines marginally but statistically significantly because of 24-HC release into the extracellular space. CYP46A1 moves from the ER to the plasma membrane and switches to the activated state. The activation depends on increases in cytosolic Ca²⁺ levels and STIM2, which detects changes in Ca²⁺ content stored in the ER [31]. Ageing is associated with increased production of reactive oxygen species that upregulate CYP46A1 expression, thus depleting cholesterol from synaptic membranes [32].

The other oxysterol is 27-HC, one of the major oxysterols in human circulation. Human physiological levels range typically from 0.15–0.73 μ M, but under pathological conditions (e.g., atherosclerosis) they can reach millimole levels [33]. All body cells are involved in the synthesis of 27-HC, taking place in mitochondria via CYP27A1 (Fig. 2). Neurons, astrocytes and oligodendrocytes are capable of producing 27-HC, although to a very low extent. Clearance of 27-HC out of the brain occurs through the BBB [34]. However, 27-HC produced in peripheral tissues can gain access to the brain (5 mg/day). The normal ratio of 27-HC to 24-HC is 1 to 8 in the frontal cortex, 1 to 5 in the occipital cortex, and 1 to 10 in basal ganglia [35]. Oxysterol-7 α -hydrolase (CYP7B1) catalyzes the conversion of 27-HC to 7 α -hydroxy-3-oxo-4-cholestenoic acid, which is eliminated via the BBB [1]. High 27-HC levels have been affiliated with hypercholesterolemia and oxidative stress [34]. Under oxidative stress conditions most brain cholesterol is metabolized into 27-HC, building up in the brain and increasing the risk of neurodegenerative diseases [33].

25-Hydroxycholesterol is a cholesterol metabolite that is produced and secreted by macrophages. The

synthesis is catalyzed by cholesterol-25-hydrolase residing in the ER. In tissues (including nerve cells) the expression of the enzyme is upregulated in response to innate immunity stimuli. Recent studies have reported that 25-HC has an antiviral effect and promotes cholesterol esterification by increasing ACAT1 activity. The brain levels of 25-HC are approximately 1 μ M and can be locally elevated in neurodegenerative disorders. It should be kept in mind that, tracing amounts of 25-HC can be synthesized by CYP46A1 and CYP27A1, and metabolized by CYP7B1 [36].

CHOLESTEROL PATCHES IN THE BRAIN

Brief characteristics of lipid rafts

The plasma membrane organization of nerve cells has a more profound effect on cellular functionality than that of other cell types. Neurons and, to a lesser extent, glial cells are highly polarized cells having distinct membrane compartments: axon, dendrites, synaptic membranes, myelin sheaths, nodes, etc. Even within one membrane domain molecules are arranged in microdomains, termed lipid rafts, enriched in cholesterol and sphingolipids. Cholesterol functions as a dynamic “glue” that holds the microdomain assembly together [37]. Sphingolipids (in particular, glycolipids) are structurally variable, and certain neuron populations and glial cells can contain rafts composed of different glycolipids. During brain development and neural differentiation, a wide variety of glycolipids are increasingly expressed [3]. The impaired synthesis of complex glycolipids in neurons causes severe neural and synaptic defects, which ultimately ends up with death within 3 weeks of birth [38]. In general, the lipid composition of rafts in the brain varies with the area, cell type, and developmental stage. Certain rafts can contain protein components (receptors, ion channels, exo- and endocytic proteins, enzymes), which are recruited into lipid rafts to form signaling complexes/specialized subcompartments [3, 24]. High cholesterol content/raft density is one of the reasons behind the poor diffusion of proteins in synaptic membranes as compared to other cell types [39]. When cholesterol and sphingolipids levels are high in the membrane, lipid rafts coalesce into larger (micrometer-scale) and more stable raft clusters (platforms). Rafts are brought together by oligomerization of raft proteins by extracellular ligands (for example, growth factor) or cytoplasmic scaffolds. Phosphorylation increases the number of protein–protein interactions, which eventually influences the clustering. The merger of rafts is essential to membrane transport, signaling, and other cellular processes [3].

Rafts are associated with numerous proteins that have been implicated as regulators of signal transduc-

tion, including caveolins. The central segment of caveolin proteins contains the scaffolding domain that binds metabotropic receptors, G-proteins, NO-synthase, adenylyl cyclase, phosphoinositol-3-kinase, MAP- and Src-kinases, protein kinase A and C [40]. In neurons, caveolin 1 is colocalized with the postsynaptic scaffolding protein PSD-95 and NMDA glutamate receptors. Caveolin-1 knockout mice exhibit a loss of synapses [41]. Cerebral ischemia may disrupt the caveolin-associated signaling complexes present in neurons. Elevated caveolin-1 expression leads to an increase in the activity of the signaling molecules that encourage the survival and growth of brain cells, conferring resistance to ischemic damage [40].

Lipid rafts and intrinsically disordered proteins

Proteins that lack a globular structure have been recognized and termed intrinsically disordered proteins. These proteins are highly abundant in eukaryotic proteomes, known as an unfoldome, and implicated in important cellular processes, such as signaling and membrane trafficking [42, 43]. The family of intrinsically disordered proteins includes α -synuclein, the amyloid precursor protein (APP), prion proteins (PrP), huntingtin protein (Htt), and tau protein. The structural organization of these proteins depends on the environment and is highly variable. Under certain conditions (overexpression, mutations, disfavored environment) α -synuclein, APP, and PrP are prone to acquiring a pathologic conformation. It is hypothesized that plasma membranes induce conformational changes of normal proteins into pathological forms. Once docked on the plasma membranes, the proteins are aggregated to form toxic oligomers. The amyloid- β peptide (proteolytically processed APP), α -synuclein, and PrP recognize specific components localized in lipid rafts, thereby further triggering their aberrant clustering [44]. The amyloid- β peptide can bind to glycosphingolipids (GM1 ganglioside, GM1 asialo-ganglioside, galactosyl ceramide) and cholesterol, α -synuclein to GM1 and GM3 gangliosides, PrP to sphingomyelin, galactosyl ceramide, GM1, and GM3 gangliosides [42]. These lipid raft components prevail in synaptic membranes [45]. The local pH value, cholesterol content, and membrane fluidity influence the strength of the interaction and aggregation state (globular or fibrillary), which ultimately determines the toxicity of the aggregate. Cholesterol increases or reduces the binding to sphingolipids containing non-hydroxylated/hydroxylated acyl groups. When GM1 ganglioside levels rise and the cholesterol and protein content drops in lipid rafts, the amyloid- β peptide assembles to form toxic fibrils on the plasma membrane, whereas an increase in membrane cholesterol concentrations inhibits the aggregation of

the amyloid- β peptide [46]. Plasma membranes can mediate the transition of mature amyloid fibrils (with low toxic effects) into neurotoxic protofibrillar forms [47]. In other words, amyloid plaques, which contain inert plaque filaments, can be resolubilized into less longer structures – the soluble amyloid protofibrils. Oligomerized amyloid- β peptides contain a structural domain capable of binding to lipid raft-associated receptors such as NMDA glutamate receptors, mGluR5 Metabotropic Glutamate Receptor, and PrP. Oligomer binding triggers the clustering of specific lipid raft proteins into aberrant pathogenic platforms at the synapse [24, 44]. Furthermore, intrinsically disordered proteins themselves can exert deleterious effects on rafts and membranes, e.g., by depleting membrane cholesterol [42, 43].

CHOLESTEROL AND SYNAPTIC TRANSMISSION

A schematic representation of signal transduction at the synapse is illustrated in *Fig. 3*. The presynaptic nerve terminals contain vesicles filled with neurotransmitters. In response to the action potential-driven Ca^{2+} influx, through potential-dependent Ca^{2+} channels, synaptic vesicles fuse with the presynaptic membrane (exocytosis), allowing the neurotransmitter to diffuse across the synaptic cleft. Following release onto the postsynaptic membrane, the neurotransmitter activates and alters the postsynaptic membrane potential. The synaptic transmission is one of the highly ordered cell processes. The efficiency of signal transduction lays the basis for integrative phenomena and can support the survival and function of neurons [37].

Presynaptic mechanisms and cholesterol

The role of cholesterol in presynaptic processes that regulate the release of a neurotransmitter is linked to the impact on membrane biophysics, the direct interaction with the proteins implicated in exo- and endocytosis, and the contribution to lipid raft formation.

Synaptic vesicle exocytosis induces membrane curvature stress, the extent of which is determined by the lipid composition of the membrane. Cholesterol, constituting 40% of total lipids in synaptic vesicles, serves as a scaffold to stabilize the curved membrane domains formed during vesicle fission and budding [48]. The apparently fast transbilayer diffusion of cholesterol (flip-flop) contributes to the relaxation of the bending energy and formation of fusion pores. Cholesterol promotes membrane merging by interacting with vesicular (synaptophysin) and presynaptic (syntaxin-1) proteins [37, 49]. The exocytic sites and membrane vesicles contain cholesterol-enriched lipid rafts [45]. The other constituents of lipid rafts are key vesicle proteins, such as the proton pump, synaptophysins, synaptotagmins, syn-

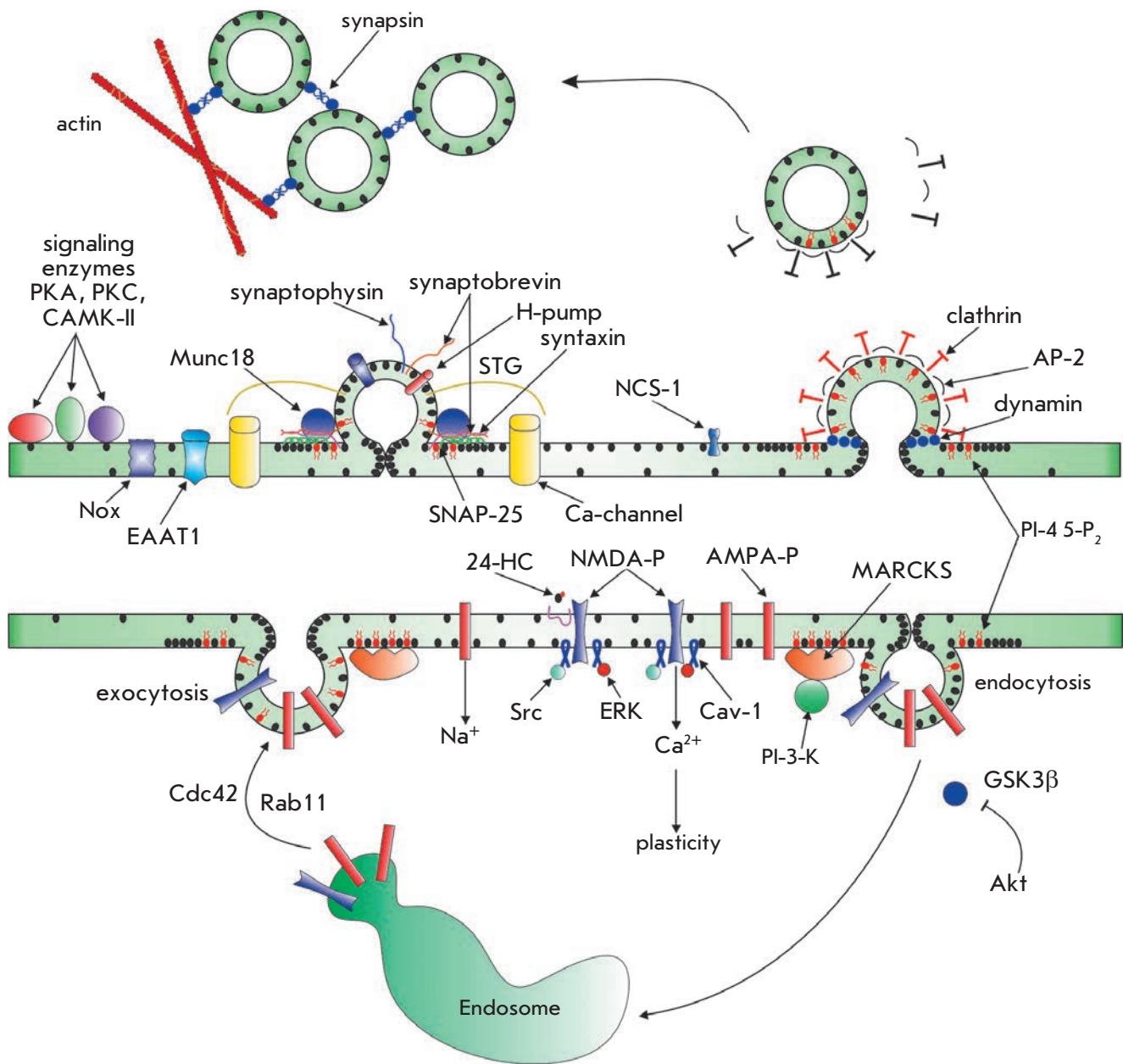


Fig. 3. Synaptic transmission: lipid-protein interactions. The neurotransmitter is released from the synaptic vesicles upon fusion (exocytosis) with the presynaptic membrane at a specific site (termed active zone) in response to Ca^{2+} influx via potential-gated Ca-channels. The vesicle fusion is governed by proteins forming a SNARE complex (synaptobrevin, syntaxin, SNAP-25) and is dictated by numerous cholesterol-binding proteins (synaptotagmin, Munc-18, NCS-1) and signaling molecules (protein kinases, NADPH-oxidase/Nox). After fusion, the protein and lipid components of the vesicles undergo clathrin-mediated endocytosis. The vast majority of synaptic vesicles form the reserve pool, which maintains neurotransmission during prolonged synaptic activity. These vesicles are translocated into the active zone through an actin-and synapsin-dependent pathway. Glutamate released from the synaptic vesicles changes the $\text{Na}^+/\text{Ca}^{2+}$ conductivity of the postsynaptic membrane by activating AMPA/NMDA receptors. The surface expression of the postsynaptic receptors is dependent on the exo-and endocytotic trafficking of these receptors, which is regulated by small GTPase (Rab11) and protein kinase (Cdc42, GSK3 β , phosphoinositol-3-kinase/PI-3-K). The receptor-dependent signaling is associated with many proteins (Src, ERK, Cav-1). As illustrated in Fig.2. Cholesterol molecules and its clusters are shown in black, phosphoinositol-4,5-bisphosphates (PI-4,5-P₂) in red, and cholesterol/PI-4,5-P₂-binding proteins. See text for a detailed explanation.

apophysins, SV2 and presynaptic membrane exocytic proteins, such as syntaxin, SNAP-25, synaptobrevin, Munc18, and potential-dependent Ca-channels [50]. The efficiency of exocytosis depends on the association of exocytic proteins with the lipid rafts. Syntaxin isoforms can cluster into isoform-specific patches in the plasma membranes, depending on the cholesterol content that defines the functional properties of sites where exocytosis occurs [51]. It is likely that membrane fusion steps are driven by the merger/separation of certain rafts. For example, although potential-dependent Ca-channels and SNARE-proteins, on the one hand, and NCS-1 protein (neuronal calcium sensor 1) that increases Ca-channel activity, on the other hand, localize to different microdomains, coalescence of these rafts favors exocytosis by clustering the proteins [52]. Ceramidase mutants, named 'slug-a-bed'(slab), exhibit impaired cholesterol distribution in the presynaptic membrane with strong reduction (by 70%) in vesicle fusion. Anion lipids and phosphatidylinositol 4,5-bisphosphates may accumulate in lipids, affecting exocytic proteins and membrane reshaping [49]. The oxysterol 5 α -cholestan-3-one disrupts the integrity of lipid rafts at the synapse, inhibits exocytosis, and decreases the number of vesicles available for neurotransmission [53]. In general, even mild cholesterol depletion reduces the evoked neurotransmitter release during both low- and high-frequency activity [54, 55]. Disorders in cholesterol metabolism negatively affect clustering of synaptic vesicles and the ion currents that contribute to the action potential [56, 57].

Membrane cholesterol specifically potentiates the evoked exocytosis, whereas, conversely, spontaneous release of synaptic vesicles is arrested by cholesterol [54, 55, 58]. It cannot be ruled out that cholesterol controls spontaneous synaptic vesicle release by preventing excess both the protein kinase activity (such as A, C, CAMK II) and the NADPH-oxidase-ROS-TRPV1-channel-Ca²⁺-calcineurin pathway activation [58–60]. For this reason, spontaneous exocytosis is sensitive to membrane cholesterol reduction, which via enhancement of spontaneous release ultimately depletes the population of synaptic vesicles, induces neurotransmitter receptor desensitization, and downregulates local protein biosynthesis. In addition, changes to the membrane cholesterol content increase non-vesicular neurotransmitter release at periphery and central synapses [61, 62].

Endocytosis of synaptic vesicles. Endocytosis of synaptic vesicles prevents synaptic vesicle pool depletion. Following endocytosis, vesicles are refilled with the neurotransmitter and recycle. Cholesterol regulates membrane invagination during endocytosis [37, 49].

Cholesterol-rich membrane domains contribute to the activation of endocytic proteins [50]. It is thought that the lipid rafts in the vesicular membranes prevent the mixing of vesicle proteins with presynaptic proteins to maintain proper sorting [45]. Raft phosphoinositides are implicated in the triggering of endocytic events and clustering of vesicular coat proteins [49]. Even slight cholesterol extraction from vesicle membranes blocks endocytosis and traps vesicular proteins in the plasma membrane [54, 62].

Postsynaptic events and cholesterol

Changes to the number and content of postsynaptic receptors are critical to synaptic plasticity, occurring through both lateral diffusion (between postsynaptic and extrasynaptic sites) and endo-exocytic traffic of these receptors (*Fig. 3*). Receptor trafficking is regulated by interaction with scaffold proteins and membrane lipid constituents [3]. Receptor activity and downstream signal transduction also depend on the membrane cholesterol content. Most postsynaptic receptors colocalize with lipid rafts [2, 3, 11, 12]. The postsynaptic density is a macromolecular assembly composed of the proteins responsible for postsynaptic signaling and membrane plasticity, attached to the lipid rafts [39, 63]. In this review, we will focus on AMPA- and NMDA-glutamate receptors.

Acute cholesterol depletion inhibits both currents through AMPA-receptors and AMPA receptor exocytosis [64]. Chronic depletion of cholesterol or sphingolipids upregulates constitutive AMPA receptor internalization [63]. Conversely, there is evidence that cholesterol reduction by 25% in naturally aging neurons causes accumulation of AMPA receptors on the cell surface, due to impaired endocytosis and lateral diffusion. In this scenario, cholesterol loss seems to provoke the detachment of MARCKS from membrane phosphoinositol-4,5-bisphosphates, which are then catalyzed by phosphoinositol-3-kinase into phosphoinositol-3,4,5-triphosphates that stabilize F-actin and increase Akt kinase activity. F-actin restricts post-synaptic AMPA-receptor mobility, and Akt kinase suppresses the glycogen synthase kinase 3 β (GSK3 β) implicated in AMPA-receptor endocytotic trafficking [12].

The oligomerization of NMDA-receptors is favored by their localization in rafts. Cholesterol depletion inhibits Ca²⁺ influxes via NMDA-receptors, promotes their desensitization, and suppresses long-term potentiation in the hippocampus [65]. Conversely, 24-HC allosterically potentiates an NMDA receptor-mediated response, facilitating long-term potentiation in hippocampal slices. Interestingly, 25-HC (in a submicromolar range) counteracts the effect of 24-HC [66]. The influx of Ca²⁺ through NMDA-receptors can drive both

synaptic plasticity and cell death (excitatory toxicity), depending on the amplitude of Ca^{2+} influx and receptor colocalization (within or outside rafts, in synaptic or extrasynaptic space). NMDA-receptors associated with rafts interact with caveolin-1, which is required for inducing the Src-kinase/ERK-kinase pathway to promote survival in neurons. Hence, their contribution to excitatory toxicity is minimized. Upon long-term exposure to agonist and ischemia, NMDA-receptors are trafficked to the non-raft membrane [67]. Overactivation of extrasynaptic NMDA-receptors has a profound impact on excitatory toxicity [12]. Lipid rafts contain the excitatory amino acid transporter EAAT1-4, and cholesterol loss reduces Na^+ -transporter-mediated glutamate uptake by glial cells and neurons [68] to trigger excitatory toxicity. Importantly, activated NMDA-receptors rapidly deplete the intracellular pool of cholesterol (probably, recycling endosomes), thereby activating Cdc42- and Rab11-dependent trafficking of AMPA-receptors to the postsynaptic membrane. This participates in the induction of long-term synaptic potentiation [69].

CHOLESTEROL AND NEURODEGENERATIVE DISORDERS

A growing body of evidence supports a role for cholesterol biosynthesis defects and impaired synaptic transduction in neurodegenerative disorders [2, 11, 12]. The importance of cholesterol in the brain has been revealed in many of the less common neurological disorders secondary to mutations in genes for cholesterol biosynthesis enzymes. We performed a literature search to collect evidence on alterations of cholesterol metabolism in CNS disorders associated with mutations in the genes implicated in the biosynthesis of cholesterol (Smith-Lemli-Opitz syndrome), intracellular trafficking (Niemann-Pick type C disorder), and synthesis regulation (Huntington's disease).

Smith-Lemli-Opitz syndrome

For some diseases, cholesterol metabolism abnormalities are the major cause of neurodegenerative disorders and birth defects. Lathosterolosis is a retardation syndrome due to a deficiency in 3β -hydroxysteroid-5-desaturase, and desmosterolosis is caused by mutations in the 3β -hydroxysteroid-24-reductase gene. Defective cholesterol-27-hydroxylase leads to cerebrotendinous xanthomatosis. The Smith-Lemli-Opitz syndrome is the most common autosomal recessive disease of this type (affects 1 in 20,000 newborns) resulting from mutations in the *dhcr7* gene encoding 7-dehydrocholesterolreductase (Dhcr7) [70]. Severe forms are deleterious for fetal development and newborn infant. Dhcr7 catalyzes the final step in the Kandutsch-Russell cholesterol biosynthetic pathway. A consequence of defec-

tive Dhcr7 is the accumulation of 7-dehydrocholesterol (7DHC) in the brain, non-neuronal tissues and plasma, and ultimately, cholesterol loss (Fig. 4). In the Smith-Lemli-Opitz syndrome, 24-HC levels drop and 27-HC levels increase in the plasma [71]. This disease involves profound brain development abnormalities, intellectual disability, as well as emotional and sleep disorders. Patients with severe cases display plasma cholesterol concentrations amounting to 2% of the normal range. In the mild form, plasma cholesterol levels may remain unaffected but that cannot stop brain developmental defects, pointing to a role for brain cholesterol in the genesis of neurological symptoms [70]. On the other hand, these symptoms could result from the accumulation of the Dhcr7 substrate 7,8-dehydrodesmosterol and its oxidized derivatives [72]. The teratogenic activity in the Smith-Lemli-Opitz syndrome seems to be attributed to a deficiency in SHH-signaling, since SHH activity (Sonic Hedgehog morphogen) requires a covalent linkage of cholesterol to SHH [70].

In the Smith-Lemli-Opitz syndrome, while cholesterol shares physicochemical properties with 7-DHC, cholesterol is depleted from the membrane and replenished with 7-DHC. These subtle changes in membrane composition lead to reduced membrane stiffness and lower the ability to stabilize the membrane curvature that affect the fission/fusion. 7-DHC can also produce defective membrane rafts with abnormal protein interface [73]. A reduced cholesterol availability has a negative effect on the signaling functions mediated via multiple receptors. Mutant mice with the Smith-Lemli-Opitz syndrome exhibit an impaired response of NMDA-receptors to glutamate [74]. 7-DHC is sensitive to oxygen, generating 7-DHC-derived oxysterols, which are active in the low micromolar range [72]. As a consequence, endo- and exocytosis could be influenced [55]. Ligand binding by serotonin(1A) receptors can be suppressed by 7-DHC [75]. In the Smith-Lemli-Opitz syndrome, hippocampal axons and dendrites exhibit increased activation of Rho GTPases (involved in actin cytoskeleton dynamics) due to the altered raft compositions [76]. Another hallmark of the Smith-Lemli-Opitz syndrome is increased phosphorylation of cofilin-1, which fails to act as an actin depolymerizing factor. Cytoskeleton stabilization could indirectly affect endo- and exocytosis, as well as trafficking of synaptic vesicles and receptors. Taken together, these alterations disrupt the release of a neurotransmitter (serotonin, dopamine) and ultimately lead to a neurological disease [77].

Niemann-Pick type C disorder

There is clear evidence linking a disordered cholesterol metabolism to brain neurodegeneration. Niemann-Pick type C is a rare autosomal recessive dis-

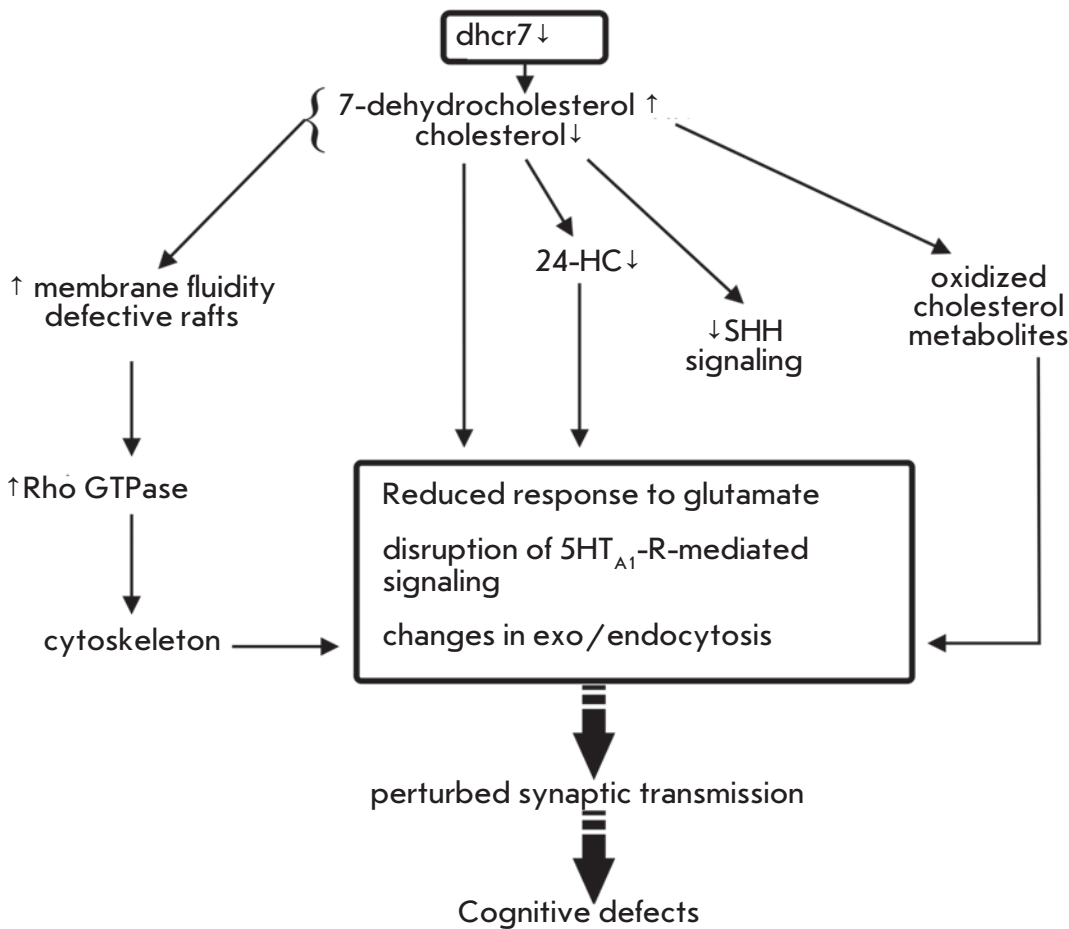


Fig. 4. Alterations in cholesterol synthesis associated with the Smith-Lemli-Opitz syndrome: an implication in synaptic dysfunction. See text for a detailed explanation.

order (affecting 1 in 150,000 newborns) characterized by progressive neuronal death and reduced life expectancy, hepatolienomegaly, and lung deficiency. The Niemann–Pick type C disease is accompanied by early loss of Purkinje cells in the cerebellum, leading to ataxia [2]. Mutations in either the NPC1 (95% of cases) or the NPC2 (5% of cases) gene render the encoded proteins non-functional (Fig. 5). Defective NPC1 or NPC2 in neurons and glial cells do not allow cholesterol and other lipids (glycolipids, in particular) to exit late endosomes/lysosomes and traffic to the plasma membrane and the ER [16]. In NPC1-deficient neurons, cholesterol is dramatically decreased in distal axons but accumulates in soma of neurons. It is likely that the defects seen in the Niemann–Pick type C disorder are caused by a reduced cholesterol content in axons: presynaptic nerve terminals, in particular. This is consistent with the evidence indicating an altered composition and organization of synaptic vesicles and recycling endosomes in nerve terminals with dysfunctional NPC1 [18]. The Niemann–Pick type C disorder is accompanied by an elevated accumulation of oxysterols, such as 3β,5α,6β-cholestantriol and 6-ketosterol, in the brain as a result of oxidative stress [2].

Neuronal soma degeneration is the final event in the pathological cascade of the Niemann–Pick type C disorder. At the onset of neurodegeneration, presynaptic nerve terminals undergo degeneration, followed by accumulation of defective NPC1 in recycling endosomes [18]. Neurodegeneration seems to originate from nerve terminals. At early stages of the disease (prior to neurological abnormalities and synapse losses) presynaptic impairments occur in the form of suppression of the evoked exocytosis and insufficient delivery of synaptic vesicles to exocytic sites [78]. These events are more severe in GABAergic nerve terminals, resulting in an imbalance of inhibitory and excitatory processes [79]. It is tempting to speculate that the alterations affecting the synaptic transmission trigger the abnormalities observed in the Niemann–Pick type C disorder manifested by ataxia, cataplexy, and a loss of reflexes. Similar changes in exocytosis of synaptic vesicles occur upon extraction of membrane cholesterol with concentrated methyl-β-cyclodextrin (MβCD) [78]. Detection of NPC1 in recycling endosomes of nerve terminals suggests a role for NPC1 in the slow vesicle recycling critical to the maintenance of synaptic vesicles during prolonged synaptic activity [18].

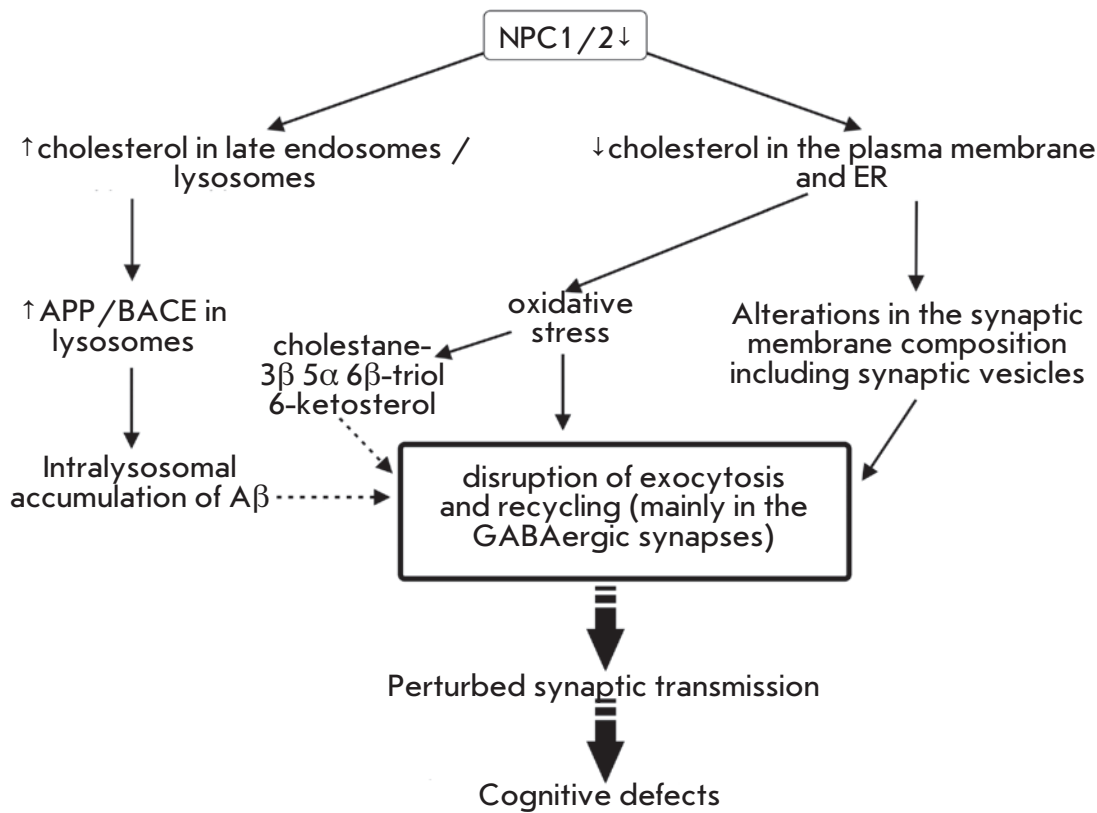


Fig. 5. Changes in cholesterol metabolism in Niemann Pick disease type C: the impact on synaptic transmission. See text for a detailed explanation.

There is no therapeutic option currently available for the treatment of the Niemann–Pick type C disorder. However, recent work raises hope for a possible intervention. Notably, a single subcutaneous administration of the cholesterol-binding agent MβCD to animals with deleted NPC1 activity delayed the development of neurodegeneration and doubled the lifespan [80]. Although MβCD cannot cross the BBB, very small amounts do pass into the brain. High levels of MβCD (5–10 mM), commonly utilized for cholesterol depletion, are toxic to neurons and block synaptic transduction [3]. Low doses of MβCD (0.1 mM) barely effect membrane cholesterol and could be taken up in neurons [62]. Endocytosed MβCD seems capable of extracting the sequestered cholesterol from the endosome/lysosome compartment and translocating it to the ER and the plasma membrane. In another study, it was discovered that injecting 2-hydroxypropyl-β-cyclodextrin into the cerebrospinal fluid reduces cholesterol accumulation in endo/lysosomes and rescues Purkinje cells [16]. Polyrotaxanes, a new class of compounds, have been shown to undergo lysosomal degradation to form β-cyclodextrins that are capable of preventing lysosomal sequestration of cholesterol [81]. It should be kept in mind that they also show neuroprotective activity in cell and mouse models of Alzheimer’s disease [82].

Neurons with Niemann–Pick Type C demonstrate β amyloid peptide accumulation (in cholesterol-laden lysosomes) and fibrillar globules of an abnormally hyperphosphorylated tau protein. The cerebrospinal fluid carries high levels of amyloid β 38, 40, and 42 species. Notably, affected individuals lack amyloid plaques, because the disorder is fatal within the first years of life [83]. Diffuse amyloid deposits occur in subjects with the ApoE4 allele, which disturbs amyloid β clearance. The ApoE4 allele carrier status is associated with increased disease severity and early onset of neurological symptoms [84].

Huntington’s disease

Huntington’s disease is an autosomal dominant neurodegenerative disease accompanied by cognitive and motor dysfunction. Huntington’s disease is caused by a genetic defect leading to an expansion of a polyglutamine stretch (over 36 residues, polyglutamine expansion) in the target protein, named huntingtin. Striatum and cortex neurons are sensitive to the toxic property of the mutated protein [85]. Huntington’s disease is associated with reduced cholesterol synthesis in the brain [10]. The mutant protein huntingtin decreases the transcriptional activity of SREBP, downregulating SREBP-regulated genes and, in turn, the cholesterol biosyn-

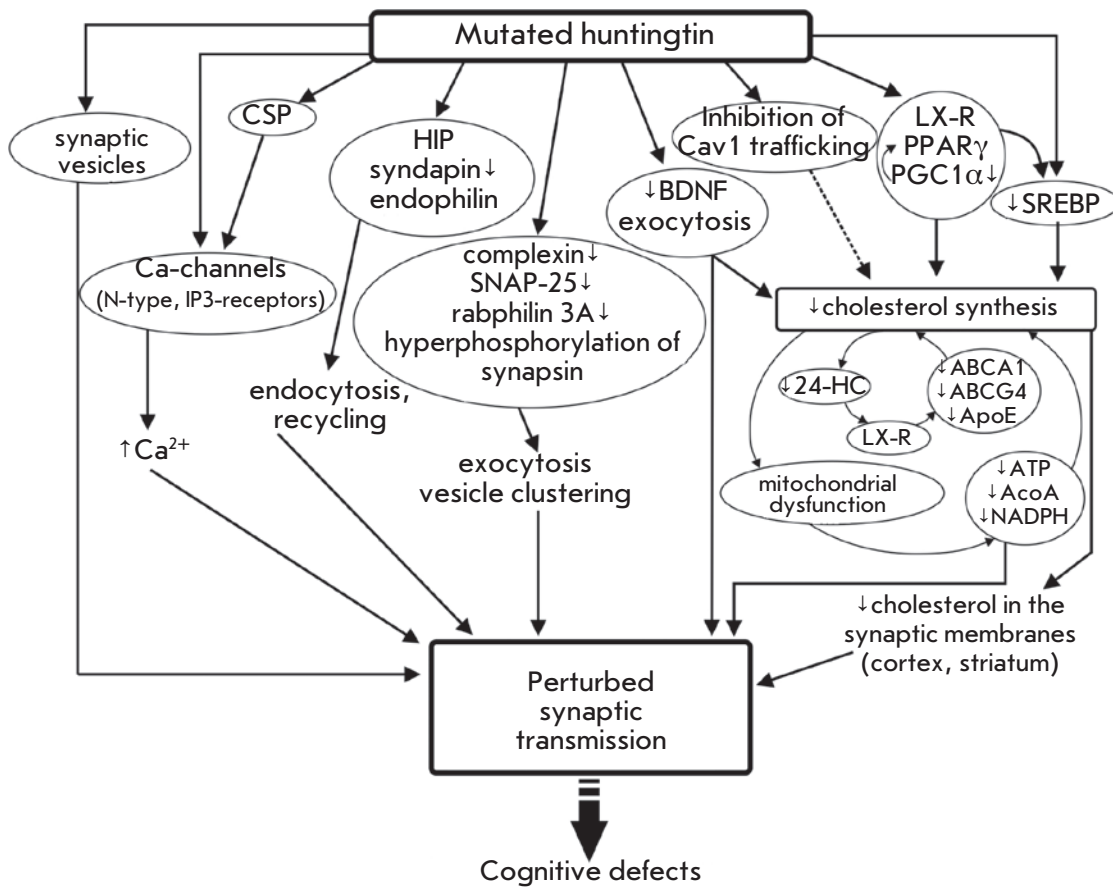


Fig. 6. Influence of the mutant huntingtin on synaptic transduction and brain cholesterol metabolism. See text for a detailed explanation.

thetic pathway in cortical and striatum neurons (Fig. 6). Cholesterol levels are first affected in synaptosomal membranes and, at later stages, in myelin sheaths. Exogenous cholesterol (up to 15 μ M) prevents the death of striatal neurons carrying the mutant protein [86]. There is a strong positive correlation between longer polyglutamine stretches and the severity of diseases and cholesterol biosynthesis disorder [34]. Huntington's disease rodents show a dramatic age-related decline in cholesterol content in brain tissue as compared to age-matched healthy individuals [86]. Cholesterol levels in fibroblasts are reduced by 50%, along with lowered total plasma cholesterol concentrations, which are detectable early in pre-manifest patients [87]. Conversely, 24-HC levels are first elevated at the onset of diseases and later dropping due to dysfunction of cholesterol biosynthesis in degenerating striatal neurons [10]. The first increase in 24-HC content could represent a response to compensate for cholesterol loss. A further decline in 24-HC levels in the brain leads to reduced cholesterol synthesis because of downregulation of LX-receptors and, correspondingly, LX-receptor-dependent protein expression (ABCA1, ABCG4, ApoE). Astrocytes bearing the mutant huntingtin produce

and secrete less ApoE. Such ApoE-particles are smaller in size and lipid-poor, failing both to efficiently transfer cholesterol from astrocytes to neurons and to clear cholesterol excess from the brain [86]. LX-receptor agonists can partially ameliorate Huntington's disease symptoms [10]. In cholesterol-deficient cells, cholesterol and its esters can form patches in plasma membranes and lysosomes/endosomes, due to prevention in efflux in the form of ApoE-particles and 24-HC. Aberrant cholesterol accumulation could be a result of defects in caveolin 1 traffic induced by the mutant huntingtin[88]. BDNF released by nerve terminals of cortical neurons in the striatum is implicated in not only synaptic plasticity and cell survival, but also induction of cholesterol synthesis in postsynaptic neurons. The mutant huntingtin inhibits cholesterol synthesis by influencing trafficking and secretion of BDNF [10].

The intact huntingtin can bind to the nuclear receptors engaged in lipid metabolism such as LX-receptor, PPAR γ (peroxisome-proliferator-activated receptor gamma), and vitamin D receptor [10]. Overexpressed wild-type huntingtin activates LX-receptors, whereas in the absence of the huntingtin, LX-receptor-mediated transcription is suppressed. It is likely that mutant

huntingtin plays a little or no role in triggering LX-receptor-dependent networks, including SREBP. In oligodendrocytes, mutant huntingtin impairs the ability of PPAR γ CoActivator 1 α (PGC1 α) to enhance both the cholesterol biosynthetic pathways and expression of myelin proteins [89]. In the pre-manifest stage of the disease, PGC1 α expression is lowered in medium spiny neurons of the striatum. This may be one of the reasons for mitochondrial dysfunction, since PGC1 α underlies mitochondrial biogenesis and oxidative metabolism and modulates the expression of the genes encoding proteins of the electron transport chain [90]. Mitochondrial dysfunction causes ATP and NADPH depletion, reducing availability of important substrate for cholesterol synthesis. The mutant protein significantly affects the membrane fluidity probably via cholesterol loss. Olesoxime, a cholesterol-like compound capable of passing into the cells and then trapped in the mitochondrial membrane, has been recently shown to exert a therapeutic effect in the correction of mitochondrial dysfunction in disease models of amyotrophic lateral sclerosis, peripheral neuropathies, and Huntington's disease. HD cells exposed to olesoxime showed a decrease in membrane fluidity, whereas long-term exposure elevates the cholesterol content [91].

In the pre-manifest stage, exo-endocytic trafficking of synaptic vesicles is perturbed (Fig. 6). The hun-

tingtin protein builds up at the presynapse and binds to synaptic vesicles. Huntington's disease mice show abnormal synapsin-1 phosphorylation and progressive decline in the concentration of complexin II, SNAP-25, and rabphilin 3A in nerve terminals of select areas of the cortex [92]. As a consequence, exocytosis is suppressed and the pool of synaptic vesicles is reduced. The level of intracellular Ca²⁺ in terminals is elevated due to the attenuation of tonic Ca²⁺ channel inhibition by CSP (cysteine-string protein), modulating N-type Ca²⁺ current, or directly by huntingtin, regulating IP₃-receptors of ER [93]. There is a group of endocytic proteins tightly binding to huntingtin, including HIP1 (huntingtin interacting protein 1), HIP1R, syndapin I, and endophilin. Syndapin I, an endocytic scaffolding protein, is eliminated from presynaptic regions, and HIP1 becomes dysfunctional and blocks endocytosis. In addition, Huntington's disease is accompanied by defective Rab11-dependent endosomal recycling, causing abnormalities in the generation of synaptic vesicles and synaptic transmission [94]. ●

This work received core financial support from an RFFI grant (№ 14-04-00094) and partial support from other RFFI (№ 16-34-00127) and RSF (№ 14-15-00847) grants.

REFERENCES

- Dietschy J.M. // Biol. Chem. 2009. V. 390. № 4. P. 287–293.
- Vance J.E. // Disease Models Mechanisms. 2012. V. 5. P. 746–755.
- Petrov A.M., Zefirov A.L. // Uspekhi fiziologicheskikh nauk. 2013. V. 44. № 1. P. 17–38.
- Saeed A.A., Genové G., Li T., Lütjohann D., Olin M., Mast N., Pikuleva I.A., Crick P., Wang Y., Griffiths W. // J. Biol. Chem. 2014. V. 289. № 34. P. 23712–23722.
- Elahy M., Jackaman C., Mamo J.C.L., Lam V., Dhaliwal S.S., Giles C., Nelson D., Takechi R. // Immunity Ageing. 2015. V. 12. A. 2.
- Sagare A.P., Bell R.D., Zhao Z., Ma Q., Winkler E.A., Ramanathan A., Zlokovic B.V. // Nat. Commun. 2013. V. 4. A. 2932.
- Russell D.W., Halford R.W., Ramirez D.M., Shah R., Kottl T. // Annu. Rev. Biochem. 2009. V. 78. P. 1017–1040.
- Saher G., Brügger B., Lappe-Siefke C., Möbius W., Tozawa R., Wehr M.C., Wieland F., Ishibashi S., Nave K.A. // Nat. Neurosci. 2005. V. 8. № 4. P. 468–475.
- Numakawa T., Suzuki S., Kumamaru E., Adachi N., Richards M., Kunugi H. // Histol. Histopathol. 2010. V. 25. № 2. P. 237–258.
- Leoni V., Caccia C. // Biochim. Biophys. Acta. 2015. pii: S1388-1981(15)00003-7.
- Anchisi L., Dessì S., Pani A., Mandas A. // Front. Physiol. 2013. V. 3. P. 1–12.
- Martin M.G., Ahmed T., Korovaichuk A., Venero C., Menchón S.A., Salas I., Munck S., Herreras O., Balschun D., Dotti C.G. // EMBO Mol. Med. 2014. V. 6. № 7. P. 902–917.
- Suzuki R., Ferris H.A., Chee M.J., Maratos-Flier E., Kahn C.R. // PLoS Biol. 2013. V. 11. № 4. P. e1001532.
- Camargo N., Brouwers J.F., Loos M., Gutmann D.H., Smit A.B., Verheijen M.H. // FASEB J. 2012. V. 26. № 10. P. 4302–4315.
- Verheijen M.H., Camargo N., Verdier V., Nadra K., de Preux Charles A.S., Médard J.J., Luoma A., Crowther M., Inouye H., Shimano H. // Proc. Natl. Acad. Sci. USA. 2009. V. 106. № 50. P. 21383–21388.
- Peake K.B., Vance J.E. // J. Biol. Chem. 2012. V. 287. P. 9290–9298.
- Bryleva E.Y., Rogers M.A., Chang C.C., Buen F., Harris B.T., Rousselet E., Seidah, N.G., Oddo S., LaFerla F.M., Spencer T.A., et al. // Proc. Natl. Acad. Sci. USA. 2010. V. 107. P. 3081–3086.
- Karten B., Campenot R.B., Vance D.E., Vance J.E. // J. Lipid Res. 2006. V. 47. P. 504–514.
- Bu G. // Nat. Rev. Neurosci. 2009. V. 10. № 5. P. 333–344.
- Hayashi H. // Biol. Pharm. Bull. 2011. V. 34. № 4. P. 453–461.
- Lane-Donovan C., Philips G.T., Herz J. // Neuron. 2014. V. 83. № 4. P. 771–787.
- Vaughan A.M., Oram J.F. // J. Lipid. Res. 2006. V. 47. № 11. P. 2433–2443.
- Karasinska J.M., de Haan W., Franciosi S., Ruddle P., Fan J., Kruit J.K., Stukas S., Lütjohann D., Gutmann D.H., Wellington C.L. // Neurobiol. Dis. 2013. V. 54. P. 445–455.
- Rushworth J.V., Griffiths H.H., Watt N.T., Hooper N.M. // J. Biol. Chem. 2013. V. 288. № 13. P. 8935–8951.
- Liu Q., Trotter J., Zhang J., Peters M.M., Cheng H., Bao J., Han X., Weeber E.J., Bu G. // J. Neurosci. 2010. V. 30. № 50.

- P. 17068–17078.
26. Rensen P.C., Jong M.C., van Vark L.C., van der Boom H., Hendriks W.L., van Berkel T.J., Biessen E.A., Havekes L.M. // *J. Biol. Chem.* 2000. V. 275. № 12. P. 8564–8571.
27. Vance J.E., Karten B. // *J. Lipid Res.* 2014. V. 55. № 8. P. 1609–1621.
28. Ignatius M.J., Gebicke-Härter P.J., Skene J.H., Schilling J.W., Weisgraber K.H., Mahley R.W., Shooter E.M. // *Proc. Natl. Acad. Sci. USA.* 1986. V. 83. P. 1125–1129.
29. Gosselet F., Saint-Pol J., Fenart L. // *Biochem. Biophys. Res. Commun.* 2014. V. 446. № 3. P. 687–691.
30. Hudry E., Van Dam D., Kulik W., De Deyn P.P., Stet F.S., Ahouansou O., Benraiss A., Delacourte A., Bougnères P., Aubourg P. // *Mol. Ther.* 2010. V. 18. № 1. P. 44–53.
31. Sodero A.O., Vriens J., Ghosh D., Stegner D., Brachet A., Pallotto M., Sassoè-Pognetto M., Brouwers J.F., Helms J.B., Nieswandt B. // *EMBO J.* 2012. V. 31. № 7. P. 1764–1773.
32. Sodero A.O., Weissmann C., Ledesma M.D., Dotti C.G. // *Neurobiol. Aging.* 2011. V. 32. № 6. P. 1043–1053.
33. Marwarha G., Ghribi O. // *Exp. Gerontol.* 2014. pii: S0531-5565(14)00270-8.
34. Brown A.J., Jessup W. // *Mol. Aspects Med.* 2009. V. 30. № 3. P. 111–122.
35. Heverin M., Bogdanovic N., Lütjohann D., Bayer T., Pikuleva I., Bretillon L., Diczfalusy U., Winblad B., Björkhem I. // *J. Lipid Res.* 2004. V. 45. № 1. P. 186–193.
36. Lathe R., Saponova A., Kotelevtsev Y. // *BMC Geriatrics.* 2014. V. 14. A. 36
37. Zefirov A.L., Petrov A.M. // *Neurosci. Behav. Physiol.* 2012. V. 42. № 2. P. 144–152.
38. Jennemann R., Sandhoff R., Wang S., Kiss E., Gretz N., Zuliani C., Martin-Villalba A., Jäger R., Schorle H., Kenzelmann M. // *Proc. Natl. Acad. Sci. USA.* 2005. V. 102. № 35. P. 12459–12464.
39. Suzuki T., Zhang J., Miyazawa S., Liu Q., Farzan M.R., Yao W.D. // *J. Neurochem.* 2011. V. 119. № 1. P. 64–77.
40. Stary C.M., Tsutsumi Y.M., Patel P.M., Head B.P., Patel H.H., Roth D.M. // *Front. Physiol.* 2012. V. 3. P. 393.
41. Head B.P., Peart J.N., Panneerselvam M., Yokoyama T., Pearn M.L., Niesman I.R., Bonds J.A., Schilling J.M., Miyanohara A., Headrick J. // *PLoS One.* 2010. V. 5. № 12. P. e15697.
42. Fantini J., Yahi N. // *Adv. Exp. Med. Biol.* 2013. V. 991. P. 15–26.
43. Uversky V.N. // *Adv. Exp. Med. Biol.* 2015. V. 855. P. 33–66.
44. Rushworth J.V., Hooper N.M. // *Int. J. Alzheimers. Dis.* 2011. P. 603052.
45. Petrov A.M., Kudryashova K.E., Odnoshivkina Yu.G., Zefirov A.L. // *Neurochem. J.* 2011. V. 5. № 1. P. 13–19.
46. Matsuzaki K. // *Int. J. Alzheimers. Dis.* 2011. V. 2011. P. 956104.
47. Martins I.C., Kuperstein I., Wilkinson H., Maes E., Vanbrabant M., Jonckheere W., van Gelder P., Hartmann D., D'Hooge R., De Strooper B. // *EMBO J.* 2008. V. 27. № 1. P. 224–233.
48. Tong J., Borbat P.P., Freed J.H., Shin Y.K. // *Proc. Natl. Acad. Sci. USA.* 2009. V. 106. № 13. P. 5141–5146.
49. Rohrbough J., Broadie K. // *Nat. Rev. Neurosci.* 2005. V. 6. № 2. P. 139–150.
50. Jia J.Y., Lamer S., Schumann M., Schmidt M.R., Krause E., Haucke V. // *Mol. Cell Proteomics.* 2006. V. 5. № 11. P. 2060–2071.
51. Sieber J.J., Willig K.I., Heintzmann R., Hell S.W., Lang T. // *Biophys. J.* 2006. V. 90. № 8. P. 2843–2851.
52. Taverna E., Saba E., Linetti A., Longhi R., Jeromin A., Righi M., Clementi F., Rosa P. // *J. Neurochem.* 2007. V. 100. № 3. P. 664–677.
53. Kasimov M.R., Giniatullin A.R., Zefirov A.L., Petrov A.M. // *Biochim. Biophys. Acta.* 2015. V. 1851. № 5. P. 674–685.
54. Petrov A.M., Kasimov M.R., Giniatullin A.R., Tarakanova O.I., Zefirov A.L. // *Neurosci. Behav. Physiol.* 2010. V. 40. № 8. P. 894–901.
55. Petrov A.M., Kasimov M.R., Giniatullin A.R., Zefirov A.L. // *Neurosci. Behav. Physiol.* 2014. V. 44. № 9. P. 1020–1030.
56. Zamir O., Charlton M.P. // *J. Physiol.* 2006. V. 571. № 1. P. 83–99.
57. Tarakanova O.I., Petrov A.M., Zefirov A.L. // *Doklady Biol. Sci.* 2011. V. 438. P. 138–140.
58. Petrov A.M., Yakovleva A.A., Zefirov A.L. // *J. Physiol.* 2014. V. 592. № 22. P. 4995–5009.
59. Smith A.J., Sugita S., Charlton M.P. // *J. Neurosci.* 2010. V. 30. № 17. P. 6116–6121.
60. Petrov A.M., Zakyrjanova G.F., Yakovleva A.A., Zefirov A.L. // *Biochem. Biophys. Res. Commun.* 2015. V. 456. № 1. P. 145–150.
61. Tarasenko A.S., Sivko R.V., Krisanova N.V., Himmelreich N.H., Borisova T.A. // *J. Mol. Neurosci.* 2010. V. 41. № 3. P. 358–367.
62. Petrov A.M., Naumenko N.V., Uzinskaya K.V., Giniatullin A.R., Urazaev A.K., Zefirov A.L. // *Neuroscience.* 2011. V. 186. P. 1–12.
63. Hering H., Lin C.C., Sheng M. // *J. Neurosci.* 2003. V. 23. № 8. P. 3262–3271.
64. Hou Q., Huang Y., Amato S., Snyder S.H., Haganir R.L., Man H.Y. // *Mol. Cell Neurosci.* 2008. V. 38. № 2. P. 213–223.
65. Korinek M., Vyklicky V., Borovska J., Lichnerova K., Kaniakova M., Krausova B., Krusek J., Balik A., Smejkalova T., Horak M. // *J. Physiol.* 2015. V. 593. № 10. P. 2279–2293.
66. Paul S.M., Doherty J.J., Robichaud A.J., Belfort G.M., Chow B.Y., Hammond R.S., Crawford D.C., Linsenbardt A.J., Shu H.J., Izumi Y. // *J. Neurosci.* 2013. V. 33. № 44. P. 17290–17300.
67. Head B.P., Patel H.H., Tsutsumi Y.M., Hu Y., Mejia T., Mora R.C., Insel P.A., Roth D.M., Drummond J.C., Patel P.M. // *FASEB J.* 2008. V. 22. № 3. P. 828–840.
68. Butchbach M.E., Tian G., Guo H., Lin C.L. // *J. Biol. Chem.* 2004. V. 279. № 33. P. 34388–34396.
69. Brachet A., Norwood S., Brouwers J.F., Palomer E., Helms J.B., Dotti C.G., Esteban J.A. // *J. Cell Biol.* 2015. V. 208. № 6. P. 791–806.
70. Nowaczyk M.J., Irons M.B. // *Am. J. Med. Genet. C Semin. Med. Genet.* 2012. V. 160C. № 4. P. 250–262.
71. Björkhem I., Starck L., Andersson U., Lütjohann D., von Bahr S., Pikuleva I., Babiker A., Diczfalusy U. // *J. Lipid Res.* 2001. V. 42. № 3. P. 366–371.
72. Korade Z., Xu L., Shelton R., Porter N.A. // *J. Lipid Res.* 2010. V. 51. № 11. P. 3259–3269.
73. Staneva G., Chachaty C., Wolf C., Quinn P.J. // *J. Lipid Res.* 2010. V. 51. № 7. P. 1810–1822.
74. Wassif C.A., Zhu P., Kratz L., Krakowiak P.A., Battaile K.P., Weight F.F., Grinberg A., Steiner R.D., Nwokoro N.A., Kelley R.I. // *Hum. Mol. Genet.* 2001. V. 10. № 6. P. 555–564.
75. Singh P., Paila Y.D., Chattopadhyay A. // *Biochem. Biophys. Res. Commun.* 2007. V. 358. № 2. P. 495–499.
76. Jiang X.S., Wassif C.A., Backlund P.S., Song L., Holtzclaw L.A., Li Z., Yergey A.L., Porter F.D. // *Hum. Mol. Genet.* 2010. V. 19. № 7. P. 1347–1357.
77. Sparks S.E., Wassif C.A., Goodwin H., Conley S.K., Lanham D.C., Kratz L.E., Hyland K., Gropman A., Tierney E., Porter F.D. // *J. Inherit. Metab. Dis.* 2014. V. 37. № 3.

- P. 415–420.
78. Hawes C.M., Wiemer H., Krueger S.R., Karten B. // *J. Neurochem.* 2010. V. 114. P. 311–322.
79. Xu S., Zhou S., Xia D., Xia J., Chen G., Duan S., Luo J. // *Neuroscience.* 2010. V. 167. P. 608–620.
80. Liu B., Turley S.D., Burns D.K., Miller A.M., Repa J.J., Dietschy J. M. // *Proc. Natl. Acad. Sci. USA.* 2009. V. 106. P. 2377–2382.
81. Tamura A., Yui N. // *J. Biol. Chem.* 2015. V. 290. № 15. P. 9442–9454.
82. Malnar M., Hecimovic S., Mattsson N., Zetterberg H. // *Neurobiol. Dis.* 2014. V. 72 Pt A. P. 37–47.
83. Yamazaki T., Chang T.Y., Haass C., Ihara Y. // *J. Biol. Chem.* 2001. V. 276. № 6. P. 4454–4460.
84. Fu R., Yanjanin N.M., Elrick M.J., Ware C., Lieberman A.P., Porter F.D. // *Am. J. Med. Genet. A.* 2012. V. 158A. № 11. P. 2775–2780.
85. Margulis B.A., Vigont V., Lazarev V.F., Kaznacheyeva E.V., Guzhova I.V. // *FEBS Lett.* 2013. V. 587. № 13. P. 1997–2007.
86. Valenza M., Leoni V., Karasinska J.M., Petricca L., Fan J., Carroll J., Pouladi M.A., Fossale E., Nguyen H.P., Riess O. // *J. Neurosci.* 2010. V. 30. P. 10844–10850.
87. Wang R., Ross C.A., Cai H., Cong W.N., Daimon C.M., Carlson O.D., Egan J.M., Siddiqui S., Maudsley S., Martin B. // *Front. Physiol.* 2014. V. 5. P. 231.
88. Trushina E., Canaria C.A., Lee D.Y., McMurray C.T. // *Hum. Mol. Genet.* 2014. V. 23. № 1. P. 129–144.
89. Xiang Z., Valenza M., Cui L., Leoni V., Jeong H.K., Brill E., Zhang J., Peng Q., Duan W., Reeves S.A. // *J. Neurosci.* 2011. V. 31. № 26. P. 9544–9553.
90. Tsunemi T., La Spada A.R. // *Prog. Neurobiol.* 2012. V. 97. № 2. P. 142–151.
91. Eckmann J., Clemens L.E., Eckert S.H., Hagl S., Yu-Taeger L., Bordet T., Pruss R.M., Muller W.E., Leuner K., Nguyen H.P. // *Mol. Neurobiol.* 2014. V. 50. № 1. P. 107–118.
92. Smith R., Klein P., Koc-Schmitz Y., Waldvogel H.J., Faull R.L., Brundin P., Plomann M., Li J.Y. // *J. Neurochem.* 2007. V. 103. № 1. P.115–123.
93. Bezprozvanny I.B. // *Acta Naturae.* 2010. V. 2. № 1(4). P. 72–80.
94. Steinert J.R., Campesan S., Richards P., Kyriacou C.P., Forsythe I.D., Giorgini F. // *Hum. Mol. Genet.* 2012. V. 21. № 13. P. 2912–2922.

Study of Antitherpetic Efficiency of Phosphite of Acycloguanosine Able to Overcome the Barrier of Resistance to Acyclovir

V. L. Andronova^{1*}, M.V. Jasko², M.K. Kukhanova², G.A. Galegov², Yr.S. Skoblov³, corresponding member of the Russian Academy of Sciences S.N. Kochetkov²

¹D.I. Ivanovsky Institute of Virology (N.F. Gamaleya Research Center of Epidemiology and Microbiology, Ministry of Healthcare of the Russian Federation), Gamaleya Str., 16, Moscow, 123098, Russia

²V.A. Engelhardt Institute of Molecular Biology, Russian Academy of Sciences, Vavilova Str., 32, Moscow, 119991, Russia

³M.M. Shemyakin-Yr.A. Ovchinnikov Institute of Bioorganic Chemistry, Russian Academy of Sciences, Miklukho-Maklaya Str., 16/10, Moscow, 117997, Russia

*E-mail: andronova.vl@yandex.ru

Received 21.08.2015

Copyright © 2016 Park-media, Ltd. This is an open access article distributed under the Creative Commons Attribution License, which permits unrestricted use, distribution, and reproduction in any medium, provided the original work is properly cited.

ABSTRACT As has been shown previously, phosphite of acycloguanosine (Hp-ACG) exhibits equal efficacy against ACV-sensitive and ACV-resistant HSV-1 strains in cell culture. Intraperitoneal administration of Hp-ACG to model mice with herpetic encephalitis caused by HSV-1 infection was shown to be effective in protecting against death. In the present work, we continue the study of the antiviral efficiency of Hp-ACG against HSV administered non-invasively; namely *in vivo*, orally and in the form of ointment formulations. It has been first shown that oral administration of Hp-ACG twice daily for five days prevents systemic infection in mice caused by HSV-1. Mortality in the control group of animals was 57%. Administration of Hp-ACG at doses of 600, 800 and 1,000 mg/kg per day significantly increased the survival and median day of death of the animals compared to the placebo-treated control group. A comparative evaluation of the therapeutic efficacy parameters of polyethylene glycol-based ACV ointment and Hp-ACG ointment was carried out after a 5-day course in the model of an experimental cutaneous infection of HSV-1 in guinea pigs. It was found that Hp-ACG has a significant therapeutic effect resulting in a statistically significant reduction in the lesion's surface area and the amount of vesicular structures. The exhibited therapeutic effect of 10% Hp-ACG in ointment form compares well with that of 5% ACV ointment.

KEYWORDS herpes simplex virus, antiviral activity, *in vitro*, *in vivo*.

ABBREVIATIONS HSV-1 and HSV-2 – Herpes Simplex virus type 1 and type 2, respectively; TK – thymidine kinase; ACV/ACG – acyclovir/acycloguanosine; Hp-ACG – phosphite of acycloguanosine; PCV – penciclovir; PEG 600 – polyethylene glycol 600; MDD – median day of death; PFA – phosphonoformic acid; CDV – cidofovir; CTD₅₀ – 50% cytotoxic dose; CPE – cytopathic effect; ID₅₀ and ID₉₅ – 50% and 95% inhibitory dose; SI – selectivity index; i.p. – intraperitoneal.

INTRODUCTION

Infections caused by the herpes simplex virus (HSV) are widespread: from 50 to 95% of the world adult population possess antibodies to HSV-1, and 20–30% are carriers of HSV-2 by the age of 15–29 years, wherein the number of seropositive persons increases with age [1, 2]. After the initial infection, herpes viruses establish a lifelong latent infection with periodic recurrences. HSV can infect various organs and tissues, leading to a variety of clinical manifestations of the infection,

including skin, the mucosas and eye lesions, and even generalized forms with damage to internal organs and CNS [3]. Therefore, it is important to have available dosage forms both for external use and systemic administration for the treatment of herpetic infections of various severities and localizations. For this purpose, nucleoside analogs are commonly used in medical practice. First of all, these are the known antitherpetic agents acyclovir (ACV, ACG, Zovirax, 9-[(2-hydroxyethoxy)methyl]-guanine) available either as 5% oint-

ment, 5% cream or 3% ophthalmic ointment and in the form of tablets, 8% suspensions for internal use, lyophilized powder for infusion solution, and lyophilized powder for injection solution (GlaxoSmithKline group of companies and etc.). Moreover, first-line antiherpetic agents include penciclovir (PCV, 1% cream) and metabolic precursors of ACV and PCV: valine ester of ACV (Valtrex, tablets with a dosage of 250, 500, and 1000 mg) and famciclovir (Famvir, film-coated tablets, 125, 250, and 500 mg dosage forms).

However, herpes viruses develop resistance to these drugs. The frequency of isolation of HSV with drug resistance in clinical practice depends on the immune status and ranges from 0.5% in immunocompetent patients to 2–36% in immunocompromised patients [4, 5]. There are cases when diseases with a severe clinical course (herpes pneumonia, meningoencephalitis, extensive mucocutaneous lesions, etc.), which can lead to the death of the patient, were associated with ACV-resistant HSV variants [6–9].

HSV resistance to ACV is due to mutations in the *UL23* gene encoding thymidine kinase (TK) and/or *UL30* encoding DNA polymerase, with which is associated a mechanism of drug action. The first stage of ACV phosphorylation resulting in ACV monophosphate formation is catalyzed by viral TK, while the next two stages are catalyzed by host cell enzymes. ACV triphosphate (the active metabolite of ACV) inhibits viral DNA polymerase and, moreover, inhibits elongation through the mechanism of termination, being incorporated in the newly synthesized DNA chain [10]. Resistance of HSV clinical isolates to ACV is in 95% of the cases due to mutations in the *UL23* gene, which, as a rule, lead to a loss or significant reduction in TK activity (96%). Mutants with altered substrate specificity to TK are much more rarely isolated (4% of all TK mutants) [6, 11].

It is important to note that due to the similarity between the mechanisms of ACV and PCV action, the resistance of HSV to these drugs has in most cases an overlapping profile, which leads to a reduction in the efficiency of the therapy using ACV, PCV or their metabolic precursors. Trisodium salt of phosphonoformic acid (PFA, foscarnet) is used in such cases in international practice [12, 13]. In addition, there is a positive experience of using CDV (cidofovir, Vistide) in the most severe cases when PFA also turned out to be ineffective [14]. These drugs are in most cases equally effective in inhibition of the reproduction of HSV variants both sensitive and resistant to ACV and PCV. Unfortunately, PFA and CDV are highly toxic and their use is prohibited in Russia. HSV mutants that share cross-resistance to ACV/PCV and PFA and/or CDV have been also described [15–17]. Therefore, the development of

agents effective against HSV and preventing a recurrence of the disease is highly relevant.

Phosphite of acycloguanosine (Hp-ACG, phosphonate of 9-[(2-hydroxyethoxy)methyl]-guanine) is an H-phosphonate derivative of ACG. We have shown earlier in an HSV-1 model that Hp-ACG exhibits antiviral activity both *in vitro* (Vero E6 cell culture) and *in vivo* (i.p. administration in infected mice). The drug is active not only against the HSV-1/L₂ reference strain, but also against the ACV-resistant laboratory strain HSV-1/L₂/R and resistant clinical isolates of HSV-1 (Avd and Sha), which have epidemic value [18–21]. Thus, Hp-ACG may be of interest to practical medicine as a drug that effectively suppresses the infection caused by ACV-sensitive and -resistant variants of HSV-1.

In the present study, we have determined the efficiency of orally administered Hp-ACG in mice with a generalized herpes infection, as well as conducted a comparative study of the ointment formulation of Hp-ACG and ACV for the development of drugs for the treatment of a cutaneous herpes infection.

EXPERIMENTAL SECTION

Compounds

Hp-ACG was synthesized at the V.A. Engelhardt Institute of Molecular Biology, RAS. ACV (9-[(2-hydroxyethoxy)methyl]-guanine) (GlaxoSmithKline, USA/UK) was used as a reference drug.

Viruses and cells

HSV-1/L₂ strain from the State Collection of viruses at the D.I. Ivanovsky Institute of Virology was used in this study. A line of Vero E6 cells (African Green Monkey Kidney Cells) was kindly provided by A.M. Butenko (D.I. Ivanovsky Institute of Virology, Ministry of Healthcare of the Russian Federation).

Animals

Agouti guinea pigs of 250 g weight (males) and BALB/c white mice weighing 8–9 g (males) were obtained from the nursery Stolbovaya Branch of the Russian Academy of Medical Sciences (Moskovskaya oblast, Chekhovskiy rayon, Stolbovaya pos.). The animals were healthy, and they had a veterinary certificate of quality and health. All procedures were carried out strictly in full compliance with the requirements stated in Rules of Work with the Use of Experimental Animals № 755 dated 08/12/1977.

Cytotoxicity

Cytotoxicity was evaluated in accordance with the conventional trypan blue exclusion method of cell stain-

ing [20, 21]. CTD_{50} was considered to be the substance concentration which ensured the death of 50% the cells after 72 h of incubation.

Antiviral activity

The antiviral activity of the compounds *in vitro* was assessed using the micromethod by their ability to protect infected cells from death by preventing the development of a virus-induced CPE in accordance with the method designed by De Clercq E. *et al.* [22] as we have previously described [20, 21]. A monolayer Vero E6 cell culture grown in plastic 96-well plates (Linbro, Flow laboratories, UK) was infected at a multiplicity of 0.1 PFU/cell; the duration of incubation was 48 hours at 37°C. In the control viral CPE was developed to 95–100%: i.e., it covered the entire monolayer of cells. Efficacy of the agent was quantitatively expressed as ID_{50} and ID_{95} , concentrations of the compound that inhibit the development of virus-induced CPE by 50% and almost completely, respectively.

Antiherpetic activity

Antiherpetic activity of the compounds was studied on an experimental model of mice with a generalized infection. HSV-1/ L_2 adapted to mouse brain was used. Infectious material was introduced i.p. in a volume of 200 μ l at a dose provoking the death of 95 or 50% of the animals in the infected, untreated control group. The infecting dose is specified for each experiment separately. The animals received the studied compounds dissolved in thrice-distilled water or saline i.p. or orally in a volume of 0.2 ml. Single doses of the compounds and the number of animals in the group are specified separately for each experiment. The compounds were administered twice daily for 5 days, and the first administration was 1 h after infection. The observation period was 21 days. The effectiveness of the drugs was evaluated based on their ability to protect the animals from death (survival rate compared to infected, untreated control group) and an increase in the MDD. For a maximum MDD has been accepted as 21 days (observation period).

A total of 96 h after infection, when infectious titer reached a maximum value in the brain of the infected animals, three mice from each group were sacrificed. Brain and lungs were isolated and homogenized in Dounce homogenizer at a temperature of 4°C, and a 10% suspension was prepared in saline, centrifuged at 5,000 rev/min and 4°C for 10 min. Infectious titer of the virus was determined in the supernatant by plaque formation by titration in cell culture as described below. The efficacy of the drug was assessed by a reduction in infectious virus titer values in organ material from animals of the experimental group receiving the drug

compared to the control (infected but not treated animals).

In order to assess drug efficacy in an experimental cutaneous infection [23], viral material was applied with its subsequent rubbing on the scarified after depilation of skin areas of the guinea pigs of about 5 cm². Viral titer was 7.87 lg PFU/ml.

At 48 h after inoculation with HSV slight redness appeared on the infected surface, followed by treatment initiated with the application of ointment twice daily for 5 days. PEG 600 was used as a base for the preparation of the ointment.

Infectious virus titer

The value of infectious virus titer in vesicle fluid was determined by plaque formation assay as described below. Vesicular fluid intake was conducted 4 days after infection. Infectious virus titer was determined by plaque assay. The 24-hour culture of cells grown in 24-well plastic plates (Costar, USA) was infected with 10-fold dilutions of the virus. After 1 h, the cell monolayer was washed from non-adsorbed virus with saline, a coating medium (2 ml/well) was added, and the cells were incubated at 37°C in 5% CO₂ atmosphere. The overlay consisted of Eagle's and 199 mediums (produced at the M.P. Chumakov Institute of Poliomyelitis and Viral Encephalitis RAMS, Russia) mixed at a ratio of 1 : 1 with 5% fetal bovine serum and 0.4% agarose (Sigma, USA). After 48 h, the overlay was removed, the infected cultures were fixed with 10% neutral formalin, stained with a 0.5% gentian violet solution, and the plaque number was counted [24].

Infectious titer T was calculated using the formula

$$T = \frac{\text{Number of plaques per well} \times \text{Dilution factor}}{\text{Inoculum volume}}$$

and expressed as lg PFU/ml, where PFU is the plaque forming unit.

RESULTS AND DISCUSSION

We have shown that Hp-ACG is equally effective in the selective inhibition of the reproduction of both ACV-sensitive and -resistant HSV strains, including laboratory strain HSV-1/ L_2 /R and the clinical isolates Avd and Sha, which circulate in the human population and now are among the most frequent TK-negative/deficient phenotypes in clinical practice [18, 19]. The corresponding data are shown in *Table 1*.

The results obtained *in vitro* were confirmed in experiments *in vivo* on a model of experimental HSV infection in BALB/c white mice. Since the infection caused by the ACV-resistant HSV-1/ L_2 /R variant was not lethal, the efficiency of Hp-ACG in i.p. adminis-

Table 1. Antiviral activity of Hp-ACG and ACV in a Vero E6 cell culture [18, 19]

Compound	Characteristic	Virus			
		HSV-1/L ₂	HSV-1/L ₂ /R	Avd	Sha
Hp-ACG	ID ₅₀ , µg/ml	15.6	31.25	31.25	31.25
	ID ₉₅ , µg/ml	31.25	62.5	250	62.5
	SI	> 64	> 32	> 32	> 32
ACV	ID ₅₀ , µg/ml	0.39	> 400	3.9	12.5
	ID ₉₅ , µg/ml	1.56	> 400	31.25	50
	SI	> 1026	> 1	> 102	> 32

Note. HSV-1/L₂ – reference virus strain; HSV-1/L₂/R – laboratory virus strain highly resistant to ACV; Avd and Sha – ACV-resistant clinical isolates of HSV-1. Multiplicity of infection – 0.1 PFU/cell. Duration of incubation – 48 h. The results of two independent experiments are presented. CTD₅₀ for ACV and Hp-ACG equal > 400 and > 1000 µg/ml, respectively. SI was calculated as the ratio of CTD₅₀ to ID₅₀.

tration was evaluated based on the influence on viral accumulation in the brain of the animals. It was demonstrated that the introduction of Hp-ACG (450 mg/kg, twice per day) led to a decrease of virus titer of 1.30 lg PFU/ml (from 3.31 ± 0.16 to 2.01 ± 0.11) of day 4. This result was close to the effect of Hp-ACG in similar conditions on the model of HSV-1 reference strain: virus titer decreased from 5.49 ± 0.25 to 4.01 ± 0.16 lg (mortality in the control in the latter case was 92.5%, mortality decreased to 67.5% in the experimental group, and MDD increased from 4.90 ± 0.75 to 10.25 ± 1.20) [18].

We have established a mechanism of resistance formation in HSV-1/L₂/R, Avd, and Sha strains. HSV-1/L₂/R and Sha strains contain mutations in the UL23 gene, which lead to R220H substitution in TK and, as a result, to a loss of enzyme activity. Such an enzyme is incapable of catalyzing the first step of ACV phosphorylation required for its conversion into active metabolite ACV triphosphate, which is capable of incorporating into a newly synthesized viral DNA chain and aborting its elongation through the mechanism of termination. Deletion deltaT66 was found in the UL23 gene of the Avd strain located in close vicinity to the ATP-binding site of the enzyme (amino acid residues 51–63), which may cause a decrease in ACV phosphorylation efficiency [20, 25]. The obtained results confirm that all the ACV-resistant HSV strains included in the study exhibit a TK-deficient phenotype and allow one to suggest that mutations in the nucleoside binding site and ATP-binding center do not substantially affect the metabolic conversions of Hp-ACG to monophosphate of ACV, which, like ACV, is further converted into di- and triphosphate of ACV. However, this conversion likely occurs through an alternative pathway by passing the stage of degradation of Hp-ACG to ACV [21].

The development of herpes encephalitis is known to be the cause of death in animals with a generalized herpes infection, and in order to exhibit antiviral activity, the drug has to overcome the blood-brain barrier and enter the brain of the infected animals. Apparently, i.p. introduction of Hp-ACG results in a concentration of the drug into the animal brain that can effectively inhibit virus reproduction. However, the bioavailability of drugs upon *per os* administration is lower than in the case of i.p. or intravenous administration and the drug dosage should be increased in order to preserve its antiviral efficacy. For example, the bioavailability of ACV when administered orally does not exceed 10–20%. The maximum concentration of ACV in blood serum upon *per os* administration of 200 mg of the drug is 0.4–0.8 µg/ml. Intravenous administration of a standard dose (5 mg/kg, three times a day) provides a significantly greater concentration of ACV in serum; about 9.8 mg/ml [26]. In a series of cases, oral administration fails to be effective. For instance, because of the extremely low bioavailability of CDV upon *per os* administration (< 5%), the drug is administered only intravenously [27]. The bioavailability of PCV upon oral administration is also very low: 5% [28]. In this regard, PCV is used only in the form of its metabolic precursor, famciclovir, for oral administration. Structural modifications allow one to increase the absolute bioavailability of PCV from famciclovir up to 77% after a single oral administration [29].

Therefore, having continued the logical development of the research we conducted on the antiherpetic activity of Hp-ACG *in vitro* and *in vivo* [18, 19], we studied the ability of Hp-ACG to protect mice with an experimental generalized infection caused by HSV-1 from death upon oral administration.

The pathogenicity of ACV-resistant HSV variants containing mutations in the TK gene is known to be defined by their phenotype, since it depends on the level of TK activity. Experiments on laboratory animals have shown that TK-negative and TK-deficient strains usually exhibit a substantially reduced virulence or are avirulent; i.e., incapable of causing lethal infection in laboratory animals and manifesting as zosteriform [30, 31]. As it has been noted, the ACV-resistant strains of HSV-1/L₂/R, Avd and Sha used in a previous series of experiments belong specifically to the TK-negative or TK-deficient phenotypes: therefore, we further infected animals with an initial parent strain HSV-1/L₂ with unchanged drug sensitivity. We would like to emphasize that the ability of TK-deficient and TK-negative strains to cause severe clinical forms of a herpes infection is caused by their natural heterogeneity. The presence of TK-positive virus particles capable of synthesizing functionally active TK in a population allows one to compensate for the lack or a low level of TK activity of ACV-resistant viral particles [6, 32].

The infected animals in experimental groups received Hp-ACG as a triple-distilled water solution as described in Experimental Section. Single doses of Hp-ACG were chosen based on the data on drug efficacy upon i.p. administration in the model of experimental infection in mice caused by HSV-1: the ability of Hp-ACG to protect infected animals from death was 3–4 times lower compared to ACV [18].

The results presented in Table 2 demonstrate that Hp-ACG administered orally is effective in protecting animals from death under the proposed experimental conditions. The protective effect is of pronounced dose-dependent nature: an increase in the Hp-ACG dose leads to increased survival rates and MDD of animals,

which is due to the inhibition of viral replication in the brain of infected animals. However, the efficiency of Hp-ACG upon oral administration was lower than in the case of i.p. administration with almost equal animal mortality in the control groups. Thus, at 57% mortality in the control group, 29 out of 40 animals receiving the drug *per os* at a dosage of 300 mg/kg died. The efficacy of Hp-ACG upon i.p. administration at the same single dose and pattern was significantly higher: only one mouse died out of 40. Mortality in the control group in this case was 60% [19].

Reduction in efficiency of Hp-ACG and ACV upon oral administration (twice daily for 5 days) in comparison with i.p. introduction in the same manner was approximately the same in both cases: oral efficacy of ACV was 3–4 times lower than i.p. Thus, in accordance with our data, the protective effect of ACV upon i.p. administration at a single dose of 25 mg/kg was 30% and the increase in MDD was 5.2 days with 65% mortality in the control group [33], which is well comparable with the efficiency values of ACV administered in mice *per os* at a dose of 100 mg/kg (Table 2).

It is important to underline the fact that the efficacy of Hp-ACG upon oral administration at a single dose of 300 mg/kg is well comparable with ACV efficiency at a single dose of 100 mg/kg administered in the same manner and under the same experimental conditions. Protection of the animals from death in the latter case was 21.67%, the increase in MDD was 3.7 days, and the reduction in viral titer in the brain was 0.73 lg.

A comparison of these data with the results shown in Table 1 indicates that the difference in the efficacy values of Hp-ACG and ACV in a generalized model of HSV infection was less significant than in *in vitro* experiments. It is possible that structural modification of

Table 2. Influence of orally administered Hp-ACG on the survival rate of BALB/c mice (8.41 ± 0.31 g) infected with HSV-1/L₂

Compound	Route of administration and dose of the drug	No. of survivors/total no. animals in the group	Mortality, %	Protection, %	MDD days	Yield of virus in brain, lg PFU/ml
–(virus control)	–	26/60	56.67 ± 3.33	–	11.35 ± 1.11	4.18 ± 0.18
Hp-ACG	300 mg/kg × 2 times daily/5 days	29/40	27.50 ± 2.50	29.17	16.40 ± 1.15	3.06 ± 0.12
Hp-ACG	400 mg/kg × 2 times daily/5 days	33/40	17.50 ± 2.50	39.17	18.13 ± 1.00	2.56 ± 0.05
Hp-ACG	500 mg/kg × 2 times daily/5 days	37/40	7.50 ± 2.50	49.17	19.78 ± 0.69	2.03 ± 0.15
ACV	100 mg/kg × 2 times daily/5 days	14/40	35 ± 0	21.67	15.05 ± 1.30	3.45 ± 0.05

Note. The infectious dose is 4×10^6 PFU/mouse (titer of virus-containing material 7.30 lg PFU/ml). The results of two independent experiments are presented.

the ACV molecule (incorporation of a H-phosphonate group) leads to a change in the pharmacokinetic parameters of the drug; for example, it increases its bioavailability upon oral administration.

The antiviral effect of Hp-ACG at a single dose of 500 mg/kg administered orally was close to the effect of Hp-ACG at a dose of 300 mg/kg upon i.p. introduction (three mice out of 40 died). The values of MDD and decrease in virus titer in the brain were also comparable (the difference in MDD from the control group was 9.64 and 8.43 days, and the decrease in virus titer was 3.47 and 2.15 lg PFU/ml upon i.p. and oral administration, respectively). Thus, we can conclude that the antiherpetic efficacy of Hp-ACG administered orally is reduced by less than 2-fold compared to i.p. administration. Since oral administration is more convenient and painless and does not require qualified medical personnel, the obtained results may be of practical interest.

The most common forms of herpes infection are lesions of the skin and mucosae, which do not affect internal organs and the CNS. For example, a recurrence of orofacial herpes (herpes *labialis*) is observed in 15–45% of the adult population [34]. Since herpetic lesions in most cases affect limited areas, the systemic administration of antiherpetic drugs may be counterproductive. Optimal dosage forms in this case are ointments, creams, and gels for topical application. In case of effective drug penetration through the skin, this method not only ensures a selective influence directly on the damaged tissues, but also provides therapeutic concentration of the antiviral agent at the site of the infection when used in much lower doses than upon systemic administration. Consequently, the toxic effect of the drug on the organism is lower, the risk of unwanted side effects is minimized, and, which is also important, the cost of the therapy is also lower. Therefore, we considered appropriate to examine the effectiveness of Hp-ACG in an ointment formulation in the next stage of the research.

Since an experimental cutaneous HSV infection in guinea pigs is caused by the same virus as in humans, and its manifestations are similar to the clinical course of a cutaneous HSV infection in humans, we used the same model for the examination of the compounds for antiherpetic activity.

The safety of skin applications of 5% and 10% Hp-ACG ointments and PEG 600, which served as the ointment base in our experiments, was first evaluated in intact guinea pigs. Ointments were applied on depilated areas of the skin twice daily for 5 days. There was no redness or ulceration of the skin at the site of ointment application, change in animal behavior, or loss of appetite.

In order to evaluate the efficacy of the ointment formulation of Hp-ACG, the animals were infected as

previously described in detail in [35] and stated in Experimental section. We used the culture HSV-1/L₂ virus, which is less neurovirulent than fresh clinical isolates, or a laboratory virus passaged through a mouse brain in order to prevent the development of a generalized infection leading to the death of the animal from encephalitis.

Since accurate calculation of the drug dosage for local use is not possible, the tested ointments were applied in a thin layer directly on to the affected skin areas. Placebo ointment, vehicle consisting of PEG-600 without the drug, was applied in the control under the same conditions.

Visual assessment of the clinical manifestations of the experimental infection was evaluated daily. The formation of local lesions typical of a herpes infection was found in the control group on the 3rd day (72 hours after infection): bullous rash (vesicles) of 2 mm both grouped and single. After another 24 hours (day 4 of infection), the intensity of the lesions reached its maximum and then gradual drying of herpetic vesicles took place with crust formation. After 7–8 days of virus inoculation, the reverse process took place (crust rejection). On day 12, a complete reepithelialization was observed.

A significant reduction in the severity of the clinical symptoms of infection, as well as reduction in the time of treatment under the action of the studied substance in comparison with the control, was used for a quantitative characterization of the compound's activity. The corresponding results are reported in Table 3.

In the case of usage of an ointment of Hp-ACG (5%), the average area of lesions in the experiment was 5.76% lower than in the control ($P < 0.05$ when evaluated using Student's t-test) after 2 days (4 days after virus inoculation), while the number of herpetic sores was 95.55% compared to the control ($P < 0.3$). The term of the start of the reverse process and cure (complete reepithelialization) was decreased by 1 day compared to the control when using a 5% Hp-ACG ointment.

The therapeutic effect of Hp-ACG was more pronounced when used as a 10% ointment and also well comparable to the effect of a 5% ACV ointment. A milder clinical course of infection was observed in both cases during the entire period of observation, which was expressed as a decrease in the number of vesicular structures and reduced lesion surface area. The difference between the values obtained in the experimental and control group was statistically significant ($P < 0.05$ using Student's t-test). The reverse process and cure of the guinea pigs occurred 1 day earlier than in the control group.

The data presented in Table 3 demonstrate that, in all cases, the use of an ointment pharmaceutical form did not lead to a significant reduction in infectious virus titer in vesicular fluid. Therefore, it would be wrong to

Table 3. Comparison of the therapeutic effect of the ointment formulation of Hp-ACG and ACV in an experimental model of a cutaneous herpetic infection in guinea pigs caused by HSV-1/L₂

Compound	Compound concentration in ointment, %	Total Lesion area		Number of herpetic sores		Virus titer in vesicular fluid, lg PFU/ml	Start of reverse process, days	Complete reepithelialization, days
		S _{mean} , cm ²	Decrease compared to control, %	n _{mean}	Decrease compared to control, %			
– (control)	0	4.62 ± 0.08	–	11.25 ± 0.49	–	4.11 ± 0.10 (3.78–4.54)	7–8	12
Hp-ACG	5	4.36 ± 0.07	5.76	10.75 ± 0.31	4.44	4.00 ± 0.08 (3.60–4.38)	6	11
	10	4.22 ± 0.07	8.60	10.00 ± 0.27	11.11	3.85 ± 0.11 (3.54–4.40)	6	11
ACV	5	4.30 ± 0.18	6.95	10.00 ± 0.38	11.11	3.89 ± 0.15 (3.40–4.48)	6	11

Note. The ointment was applied twice daily for 5 days. The first application was 48 hours after infection when a slight redness appeared. The results were registered 4 days after infection. Virus titer in vesicular fluid was determined after 4 days of inoculation when the clinical severity of herpetic manifestations reached their maximum value in the control. The results of two independent experiments are presented.

assume that the ability of Hp-ACG to inhibit the development of a cutaneous herpes infection in guinea pigs caused by a HSV-1/L₂ reference strain is due to the inhibition of viral replication at the site of the infection. However, the obtained results are in good agreement with the published data on the influence of ACV upon local administration on infectious titer of HSV under similar experimental conditions. At the same time, a statistically significant decrease in the number of herpetic vesicular formations and a reduction in the lesion surface area were noted [36–38]. Apparently, the effect of Hp-ACG upon local administration has a primarily preventive character, which is expressed in a prevention of the formation of herpetic sores upon drug application during the prodromal phase at the stage of the appearance of a slight redness but not in the inhibition of virus replication in already-formed vesicles.

CONCLUSION

Thus, our study of the therapeutic efficacy of Hp-ACG action in *in vivo* experiments revealed that Hp-ACG effectively influences a generalized and cutaneous infection caused by HSV-1 upon *per os* administration or as an ointment pharmaceutical form. Despite the fact that this compound is inferior to ACV (the concentration of Hp-ACG must be increased 2-fold in order to achieve a comparable therapeutic effect), it can inhibit the reproduction of ACV-resistant virus variants, as we have shown in experiments *in vitro* and *in vivo*. This makes possible the use of Hp-ACG when ACV is no longer effective. ●

This work was supported by RFBR Grant № 14-04-00198.

REFERENCES

- Díaz-Ramón J.L., Díaz-Pérez J.L. // *Eur. J. Dermatol.* 2008. V. 18. № 1. P. 108–111.
- Smith J.S., Robinson N.J. // *J. Infect. Dis.* 2002. V. 186. Suppl. 1. P. S3–S28.
- Pereira F.A. // *J. Am. Acad. Dermatol.* 1996. V. 35. № 4. P. 503–520.
- Danve-Szatanek C., Aymard M., Thouveno D., Morfin F., Agius G., Bertin I., Billaudel S., Chanzy B., Coste-Burel M., Finkielstejn L., et al. // *J. Clin. Microbiol.* 2004. V. 42. № 1. P. 242–249.
- Langston A.A., Redei I., Caliendo A.M., Somani J., Hutcherson D., Lonial S., Bucur S., Cherry J., Allen A., Waller E.K. // *Blood.* 2002. V. 99. № 3. P. 1085–1088.
- Andrei G., Georgala A., Topalis D., Fiten P., Aoun M., Opendakker G., Snoeck R. // *J. Infect. Dis.* 2013. V. 207. № 8. P. 1295–1305.
- Gateley A., Gander R.M., Johnson P.C., Kit S., Otsuka H., Kohl S. // *J. Infect. Dis.* 1990. V. 161. № 4. P. 711–715.
- Ljungman P., Ellis M.N., Hackman R.C., Shepp D.H., Meyers J.D. // *J. Infect. Dis.* 1990. V. 162. № 1. P. 244–248.
- Marks G.L., Nolan P.E., Erlich K.S., Ellis M.N. // *Rev. Infect. Dis.* 1989. V. 11. № 3. P. 474–476.
- Reardon J.E., Spector T. // *J. Biol. Chem.* 1989. V. 264. № 13. P. 7405–7411.
- Gaudreau A., Hill E., Balfour H. H., Erice A., Boivin G. // *J. Infect. Dis.* 1998. V. 178. № 2. P. 297–303.
- Andrei G., De Clercq E., Snoeck R. // *Antiviral Res.* 2004. V. 61. № 3. P. 181–187.
- Sauerbrei A., Bohn K., Heim A., Hofmann J., Weissbrich B., Schnitzler P., Hoffmann D., Zell R., Jahn G., Wutzler P., et al. // *Antivir. Ther.* 2011. V. 16. № 8. P. 1297–1308.
- Lalezari J.P., Drew W.L., Glutzer E., Miner D., Safran S., Owen W.F. Jr., Davidson J.M., Fisher P.E., Jaffe H.S. // *J.*

- Infect. Dis. 1994. V. 170. № 3. P. 570–572.
15. Gibbs J.S., Chiou H.C., Bastow K.F., Cheng Y.C., Coen D.M. // Proc. Natl. Acad. Sci. USA. 1988. V.85. № 18. P. 6672–6676.
16. Larder B.A., Kemp S.D., Darby G. // EMBO J. 1987. V. 6. № 1. P. 169–175.
17. Saijo M., Suzutani T., Morikawa S., Kurane I. // Antimicrob. Agents Chemother. 2005. V. 49. № 2. P. 606–611.
18. Andronova V.L., Galegov G.A., Jasko M.V., Kukhanova M.K., Skoblov Y.S. // Voprosy Virusologii. 2010. V. 55. № 1. P. 31–34.
19. Andronova V.L., Galegov G.A., Jasko M.V., Kukhanova M.K., Kochetkov S.N., Skoblov Y.S. // Voprosy Virusologii. 2011. V. 56. № 5. P. 37–40.
20. Korovina A.N., Gus'kova A.A., Skoblov M.Y., Andronova V.L., Galegov G.A., Kochetkov S.N., Kukhanova M.K., Skoblov Y.S. // Mol. Biol. 2010. V. 44. № 3. P. 488–496.
21. Karpenko I.L., Jasko M.V., Andronova V.L., Ivanov A.V., Kukhanova M.K., Galegov G.A., Skoblov Y.S. // Nucleosides Nucleotides Nucl. Acids. 2003. V. 22. № 3. P. 319–328.
22. De Clercq E., Descamps J., Verheist G., Walker R.T., Jones A.S., Torrence P.F., Shugar D. // J. Infect. Dis. 1980. V. 141. № 5. P. 563–573.
23. McKeough M.B., Spruance S.L. // Arch. Dermatol. 2001. V. 137. № 9. P. 1153–1158.
24. Sarisky R.T., Nguyen T.T., Duffy K.E., Wittrock R.J., Leary J.J. // Antimicrob. Agents Chemother. 2000. V. 44. № 6. P. 1524–1529.
25. Gus'kova A.A., Zagurnyĭ A.V., Skoblov M.Y., Baranova A.V., Andronova V.L., Iankovskii N.K., Galegov G.A., Skoblov Y.S. // Mol. Biol. 2005. V. 39. № 1. P. 155–158.
26. Wagstaff A.J., Faulds D., Goa K.L. // Drugs. 1994. V. 47. № 1. P. 153–205.
27. Cundy K.C. // Clin. Pharmacokinetics. 1999. V. 36. № 2. P. 127–143.
28. Harden M.R., Jarvest R.L. // Tetrahedron Lett. 1985. V. 26. P. 4265–4268.
29. Perry C.M., Wagstaff A.J. // Drugs. 1995. V. 50. № 2. P. 396–415.
30. Coen D.M. // Trends. Microbiol. 1994. V. 2. № 12. P. 481–485.
31. Efsthathiou S., Kemp S., Darby G., Minson A.C. // J. Gen. Virol. 1989. V. 70. Pt. 4. P. 869–879.
32. Horsburgh B.C., Chen S.H., Hu A., Mulamba G.B., Burns W.H., Coen D.M. // J. Infect. Dis. 1998. V. 178. № 3. P. 618–625.
33. Andronova V.L., Grokhovskiy S.L., Surovaya A.N., Gurskiy G.V., Galegov G.A. // Doklady Biochemistry and Biophysics. 2007. V. 413. № 6. P. 830–834.
34. Harmenberg J., Oberg B., Spruance S. // Acta Derm. Venereol. 2010. V. 90. № 2. P. 122–130.
35. Andronova V.L., Grokhovskiy S.L., Surovaya A.N., Gurskiy G.V., Deryabin P.G., L'vov D.K., Galegov G.A. // Voprosy Virusologii. 2013. V. 58. № 1. P. 32–35.
36. Spruance S.L., Freeman D.J., Sheth N.V. // Antimicrob. Agents Chemother. 1985. V. 28. № 1. P. 103–106.
37. Spruance S.L., McKeough M.B., Cardinal J.R. // Antimicrob. Agents Chemother. 1984. V. 25. № 1. P. 10–15.
38. Spruance S.L., Freeman D.J., Sheth N.V. // Antimicrob. Agents Chemother. 1986. V. 30. № 1. P. 196–198.

Molecular Mechanism Underlying the Action of Substituted Pro-Gly Dipeptide Noopept

Y. V. Vakhitova^{1,2*}, S. V. Sadovnikov², S. S. Borisevich^{2,3}, R. U. Ostrovskaya¹, T. A. Gudasheva¹, S. B. Seredenin¹

¹State Zakusov Institute of Pharmacology, Baltiyskaya Str., 8, 125315, Moscow, Russia

²Institute of Biochemistry and Genetics of Ufa Scientific Centre RAS, Prospekt Oktyabrya, 71, 450065, Ufa, Russia

³Ufa Institute of Chemistry RAS, Prospekt Oktyabrya, 71, 450065, Ufa, Russia

*E-mail: juvv73@gmail.com

Received 16.06.2015

Copyright © 2016 Park-media, Ltd. This is an open access article distributed under the Creative Commons Attribution License, which permits unrestricted use, distribution, and reproduction in any medium, provided the original work is properly cited.

ABSTRACT This study was performed in order to reveal the effect of Noopept (ethyl ester of N-phenylacetyl-L-prolylglycine, GVS-111) on the DNA-binding activity of transcriptional factors (TF) in HEK293 cells transiently transfected with luciferase reporter constructs containing sequences for CREB, NFAT, NF- κ B, p53, STAT1, GAS, VDR, HSF1, and HIF-1. Noopept (10 μ M) was shown to increase the DNA-binding activity of HIF-1 only, while lacking the ability to affect that of CREB, NFAT, NF- κ B, p53, STAT1, GAS, VDR, and HSF1. Noopept provoked an additional increase in the DNA-binding activity of HIF-1 when applied in conditions of CoCl₂-induced HIF-1 stabilization. The degree of this HIF-positive effect of Noopept was shown to be concentration-dependent. Piracetam (1 mM) failed to affect significantly any of the TF under study. The results of molecular docking showed that Noopept (*L*-isomer), as well as its metabolite, *L*-isomer of N-phenyl-acetylprolyl, unlike its pharmacologically ineffective *D*-isomer, is able to bind to the active site of prolyl hydroxylase 2. Taking into account the important role of the genes activated by HIF-1 in the formation of an adaptive response to hypoxia, data on the ability of Noopept to provoke a selective increase in the DNA-binding activity of HIF-1 explain the wide spectrum of neurochemical and pharmacological effects of Noopept revealed before. The obtained data allow one to propose the HIF-positive effect as the primary mechanism of the activity of this Pro-Gly-containing dipeptide.

KEYWORDS Noopept, transcriptional factors, HIF-1, hypoxia, HIF-prolyl hydroxylase 2, docking, neuroprotection.

ABBREVIATIONS CREB – cAMP responsive element-binding protein; NFAT – nuclear factor of activated T-cells; NF- κ B – nuclear factor kappa-light-chain-enhancer of activated B-cells; STAT1 – signal transducer and activator of transcription; GAS – interferon- γ -activated sequence; VDR – vitamin D₃ receptor; HSF1 – heat shock transcriptional factor 1; HIF-1 – hypoxia-inducible factor 1.

INTRODUCTION

Noopept (ethyl ester of N-phenylacetyl-L-prolylglycine) was designed as a drug at State Zakusov Institute of Pharmacology. The synthesis of the drug is based on the original hypothesis of peptide design, according to which structures similar to known psychotropic agents are reproduced using appropriate amino acids [1]. The non-peptide prototype of Noopept is the nootropic drug Piracetam. The pharmacological activity of the new compound turned out to be generally similar to the activity of Piracetam; but, it manifestes itself at doses 1,000 times lower than those for Piracetam [2, 3]. Moreover, Noopept has more pronounced anxiolytic [4] and neuroprotective properties [5–7].

A clinical study of Noopept (registration number 015770) confirmed the nootropic effects established

experimentally. In patients with mild cognitive impairment of cerebrovascular and post-traumatic origin, the drug decreased cognitive impairment, showed an anxiolytic effect, and vegetostabilizing activity (www.noopept.ru).

The mechanism of Noopept action has been studied since its synthesis. It has been established that the drug increases the expression of NGF and BDNF in the hippocampus [8], exhibits choline-positive properties at behavioral and neuronal levels [9], reduces oxidative stress and enhances the activity of antioxidant systems [7, 10], and represses kinases pSAPK/JNK and pERK1 induced by stress [11]. However, the study of the primary interactions of Noopept with more than 100 known receptors conducted according to our protocol by the CEREP company (France) did not lead to

the expected identification of the primary targets. At the same time, the wide range of the neurochemical and pharmacological effects of Noopept prompted the further search for its targets.

In order to obtain more exhaustive information on the targets of Noopept, we analyzed *in vitro* the influence of the drug on the DNA-binding activity of pharmacologically significant biological targets, the transcription factors (TF) CREB, NFAT, NF- κ B, p53, STAT1, GAS, VDR, HSF1, and HIF-1. Having identified the selective influence of Noopept on HIF-1, we examined the effect of the drug on the activity of this transcription factor under conditions mimicking the hypoxia *in vitro*.

EXPERIMENTAL

Cell culturing

A HEK 293 cell line (human embryonic kidney cells; Russian Collection of Cell Cultures, Institute of Cytology, RAS, St. Petersburg) was used in the study. The cells were cultured at 37°C, 5% CO₂ in DMEM medium (Biolot, Russia) with 10% fetal bovine serum (Sigma, USA), 2 mM L-glutamine, 50 µg/ml gentamycin sulfate, and 2.5 µg/ml amphotericin B (PanEco, Russia).

The influence of Noopept on the DNA-binding activity of transcription factors was examined using luciferase reporter constructs containing binding sites for CREB, NFAT, NF- κ B, p53, STAT1, GAS, VDR, HSF1, and HIF-1 according to [12].

For transfection, HEK293 cells were seeded (4×10^3 cells/per well) in 96-well plates in 100 µl of a DMEM medium containing 10% fetal bovine serum and 2 mM L-glutamine without an antibiotic. Reporter vector constructs containing binding sites for the transcription factors CREB, NFAT, NF- κ B, p53, STAT1, GAS, VDR, HSF1, and HIF-1 were obtained on the basis of the pTL-Luc plasmid vector (Panomics, USA; carries the *Photinus pyralis* luciferase gene) [13]. The HEK293 cells were transiently transfected with the constructs using the Lipofectamine 2000 reagent (Invitrogen, USA) according to the manufacturer's recommendations. The medium was replaced with a medium containing an antibiotic (DMEM, 10% fetal bovine serum, 2 mM L-glutamine, 50 µg/ml gentamicin sulfate) 6 hours after transfection, and the studied drugs (Noopept 10 µM; Piracetam, 1 mM) were added after 18 h. The cells were incubated in the presence of either Noopept or Piracetam for another 24 hours. Luciferase activity in cell lysates was determined using a Dual Luciferase Reporter Assay System (Promega, USA) on the plate reader 2300 EnSpire® Multimode Plate Reader (Perkin Elmer, USA). Co-transfection with plasmid pRL-TK (Promega, USA) encoding the *Renilla reniformis*

luciferase gene was used as an internal control for transfection. The values of the *P. pyralis* luminescence were normalized to the luminescence of *R. reniformis* in each measurement.

Experimental simulation of hypoxia was performed using CoCl₂, as pharmacological inducer of hypoxia, causing stabilization of HIF-1 [14]. The luciferase construct for the analysis of HIF-1 activity contains four copies of a consensus sequence 5'-ACGTG-3', an HIF-1 protein-binding site (HIF-1-Luc construct). The cells transfected with the plasmid vector HIF-1-Luc were preincubated with Noopept for 8 hours (final concentrations 1, 10, and 100 µM; double administration every 4 hours), then the hypoxia inductor CoCl₂ was added at a working concentration of 50 µM, and combined incubation with Noopept and CoCl₂ proceeded for an additional 16 hours. After that, luciferase activity was determined as described above.

Statistical analysis

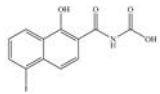
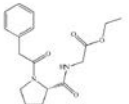
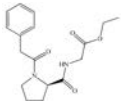
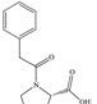
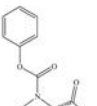
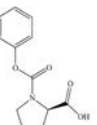
The arithmetic mean of the values obtained for two repeats in each experiment in a series of three independent experiments and the standard error of the mean value were calculated using the Statistica 6.1 software (StatSoft Inc., USA). Experimental groups were compared using a paired Student's t-test for dependent samples.

Molecular docking

The three-dimensional structure of the target protein prolyl hydroxylase 2 (PHD2; hypoxia-inducible factor-L-proline, 2-oxoglutarate: oxygen oxidoreductase, [1.14.11.29]; PDB code: 2G19) in a complex with the native inhibitor (ZINC code: 24800213; IC₅₀ 1.4 µM) was used for construction and validation of the docking model [15, 16]. Noopept and its D-enantiomer (ZINC codes: 1542824 and 3812682, respectively), Noopept metabolite L-N-phenylacetyl-proline (ZINC code: 76075), and stereoisomers of the previously described [31] prolyl hydroxylase inhibitor (PA2L and PA2D) (Table) were considered as ligands. The geometrical parameters of the majority of the molecules were extracted from the ZINC database [17] or modeled using the ChemCraft v1.7 software [18] and optimized by the HF/6-311G(d,p) method on the GAUSSIAN 09 C.01 software [19]. Preparation of target and ligand structures for docking, as well as docking, was performed using the LeadIT 2.1.8 software [20]. All quantum chemical calculations were performed on a cluster supercomputer at the Ufa Institute of Chemistry, RAS.

The surrounding area of the native inhibitor (ZINC: 24800213) with adjacent amino acid residues is 6.5 Å and contains Arg383, Tyr310, Tyr303 and Fe²⁺. Analysis

In silico estimation of the energies of interaction between ligand and receptor

Ligand code	Ligand structure	$\Delta G_{\text{FlexX}}^1$ kJ/mol ¹	RMSD ²	ΔG_{HYDE}^3 kJ/mol ³	LE ⁴
ZINC24800213		-31.8	0.42	-63	0.79 (H)
ZINC1542824_L		-17.0	0.48	-44	0.45 (HA)
ZINC3812682_D		-17.5	1.10	-42	0.42 (HA)
ZINC76075_L		-24.1	0.47	-38	0.53 (H)
PA2_L		-27.2	0.55	-49	0.55 (H)
PA2_D		-28.2	0.73	-41	0.47 (HA)

¹ ΔG_{FlexX} – free binding energy, kJ/mol.

²RMSD – root-mean square deviation of ligand position in active site.

³ ΔG_{HYDE} – affinity energy between ligand and binding site, kJ/mol.

⁴LE – ligand efficiency (LE = $|\Delta G_{\text{HYDE}}|/N$ [22, 23], where N – number of heavy, i.e. not hydrogen atoms), where ligand efficiency can be evaluated as H – high efficiency, HA – higher than average efficiency [22].

of the 2G19 enzyme active center showed that Arg383 and Tyr329 form hydrogen bonds with the carboxyl group of the ZINC 24800213 native inhibitor; Tyr310 and Tyr303 form a π - π electron interaction with the aromatic rings of the ligand. The amino acid residues Trp389, Trp258, Met299, and Ile256 form a hydrophobic pocket (*Fig. 1*). All water molecules were removed from the active center during preparation of the enzyme structure for the docking procedure. Re-docking of the native ligand into the PHD2 enzyme active site accurately reproduces the mode of binding between the ligand and enzyme that has been determined crystallographically. The root-mean-square deviation is 0.44 Å. The subprogram FlexX [21] allows to perform the procedure of ligand docking (*Table*) and estimate the energy of binding between the ligand and receptor in the active site. The number of docking decisions can be large enough, and the choice of an optimal solution is based on the minimum value of the binding energy

in combination with a minimum root-mean-square deviation (RMSD) value when the ligand is in the binding site. Next, the selected position is subjected to further calculation: assessment of the affinity energy between the ligand and binding site (ΔG_{HYDE} , kJ/mol) and evaluation of ligand effectiveness [22, 23]. A detailed algorithm of the calculation is described in [22]. It is noted that it is optimal to use two successive stages of the selection of the leader compound among the ligands.

RESULTS AND DISCUSSION

The data presented in *Fig. 2A* indicate that incubation with Noopept at a concentration of 10 μM for 24 hours enhances the DNA-binding activity of HIF-1 by 43% and does not caused any statistically significant changes in the DNA-binding activity of the factors CREB, NFAT, NF- κB , p53, STAT1, GAS, VDR, and HSF1. As follows from the data presented in *Fig. 3*, Noopept at concentrations of 10 and 100 μM increases the level of

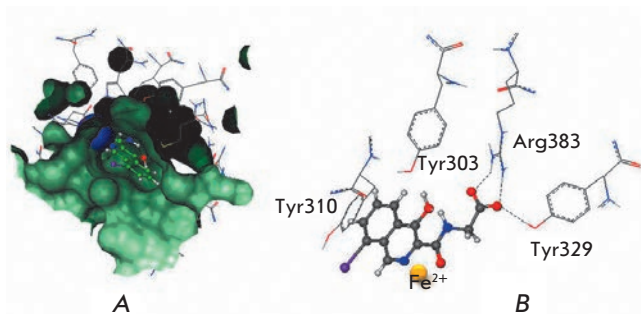


Fig. 1. Analysis of the active site of prolyl hydroxylase enzyme 2. *A* – active center occupied by “native” ligand. *B* – interaction between inhibitor and amino acid residues of the enzyme (docking solution)

luciferase induction. It was shown that Piracetam at either an equimolar (10 μM , data not shown) or higher concentration (1 μM) does not cause statistically significant changes in the DNA-binding activity of the studied transcription factors (*Fig. 2B*).

The next stage of the study included the analysis of the influence of Noopept on the DNA-binding activity of HIF-1 in the presence of a pharmacological mimetic of hypoxia CoCl_2 . In full accordance with the well known data concerning CoCl_2 action, an increase in HIF-1 activity was observed. Addition of Noopept at concentrations of 10 and 100 μM resulted in a further increase in HIF-1-dependent luciferase activity (*Fig. 3*). Thus, it has been established for the first time that Noopept is able to increase both the basal activity

of HIF-1 and the activity induced by a pharmacological mimetic of hypoxia *in vitro*.

The factor induced by hypoxia (HIF-1) is a heterodimer composed of two subunits: a HIF-1 α subunit sensitive to oxygen and constitutively expressed HIF-1 β . Hypoxia promotes an increase in the HIF-1 α level, its dimerization with HIF-1 β , mobilization of coactivators (p300/CBP), and binding of this complex to HRE (hypoxia-response element) in the regulatory regions of target genes. In normoxic conditions, oxygen-dependent hydroxylation of proline residues in the HIF-1 α molecule by prolyl hydroxylases is necessary for binding by the component of ubiquitin-protein ligase E3, von Hippel-Lindau (VHL) protein. Ubiquitinated HIF-1 α becomes a target for degradation by 26S proteasomes. The asparagine residue at the C-terminal transactivation domain (C-TAD) of HIF-1 α is hydroxylated by asparagin hydroxylase (FIH1, factor inhibiting HIF-1) in the presence of oxygen, thereby blocking its interaction with the transcriptional coactivator p300/CBP. Thus, PHD and FIH inactivate HIF-1 α in normoxia, suppressing HIF-1-dependent expression of the target genes. PHD and FIH activity decreases under conditions of hypoxia, leading to a decrease in HIF-1 α degradation and transcriptional activation of its dependent genes [24]. It has been shown [25] that HIF-1 activates a total of up to 100 genes. *Figure 4* presents the main targets of HIF-1, which include the genes involved in angiogenesis through activation of the vascular endothelial growth factor, enhanced synthesis of erythropoietin, activation of the systems of glucose transport through membranes, cytoprotection by neurotrophic factors, normalization of cell cycle and

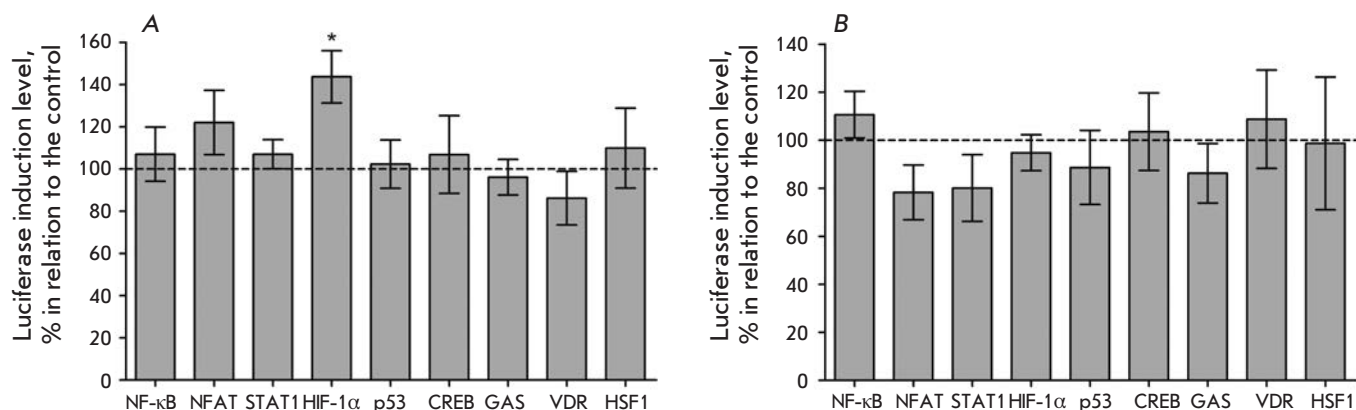


Fig. 2. Effect of Noopept, 10 μM (*A*), and piracetam, 1 mM (*B*), on the basal DNA-binding activity of the transcriptional factors NF- κ B, NFAT, STAT1, HIF-1 α , p53, CREB, GAS, VDR, and HSF1 *in vitro*. The statistical significance of the differences was assessed using a paired Student's t-test for dependent samples ($n = 3$, $*p < 0.05$)

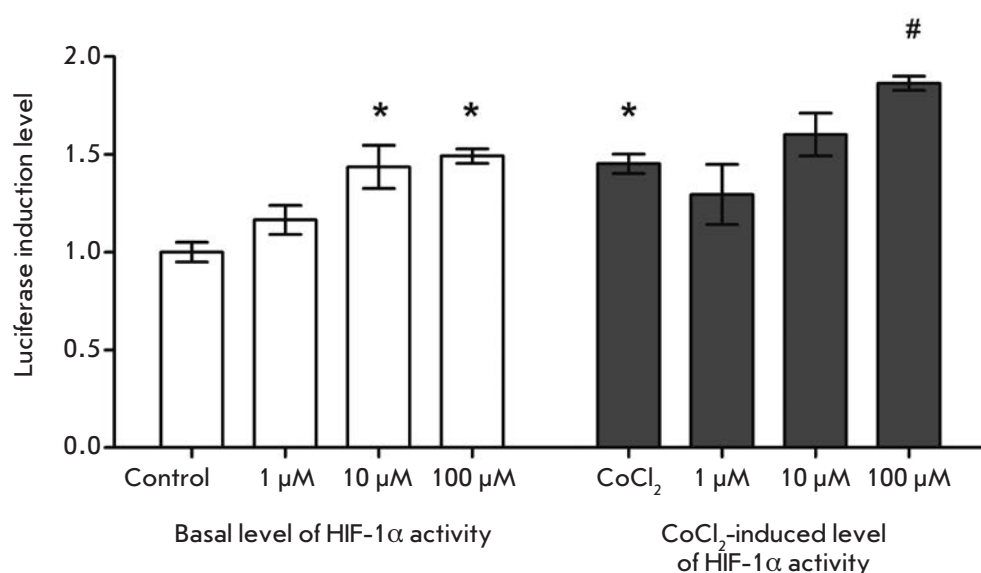


Fig. 3. The effect of Noopept on the basal and induced activity of HIF-1. "Control" group – values of the basal activity of HIF-1 in unstimulated cells; "CoCl₂" group – HIF-1 activity values in CoCl₂-stimulated cells. The data are presented as arithmetic mean ± standard error of the mean ($n = 3$; * $p < 0.05$ with respect to "control" group; # $p < 0.05$ with respect to "CoCl₂" group)

metabolism at the mitochondrial level, as well as the activity of antioxidant enzymes: superoxide dismutase and catalase. The combination of these effects allows the implementation of an adaptive response to hypoxic exposure. Alongside with this, HIF-1 affects the state of many neurotransmitter systems: it activates the protein responsible for control of GABA receptors (GABA-RBP) [26] and increases tyrosine hydroxylase activity [27]. The close relation between HIF-1 and cholinergic receptors has been described [28].

As shown in our study, Noopept causes a concentration-dependent increase in the basal DNA-binding activity of HIF-1. Upon stabilization of HIF-1 with CoCl₂, a chemical inducer of this transcription factor [29, 30], Noopept provides an additional increase in the HIF-1 DNA-binding activity. The effect on HIF-1 is specific for Noopept: the classical nootropic drug Piracetam does not affect the activity of this transcription factor. Noopept enhances the DNA-binding activity of HIF-1 alone, while the activity of other transcription factors (CREB, NFAT, NF- κ B, p53, STAT1, GAS, VDR and HSF1) is not increased. Since prolyl hydroxylase is directly involved in HIF-1 deactivation, and proline analogs are described as effective inhibitors of this enzyme [31], it can be assumed that the increase in the DNA-binding activity of HIF-1 by Noopept is associated with the inhibition of this enzyme.

The comparison of the structures of prolyl hydroxylase inhibitors presented by Ma *et al.* [31] with that of Noopept and its metabolites suggests a similarity between the PA2 (benzyloxycarbonyl-Pro) compound and an N-terminal fragment of the Noopept molecule, N-phenylacetyl-Pro (Table) [32, 33]. It should be noted

that the range of concentrations at which PA2 inhibits prolyl hydroxylase ($K_i = 2.38 \mu\text{M}$, $EC_{50} = 3.17 \mu\text{M}$) [31] is close to the level of effective concentrations for Noopept identified in the present study.

According to the results of the molecular docking, Noopept and *L*-isomer of N-phenylacetyl-Pro binds to the active site of prolyl hydroxylase at a level of efficiency comparable with that of RA2L *L*-isomer (Table). The qualitative effectiveness of the ligand is estimated as high. *L*- stereoisomer of N-phenylacetyl-Pro forms hydrogen bonds with Arg383 and Tyr329 in the active site of the enzyme, and the PA2L molecule is coordinated by oxygens around the Fe atom (Fig. 5). It should be underlined that the pharmacologically inactive *D*-isomer of Noopept has a lower binding energy. Thus, it can be assumed that Noopept and its metabolite, *L*-isomer of N-phenylacetyl-Pro, may bind to the active site of prolyl hydroxylase 2 and, probably, inhibit its enzymatic activity. Apparently, the final conclusion requires further experimental study of the effect of Noopept and its metabolite on the activity of prolyl hydroxylase. Possible interaction of Noopept with asparagine hydroxylase also requires additional studies.

Returning to the question of the interaction between Noopept and HIF-1 while lacking that for Piracetam, it should be noted that Noopept is designed as a dipeptide analogue of Piracetam. However, the effective doses of Noopept are three times lower than that of Piracetam [2]. The new drug and its non-peptide prototype demonstrate different spectrum of pharmacological activity. Thus, Noopept facilitated all phases of information processing, while Piracetam influenced mainly initial phases [1]. Noopept exhibited pronounced neuroprotec-

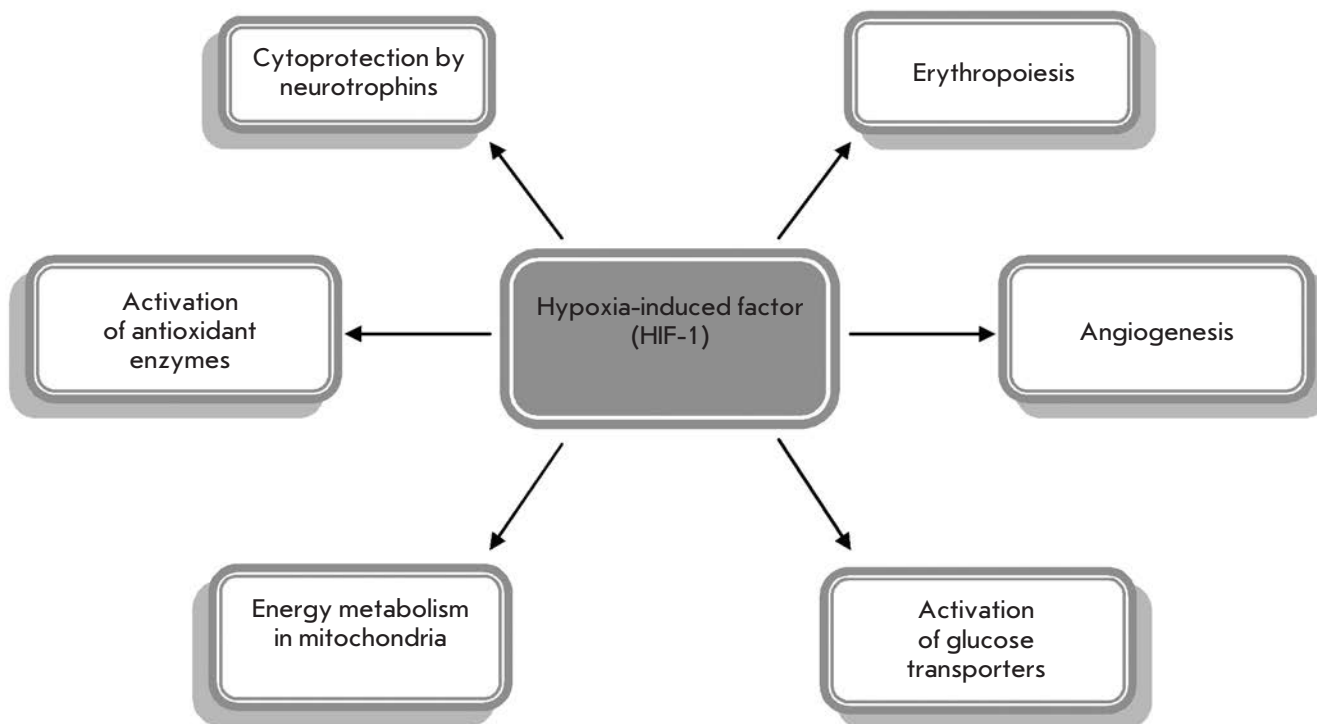


Fig. 4. Hypoxia-induced factor HIF-1 and its targets. Modified according to [24]

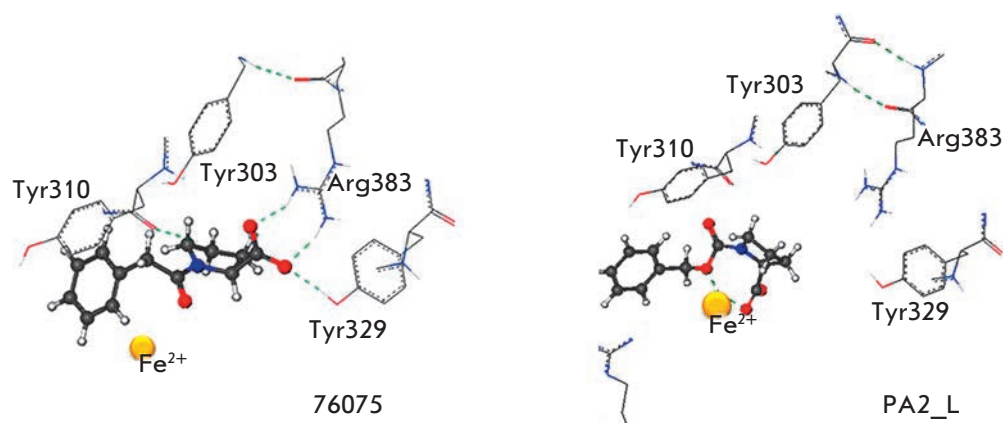


Fig. 5. Results of molecular docking: location of ligands in the active site of prolyl hydroxylase (hydrogen bonds are shown in dashed line)

tive properties, whereas in Piracetam they, depending on the estimated parameter, were mild [7, 34] or absent [35]. From a pharmacological position, such differences must be based on the specificity of the mechanism of action, which includes the effect of Noopept interaction with HIF-1 identified by us.

Regardless of the details of this interaction, it is important that this Pro-containing dipeptide enhances HIF-1 activity. It is known that activation of the HIF system is now regarded as one of the main mechanisms of neuroprotection during hypoxia, cerebral ischemia, and neurodegenerative diseases [24, 36]. During many

years of study, these states have been defined as pharmacological targets for Noopept action on a broad spectrum of relevant experimental models.

Following the ability of Noopept to increase animal survival in hyperbaric hypoxia [37] detected at the beginning of the study of this dipeptide, it has been shown that it reduces the volume of ischemic brain damage in circulatory hypoxia models: for example, cortical photochemically induced thrombosis [6] and ligation of the middle artery [5]. The ability of Noopept to attenuate the severity of oxidative stress was established in neuronal cultures of various types: granular

cerebellar cells [35], cortical neuron culture of aborted fetuses with diagnosed Down syndrome [7], PC12 culture [38], SH-SY5Y culture [39], and in vivo experiments on brain tissue and rat plasma [40]. The ability to enhance superoxide dismutase and catalase activity was shown both in the experiment [10] and in clinical conditions [34].

The ability of Noopept not only to eliminate the manifestations of cognitive deficit [41], but to exert also a neuroprotective effect was shown in models of Alzheimer's disease: it attenuated the disturbance of oxidative processes and calcium homeostasis, enhanced neurogenesis, prevented the tau protein aggregation caused by a fragment of β -amyloid₂₅₋₃₅ [38], and eliminated NGF and BDNF deficit caused by diabetogenic toxin streptozotocin administration into brain ventricles [42]. Noopept is capable of reducing the cytotoxic effect of aggregated α -synuclein in a cell model of Parkinson's disease [39]. All these numerous effects can be explained by the activation of the HIF-1 transcription factor.

In the past years, we have shown that Noopept has an antidiabetic effect on the streptozotocin model of diabetes [43]. This fact was interpreted by us as a result of the multifactorial metabolic action of the drug: attenuation of the deficit in the antioxidant systems and neurotrophic factors and increased production of pro-inflammatory cytokines typical of diabetes [44]. The results obtained in the present study have drawn our attention to the data on the role of HIF-1 in the development of pathological processes in diabetes mellitus. For instance, the ability of insulin to disrupt HIF-1 formation and the role of this factor deficiency in the development of diabetes type 1 and 2 and its complications have been reported [45]. The impaired function of the glucose transport system GLUT1 and GLUT3 through cellular barriers observed in HIF-1 deficiency promotes the development of insulin resistance in both

Alzheimer's disease and diabetes mellitus [46]. The involvement of HIF-1 in the expression of incretins, important factors of pancreatic β -cell cytoprotection, has been proved [47]. A summary of these data allows to suggest that the HIF-1-positive effect of Noopept participates in the realization of its anti-diabetic effect, including the newly identified one by us ability to increase the level of incretin, a glucagon-like peptide-1 (GLP-1) [44].

CONCLUSION

The data obtained on the ability of the effective nootropic and neuroprotective drug Noopept to cause an increase in the DNA-binding activity of HIF-1 allow one to advance a novel interpretation of the wide spectrum of its action: namely, assume that the HIF-1-positive effect of the drug can be considered as the primary mechanism of its action. Clarification of the molecular mechanisms underlying the HIF-1-positive action of Noopept certainly requires further investigation; but the presence of this effect definitely has a significant value, since it allows one to explain almost all known to date effects of Noopept and, probably, the effects of other biologically active Pro-Gly peptides. These data provide additional evidence for current concepts of the importance of the components of the HIF-1-dependent signaling pathway and the compensation processes activated by this transcription factor in the mechanisms of neuroprotection. ●

The studies were performed using equipment from Biomika (Department of Biochemical Methods of Research and Nanobiotechnology Agidel, Ufa) and KODINK.

This work was supported by a Russian President grant for leading scientific schools (5923.2014.4).

REFERENCES

- Gudasheva T.A. // Bulletin of the Russian Academy of Medical Sciences. 2011. № 7. P. 8–16.
- Seredenin S.B., Voronina T.A., Gudasheva T.A., Ostrovskaya R.U., Rozantsev G.G., Skoldinov A.P., Trofimov S.S., Halikas J., Garibova T.L. Biologically active N-acylprolyldipeptides having anti-amnesic, antihypoxic effects. Patent 5.439.930 USA. 1995.
- Gudasheva T.A., Voronina T.A., Ostrovskaya R.U., Rozantsev G.G., Vasilevich N.I., Trofimov S.S., Kravchenko E.V., Skoldinov A.P., Seredenin S.B. // Eur. J. Med. Chem. 1996. V. 31. P. 151–157.
- Ostrovskaya R.U., Seredenin S.B., Voronina T.A., Molodavkin G.M., Gudasheva T.A. // In Animal models in biological psychiatry / Ed. Kalueff A.V. N.-Y.: Nova Sci. Publ. Inc., 2006. P. 165–182.
- Gavrilova S.A., Us K.S., Ostrovskaya R.U., Koshelev V.B. // Eksp. Klin. Farmakol. 2006. V. 69. № 4. P. 16–18.
- Ostrovskaya R.U., Romanova G.A., Barskov I.V., Shani-na E.V., Gudasheva T.A., Victorov I.V., Voronina T.A., Seredenin S.B. // Behav. Pharmacol. 1999. V. 10. P. 549–553.
- Pealsman A., Hoyo-Vadillo C., Seredenin S.B., Gudasheva T.A., Ostrovskaya R.U., Busciglio J. // Int. J. Dev. Neurosci. 2003. V. 21. P. 117–124.
- Ostrovskaya R.U., Gudasheva T.A., Tsaplina A.P., Vakhitova Yu.V., Salimgareeva M.H., Yamidanov R.S., Seredenin S.B. // Bull. Exp. Biol. Med.. 2008. V. 146. № 9. P. 309–312.
- Ostrovskaya R.U., Mirzoev T.H., Firova F.A., Trofimov S.S., Gudasheva T.A., Grechenko T.N., Gutyrchik E.F., Barkova E.B. // Eksp. Klin. Farmakol. 2001. V. 64. № 2. P. 11–14.
- Mendzheritskiy A.M., Lysenko A.V., Demyanenko S.V., Prokofyev V.N., Gudasheva T.A., Ostrovskaya R.U. // J. Neurochemical. 2003. V. 20. № 4. P. 281–286.
- Ostrovskaya R.U., Vakhitova Y.V., Salimgareeva M.H., Yamidanov R.S., Sadovnikov S.V., Kapitsa I.G., Seredenin S.B. // Eksp. Klin. Farmakol. 2010. V. 73. № 12. P. 2–5.

12. Phippard D., Manning A.M. // *Methods Mol. Biol.* 2003. V. 225. P. 19–23.
13. Salimgareeva M.H., Sadovnikov S.V., Farafontova E.I., Zaynullina L.F., Vakhitov V.A., Vakhitova Y.V. // *Prikladnaya biokhimiya i microbiologiya.* 2014. V. 50. № 2. P. 219–225.
14. Piret J.P., Mottet D., Raes M., Michiels C. // *Ann. N.Y. Acad. Sci.* 2002. V. 973. P. 443–447.
15. Rose P.W., Prlić A., Bi C., Bluhm W.F., Christie C.H., Dutta S., Green R.K., Goodsell D.S., Westbrook J.D., Woo J., et al. // *Nucl. Acids Res.* 2015. V. 43. P. 345–356. <http://www.rcsb.org/>
16. McDonough M.A., Li V., Flashman E., Chowdhury R., Mohr C., Liénard B.M., Zondlo J., Oldham N.J., Clifton I.J., Lewis J., et al. // *Proc. Natl. Acad. Sci. USA.* 2006. V. 103. № 26. P. 9814–9819.
17. Irwin J.J., Shoichet B.K. // *J. Chem. Inform. Model.* 2005. V. 45. P. 177–182.
18. Zhurko G.A., Zhurko D.A. // *ChemCraft.* v. 1.7. 2013.
19. Frisch M.J., Trucks G.W., Schlegel H.B., Scuseria G.E., Robb M.A., Cheeseman J.R., Scalmani G., Barone V., Mennucci B., Petersson G.A., et al. // *Gaussian 09, Revision C.01*, Gaussian Inc., Wallingford CT, 2010.
20. Claussen H., Dramburg I., Gastreich M., Hindle S., Kamper A., Kramer B., Lilienthal M., Mueller G., Rarey M., Wefing S., et al. // *LeadIT. V. 2.1.8 BioSolveIT CmbH*, 2014.
21. Rarey M., Kramer B., Lengauer T., Klebe G. // *J. Mol. Biol.* 1996. V. 261. P. 470–489.
22. Schneider N., Hindle S., Lange G., Klein R., Albrecht J., Briem H., Beyer K., Claußen H., Gastreich M., Lemmen Ch., Rarey M. // *J. Comput Aided Mol. Des.* 2012. V. 26. P. 701–723.
23. Kuntz I.D., Chen K., Sharp K.A., Kollman P.A. // *Proc. Natl. Acad. Sci. USA.* 1999. V. 96. № 18. P. 9997–10002.
24. Semenza G. // *Cell.* 2012. V. 148. № 3. P. 399–408.
25. Zheng H., Fridkin M., Youdim M. // *Persp. Med. Chem.* 2015. V. 7. P. 1–8.
26. Park S.H., Kim B.R., Lee J.H., Park S.T., Lee S.H., Dong S.M., Rho S.B. // *Cell Signal.* 2014. V. 26. № 7. P. 1506–1513.
27. Schnell P.O., Ignacak M.L., Bauer A.L., Striet J.B., Paulding W.R., Czyzyk-Krzeska M.F. // *J. Neurochem.* 2003. V. 85. № 2. P. 483–491.
28. Hirota K., Ryo Fukuda R., Takabuchi S., Kizaka-Kondoh S., Adachi T., Kazuhiko Fukuda K., Semenza G.L. // *J. Biol. Chem.* 2004. V. 279. № 40. P. 41521–41528.
29. Epstein A.C., Gleadle J.M., McNeill L.A., Hewitson K.S., O'Rourke J., Mole D.R., Mukherji M., Metzén E., Wilson M.I., Dhanda A., et al. // *Cell.* 2001. V. 107. № 1. P. 43–54.
30. Yuan Y., Hilliard G., Ferguson T., Millhorn D.E. // *J. Biol. Chem.* 2003. V. 278. № 18. P. 15911–15916.
31. Ma X., Wang X., Cao J., Geng Z., Wang Z. // *PLoS One.* 2014. V. 9. № 4. e95692.
32. Boyko S.S., Zherdev V.P., Dvoryaninov A.A., Gudasheva T.A., Ostrovskaya R.U., Voronina T.A., Rozantsev G.G., Seredenin S.B. // *Eksp. Klin. Farmakol.* 1997. V. 60. № 2. P. 101–104.
33. Gudasheva T.A., Boyko S.S., Akparov V.Kh., Ostrovskaya R.U., Skoldinov S.P., Rozantsev G.G., Voronina T.A., Zherdev V.P., Seredenin S.B. // *FEBS Lett.* 1996. V. 391. P. 149–151.
34. Fedorova T.N., Us K.S., Ostrovskaya R.U. // *J. Neurochemical.* 2007. V. 24. № 1. P. 69–73.
35. Andreeva N.A., Stemalshuk E.V., Isaev N.K., Ostrovskaya R.U., Gudasheva T.A., Viktorov I.V. // *Bull. Exp. Biol. Med.* 2000. V. 130. № 10. P. 418–421.
36. Zhang Z., Yan J., Chang Y., ShiDu Yan S., Shi H. // *Curr. Med. Chem.* 2011. V. 18. № 28. P. 4335–4343.
37. Firova F.A. The range of neurotropic activity of the original substituted prolyl-dipeptide GVS-111. Extended abstract of PhD dissertation (Medicine). Institute of Pharmacology RAMS. Moscow. 1994. (in Russian).
38. Ostrovskaya R.U., Vakhitova Y.V., Kuzmina U.Sh., Salimgareeva M., Zainullina L.F., Gudasheva T.A., Vakhitov V.A., Seredenin S.B. // *J. Biomed. Sci.* 2014. V. 21. P. 74–82.
39. Jia X., Gharibyan A., Öhman A., Liu Y., Olofsson A., Morozova-Roche L.A. // *J. Mol. Biol.* 2011. V. 414. P. 699–712.
40. Lysenko A.V., Uskova N.I., Ostrovskaya R.U., Gudasheva T.A., Voronina T.A. // *Eksp. Klin. Farmakol.* 1997. V. 60. № 3. P. 15–18.
41. Ostrovskaya R.U., Gruden M.A., Bobkova N.A., Sewell R.D.E., Gudasheva T.A., Samokhin A.N., Seredenin S.B., Noppe W., Sherstnev V.V., Morozova-Roche L.A. // *J. Psychopharmacol.* 2007. V. 21. P. 611–619.
42. Ostrovskaya R.U., Tsaplina A.P., Vakhitova Yu.V., Salimgareeva M.Kh., Yamidanov R.S. // *Eksp. Klin. Farmakol.* 2010. V. 73. № 1. P. 2–6.
43. Ostrovskaya R.U., Ozerova I.V., Gudasheva T.A., Kapitsa I.G., Ivanova E.A., Voronina T.A., Seredenin S.B. // *Bull. Exp. Biol. Med.* 2013. V. 156. № 9. P. 317–321.
44. Ostrovskaya R.U., Zolotov N.N., Ozerova I.V., Ivanova E.A., Kapitsa I.G., Taraban K.V., Michunskaya A.B., Voronina T.A., Gudasheva T.A., Seredenin S.B. // *Bull. Exp. Biol. Med.* 2014. V. 157. № 3. P. 321–327.
45. Cheng K., Ho K., Stokes R., Scott C., Lau S.M., Hawthorne W.J., O'Connell P.J., Loudovaris T., Kay T.W., Kulkarni R.N., et al. // *J. Clin. Invest.* 2010. V. 120. № 6. P. 2171–2183.
46. Liu Y., Liu F., Iqbal K., Grundke-Iqbal I., Gong C.X. // *FEBS Lett.* 2008. V. 582. P. 359–364.
47. van de Velde S., Hogan M.F., Montminy M. // *Proc. Natl. Acad. Sci. USA.* 2011. V. 108. № 41. P. 16876–16882.

Binding of Protein Factor CTCF within Chicken Genome Alpha-Globin Locus

E. S. Kotova¹, S. B. Akopov¹, D. A. Didych¹, N. V. Petrova², O. V. Iarovaia², S. V. Razin², L. G. Nikolaev^{1*}

¹Shemyakin-Ovchinnikov Institute of Bioorganic Chemistry, Russian Academy of Sciences, 16/10 Miklukho-Maklaya St., Moscow 117997, Russia

²Institute of Gene Biology, Russian Academy of Sciences, 34/5 Vavilov St., Moscow 119334, Russia

*E-mail: lev@ibch.ru

Received: 16.10.2015

Copyright © 2016 Park-media, Ltd. This is an open access article distributed under the Creative Commons Attribution License, which permits unrestricted use, distribution, and reproduction in any medium, provided the original work is properly cited.

ABSTRACT A systematic search for DNA fragments containing potential CTCF transcription factor binding sites in the chicken alpha-globin domain and its flanking regions was performed by means of the two-dimension electrophoretic mobility shift assay. For the alpha-globin domain fragments selected, the occupancy by the CTCF in erythroid and lymphoid chicken cells was tested by chromatin immunoprecipitation. Only one of 13 DNA fragments capable of CTCF binding *in vitro* was efficiently bound to this protein *in vivo* in erythroid cells, and somewhat less efficiently – in lymphoid cells. So, binding of CTCF to the DNA fragment *in vitro* in most cases does not mean that this fragment will be occupied by CTCF in the cell nucleus. Yet, CTCF binding *in vivo*, as a rule, is accompanied by the binding of the protein to this DNA region *in vitro*. During the erythroid differentiation, no significant changes in CTCF binding to the DNA fragments studied were detected.

KEYWORDS globin genes, transcription factor CTCF, erythroid differentiation

ABBREVIATIONS EMSA – Electrophoretic Mobility Shift Assay; PBS – Phosphate Buffered Saline; AEBSEF - 4-(2-AminoEthyl) BenzeneSulfonyl Fluoride; ChIP – Chromatin ImmunoPrecipitation; ChIP-seq – Chromatin ImmunoPrecipitation with the subsequent mass sequencing.

INTRODUCTION

In chicken, alpha-globin encoding genes *HBZ*, *HBAD*, and *HBAA* are located in the alpha-globin domain on chromosome 14. The chicken alpha-globin domain belongs to a class of open domains which have certain inherent peculiarities; it is located in a gene-rich region, is sensitive to nucleases in all types of cells, and is replicated in the early S-phase of the cell cycle. The cluster of alpha-globin genes is flanked by housekeeping genes, which are actively transcribed in all studied cell types [1]. The major regulatory element (MRE) of the domain is located approximately 20 kbp upstream from the globin genes [2] and contains an erythroid-specific promoter of whole domain transcript [3]. The enhancer and silencer active in chicken erythroblasts are found near the 3'-end of the *HBAA* gene. In erythroid differentiation, the acetylation status of histone H4 changes in the entire domain [4].

The CTCF transcription factor is thought to participate in various gene regulatory networks, including transcription activation and repression, formation of independently functioning chromatin domains, regula-

tion of imprinting, etc. The fundamental properties of CTCF allow it to act as a transcription factor, an insulator protein, and as a component of boundary elements distributed throughout the genome, which can recruit various factors that appear in response to different internal and external signals [5, 6]. Previously, several CTCF-binding sites were identified in chicken alpha-globin locus. First of all, the M9 and C10–C14 sites located in sequences with insulator functions which bind to CTCF in erythroid and non-erythroid cells [7], and a CTCF-dependent silencer (CDS [8]) which binds to CTCF in HD3 and 6C2 erythroid cells. In addition, the ChIP-seq technique allowed researchers to identify several CTCF-binding sites in the erythrocytes of five- and ten-day chick embryos (referred to herein as 5d1–5d3, 10d1–10d3 [9]). One of these sites, 5d1/10d2, may be involved in the switching-on of the globin genes activity in development [10].

In this work, we have undertaken a systematic search for potential CTCF-binding sites in the chicken alpha-globin domain and its flanking regions using a two-dimensional electrophoretic mobility shift assay

(2D-EMSA) developed by us earlier [11, 12]. Chromatin immunoprecipitation and real-time PCR analysis were used for further identification of fragments that are occupied by CTCF in erythroid and non-erythroid cells among the selected fragments.

MATERIALS AND METHODS

Cell cultures

The chicken erythroblasts line HD3, transformed by the avian erythroblastosis virus (clone A6, line LSCC, [13]), and the chicken B-lymphoid DT40 cell line (CRL-2111), were grown in a DMEM/F12 (1:1) medium (Invitrogen) supplemented with 2% chicken and 8% fetal calf serum at 37°C and 5% CO₂. For DT40 cultivation, the medium was further supplemented with 2-mercaptoethanol to a concentration of 50 µM. Terminal erythroid differentiation of HD3 cells was induced by incubation of the cells for 12 hours in the presence of 20 µM of a iso-H-7 protein kinase inhibitor (1-(5-isoquinolinylnsulfonyl)-3-methylpiperazine dihydrochloride, Sigma-Aldrich) at pH 8.0 and 42°C in 100% air atmosphere as described previously [14]. Benzidine staining was used to control cells differentiation [15]. 1 µL of a 30% H₂O₂ solution was added to 25 µL of a 0.4% (w/v) benzidine solution (Sigma) in 4% acetic acid, the resulting solution was mixed with 25 µL of the cell suspension, incubated for 10 min, and a light microscope was used to identify benzidine-positive cells stained with a dark blue color. Hemoglobin-containing (benzidine-positive) cells accounted for 21% of the cells after 12 hours of incubation. Under these conditions, the alpha-globin gene transcriptional level is close to its maximum but continues to increase [16].

CTCF protein and antibodies

The full-length chicken CTCF protein, containing a polyhistidine (6 × His) sequence, was synthesized in COS-1 cells and partially purified by the method described previously [17]. Rabbit polyclonal antibodies to a fragment of chicken CTCF (residues 86–233) were prepared according to [17, 18].

Construction of the alpha-globin locus short fragments library

DNA of CH261-75C12 clone of bacterial artificial chromosome (BAC, obtained from CHORI BACPAC Resource Center, <https://bacpac.chori.org>) containing a 227,366 bp chicken alpha-globin locus insert was purified using a Plasmid Midi Kit (Qiagen) and treated with Plasmid-Safe ATP-Dependent DNase (Epicentre) according to the manufacturers' recommendations.

The library of short fragments was obtained essentially according to [19]. Two BAC DNA samples were

digested with either Sau3AI or Csp6I (Fermentas), and ACTGAGGTCTGACTATCCATGAACA library primer was attached to the sticky ends. The obtained sub-libraries were amplified by PCR (21–24 cycles) using the same primer and a Encyclo PCR kit (Evrogen) in the presence of 1.5 M betaine and 5% dimethyl sulfoxide as follows: 95°C, 30 sec; 55°C, 30 sec; 72°C, 90 sec. The sub-libraries were combined and purified using a QIAquick PCR Purification Kit (Qiagen).

PCR amplification of the M9, CDS, and HBAD fragments with the obtained libraries as templates was performed using an Encyclo PCR kit (Evrogen) in the presence of 1.5 M betaine, and 5% dimethyl sulfoxide. The following pairs of primers were used: TCAG-GAAGAAAGAATGGGAAA and CCTGCGTTT-TAGCTGATTGG for M9; TCCCAGCACCTCGCAGT-GCA and GCACAAGGCTCAAAGGTGAGACA for CDS; CCCAGACCAAGACCTACTTCC and GCTGAG-GTTGTCCACGTTCTT for HBAD.

Starting with the 24th PCR cycle, 2.5 µL aliquots were taken from the reaction mixture every three cycles and analyzed in 1% agarose gel.

Electrophoretic mobility shift assay (EMSA)

The selected fragments 1–13 were amplified on a plasmid DNA template, isolated from the corresponding clones of the arrayed library, for 10 cycles (94°C, 30 sec; 60°C, 30 sec; 72°C, 90 sec) using the library primer. Next, an aliquot of the reaction mixture was used for PCR radiolabelling according to [12]. For electrophoretic mobility shift assay ~5 ng (30000–50000 cpm) of the labeled DNA fragment were mixed with 1 µg of poly(dI-dC), 1–2 µg (as protein) of a nuclear or cytoplasmic extract or 2 µL of a purified CTCF protein solution in 20 µL of a final volume of 12 mM HEPES-KOH pH 7.9, 12% glycerol, 60 mM KCl, 0.3 mM EDTA, and 0.6 mM DTT. 4.5 µg of anti-CTCF antibodies or 3 µg of monoclonal antibodies to poly-histidine (Sigma, H1029) were added for the supershift assay. The mixture was incubated for 20 min at room temperature, resolved in 5–7.5% polyacrylamide gel prepared with a 50 mM Tris-borate buffer, pH 8.3, 0.5 mM EDTA, and autoradiographed for 16–40 hours.

A two-dimensional electrophoretic mobility shift assay (2D-EMSA) was performed as described previously [12] with minor modifications. PCR amplification was done in the presence of 1.5 M betaine and 5% dimethyl sulfoxide using the Encyclo PCR kit (Evrogen). 10 µL of the protein fraction containing ca. 0.5 pmol CTCF was used for the first round of two-dimensional EMSA, and 1 µL of the same fraction was used for the second round. The resulting library of CTCF-binding DNA fragments was cloned into pGEM-T plasmid (Promega) and arrayed in 96-well plates. A total of 230 clones were

sequenced and mapped on the *Gallus gallus* genome (galGal4).

Chromatin immunoprecipitation (ChIP)

Chromatin immunoprecipitation was performed according to the previously described method [20]. Approximately 3×10^7 exponentially growing (for DT40 and HD3) or collected 12 hours after the initiation of induction (for induced HD3) were fixed with 1% (v) of formaldehyde in 60 mL of a DMEM/F12 medium (1:1) for 8 min. The cells were pelleted by centrifugation for 4 min at 700 *g* and 4°C, washed with PBS, containing 1 mM AEBSF and a 1 µL/mL protease inhibitor cocktail (Sigma, P8340), re-pelleted, re-suspended in 200 µL of 50 mM Tris-HCl pH 8.0, 1% SDS, 10 mM EDTA and incubated for 10 min on ice for lysis. The cells were then sonicated using a Cole-Parmer CP750 processor (30% amplitude, 30 3-sec cycles with 10-sec intervals). Cell debris were removed in a microcentrifuge (10 min, 13,000 rpm, 4°C), the supernatant was diluted 10 times with 16.7 mM Tris-HCl pH 8.0, 16.7 mM NaCl, 1.2 mM EDTA, 1% Triton X-100, 0.01% SDS, 1 mM PMSF and the 1 µL/mL protease inhibitor cocktail. At this stage, an input control aliquot was withdrawn. Cell lysate was purified from nonspecifically bound proteins by pre-incubation with protein-A-agarose (Invitrogen) and then incubated with 2 µg of polyclonal antibodies to CTCF or control rabbit polyclonal antibodies to thau-matin (kindly provided by E.A. Stukacheva) overnight at 4°C and constant stirring. DNA-protein complexes were collected on protein-A-agarose, washed and eluted from the vehicle with elution buffer (1% SDS, 0.1 M NaHCO₃, 2 x 15 min) at room temperature. NaCl was added to the solution to a concentration of 0.2 M, followed by RNase A and proteinase K, and the mixture was incubated at 65°C for 4 hours to reverse the cross-links. DNA was extracted twice with a phenol-chloroform mixture and precipitated with ethanol overnight at 4°C in the presence of 20 µg glycogen as a carrier. The DNA fragments were collected by centrifugation, dissolved in water, and analyzed using quantitative real-time PCR on a MX3000P thermocycler (Stratagene) and qPCRmix-HS SYBR reaction mixture (“Evrogen”) in a volume of 25 µl for 40 cycles: 95°C, 30 sec; 61–65°C (for different primers), 30 sec; and 72°C, 60 sec. The efficiency of PCR was calculated using the LinRegPCR software [21].

A fragment of a chicken lysozyme gene F1 silencer [22] and a fragment of the promoter region of the chicken *MYC* gene [23] were used as positive controls for quantitative PCR. A CTCF non-binding enhancer fragment from the chicken beta-globin locus [8] and a fragment of the alpha-*D*-globin (*HBAD*) exon gene were used as negative controls. DNA fragments were

amplified on the chicken genomic DNA template using the following primers: CAGCACAGTTCTGGC-TATGAAA and CCTCAGCTGGGGTCAATAAGT (lysozyme gene silencer); AAGCAGCGAGGAGC-GCCCTTT and TACTACAAGGAGAGGTCGGAAGT (*MYC* gene promoter); GGGCAGGTTGCAGATAAAA-CA and TAACCCCTCTCTTCCCTCA (enhancer from beta-globin locus); CCCAGACCAAGACCTACTTCC and GCTGAGGTTGTCCACGTTCTT (*HBAD* gene exon); TGTGGTCATCCATGTCCTCAATC and GGAAGCTTTTTTGCCAAGGAGAA for 10d1; GCTCTTCTCACCCAGGTTTCT and CATCCAGCCCTCTCCAAACA (10d2, 8, and 5d1); TGACCCATCTTGCAATGGATACT and GTTTGGGAACCTCTCTCCATCC (10d3); ATAG-GACTTCCCTGCTTCCATCT and GTTGGAGT-GTTGTGGTCTTCTCC (5d2); GTGAGGAGAGGGC-GAAGTTTATT and GCTCCCTGAGCTCCTCACCT (5d3); ATAACCTGGCAGCAAACCTAGCA and TTTGGAAAGTGCTGTGGGTAAAG (fragment 1); TTCTACACTTGTCCCTCCTTTTCA and CCTATTTTGTGGCTGCATTCTTC (fragment 2); GGAGCTCAGCAGGCAGAAACTA and GCTAAGGCAAAGGCTCTGTTGT (fragment 3); CTCTGCATTGCTGTGTGTGTTTT and ATGGTGGTTATCTCAGGGGTTTT (fragment 4); GGTACGTTCTCAGTGCCCAAAC and CCACCTGCAGACCTAACCTGTC (fragment 5); CAGCTCTTCTGGCTCATTTGTCT and ATCTCCCTTTCAGTCCCCTTCTC (fragment 6); TTTCACCCCGAAGTTCATGCT and CCCAGTGTGGAAGCCATTTATC (fragment 7); CATGGGCAGCAAACACACAG and TC-CATTTCCAGCGTTTCTTATC (fragment 9); AG-GTAGGACTCAGCAGGGACAG and GGGA-CAAGTAGCTGGGACAAAA (fragment 10); CTGGAGATACCCATGGCAGAAC and TTTGTG-GCCAACGTCAAACCTAC (fragment 11); GGTTT-GCCTTTCTTGCTCTG and ATGCCCATCTCACTT-GCTCT (fragment 12); CGTACCAGCACCAGACAAACAG and TCGACTGTTGAAGGAGGCATAA (fragment 13).

Data were analyzed using genome browser resources (UCSC Genome Browser, <http://genome.ucsc.edu>) [24] and NCBI-BLAST (<http://blast.ncbi.nlm.nih.gov/Blast.cgi>).

RESULTS AND DISCUSSION

Selection of CTCF-binding sequences using 2D-EMSA

To obtain libraries of CTCF-binding sequences by two-dimensional EMSA (2D-EMSA, [12]), the artificial bacterial chromosome (BAC) containing a 227366 bp

insert, which overlaps the chicken alpha-globin locus and includes extensive flanking regions, was digested to completion with either the *Sau3AI* or *Csp6I* restriction enzyme. Synthetic adapters were attached to the resulting sticky ends, amplified by PCR, and both hydrolysates were mixed in equal proportions. The resulting library of short fragments (approximately 1,000 fragments with an average length of ca. 500 bp) was ^{32}P -labeled and mixed with a protein fraction enriched in full-length CTCF, expressed in COS-1 cells [17]. The reaction mixture was then electrophoretically separated by non-denaturing polyacrylamide gel (first dimension). The region with the sample was cut out, incubated in SDS-containing buffer to disrupt the DNA-protein complexes, and the DNA fragments were separated in SDS-containing gel (second dimension). The region containing the most fragments originally bound to CTCF (outlined by the oval in *Fig. 1A*) was cut out from the gel and the DNA fragments were eluted and amplified. The procedure was repeated to improve the efficiency of selection.

The specificity of selection was checked by amplification of the resulting and the original libraries with primers to chicken alpha-globin locus sequences, which bind to CTCF according to the published data: namely, CDS (CTCF-dependent silencer) [8] and the M9 sequence [7]. The sequence of *HBAD* exon which does not bind to CTCF was used as a negative control. The results of amplification are shown in *Fig. 1B*.

As can be seen from *Fig. 1*, after two rounds of selection PCR products of the CDS and M9 regions become visible after 24 and 27 cycles of amplification, respectively, while the product of the control *HBAD* gene fragment that does not bind to CTCF becomes visible only after 33 cycles. Since all three fragments are amplified from the original library with approximately equal efficiency (see the input lane in *Fig. 1B*) a rough estimation of the degree of enrichment with the CTCF-binding fragments for the library obtained is ~64–512 times.

The DNA fragments obtained after the second round of the selection were cloned into a pGEM-T vector, white colonies (230) were arrayed in 96-well plates, and their inserts were sequenced. Among these sequences, 22 corresponded to fragments of BAC, *Escherichia coli* genomic DNA or chimeric fragments, and 208 belonged to the alpha-globin locus. 79 unique sequences were identified. The constructed rarefaction curve (*Fig. 1B*) indicates that the sequencing was performed with a depth sufficient to identify most of the potential CTCF-binding fragments of the locus.

Ten selected DNA fragments (1–4, 6–10, 13) were used as probes to test their ability to bind CTCF by electrophoretic mobility shift and supershift assays

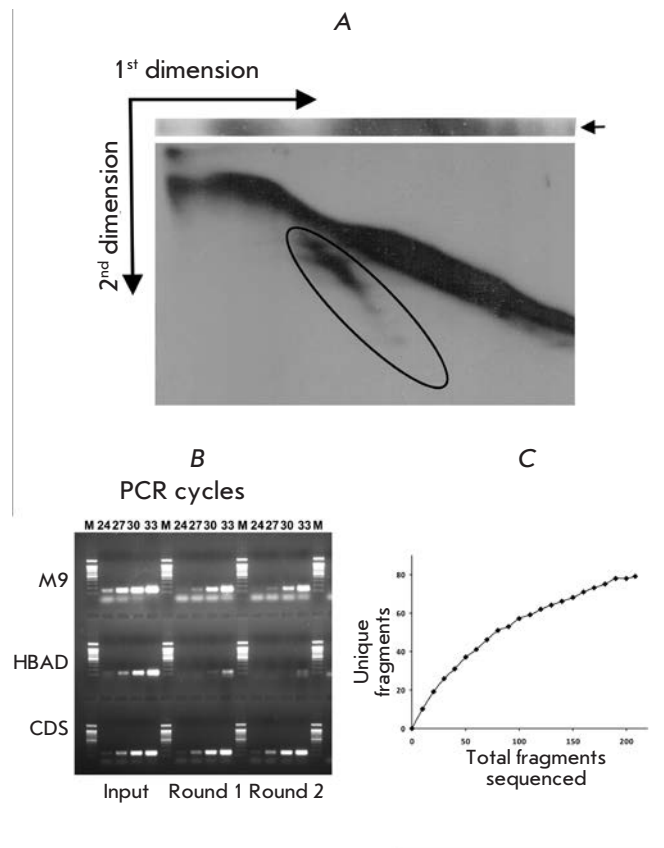


Fig. 1. Preparation and characterization of the library of CTCF-binding fragments. (A) Selection of CTCF-binding fragments by means of the two-dimensional electrophoretic mobility shift assay (2D-EMSA). The results of two-dimensional electrophoresis for the second selection round are shown. Region containing selected CTCF-binding fragments is outlined by the oval. For detail, see text. (B) Estimation of the degree of enrichment with the CTCF-binding fragments for the library obtained. Initial DNA and DNA after first and second 2D-EMSA selection rounds were used as a template for PCR with primers targeted to CTCF-binding sequences from the chicken alpha-globin locus: CDS (CTCF-dependent silencer) and M9 sequence. Sequence from *HBAD* gene exon which does not bind CTCF was used as a negative control. (C) Rarefaction curve obtained during sequencing of the CTCF-binding fragments library

(EMSA, supershift). Two fragments (10 and 13) are shown in *Fig. 2*. All 10 fragments were able to bind CTCF, which indicates the high efficiency of the selection.

Distribution of potential CTCF binding sites

All 208 sequenced fragments were mapped to the *Gallus gallus* genome (galGal4, 2011). A table with

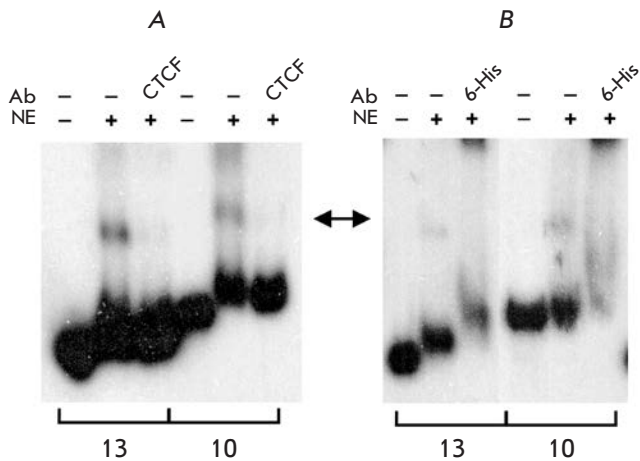


Fig. 2. CTCF binding to selected DNA fragments 10 and 13. Anti-CTCF (A) and anti-polyHistidine (B) antibodies were used for the supershift assay. AB – antibodies, NE – nuclear extract

the coordinates of all mapped DNA fragments in BED format is available upon request. A full map of the fragments distribution is presented in the upper part of *Fig. 3*. As can be seen, the locus had a number of sites with higher selection efficiency (indicated by vertical arrows); i.e., with higher affinity for CTCF in EMSA conditions. The bottom part of *Fig. 3* shows an enlarged map of the immediate surroundings of the globin genes with indicated genes positions (RefSeq), as well as some previously identified regulatory elements, in particular the enhancer/silencer [25] and MRE (Major Regulatory Element, [2]). It also shows DNA fragments that had been previously identified in various cell types and tissues as capable of binding CTCF: M9, C10-C14 [7], and a fragment of the CTCF-dependent silencer [8]. CTCF-binding fragments 5d1–5d3 and 10d1–10d3 have been previously identified by ChIP-seq in five- and ten-day chick embryos, respectively [9].

As can be seen from *Fig. 3*, the vast majority of previously identified CTCF binding sites are located in or very close to the regions of high selection efficiency; i.e., strong CTCF-binding in EMSA conditions. The binding site 10d1, located outside the enlarged section of the map, is also located in the area with high affinity to CTCF. It should be noted that the binding site and the cross-linking position in chromatin immunoprecipitation may not match exactly due to DNA bending [26, 27]; i.e., fragments identified by EMSA and ChIP do not necessarily overlap, even though they should be located close to one another.

CTCF binding *in vitro* and *in vivo* in the region of alpha-globin genes

To compare the CTCF binding to DNA in a living cell and detected by EMSA, we performed chromatin immunoprecipitation for 13 DNA fragments from the globin region, as well as for the 5d1–5d3 and 10d1–10d3 fragments [9] in three cell types: HD3 cells, HD3 induced to erythroid differentiation, and B-lymphoid DT40. The positions of DNA fragments amplified during chromatin immunoprecipitation are shown in *Fig. 3* (ChIP panel), and the results of immunoprecipitation are presented in *Fig. 4*.

Figure 4 demonstrates that fragment 10, located near the 3'-end of *HBAA*, is the only one to display a high degree of occupancy by CTCF, close to that observed for the positive controls (F1, MYC). A high degree of CTCF binding is observed in HD3 cells and induced HD3 cells, while CTCF binding to this site in DT40 cells is significantly lower. Remarkably, the position of fragment 10 coincides with the position of the genomic region fragment with the strongest CTCF binding *in vitro* (*Fig. 3*).

In addition to fragment 10, another fragment to stand out is 5d3, whose CTCF occupancy is reliably above the negative control level for all three cell types but is substantially lower than that of fragment 10 in HD3 and HD3-ind cells. Some excess over the negative control is observed also for fragments 4, 5, 9, and 10d3 in HD3-ind cells only, but the extent of this excess is small and does not allow us to claim with certainty that these fragments bind CTCF.

Thus, most DNA fragments (17 out of 18) that bind to the purified CTCF protein in EMSA conditions are not occupied by CTCF in the cell nucleus of the studied cell types. This fact can be attributed to the following reasons:

1. Methylation of cytosine in CpG dinucleotides disrupts its binding to CTCF [28, 29]. However, only about 30% of CTCF binding sites contain the CpG sequence [30]: therefore, DNA methylation at the CTCF site can only partially explain the results.

2. CTCF binding is limited to sites with a suitable structure of chromatin/histone modifications and/or presence of other transcription factors nearby that facilitate CTCF binding [31].

Most likely, both reasons play a role in limiting CTCF binding [32].

Obviously, some of the sites that were not occupied by CTCF in our chromatin immunoprecipitation experiments (*Fig. 4*) can bind this protein in other types of cells and tissues. For example, the DNA fragments 5d1, 5d2, 10d1–10d3, which do not bind CTCF in DT40 and HD3 cells (*Fig. 4*), bind to it in chick embryo erythroblasts [9].

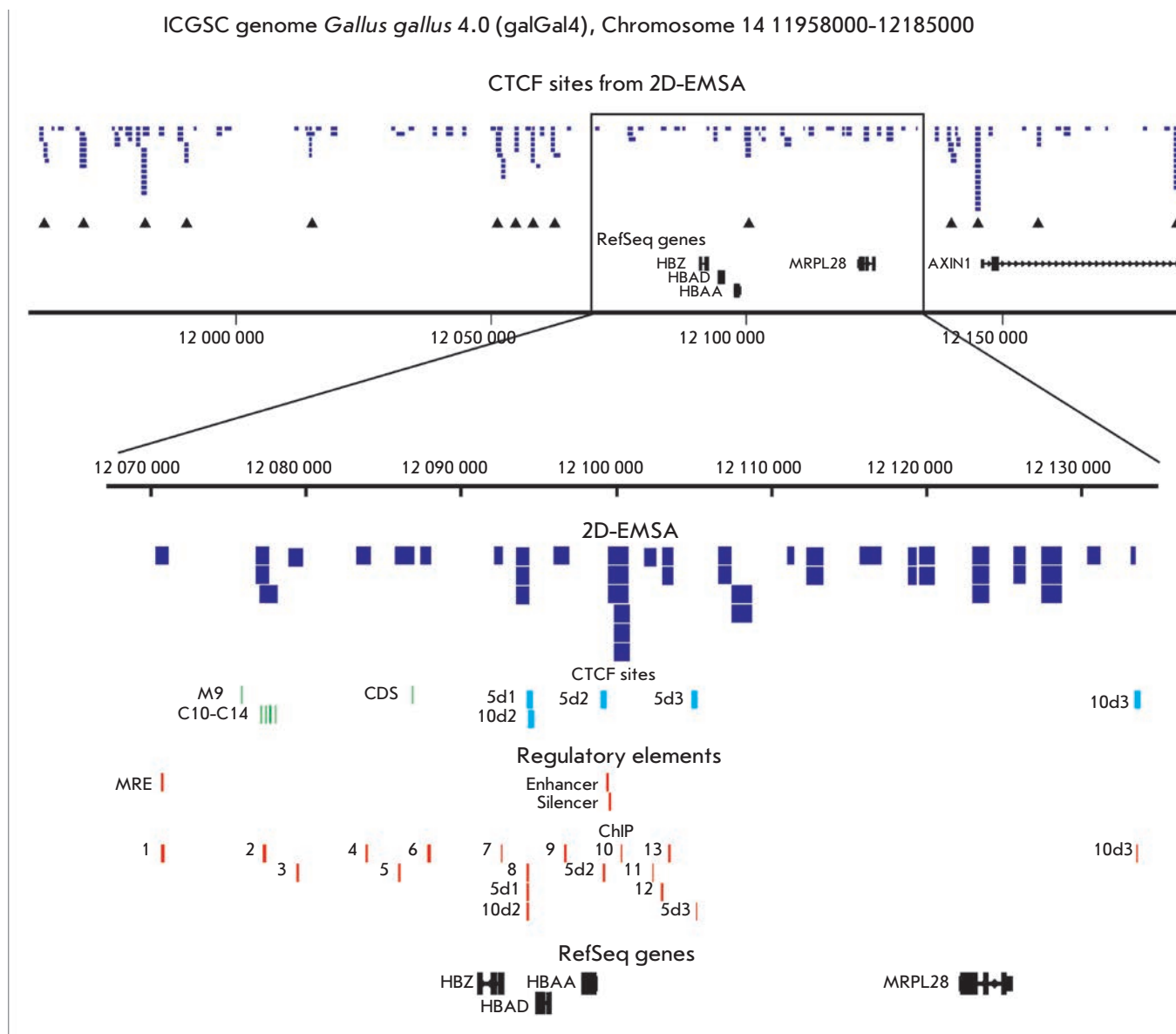


Fig.3. Distribution of CTCF binding sites and some regulatory elements in the region overlapping the chicken genome alpha-globin domain. Upper map shows the positions of all selected DNA fragments. The arrows indicate DNA regions with high affinity to CTCF. Lower part shows the enlarged map of the immediate surroundings of the globin genes. In the "CTCF sites" panel the identified previously CTCF binding sites M9, C10-C14 [7], CDS [8] and 5d1-5d3, 10d1-10d3 [9] are shown, the "Regulatory elements" panel demonstrates the positions of the MRE [2] and the enhancer and silencer [25]. In the ChIP region the positions of DNA fragments amplified in the chromatin immunoprecipitation experiment are shown (see text)

The 5d3 fragment is a special case. It binds CTCF according to the results of chromatin immunoprecipitation (Fig. 4) and according to [9], but it does not overlap with any of the selected fragments. The CTCF-binding M9 fragment behaves similarly [7], but its presence in the library is confirmed by PCR (Fig. 1B). Perhaps both of these DNA fragments did not fall into the sequenced pool.

CONCLUSION

On the basis of these experiments we can conclude that there is a unilateral relationship between the CTCF-binding efficiency of a fragment under EMSA conditions (*in vitro*) and its degree of occupancy by a CTCF protein in ChIP conditions. Binding of CTCF to a DNA fragment *in vitro* in most cases does not mean that this fragment will be occupied by CTCF in the cell

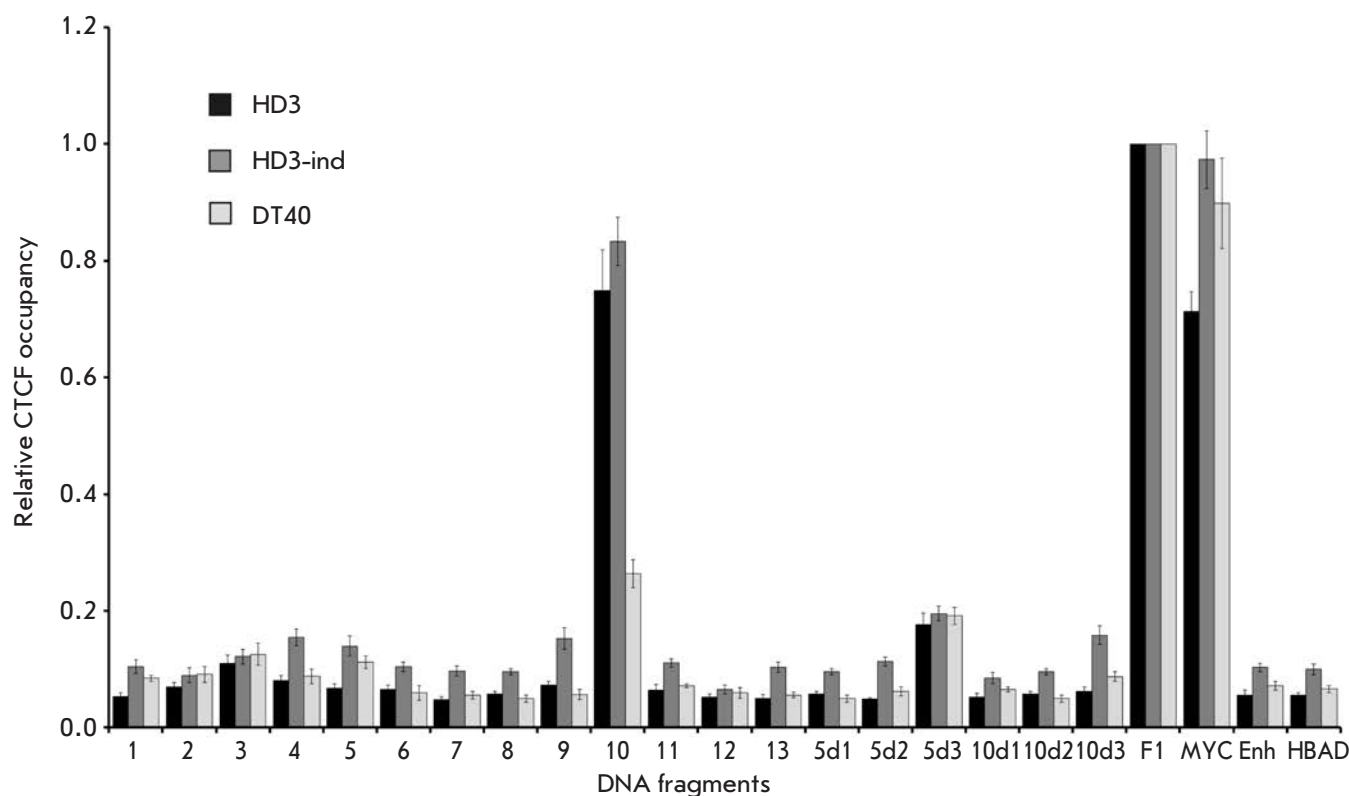


Fig.4. CTCF binding to DNA regions *in vivo* as revealed by chromatin immunoprecipitation and a real-time PCR analysis. The results for HD3 cells, HD3 induced to erythroid differentiation, and for B-lymphoid DT40 cells are presented. Primers were targeted to the DNA fragments selected in this work (1-13) and to six fragments identified in [9] (5d1-5d3, 10d1-10d3). F1, MYC – positive controls; Enh, HBAD – negative controls. The data are normalized to binding CTCF with the F1 fragment. Error bars indicate the standard errors of the mean.

nucleus. In contrast, CTCF binding *in vivo*, as a rule, is accompanied by the binding of the protein to this DNA region *in vitro*. Furthermore, these results show that erythroid differentiation has no significant impact on the CTCF binding of the studied DNA fragments.

The only site which strongly binds CTCF in erythroid cells, HD3 and HD3-ind, binds this protein in lymphoid DT40 cells with significantly (2–3 times) weaker efficiency; i.e., CTCF binding to this site is distinctly tissue-specific. At the same time, there are no significant differences in CTCF binding in a HD3 eryth-

roblast cell line and in cells of the same line stimulated to erythroid differentiation. ●

The authors are grateful to EA Stukacheva for antibodies to thaumatin.

This work was supported by the Russian Leading Scientific Schools program (project NSH_1674.2012.4), Presidium of RAS Molecular and Cellular Biology program and RFBR (projects № 10-04-01365, 10-04-01472, 14-04-00010).

REFERENCES

- Razin S. V., Ulianov S. V., Ioudinkova E. S., Gushchanskaya E. S., Gavrilov A. A., Iarovaia O. V. // *Biochemistry (Mosc)*. 2012. V. 77. P. 1409–1423.
- Flint J., Tufarelli C., Peden J., Clark K., Daniels R.J., Hardison R., Miller W., Philipsen S., Tan-Un K.C., McMorrow T., et al. // *Hum. Mol. Genet.* 2001. V. 10. P. 371–382.
- Razin S.V., Rynditch A., Borunova V., Ioudinkova E., Smalko V., Scherrer K. // *J. Cell Biochem.* 2004. V. 92. P. 445–457.
- Anguita E., Johnson C.A., Wood W.G., Turner B.M., Higgs D.R. // *Proc. Natl. Acad. Sci. USA*. 2001. V. 98. P. 12114–12119.
- Holwerda S.J., de Laat W. // *Philos. Trans. R. Soc. Lond. B Biol. Sci.* 2013. V. 368. P. 20120369.
- Nikolaev L.G., Akopov S.B., Didych D.A., Sverdlov E.D. // *Curr. Genomics*. 2009. V. 10. P. 294–302.
- Valadez-Graham V., Razin S.V., Recillas-Targa F. // *Nucl. Acids Res.* 2004. V. 32. P. 1354–1362.
- Klochkov D., Rincon-Arango H., Ioudinkova E.S., Valadez-

- Graham V., Gavrilov A., Recillas-Targa F., Razin S.V. // *Mol. Cell Biol.* 2006. V. 26. P. 1589–1597.
9. Martin D., Pantoja C., Fernandez Minan A., Valdes-Quezada C., Molto E., Matesanz F., Bogdanovic O., de la Calle-Mustienes E., Dominguez O., Taher L., et al. // *Nat. Struct. Mol. Biol.* 2011. V. 18. P. 708–714.
10. Valdes-Quezada C., Arriaga-Canon C., Fonseca-Guzman Y., Guerrero G., Recillas-Targa F. // *Epigenetics.* 2013. V. 8. P. 827–838.
11. Chernov I.P., Akopov S.B., Nikolaev L.G., Sverdlov E.D. // *Biotechniques.* 2006. V. 41. P. 91–96.
12. Vetchinova A.S., Akopov S.B., Chernov I.P., Nikolaev L.G., Sverdlov E.D. // *Anal. Biochem.* 2006. V. 354. P. 85–93.
13. Beug H., von Kirchbach A., Doderlein G., Conscience J.F., Graf T. // *Cell.* 1979. V. 18. P. 375–390.
14. Nicolas R.H., Partington G., Major G.N., Smith B., Carne A.F., Huskisson N., Goodwin G. // *Cell Growth Differ.* 1991. V. 2. P. 129–135.
15. Orkin S.H., Harosi F.I., Leder P. // *Proc. Natl. Acad. Sci. USA.* 1975. V. 72. P. 98–102.
16. Gavrilov A.A., Razin S.V. // *Nucl. Acids Res.* 2008. V. 36. P. 4629–4640.
17. Kotova E. S., Sorokina I. V., Akopov S. B., Nikolaev L. G., Sverdlov E. D. // *Biochemistry (Mosc).* 2013. V. 78. P. 879–883.
18. Gushchanskaya E.S., Artemov A.V., Ulyanov S.V., Logacheva M.D., Penin A.A., Kotova E.S., Akopov S.B., Nikolaev L.G., Iarovaia O.V., Sverdlov E.D., et al. // *Epigenetics.* 2014. V. 9. P. 951–963.
19. Nikolaev L.G., Tsevegijn T., Akopov S.B., Ashworth L.K., Sverdlov E.D. // *Nucl. Acids Res.* 1996. V. 24. P. 1330–1336.
20. Orlando V. // *Trends Biochem. Sci.* 2000. V. 25. P. 99–104.
21. Ruijter J.M., Ramakers C., Hoogaars W.M., Karlen Y., Bakker O., van den Hoff M.J., Moorman A.F. // *Nucl. Acids Res.* 2009. V. 37. P. e45.
22. Kohne A.C., Baniahmad A., Renkawitz R. // *J. Mol. Biol.* 1993. V. 232. P. 747–755.
23. Filippova G.N., Fagerlie S., Klenova E.M., Myers C., Dehner Y., Goodwin G., Neiman P.E., Collins S.J., Lobanenkov V.V. // *Mol. Cell Biol.* 1996. V. 16. P. 2802–2813.
24. Meyer L.R., Zweig A.S., Hinrichs A.S., Karolchik D., Kuhn R.M., Wong M., Sloan C.A., Rosenbloom K.R., Roe G., Rhead B., et al. // *Nucl. Acids Res.* 2013. V. 41. P. D64–D69.
25. Targa F.R., de Moura Gallo C.V., Huesca M., Scherrer K., Marcaud L. // *Gene.* 1993. V. 129. P. 229–237.
26. Arnold R., Burcin M., Kaiser B., Muller M., Renkawitz R. // *Nucl. Acids Res.* 1996. V. 24. P. 2640–2647.
27. MacPherson M.J., Sadowski P.D. // *BMC Mol. Biol.* 2010. V. 11. P. 101.
28. Bell A.C., Felsenfeld G. // *Nature.* 2000. V. 405. P. 482–485.
29. Hark A.T., Schoenherr C.J., Katz D.J., Ingram R.S., Levorse J.M., Tilghman S.M. // *Nature.* 2000. V. 405. P. 486–489.
30. Nakahashi H., Kwon K.R., Resch W., Vian L., Dose M., Stavreva D., Hakim O., Pruett N., Nelson S., Yamane A., et al. // *Cell Rep.* 2013. V. 3. P. 1678–1689.
31. The ENCODE Project Consortium. // *Nature.* 2012. V. 489. P. 57–74.
32. Teif V.B., Beshnova D.A., Vainshtein Y., Marth C., Mallm J.P., Hofer T., Rippe K. // *Genome Res.* 2014. V. 24. P. 1285–1295.

Human Interleukin-2 and Hen Egg White Lysozyme: Screening for Bacteriolytic Activity against Various Bacterial Cells

P. A. Levashov^{1*}, E. D. Ovchinnikova¹, O. A. Morozova², D. A. Matolygina¹, H. E. Osipova¹, T. A. Cherdyntseva³, S. S. Savin¹, G. S. Zakharova^{1,4}, A. A. Alekseeva^{1,4}, N. G. Belogurova¹, S. A. Smirnov¹, V. I. Tishkov^{1,4*}, A. V. Levashov¹

¹Department of Chemical Enzymology, Faculty of Chemistry, M.V. Lomonosov Moscow State University, Leninskie Gory, 1-3, 119991, Moscow, Russian Federation

²Clinical Center, I.M. Sechenov First Moscow State Medical University, Bolshaya Pirogovskaya St., 2-4, 119881, Moscow, Russian Federation

³Department of Microbiology, Faculty of Biology, M.V. Lomonosov Moscow State University, Leninskie Gory, 1-12, 119991, Moscow, Russian Federation

⁴A.N. Bach Institute of Biochemistry, Federal Research Centre "Fundamentals of Biotechnology" of the Russian Academy of Sciences, Leninsky Pr., 33-2, 119071, Moscow, Russian Federation

* E-mail: levashov@yahoo.com, vitishkov@gmail.com

Received 01.12.2015

Copyright © 2016 Park-media, Ltd. This is an open access article distributed under the Creative Commons Attribution License, which permits unrestricted use, distribution, and reproduction in any medium, provided the original work is properly cited.

ABSTRACT The bacteriolytic activity of interleukin-2 and hen egg white lysozyme against 34 different species of microorganisms has been studied. It was found that 6 species of microorganisms are lysed in the presence of interleukin-2. All interleukin-2-sensitive microorganisms belong either to the Enterobacteriaceae, Bacillaceae, or the Lactobacillaceae family. It was also found that 12 species of microorganisms are lysed in the presence of lysozyme, and 16 species of microorganisms are lysed in the presence of sodium dodecyl sulfate (SDS). The bacteriolytic activity of interleukin-2 and lysozyme was studied at various pH values.

KEYWORDS lysozyme, interleukin-2, bacteriolytic activity

ABBREVIATIONS CFU – the number of colony forming units; SDS – sodium dodecyl sulfate

INTRODUCTION

Interleukin-2 (IL-2) is one of the most important regulators of vital activity. This lymphokine is involved in the regulation of such processes as proliferation and differentiation of T lymphocytes, increase of the cytolytic activity of NK cells, proliferation of B lymphocytes, immunoglobulin secretion, etc. We have recently shown that human IL-2 is able to exhibit bacteriolytic activity [1-3]. A comparative test with several bacterial strains has shown that IL-2 has a narrower substrate specificity compared to hen egg white lysozyme. IL-2, as well as lysozyme, is capable of lysing *Escherichia coli* and *Lactobacillus plantarum* cells, but, unlike lysozyme, it shows no effect on *Micrococcus luteus* and *Bacillus subtilis* [1-3]. The detection of IL-2 activity against *E. coli* and *L. plantarum* turned out to be surprising. The mechanism of the bacteriolytic action of IL-2 still remains unknown, and its elucidation requires a study of the influence of IL-2 on other bacterial species. Since IL-2 plays an important role in the development of the immune response and

is used as a drug, it is of primal importance to examine its action on the bacteria that are often in contact with humans, including the components of symbiotic microflora.

The main objective of the study was to screen IL-2 for bacteriolytic activity against microorganisms that are found on human skin and mucous membranes and can be detected in a wound discharge. For comparison, we decided to examine the effect of lysozyme on microorganisms and lysis of the same bacterial cells in the presence of sodium dodecyl sulfate (SDS), which is part of IL-2-based drugs.

EXPERIMENTAL SECTION

The following reagents were used: roncoleukin (0.25 mg/mL solution of purified interleukin-2 for intravenous and subcutaneous administration, Biotech, Russia); MES, Tris ("extra pure," Amresco, USA); lyophilized hen egg lysozyme (95% purity, Sigma Aldrich, USA); NaOH (98% purity, AppliChem Panreac, Germany); CH₃COOH ("AR grade," Reachim, Russia); HCl

(Germed, Germany); and a 10% water solution of SDS (BioRad, USA).

Microbial strains isolated from clinical specimens (urine, sputum, feces, wound discharge, etc.) were kindly provided by I.M. Sechenov First MSMU. The species of microorganisms were identified by direct protein profiling using MALDI-TOF mass spectrometry (FLEX series, Bruker Daltonic GmbH, Germany). A solid agar medium, 5% Colombia blood agar (Oxoid, UK), pH 7.3, was used for cultivation. The cell culture was grown at 35 °C and 5% CO₂ for 24 hours.

Strains from the museum collection of microorganisms (CM) of the Department of Microbiology at M.V. Lomonosov Moscow State University (referred to as MSU CM) were also used for the study. *Lactobacillus acidophilus* MSU CM 146, *Lactobacillus casei* MSU CM 153, and *Lactococcus lactis* MSU CM 165 were grown in a MRS liquid medium at 37 °C under anaerobic conditions [4]. *Clostridium butyricum* MSU CM 19 was grown in a medium of the following composition: 10 g/L glucose, 10 g/L peptone, 1 g/L K₂HPO₄, 5 g/L CaCO₃, tap water; at 37 °C under anaerobic conditions [5]. *Alcaligenes faecalis* MSU CM 82, *Bacillus megaterium* MSU CM 17, *Bacillus mycoides* MSU CM 31, *Bacillus cereus* MSU CM 9, *Pseudomonas aeruginosa* MSU CM 47, *Pseudomonas fluorescens* MSU CM 71, *Serratia marcescens* MSU CM 208, and *Staphylococcus aureus* MSU CM 144 were grown in a meat-peptone broth at 30 °C under aerobic conditions [6].

Lyophilized *Bifidobacterium bifidum* (Microgen, Russia) was used for the preparation of a suspension (10 mL of water per ampoule) at the initial stages of the study. Based on the analogy with the sample of lyophilized *L. plantarum* cells, it was assumed that the lyophilized bacterial sample differs little in the change of lysis rate from freshly grown cells [7].

Thermus aquaticus cells were graciously provided by A.A. Belogurov. Cells were grown according to the standard procedure for the culture at 75 °C under aerobic conditions [8].

Before measurements, all samples of bacterial cells were centrifuged at 3500 rpm for 4 min in a Minispin centrifuge (Eppendorf, Germany) then re-suspended in the buffer solution that was used for measuring the activity. The hen egg lysozyme solution was prepared immediately before the experiment using the same buffer as for activity measurement. A ready-to-use sample of IL-2 was used without additional treatment as a standard solution, and the ampoule was opened immediately before the experiment. Since the initial solution of IL-2 contained SDS (2.5 mg/mL), experiments on the effect of this component on background cell lysis were conducted. In order to determine the changes in absorption upon cell lysis, double-beam spectropho-

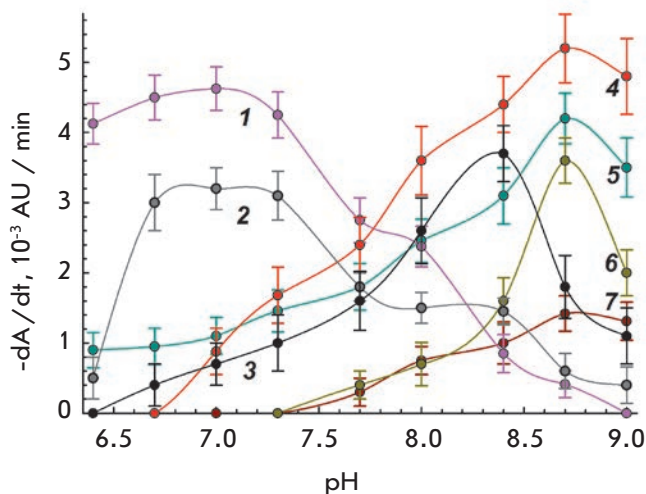


Fig. 1. Dependence of cell lysis rate on pH in the presence of lysozyme. 1 – *Streptococcus agalactiae*, lysozyme 5.0 µg/mL. 2 – *Lactobacillus acidophilus* MSU CM 146, lysozyme 0.8 µg/mL. 3 – *Serratia marcescens* MSU CM 208, lysozyme 0.2 µg/mL. 4 – *Bacillus megaterium*, lysozyme 0.8 µg/mL. 5 – *Pseudomonas aeruginosa*, lysozyme 0.2 µg/mL. 6 – *Proteus vulgaris*, lysozyme 2 µg/mL. 7 – *Staphylococcus haemolyticus*, lysozyme 0.4 µg/mL

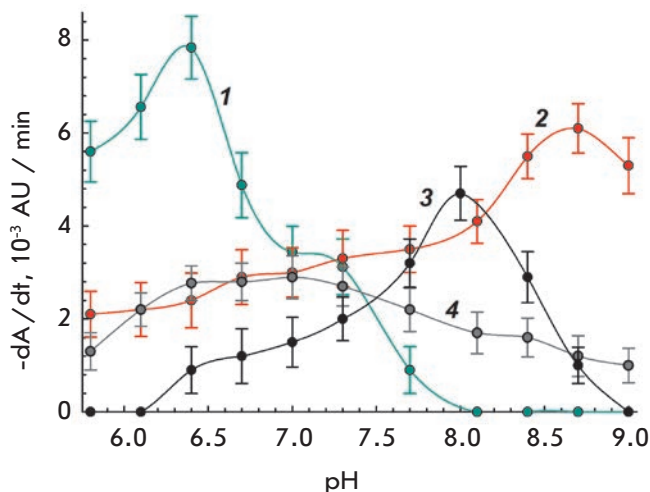


Fig. 2. pH-dependence of cell lysis rate in the presence of interleukin-2. 1 – *Enterobacter aerogenes*, interleukin-2 2.0 µg/mL. 2 – *Bacillus megaterium*, interleukin-2 15 µg/mL. 3 – *Serratia marcescens* MSU CM 208, interleukin-2 30 µg/mL. 4 – *Lactobacillus acidophilus* MSU CM 146, interleukin-2 5.0 µg/mL

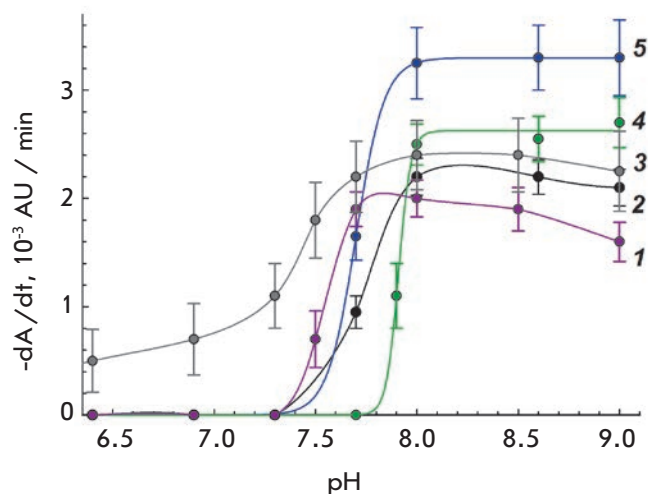


Fig. 3. pH-dependence of cell lysis rate in the presence of SDS. 1 – *Morganella morganii*, SDS 40 $\mu\text{g}/\text{mL}$. 2 – *Proteus vulgaris*, SDS 60 $\mu\text{g}/\text{mL}$. 3 – *Lactobacillus acidophilus* MSU CM 146, SDS 50 $\mu\text{g}/\text{mL}$. 4 – *Pseudomonas putida*, SDS 0.2 mg/mL. 5 – *Stenotrophomonas maltophilia*, SDS 0.15 mg/mL

tometers UV-1800 or UV-1601PC (Shimadzu, Japan) were used. Measurements were performed in cells with an optical path length of 1 cm and a volume of 0.5 mL.

Bacteriolytic activity was determined turbidimetrically by a decrease in absorbance of cell suspension [7, 9] at a wavelength of 650 nm and a temperature of 37°C. A change in absorbance (A_{650}) in the range of 5 to 20–30 s from the start of the reaction was used as the initial cell lysis rate. If background spontaneous lysis of cells took place in the absence of bacteriolytic factors, then its value was subtracted from the value of activity in the presence of bacteriolytic additives. In case of cell lysis in the presence of SDS, the value of the lysis rate in the presence of IL-2 was taken into account as a correction proportionally to the content of SDS in the sample. Cell suspension with an initial absorbance $A_{650} = 0.4$ was used for the determination of the cell lysis rate. The activity was measured in a 10 mM buffer solution of MES-Tris- CH_3COOH at different pH values. As a relative value of activity, values of changes in the initial absorbance $-\text{d}A/\text{d}t$ (AU/min) are presented, which (with the coefficients for corresponding cells) are proportional to the rate of change in the number of living cells or colony-forming units ($-\text{dCFU}/\text{d}t$), proportional to the changes in the lysis rate $\text{d}\Theta/\text{d}t$ ($\Theta = 0$ if all cells remained intact, and $\Theta = 1$ in case of 100% cell lysis) [7, 9].

RESULTS AND DISCUSSION

The Table shows data on the effects of IL-2, lysozyme, and SDS on the cells of 37 strains of 34 different bacterial species. As one can see, 12 bacterial species are susceptible to lysis in the presence of lysozyme, 16 species are lysed in the presence of SDS, and only six species are sensitive to IL-2: *L. acidophilus*, *B. megaterium* (confirmed for two strains of the species), *B. mycoides*, *B. cereus*, *S. marcescens*, and *Enterobacter aerogenes*. At the same time, lysozyme, IL-2, and SDS are active against *L. acidophilus* and *B. mycoides*. *B. megaterium*, *B. cereus*, and *S. marcescens* are susceptible to lysozyme and IL-2 but not SDS. *Ent. aerogenes* is only susceptible to IL-2. In general, the spectra of microorganisms sensitive to lysozyme and interleukin-2 are not identical, though they overlap. Apparently, the mechanisms of action differ starkly for lysozyme and IL-2.

The pH-dependence of the rate of cell lysis by lysozyme and IL-2 is presented in Figs. 1 and 2. As can be seen, the values of pH-optimum activity for IL-2 and lysozyme against *B. megaterium* cells are identical and equal to 8.7. In the case of *L. acidophilus*, the pH-optima of lysozyme and IL-2 activity are also similar (6.5–7.0 and 6.7–7.3). Activity optima for lysozyme and IL-2 are similar for *B. mycoides* and *B. cereus* (not presented on the graphs due to the similarity with the dependencies for *B. megaterium*). A similar shift in lysozyme and IL-2 activity optima depending on the substrate (species of bacteria) was also observed in the case of *E. coli* and *L. plantarum* [3].

Figure 3 shows the pH-dependence of the cell lysis rate in the presence of SDS. The graph presents data for only five of the 16 microorganisms sensitive to SDS. For the other 11 microorganisms, pH-dependences of the cell lysis rate in the presence of SDS are similar. As it can be seen, SDS acts best on cells in an alkaline medium, which is inherent to various microorganisms. SDS is active at pH higher than 7.3–8.0. It is possible that such a tendency of pH-dependence is somehow connected to the range of pK values of the phosphate groups of cell membrane phospholipids. It is also possible that the components of the buffer solution (for example, Tris) can influence the nature of the pH-dependence. Identification of the exact molecular reason for such pH-dependency of the SDS action is beyond the scope of our study.

IL-2 acts on individual members of the Gram-negative family Enterobacteriaceae, including *Ent. aerogenes* and *S. marcescens*, as shown in our work, and, as previously established, on *E. coli* [1–3]. IL-2 is active against such Gram-positive members of the family Lactobacillaceae as *L. acidophilus* (current paper) and *L. plantarum* [3]. It was also found that IL-2 acts on *B. megaterium*, *B. mycoides*, and *B. cereus*, Gram-positive

Lysis of bacteria in the presence of interleukin-2, lysozyme and sodium dodecyl sulfate (SDS)

№	Microorganism	Cell lysis rate in the presence of an additive		
		lysozyme	interleukin-2	SDS
1	<i>Acinetobacter baumannii</i>	0	0	0
2	<i>Alcaligenes faecalis</i> MSU CM 82	3.2/2.0/6.4	0	1.1/100/8.0
3	<i>Bacillus megaterium</i>	5.2/0.8/8.7	6.1/15/8.7	0
4	<i>Bacillus megaterium</i> MSU CM 17	2.2/2.0/8.5	2.6/30/8.5	0
5	<i>Bacillus mycoides</i> MSU CM 31	4.5/4.0/8.0	3.6/10/8.0	0.7/100/8.0
6	<i>Bacillus cereus</i> MSU CM 9	4.5/4.0/8.5	0.9/30/8.5	0
7	<i>Bifidobacterium bifidum</i>	0	0	0
8	<i>Citrobacter braakii</i>	0	0	0
9	<i>Clostridium butiricum</i> MSU CM 19	0	0	2.5/400/8.0
10	<i>Corynebacterium amycolatum</i>	0	0	0
11	<i>Enterobacter aerogenes</i>	0	7.8/2.0/6.4	0
12	<i>Enterobacter cloacae</i>	0	0	0.9/200/8.0
13	<i>Enterococcus faecalis</i>	0	0	1.9/50/8.0
14	<i>Klebsiella pneumoniae</i>	0	0	0
15	<i>Lactobacillus acidophilus</i> MSU CM 146	3.2/0.8/7.0	2.9/5.0/7.0	2.4/50/8.0
16	<i>Lactobacillus casei</i> MSU CM 153	0	0	0
17	<i>Lactococcus lactis</i> MSU CM 165	0	0	0
18	<i>Morganella morganii</i>	0	0	2.0/40/8.0
19	<i>Neisseria perflava</i>	0	0	0
20	<i>Proteus mirabilis</i>	0	0	2.9/50/8.0
21	<i>Proteus vulgaris</i>	3.6/2.0/8.7	0	2.2/60/8.0
22	<i>Pseudomonas aeruginosa</i>	4.2/0.2/8.7	0	5.8/50/8.0
23	<i>Pseudomonas aeruginosa</i> MSU CM 47	7.3/0.4/7.7	0	1.1/100/8.0
24	<i>Pseudomonas fluorescens</i> MSU CM 71	3.5/0.5/8.4	0	0
25	<i>Pseudomonas putida</i>	0	0	2.5/200/8.0
26	<i>Rothia mucilaginosa</i>	0	0	0
27	<i>Serratia marcescens</i> MSU CM 208	3.7/0.2/8.4	4.7/30/8.0	0
28	<i>Staphylococcus aureus</i>	0	0	6.2/50/8.0
29	<i>Staphylococcus aureus</i> MSU CM 144	1.6/1.0/7.7	0	0
30	<i>Staphylococcus capitis</i>	0	0	0
31	<i>Staphylococcus epidermidis</i>	0	0	0
32	<i>Staphylococcus haemolyticus</i>	1.4/0.4/8.7	0	4.9/20/8.0
33	<i>Staphylococcus lugdunensis</i>	0	0	0
34	<i>Stenotrophomonas maltophilia</i>	0	0	3.3/150/8.0
35	<i>Streptococcus agalactiae</i>	4.6/5.0/7.0	0	4.1/50/8.0
36	<i>Streptococcus pyogenes</i>	0	0	0
37	<i>Thermus aquaticus</i>	0	0	3.6/125/8.0

Note. Values of the lysis rate are presented in the form X/Y/Z, wherein X is the lysis rate, AU, $10^{-3} \times \text{min}^{-1}$, Y is the concentration of an additive, $\mu\text{g} \times \text{mL}^{-1}$, and Z is pH of the medium in which the measurements were made. Values of pH-optimum are presented for lysozyme and interleukin-2: all rate values for SDS were obtained at pH 8.0. Zeroes indicate that no absorbance change was obtained for 3 min at concentrations of up to 5 $\mu\text{g}/\text{mL}$, 50 $\mu\text{g}/\text{mL}$ and 0.5 mg/mL for lysozyme, interleukin-2, and SDS, respectively.

spore-forming bacilli of the Bacillaceae family, which differ in cell wall structure and composition from the bacteria of the Enterobacteriaceae and Lactobacillaceae families. It can be assumed that the cell walls of *E. coli*, *Ent. aerogenes*, *S. marcescens*, *L. plantarum*, *L. acidophilus*, *B. mycoides*, *B. megaterium* and *B. cereus* have some similar structures. Indeed, structures containing diaminopimelic acid have been detected in the cell wall of *B. megaterium*, *B. cereus* and *L. plantarum* [10–13], which are not typical for many Gram-positive microorganisms but quite common among representatives of the family Enterobacteriaceae [13, 14]. The cell wall of *L. acidophilus* is believed not to contain significant amounts of diaminopimelic acid [15]. However, we can assume by analogy with *L. plantarum* that diaminopimelic acid may comprise the cell wall of certain strains of *L. acidophilus*. We have not found any publications demonstrating accurate data on the presence and quantity of diaminopimelic acid in *B. mycoides*, but we can assume that the structure of the cell wall of this bacterium, *B. megaterium* and *B. cereus*, can be partially similar. Apparently, similarity in susceptibility to IL-2 of such unrelated microorganisms can be explained by the presence of common structures containing diaminopimelic acid. We have previously shown that IL-2 has no effect on *B. subtilis* cells [1, 2], which also belong to the family Bacillaceae. However, some data have been published according to which, in contrast to many other members of this family, *B. subtilis* contains diaminopimelic acid, which is presented in amidated form [16]. Thus, the resistance of *B. sub-*

tilis to IL-2 actually confirms our hypothesis. In general, it is too early to draw accurate conclusions at this stage of the study about what types of microorganisms are sensitive to IL-2. Moreover, sensitivity to bacteriolytic agents can vary depending on the presence and composition of the capsule in bacteria, as well as vary even among different strains of the same species [17]. It should be noted that there is ongoing debate on the mechanisms of lysozyme action, which has been studied for a long time, against various microorganisms. There are reasons to believe that lysozyme can act not only on bacterial cells as an enzyme, but also as a cationic antibacterial protein [18]. As a result of our work, we established the spectrum of microorganisms sensitive to interleukin-2, which will help further study the molecular mechanisms of susceptibility or immunity of microorganisms to this bacteriolytic factor. ●

The authors express their gratitude to the members of Interclinical Bacteriological Laboratory at I.M. Sechenov First MSMU for the opportunity to cultivate microorganisms and determine their species. The authors also express their gratitude to the members of the Department of Microbiology of the Faculty of Biology at M.V. Lomonosov Moscow State University for the opportunity to work with microorganisms of the museum collection.

This work was supported by the Russian Science Foundation (project № 15-14-00012).

REFERENCES

- Levashov P.A., Sedov S.A., Belogurova N.G., Shipovskov S.V., Levashov A.V. // *Biochemistry (Moscow)*. 2012. V. 77. № 11. P. 1312–1314.
- Sedov S.A., Belogurova N.G., Shipovskov S.V., Semenova M.V., Gitinov M.M., Levashov A.V., Levashov P.A. // *Rus. J. Bioorg. Chem.* 2012. V. 38. № 3. P. 274–281.
- Levashov P.A., Matolygina D.A., Osipova H.E., Savin S.S., Zaharova G.S., Gasanova D.A., Belogurova N.G., Ovchinnikova E.D., Smirnov S.A., Tishkov V.I., Levashov A.V. // *J. Moscow Univ. Chem. Bull.* 2015. V. 70. № 6. P. 257–261.
- de Man J.D., Rogosa M., Sharpe M.E. // *J. Appl. Bacteriol.* 1960. V. 23. P. 130–135.
- Galyntkin V.A., Zaikina N.A., Kocherovets V.I., Kurbanova I.Z. // *Nutrient media for microbiological quality control of medicines and food products. Reference book*, St.P.: Prospekt Nauki, 2006.
- Netrusov A.I., Egorova M.A., Zakharchuk L.M. // *Praktikum po mikrobiologii*. M.: Akademiya, 2005.
- Matolygina D.A., Osipova H.E., Smirnov S.A., Belogurova N.G., Ereemeev N.L., Tishkov V.I., Levashov A.V., Levashov P.A. // *Moscow Univ. Chem. Bull.* 2015. V. 70. № 6. P. 262–267.
- Brock T.D., Edwards M.R. // *J. Bacteriol.* 1970. V. 104. P. 509–517.
- Levashov P.A., Sedov S.A., Shipovskov S.V., Belogurova N.G., Levashov A.V. // *Anal. Chem.* 2010. V. 82. P. 2161–2163.
- Bricas E., Ghuysen J.-M., Dezélee P. // *Biochem.* 1967. V. 6. № 8. P. 2598–2607.
- Okada S., Suzuki Y., Kozaki M. // *J. Gen. Appl. Microbiol.* 1979. V. 25. P. 215–221.
- van Heijenoort J., Elbaz L., Dezelee P., Petit J.F., Bricas E., Ghuysen J.M. // *Biochem.* 1969. V. 8. № 1. P. 207–213.
- Day A., White P.J. // *Biochem J.* 1977. V. 161. № 3. P. 677–685.
- Berges D.A., DeWolf W.E. Jr., Dunn G.L., Grappel S.F., Newman D.J., Taggart J.J., Gilvarg C. // *J. Med. Chem.* 1986. V. 29. № 1. P. 89–95.
- Ikawa M., Snell E.E. // *J. Biol. Chem.* 1960. V. 235. P. 1376–1382.
- Warth A.D., Strominger J.L. // *Proc. Natl. Acad. Sci. USA.* 1969. V. 64. № 2. P. 528–535.
- Campos M.A., Vargas M.A., Regueiro V., Llompert C.M., Albertí S., Bengoechea J.A. // *Infection Immunity*. 2004. V. 72. № 12. P. 7107–7114.
- Ginsburg A., Koren E., Feuerstein O. // *SOJ Microbiol. Infect. Dis.* 2015. V. 3. № 1. P. 1–8.

Thermodynamics of Damaged DNA Binding and Catalysis by Human AP Endonuclease 1

A. D. Miroshnikova¹, A. A. Kuznetsova¹, N. A. Kuznetsov^{1,2*}, O. S. Fedorova^{1,2*}

¹Institute of Chemical Biology and Fundamental Medicine, Siberian Branch of the Russian Academy of Sciences. Prosp. Acad. Lavrent'eva, 8, Novosibirsk, 630090, Russia;

²Department of Natural Sciences, Novosibirsk State University, Pirogova St., 2, Novosibirsk, 630090, Russia.

*E-mail: fedorova@niboch.nsc.ru, nikita.kuznetsov@niboch.nsc.ru

Received: 01.07.2015

Copyright © 2016 Park-media, Ltd. This is an open access article distributed under the Creative Commons Attribution License, which permits unrestricted use, distribution, and reproduction in any medium, provided the original work is properly cited.

ABSTRACT Apurinic/aprimidinic (AP) endonucleases play an important role in DNA repair and initiation of AP site elimination. One of the most topical problems in the field of DNA repair is to understand the mechanism of the enzymatic process involving the human enzyme APE1 that provides recognition of AP sites and efficient cleavage of the 5'-phosphodiester bond. In this study, a thermodynamic analysis of the interaction between APE1 and a DNA substrate containing a stable AP site analog lacking the C1' hydroxyl group (F site) was performed. Based on stopped-flow kinetic data at different temperatures, the steps of DNA binding, catalysis, and DNA product release were characterized. The changes in the standard Gibbs energy, enthalpy, and entropy of sequential specific steps of the repair process were determined. The thermodynamic analysis of the data suggests that the initial step of the DNA substrate binding includes formation of non-specific contacts between the enzyme binding surface and DNA, as well as insertion of the amino acid residues Arg177 and Met270 into the duplex, which results in the removal of "crystalline" water molecules from DNA grooves. The second binding step involves the F site flipping-out process and formation of specific contacts between the enzyme active site and the everted 5'-phosphate-2'-deoxyribose residue. It was shown that non-specific interactions between the binding surfaces of the enzyme and DNA provide the main contribution into the thermodynamic parameters of the DNA product release step.

KEYWORDS thermodynamics, pre-steady-state kinetics, kinetic mechanism, apurinic/aprimidinic site, human AP endonuclease.

ABBREVIATIONS APE1 – AP endonuclease; BER – base excision repair, AP site – apurinic/aprimidinic site; F site – (3-hydroxy-tetrahydrofuran-2-yl) methyl phosphate.

INTRODUCTION

One of the most frequent DNA damages are apurinic/aprimidinic sites (AP sites) [1, 2] that are formed in DNA during spontaneous or DNA glycosylase-catalyzed hydrolysis of N-glycosidic bonds [3]. Every day, up to 10,000 AP sites may form in the human cell. The high mutagenicity of AP sites is related to both the lack of an encoding nitrogenous base and the increased ability of AP sites to cause nicks in the DNA ribose phosphate backbone.

The key enzyme of the base excision repair (BER) system is human apurinic/aprimidinic endonuclease 1 (APE1) that is responsible for recognition and initiation of removal of AP sites in DNA [4, 5]. Its major physiological function is hydrolysis of the DNA phosphodies-

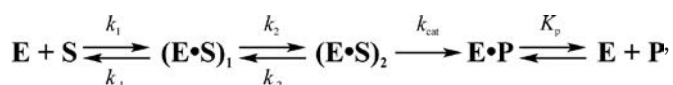
ter bond located upstream of the AP site, which results in a ribose phosphate backbone breakage to form chain fragments containing a 3'-hydroxyl group and 2'-deoxyribose 5'-phosphate [6, 7].

An analysis of the crystal structures of the free APE1 enzyme [8–10] and APE1-DNA covalent complexes [11–13] showed that catalysis in the APE1-DNA complex requires contacts whose formation leads to flipping of an AP site out of the double helix. *Figure 1* presents a scheme of the contacts in the enzyme-substrate complex between APE1 and DNA containing the F site lacking an OH-group in the C1' position of deoxyribose (PDB ID 1DE8). It is seen that enzyme amino acid residues interact preferentially with one of the duplex strands to form usually hydrogen bonds and

electrostatic contacts between DNA phosphate groups and amino acid side chains and also amide groups of peptide bonds of the protein. The enzyme active site is formed by Asp308, His309, Glu96, Asp210, Tyr171, Asn212, and Asn174 residues. The flipped out AP site conformation is stabilized by Met270 and Arg177 residues. Met270 is embedded into the DNA minor groove, thereby displacing the base opposite to the AP site. The Arg177 residue is inserted on the DNA major groove side and forms a hydrogen bond with a phosphate group located downstream of the AP site. In the enzyme-substrate complex, which is in a catalytically competent state, a phosphate residue located upstream of the AP site is coordinated by Asn174, Asn212, and His309 residues. The catalytic reaction begins with the nucleophilic attack of a water molecule that is coordinated, directly or indirectly through a Mg^{2+} ion, by Asp210 on a 5'-phosphate group [11, 13].

Previously, a stopped-flow technique with detection of changes in the fluorescence intensity of enzyme tryptophans [14, 15] and 2-aminopurines located downstream and upstream of the AP site [16] was used to elucidate the kinetic mechanism of interaction between APE1 and DNA substrates (*Scheme*). DNA duplexes containing a native AP site or its analog (F site) without an OH-group in the C1' position of deoxyribose were used as substrates. The interaction between APE1 and substrates was shown to include at least two steps of DNA binding and AP site recognition that lead to the formation of a catalytically competent complex. An irreversible step of catalytic hydrolysis of a 5'-phosphodiester bond of the AP site occurs in this complex. The last step of the kinetic mechanism describes equilibrium dissociation of the enzyme-product complex.

Scheme. The kinetic mechanism of interaction between APE1 and a DNA substrate



where E is the enzyme; S is the substrate; $(E \cdot S)_1$ and $(E \cdot S)_2$ are enzyme-substrate complexes; P is a product of the enzyme-catalyzed reaction; $(E \cdot P)$ is the enzyme-product complex; k_i and k_{-i} are rate constants of the forward and reverse reactions of equilibrium steps; k_{cat} is the rate constant of the catalytic step; and K_p is the equilibrium dissociation constant of the EP complex.

According to the X-ray data, DNA binding leads only to minor structural rearrangements in APE1 (*Fig. 2*). Comparison of the structures of free APE1 (PDB ID 4LND) and a complex between APE1 and

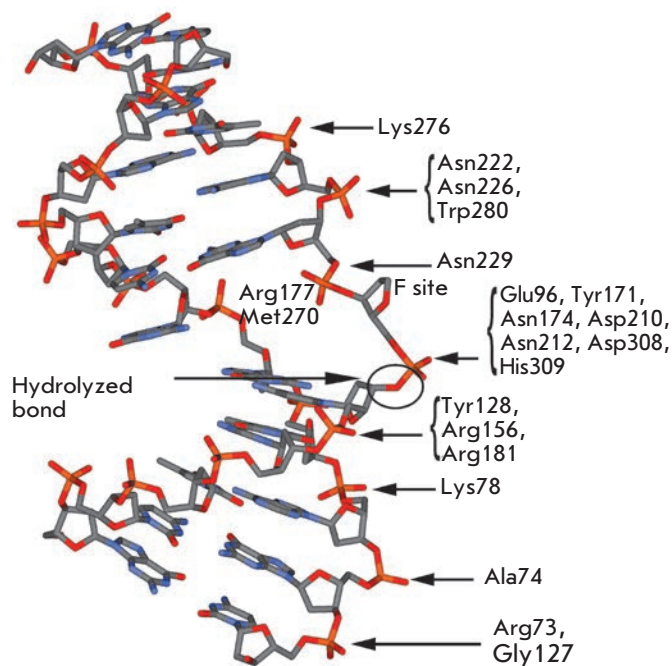


Fig. 1. Schematic representation of contacts in the complex between APE1 and DNA containing the F site (PDB ID 1DE8 [11]).

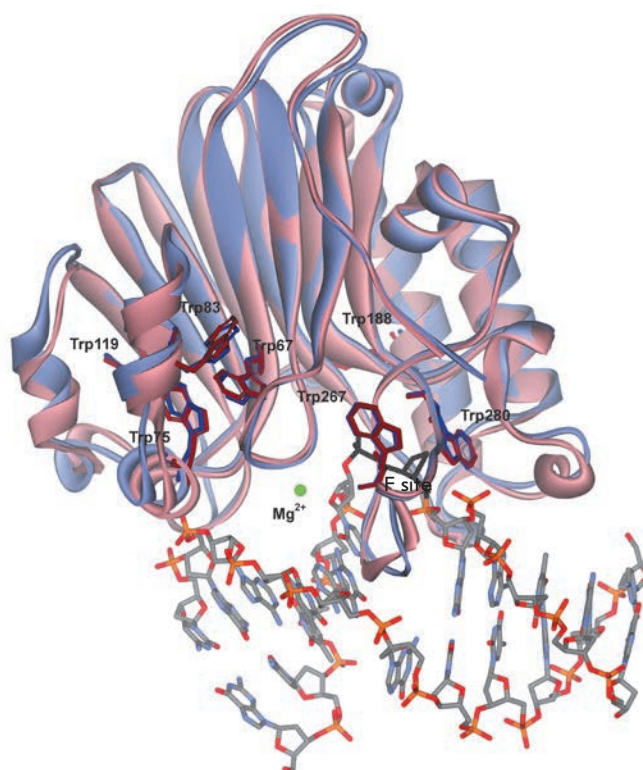


Fig. 2. Overall structures of free APE1 (pink, PDB ID 4LND) and APE1 associated with damaged DNA (violet, PDB ID 1DE8).

DNA containing the F site (PDB ID 1DE8) demonstrates that one of the seven tryptophan residues of the enzyme molecule, Trp280, is located in the DNA-binding site and forms a hydrogen bond with a DNA phosphate group. Therefore, the observed changes in Trp fluorescence are likely related to enzyme conformational changes in the Trp280 region.

The aim of this work was to determine the thermodynamic parameters of the APE1 conformational rearrangements associated with specific recognition of a damaged DNA site and the catalytic step of the enzymatic reaction during base excision repair based on the kinetic data of the enzymatic process at different temperatures. This approach made it possible to determine the thermodynamic parameters for steps of formation of the catalytically active enzyme form, including an intermediate enzyme-substrate complex, in contrast to the data [17] obtained previously for an inactive form of APE1.

MATERIAL AND METHODS

Oligodeoxyribonucleotides

Oligonucleotides were purified by HPLC on an ion exchange column (PRP-X500 Hamilton Company, 3.9×300 mm, 12–30 μ m particle size) and subsequent reverse phase chromatography (Nucleoprep 100-20 C₁₈, 10×250 mm, Macherey-Nagel, Germany). Oligonucleotide purity was evaluated using 20% denaturing polyacrylamide gel electrophoresis (PAGE). The oligonucleotide concentration was measured by absorbance of solutions at 260 nm in their electronic absorption spectra and calculated according to the Lambert-Bouguer-Beer law based on a molar extinction coefficient determined using the nearest-neighbor approximation [18]. A DNA substrate of the APE1 enzyme (F substrate) was a 17-mer duplex consisting of oligodeoxyribonucleotides

5'-TCTCTCTCFCTTCCTT-3' and
3'-AGAGAGAGGGGAAGGAA-5'.

APE1 enzyme

The APE1 enzyme was isolated from *Escherichia coli* Rosetta 2 cells transformed with the plasmid pET11a carrying the human AP endonuclease gene. The *E. coli* Rosetta 2 cell culture was grown in a LB medium (1 L) containing 50 μ g/mL of ampicillin at 37°C to an optical density of 0.6–0.7 at 600 nm. Then, the temperature was lowered to 20°C, and transcription was induced by adding isopropyl- β -D-thiogalactopyranoside to a final concentration of 0.2 mM. After induction, the cell culture was incubated for 16 h. Then, the cells were pelleted by centrifugation (12,000 rpm, 10 min), and a cell

suspension was prepared in 30 mL of buffer I (20 mM HEPES-NaOH, pH 7.8) containing 40 mM NaCl. Cells were lysed using a French-press. All subsequent procedures were performed at 4°C. The cell lysate was centrifuged (30,000 rpm, 40 min), and the supernatant was loaded onto column I (Q-Sepharose Fast Flow, Amersham Biosciences, Sweden) and washed with buffer I (20 mM HEPES-NaOH, pH 7.8) containing 40 mM NaCl. Fractions containing the APE1 protein were collected and loaded onto column II (HiTrap-Heparin™, Amersham Biosciences, Sweden). Chromatography was performed in buffer I with a linear gradient of 40 → 600 mM of NaCl; the solution's absorbance was detected at 280 nm. The APE1 protein purity was determined by gel electrophoresis. Fractions containing the APE1 protein were dialyzed in buffer II (20 mM HEPES-NaOH, 1 mM EDTA, 1 mM dithiothreitol, 250 mM NaCl, 50% glycerol, pH 7.5) and stored at -20°C. The enzyme concentration was calculated using protein absorbance values at 280 nm and a molar extinction coefficient of 56,818 M⁻¹cm⁻¹ [19].

Stopped-flow kinetic measurements

Kinetic fluorescence curves were acquired using a SX20 stopped-flow spectrometer (Applied Photophysics, UK). The fluorescence excitation wavelength was 290 nm. Fluorescence was recorded at wavelengths longer than 320 nm (Schott filter WG 320). Since the APE1 molecule contains 7 Trp residues and 11 Tyr residues, more than 90% of the detected protein fluorescence intensity was due to Trp fluorescence under the experimental conditions used. The instrument dead time was 1.1 ms, and the maximum signal acquisition time was 200 s. All experiments were performed in a buffer solution simulating BER conditions (50 mM Tris-HCl, 50 mM KCl, 5 mM MgCl₂, 1 mM dithiothreitol, 7% glycerol, pH 7.5) at 10–37°C. Each kinetic curve was an average of at least three experimental curves.

Analysis of the hydrolysis extent of the 5'-phosphodiester bond at the AP site

The dependence of the hydrolysis extent of the 5'-phosphodiester bond at the AP site on time was studied by mixing enzyme and ³²P-labeled substrate solutions. The label was attached to the 5'-end of an F-containing oligonucleotide using T4 polynucleotide kinase (SibEnzyme, Novosibirsk) and [γ -³²P] ATP (BIO-SAN, Novosibirsk) according to [20, 21]. Further, 2 μ L aliquots were taken from the reaction mixture and transferred to prepared test tubes containing 3 μ L of a 7 M urea solution, 0.1% bromophenol blue, and 0.1% xylene cyanol FF. PAGE was carried out at 50 V/cm. Gel was autoradiographed on an Agfa CP-BU New X-ray film (Agfa-Geveart, Belgium) at -20°C for 12–60 h.

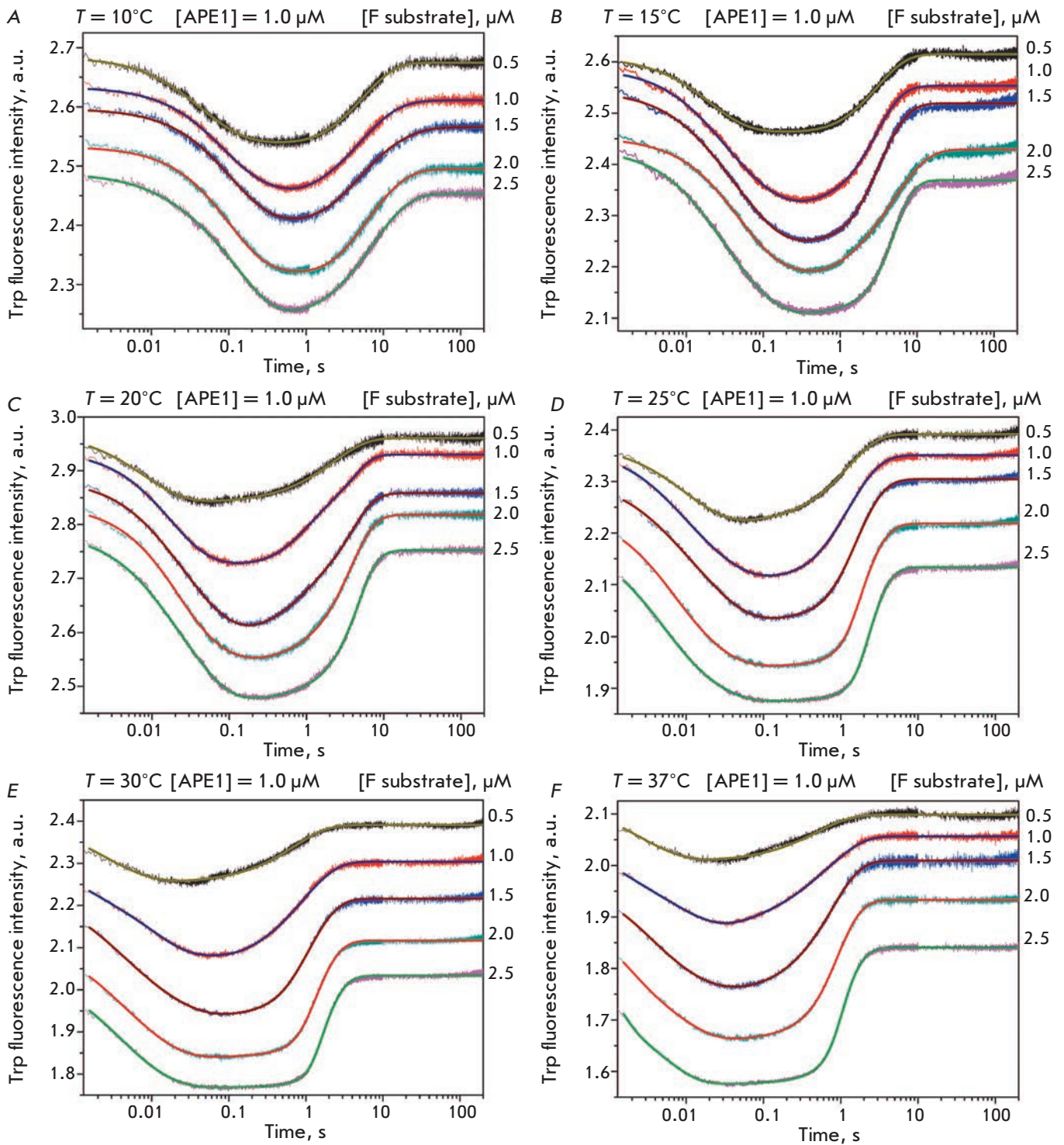


Fig. 3. Changes in the Trp fluorescence intensity during interaction between APE1 and the F substrate at 10°C (A), 15°C (B), 20°C (C), 25°C (D), 30°C (E), and 37°C (F). Experimental curves were smoothed using the kinetic model (*Scheme*). The F substrate concentration was varied from 0.5 to 2.5 μM ; the APE1 concentration was 1.0 μM .

Analysis of kinetic curves

To calculate the rate constants of conformational transitions, a number of kinetic curves for different substrate concentrations at different temperatures were obtained. Detection was carried out under conditions appropriate for one enzyme turnover, i.e. at enzyme and substrate concentrations of the same order. DynaFit software (BioKin, USA) [22] was used to determine the minimum kinetic scheme describing the enzyme-substrate interaction and to calculate the rate constants of elementary steps of the reaction. Quantitative processing of experimental data was conducted by optimizing the parameters included in the kinetic schemes as described previously [23–25].

The obtained values of rate constants of individual reaction steps were used to calculate the equilibrium constants (K_i) for the steps (k_i/k_{-i} , where i is the step number) at different temperatures. Standard thermodynamic parameters of the i -th equilibrium step were determined using the van't Hoff equation (1) [26, 27]

$$\ln(K_i) = -\Delta G_i/RT = -\Delta H_i/RT + \Delta S_i/R. \quad (1)$$

The $\ln(K_i)$ vs $1/T$ dependences were linear.

An analysis of the temperature dependence of the reaction rate constant k_{cat} using the Eyring equation (2) provided the standard activation enthalpy (ΔH^{\ddagger}) and standard activation entropy (ΔS^{\ddagger}) of the transition state [26]

$$\ln(k_{\text{cat}}/T) = \ln(k_B/h) + (\Delta S^{\ddagger}/R) - (\Delta H^{\ddagger}/RT), \quad (2)$$

where k_B and h are the Boltzmann and Planck constants, respectively; R is the gas constant; and T is absolute temperature in degrees Kelvin.

RESULTS AND DISCUSSION

To clarify the nature of the processes occurring during sequential stages of F site recognition in the DNA-substrate complex, catalysis, and enzyme-product complex dissociation, we conducted a stepwise thermodynamic analysis of the interaction between APE1 and the F substrate. Stopped-flow measurements of the Trp fluorescence intensity provided kinetic curves characterizing the interaction between APE1 and the 17-mer F substrate at one enzyme turnover conditions and temperature of 10 to 37°C (Fig. 3). It is seen that the interaction between APE1 and the F substrate leads to multiphase changes in the Trp fluorescence intensity. According to the previously obtained data [14, 15], a decrease in the fluorescence intensity in the initial part of the kinetic curves characterizes the formation of a catalytically competent complex. The catalytic reaction step leading to the formation of products and sub-

sequent dissociation of the enzyme-product complex is accompanied by an increase in the Trp fluorescence intensity at longer times (>1 s). As is evident from the kinetic curves (Fig. 4), both phases of the changes in the fluorescence intensity are temperature-dependent.

An analysis of the kinetic curves of the protein fluorescence intensity demonstrated that the minimum kinetic mechanism of the interaction between APE1 and the DNA substrate containing the F site as damage involves a two-step equilibrium binding, irreversible formation of the enzyme-product complex, and equilibrium dissociation of the complex. As previously [14–16], the mechanism is described by the *Scheme*.

The rate constants of the forward and reverse reactions that describe the APE1-DNA substrate interaction at different temperatures were calculated by a nonlinear regression, including numerical integration of differential equations related to the *Scheme*, as described previously [28, 29]. The resulting rate constants were used to determine the equilibrium constants K_i and K_p (Table 1).

As shown in Figure 5, the $\ln(K_i)$ and $\ln(k_{\text{cat}}/T)$ vs $1/T$ dependences are linear, which enables calculation of thermodynamic parameters for equilibrium steps using the van't Hoff equation (1), as well as parameters of the transition state in the catalytic step using the Eyring equation (2) (Table 2).

According to the obtained data, the formation of the primary enzyme-substrate complex (the first step in the *Scheme*) is characterized by a positive standard enthalpy value (14.3 kcal/mol) and a positive entropy

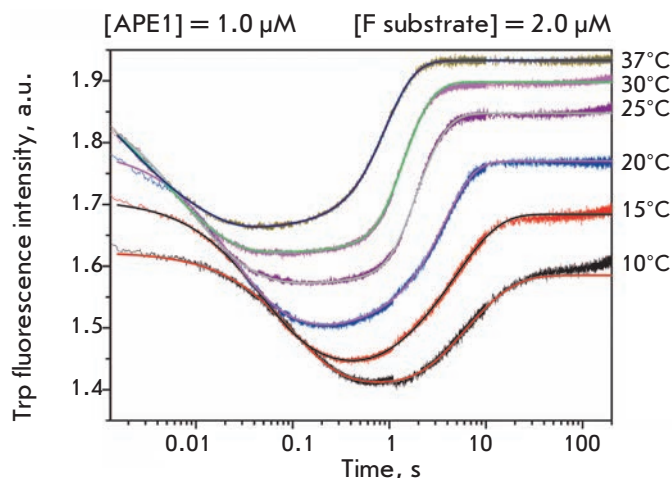


Fig. 4. Changes in the Trp fluorescence intensity during interaction between APE1 and the F substrate at different temperatures. [APE1] = 1.0 μM , [F substrate] = 2.0 μM .

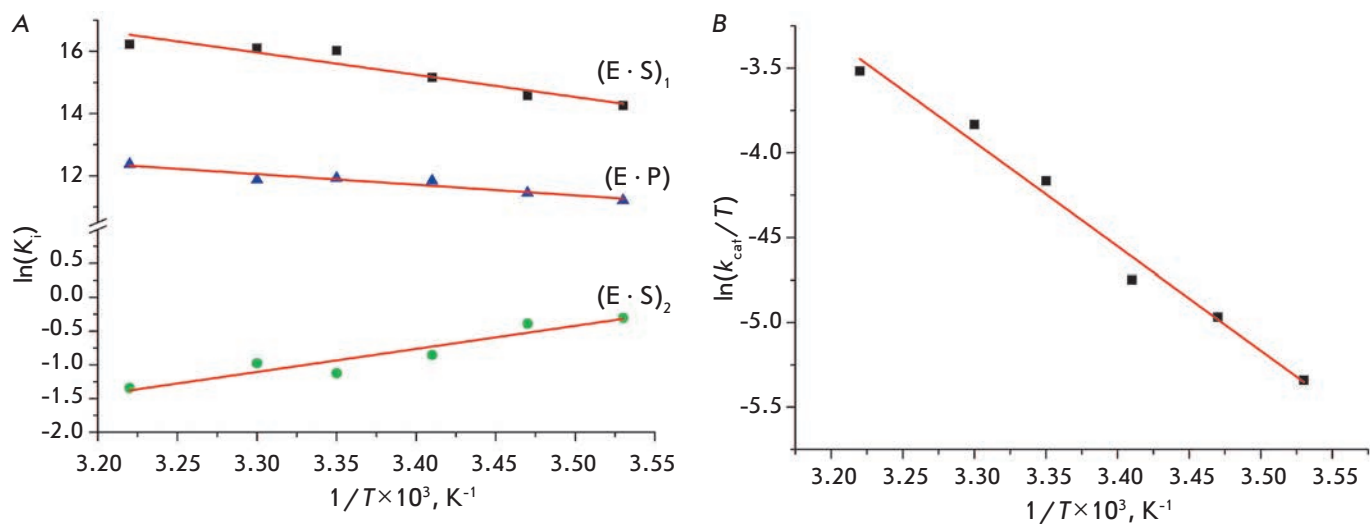
Table 1. Rate constants for individual steps of the interaction between APE1 and the F substrate under BER conditions and dissociation constants of the enzyme-product complex.

Temperature Constant	10°C	15°C	20°C	25°C	30°C	37°C
$k_1, M^{-1}s^{-1}$	$(5.1 \pm 2.1) \times 10^6$	$(16.0 \pm 3.4) \times 10^6$	$(46.0 \pm 12.0) \times 10^6$	$(100 \pm 12) \times 10^6$	$(190 \pm 32) \times 10^6$	$(520 \pm 20) \times 10^6$
k_{-1}, s^{-1}	3.3 ± 0.4	7.3 ± 3.6	12.0 ± 5.1	11.0 ± 2.5	19.0 ± 5.2	47.0 ± 13.0
K_1^*, M	0.65×10^{-6}	0.47×10^{-6}	0.26×10^{-6}	0.11×10^{-6}	0.10×10^{-6}	0.09×10^{-6}
k_2, s^{-1}	4.2 ± 2.6	3.7 ± 1.2	8.2 ± 3.9	8.8 ± 4.4	15.0 ± 1.8	24.0 ± 9.0
k_{-2}, s^{-1}	5.7 ± 1.9	5.5 ± 2.9	19.0 ± 3.7	27.0 ± 4.2	40.0 ± 6.6	93.0 ± 17.4
K_2	1.27	0.51	0.68	0.81	0.79	0.52
k_{cat}, s^{-1}	1.4 ± 0.6	2.0 ± 0.7	2.5 ± 1.2	4.6 ± 2.2	6.6 ± 2.2	9.2 ± 1.0
K_p, M	$(13.5 \pm 3.9) \times 10^{-6}$	$(10.6 \pm 1.9) \times 10^{-6}$	$(7.2 \pm 1.8) \times 10^{-6}$	$(6.6 \pm 2.3) \times 10^{-6}$	$(6.9 \pm 1.2) \times 10^{-6}$	$(4.2 \pm 0.6) \times 10^{-6}$

*Equilibrium association constants were calculated using the formula $K_i = k_{-i}/k_i$.

Table 2. Thermodynamic parameters of the interaction between APE1 and F-substrate.

Parameter Step (number)	$\Delta G_{i,298}^\circ, kcal/mol$	$\Delta H_i^\circ, kcal/mol$	$\Delta S_i^\circ, cal/(mol \times K)$
Primary DNA binding (1)	-9.2	14.3 ± 2.2	79.0 ± 7.6
Specific recognition of the F site (2)	0.5	-6.8 ± 1.2	-24.6 ± 4.0
Overall parameter value for binding steps $\sum_{i=1}^2$	-8.7	7.5 ± 3.4	54.4 ± 11.7
Transition state of the catalytic step (3)	16.6	12.2 ± 0.8	-14.8 ± 2.8
Enzyme-product complex formation (4)	-7.0	6.8 ± 1.0	46.6 ± 3.5

**Fig. 5.** Analysis of the temperature dependence of $\ln(K_i)$ (A) and $\ln(k_{cat}/T)$ (B).

value (79.0 cal/(mol×K)). An increase in entropy during interaction between DNA-binding proteins and DNA is known to be usually due to two factors: desolvation of polar groups at the DNA-protein interface [30] and removal of highly ordered molecules of “crystalline water” from the DNA grooves [31]. It may be assumed that the bonds between amino acid residues of the DNA-binding site and the DNA duplex form at this stage. The interaction between DNA duplex phosphate groups situated upstream and downstream of the F site and Arg73, Ala74, Lys78, Trp280, Asn222, Asn226, and Asn229 residues is of special interest (*Fig. 1*). Furthermore, incorporation of the Arg177 residue into the DNA duplex on the major groove side and formation of a hydrogen bond with a phosphate group located downstream of the F site may occur at this moment. The Met270 residue is incorporated into the DNA duplex on the minor groove side and may also displace “crystalline” water. Previously, studies of *E. coli* Fpg [28] and human OGG1 [29] DNA-glycosylases, which belong to different structural classes and, consequently, interact with DNA through contacts of different nature, demonstrated that the steps of enzyme-substrate complex formation and isomerization of the complex into a catalytically competent state are characterized by a significant increase in entropy that is apparently caused by desolvation of the interacting protein and DNA surfaces.

The second stage of the interaction between APE1 and the F substrate is a specific rearrangement of the $(E \cdot S)_1$ complex and is characterized by negative changes in both enthalpy ($\Delta H^\circ_2 = -6.8$ kcal/mol) and entropy ($\Delta S^\circ_2 = -24.6$ cal/(mol×K)). The negative ΔH°_2 value indicates stabilization of the complex during formation of new, energetically favorable bonds among interacting atoms, while the negative ΔS°_2 value suggests an increase in the rigidity of the complex; i.e. a reduction in its internal degrees of freedom. This step probably involves flipping the F site into the enzyme active site and stabilizing this state by Arg177 and Met270 residues that are inserted into the major and minor DNA grooves, respectively. Furthermore, bonds between a phosphate group located upstream of the F site (*Fig. 1*) and the Asn174, Asn212, and His309 residues and the Mg^{2+} ion that are located in the enzyme active site may form at this moment.

Activation enthalpy (ΔH^\ddagger) and entropy (ΔS^\ddagger) for the transition complex formation were calculated for the third catalytic step. The resulting activation enthalpy value is 12.2 kcal/mol. It should be noted that this value is related to the step of phosphodiester bond hydrolysis by the APE1 enzyme and lies within the range of

6.0–18.6 kcal/mol obtained previously for the catalytic steps of N-glycosidic bond cleavage and β -elimination of phosphate groups by Fpg and hOGG1 DNA glycosylases [28, 29].

The thermodynamic parameters of the complex formation between APE1 and AP-containing DNA were obtained previously using SPR, i.e. under heterophase conditions, for a catalytically inactive enzyme in the absence of Mg^{2+} ions [17]. The approach used in the present study [28, 29] enables the calculation of thermodynamic data for processes occurring in an aqueous solution, i.e. under homophase conditions, and involving catalytically active forms of enzymes, including transient enzyme-substrate intermediates.

Interestingly, the thermodynamic parameters for the step of the complex formation between the enzyme and a reaction product correlate with those of the primary complex formation. Similarly to the first step, this process is characterized by positive standard enthalpy and entropy changes (6.8 kcal/mol and 46.6 cal/(mol×K), respectively). This indicates that the thermodynamic parameters of this step are largely determined by the same interactions that occur at the first step of APE1 binding to the DNA substrate – non-specific contacts between the DNA-binding site and the ribose-phosphate backbone of the DNA duplex. However, the enzyme-product complex ($E \cdot P$) may be considered a true non-specific complex, while the formation of the primary complex $(E \cdot S)_1$ in the case of a short DNA substrate involves some elements of specific recognition of the F site. Therefore, the $(E \cdot S)_1$ complex formation is energetically more favorable compared to the $E \cdot P$ complex ($\Delta \Delta G^\circ_{298} = -2.2$ kcal/mol, $\Delta \Delta H^\circ = 7.5$ kcal/mol, $\Delta \Delta S^\circ = 32.4$ cal/(mol×K)).

Thus, we obtained the thermodynamic parameters of conformational APE1 rearrangements associated with specific recognition of a damaged DNA fragment and the catalytic step. These findings led to a conclusion on the molecular nature of the individual steps of the kinetic mechanisms that describe the enzyme function. ●

This work was supported by the Federal Agency for Scientific Organizations, Russian Academy of Sciences (grant 6.11 under the program Molecular and Cell Biology), Leading Scientific Schools (grant NSH-7564.2016.4), and Russian Foundation for Basic Research (grants No. 16-04-00037, 15-34-20121, and 15-04-00467). Part of the work, including analysis of the experimental data, was supported by a grant of the Russian Science Foundation (No. 14-14-00063).

REFERENCES

1. Lindahl T. // *Nature*. 1993. V. 362. P. 709–715.
2. Wilson III D.M., Barsky D. // *Mutat. Res.* 2001. V. 485. P. 283–307.
3. Friedberg E.C., Walker G.C., Siede W., Wood R.D., Schultz R.A., Ellenberger T. *DNA Repair and Mutagenesis*. Washington: ASM Press, 2006.
4. Mol C.D., Parikh S.S., Putnam C.D., Lo T.P., Tainer J.A. // *Annu. Rev. Biophys. Biomol. Struct.* 1999. V. 28. P. 101–128.
5. David S.S., Williams S.D. // *Chem. Rev.* 1998. V. 98. P. 1221–1261.
6. Demple B., Sung J.-S. // *DNA Repair (Amst.)*. 2005. V. 4. P. 1442–1449.
7. Dyrkheeva N.S., Khodyreva S.N., Lavrik O.I. // *Mol. Biol. (Mosk.)*. 2007. V. 41. P. 450–466.
8. Gorman M.A., Morera S., Rothwell D.G., de La Fortelle E., Mol C.D., Tainer J.A., Hickson I.D., Freemont P.S. // *EMBO J.* 1997. V. 16. P. 6548–6558.
9. Beernink P.T., Segelke B.W., Hadi M.Z., Erzberger J.P., Wilson D.M., 3rd, Rupp B. // *J. Mol. Biol.* 2001. V. 307. P. 1023–1034.
10. Manvilla B.A., Pozharski E., Toth E.A., Drohat A.C. // *Acta Crystallogr. D Biol. Crystallogr.* 2013. V. 69. P. 2555–2562.
11. Mol C.D., Izumi T., Mitra S., Tainer J.A. // *Nature*. 2000. V. 403. P. 451–456.
12. Mol C.D., Hosfield D.J., Tainer J.A. // *Mutat. Res.* 2000. V. 460. P. 211–229.
13. Tsutakawa S.E., Shin D.S., Mol C.D., Izumi T., Arvai A.S., Mantha A.K., Szczesny B., Ivanov I.N., Hosfield D.J., Maiti B., Pique M.E., Frankel K.A., Hitomi K., Cunningham R.P., Mitra S., Tainer J.A. // *J. Biol. Chem.* 2013. V. 288. P. 8445–8455.
14. Timofeyeva N.A., Koval V.V., Knorre D.G., Zharkov D.O., Sapparbaev M.K., Ishchenko A.A., Fedorova O.S. // *J. Biomol. Struct. Dyn.* 2009. V. 26. P. 637–652.
15. Kanazhevskaya L.Y., Koval V.V., Zharkov D.O., Strauss P.R., Fedorova O.S. // *Biochemistry*. 2010. V. 49. P. 6451–6461.
16. Kanazhevskaya L.Y., Koval V.V., Vorobjev Y.N., Fedorova O.S. // *Biochemistry*. 2012. V. 51. P. 1306–1321.
17. Adhikari S., Uren A., Roy R. // *J. Biol. Chem.* 2008. V. 283. P. 1334–1339.
18. Fasman G.D. *Handbook of Biochemistry and Molecular Biology*, 3ed. Cleveland: CRC Press, 1975.
19. Gill S.C., von Hippel P.H. // *Anal. Biochem.* 1989. V. 182. P. 319–326.
20. Kuznetsov N.A., Koval V.V., Zharkov D.O., Fedorova O.S. // *DNA Repair (Amst.)*. 2012. V. 11. P. 884–891.
21. Kuznetsov N.A., Zharkov D.O., Koval V.V., Buckle M., Fedorova O.S. // *Biochemistry*. 2009. V. 48. P. 11335–11343.
22. Kuzmic P. // *Anal. Biochem.* 1996. V. 237. P. 260–273.
23. Kuznetsov N.A., Koval V.V., Nevinsky G.A., Douglas K.T., Zharkov D.O., Fedorova O.S. // *J. Biol. Chem.* 2007. V. 282. P. 1029–1038.
24. Kuznetsov N.A., Koval V.V., Zharkov D.O., Vorobiev Y.N., Nevinsky G.A., Douglas K.T., Fedorova O.S. // *Biochemistry*. 2007. V. 46. P. 424–435.
25. Koval V.V., Kuznetsov N.A., Ishchenko A.A., Sapparbaev M.K., Fedorova O.S. // *Mutat. Res.* 2010. V. 685. P. 3–10.
26. Atkins P., Paula J., Atkins' *Physical Chemistry*. 8th Edition. N.Y.: Oxford Univ. Press, 2006.
27. Ragone R., Colonna G., Ambrosone L. // *J. Phys. Chem.* 1995. V. 99. P. 13050–13050.
28. Kuznetsov N.A., Vorobjev Y.N., Krasnoperov L.N., Fedorova O.S. // *Nucl. Acids Res.* 2012. V. 40. P. 7384–7392.
29. Kuznetsov N.A., Kuznetsova A.A., Vorobjev Y.N., Krasnoperov L.N., Fedorova O.S. // *PLoS One*. 2014. V. 9. P. e98495.
30. Jen-Jacobson L., Engler L.E., Jacobson L.A. // *Structure*. 2000. V. 8. P. 1015–1023.
31. Privalov P.L., Dragan A.I., Crane-Robinson C. // *Nucl. Acids Res.* 2011. V. 39. P. 2483–2491.

Combinations of Polymorphic Markers of Chemokine Genes, Their Receptors and Acute Phase Protein Genes As Potential Predictors of Coronary Heart Diseases

T.R. Nasibullin¹, L.F. Yagafarova², I.R. Yagafarov², Y.R. Timasheva¹, V.V. Erdman¹, I.A. Tuktarova¹, O.E. Mustafina¹

¹Institute of Biochemistry and Genetics, Ufa Research Center of the Russian Academy of Sciences, Ufa, the Republic of Bashkortostan, Prospect Octyabrya, 71, 450054, Russia

²Medical and sanitary unit of PJSC "Tatneft" and the city of Almetyevsk, Almetyevsk, the Republic of Tatarstan, Radischeva Str., 67, 423450, Russia

*E-mail: NasibullinTR@yandex.ru

Received 21.07.2015

Copyright © 2016 Park-media, Ltd. This is an open access article distributed under the Creative Commons Attribution License, which permits unrestricted use, distribution, and reproduction in any medium, provided the original work is properly cited.

ABSTRACT Atherosclerosis, the main factor in the development of coronary heart diseases (CHD), is an inflammatory response to endothelial layer damage in the arterial bed. We have analyzed the association between CHD and the polymorphic markers of genes that control the synthesis of proteins involved in the processes of adhesion and chemotaxis of immunocompetent cells: rs1024611 (-2518A>G, *CCL2* gene), rs1799864 (V64I, *CCR2* gene), rs3732378 (T280M, *CX3CR1* gene), rs1136743 (A70V, *SAA1* gene), and rs1205 (2042C>T, *CRP* gene) in 217 patients with CHD and 250 controls. Using the Monte Carlo method and Markov chains (APSampler), we revealed a combination of alleles/genotypes associated with both a reduced and increased risk of CHD. The most significant alleles/genotypes are *SAA1**T/T+*CRP**C+*CX3CR1**G/A ($P_{\text{perm}} = 0.0056$, OR = 0.07 95%CI 0.009–0.55), *SAA1**T+*CRP**T+*CCR2**G/A+*CX3CR1**G ($P_{\text{perm}} = 0.0063$, OR = 14.58 95%CI 1.88–113.04), *SAA1**T+*CCR2**A+*CCL2**G/G ($P_{\text{perm}} = 0.0351$, OR = 10.77 95%CI 1.35–85.74).

KEYWORDS coronary heart disease, genetic polymorphism, complex traits, APSampler.

ABBREVIATIONS CHD – coronary heart disease; MI – myocardial infarction; CRP – C-reactive protein; SAA – serum amyloid A.

INTRODUCTION

Coronary heart diseases (CHD) and the main factor of their development, atherosclerosis, are among the most frequent causes of disability and mortality in the majority of developed countries. The molecular and genetic basis of hereditary predisposition to CHD is actively studied, and one of the important directions in such research is the analysis of the association between polymorphic DNA markers and the disease. Genome-wide association studies (GWAS) using high-density microarrays and analysis of individual polymorphic markers located in the regions of the genes encoding for products involved in the pathogenesis of the disease (candidate genes) are used for this purpose. Most studies analyze the contribution of individual polymorphic markers in the formation of hereditary predisposition to the disease. At the same time, since atherosclerosis, with the exception of rare monogenic variants, is a multifactorial polygenic disease caused by complex in-

teractions between genetic and environmental factors, the analysis of the combinations of factors determining the activity of individual pathogenetic links appears to be more promising.

According to modern concepts, atherosclerotic lesion of the vascular wall is caused by an inflammatory reaction developing in response to damage to vascular endothelium [1]. The inflammatory process at all stages of atherosclerosis involves immune cells, the participation of which in endothelial damage includes their mobilization from the bone marrow, adhesion, chemotaxis, transformation, change in the ratio of different leukocyte subclasses, etc. All these processes are controlled by a variety of proteins and inflammatory mediators, including chemokines and acute-phase proteins.

Chemokines are a group of low-molecular-weight cytokines the primary function of which is mediating the migration of various cells expressing chemokine receptors from the bloodstream to inflammation or tumor

Table 1. List of the polymorphic markers included in the study, their localization, primer sequences, restriction enzymes, and allele nomenclature

Gene, chromosome localization	Polymorphism, localization	Primer sequence, restriction enzyme	Allele, fragment size, bp
<i>CCL2</i> 17q12	rs1024611 -2518A>G 5'-end	F 5'-ctc acg cca gca ctg acc tcc-3' R 5'-agc cac aat cca gag aag gag acc-3' <i>PvuII</i>	A – 300 G – 228 and 72
<i>CCR2</i> 3p21.31	rs1799864 V64I exon 2	F 5'-tgc ggt gtt tgt gtt gtg tgg tca-3' R 5'-aga tgg cca ggt tga gca ggt-3' <i>FokI</i>	G(V) – 282 and 74 A(I) – 198, 84 and 74
<i>CX3CR1</i> 3p21.3	rs3732378 T280M exon 2	F 5'-gga ctg agc gcc cac aca gg-3' R 5'-agg ctg gcc ctc agt gtg act-3' <i>Alw26I</i>	A(M) – 148 G(T) – 128 and 20
<i>SAA1</i> 11p15.1	rs1136743 A70V exon 3	F 5'-ccc ctc taa ggt gtt gtt gga-3' R 5'-ctc cac aag gag ctc gtc tc-3' <i>BshNI</i>	T(V) – 289 C(A) – 183 and 106
<i>CRP</i> 1q23.2	rs1205 2042C>T 3'-untranslated region	F 5'-aga aaa cag ctt gga ctc act ca-3' R 5'-tga gag gac gtg aac ctg gg-3' C 5'-cca gtt tgg ctt ctg tcc tca c-3' T 5'-cca gtt tgg ctt ctg tcc tca t-3'	IC* – 235 Allele – 82

*IC – internal control containing studied mutation

sites. Chemokine CCL2 (monocyte chemoattractant protein-1, MCP-1) and its receptor CCR2 play a central role in monocyte chemotaxis and infiltration of vascular wall as shown in the experiments in mice that demonstrated enhanced expression of CCR2 gene on the surface of monocytes and increased synthesis of CCL2 in hyperlipidemic conditions [2, 3]. Chemokine CX3CL1 (fractalkine) exists in two forms: a membrane-bound form, providing the adhesion of leukocytes to endothelium of blood vessels, and a soluble form acting as chemoattractant [4]. CX3CL1 interacts with CX3CR1 receptor found on the membranes of T-lymphocytes, monocytes, dendritic cells, natural killer cells, and smooth muscle cells, thereby providing their migration, adhesion, and proliferation [5].

C-reactive protein (CRP) and serum amyloid A (SAA) are major acute phase inflammatory proteins. During the first hours of injury, their level increases by 20-100 times, in some cases by 1,000 times and more, which makes these proteins universal markers of acute inflammatory response. It has been demonstrated *in vitro* that CRP is capable of inducing the expression of adhesion molecules and chemokine CCL2 in endothelial cells [6, 7]. SAA also promotes the migration of monocytes and lymphocytes, increasing chemokine expression [8].

The aim of our study was to analyze the contribution of combinations of the polymorphic markers rs1024611 (-2518A>G, *CCL2* gene), rs1799864 (V64I, *CCR2* gene), rs3732378 (T280M, *CX3CR1* gene), rs1136743 (A70V, *SAA1* gene), and rs1205 (2042C>T, *CRP* gene) to the formation of genetic predisposition to CHD.

EXPERIMENTAL

The study group consisted of unrelated male patients ($N = 217$) with verified diagnosis of CHD (165 cases of myocardial infarction, 52 cases of functional class 3–4 cardiac angina) treated in the Medical and Sanitary Unit of PJSC Tatneft in the city of Almetyevsk. Coronary artery atherosclerosis was confirmed by angiography. The average age of patients at enrollment in the study was 53.55 ± 5.78 years. Patients with diabetes and other endocrine disorders were excluded from the study. The control group consisted of unrelated sex- and age-matched (average age 50.48 ± 6.03) individuals ($N = 250$). All members of the control group did not have any signs of cardiovascular disease according to their medical history, clinical examination and electrocardiography. All participants in the study belonged to the Tatar ethnic group. All participants gave their informed consent.

DNA samples were isolated from peripheral blood leukocytes by phenol-chloroform extraction [9]. All polymorphic markers, except for rs1205, were genotyped by polymerase chain reaction (PCR), followed by treatment of the amplification products with the appropriate restriction enzyme. Polymorphic marker rs1205 was genotyped by site-specific PCR. Amplicons were separated by electrophoresis in 7% polyacrylamide or 2% agarose gel. Primers and restriction enzymes specific to each marker were selected using the DNASTAR 5.05 software package and <http://www.ncbi.nlm.nih.gov/snp> database. Primer sequences, restriction enzymes, and the resulting fragment lengths are presented in *Table 1*.

Table 2. Results of the analysis of association between polymorphic DNA markers and the risk of coronary heart disease

Genotype/ Allele	Control, %		Cases, %		P
	n	Frequency (95%CI)	n	Frequency (95%CI)	
<i>CRP</i> rs1205 (2042C>T)					
*C/C	83	33.2 (27.39–39.41)	57	26.27 (20.54–32.65)	0.1065
*C/T	127	50.8 (44.43–57.16)	106	48.85 (42.02–55.71)	0.7108
*T/T	40	16 (11.68–21.14)	54	24.88 (19.28–31.19)	0.0205
*C	293	58.6 (54.14–62.96)	220	50.69 (45.88–55.49)	0.0176
*T	207	41.4 (37.04–45.86)	214	49.31 (44.51–54.12)	
<i>SAA1</i> rs1136743 (A70V)					
*C/C	71	28.4 (22.9–34.42)	48	22.12 (16.78–28.24)	0.1363
*T/C	135	54 (47.61–60.3)	142	65.44 (58.7–71.75)	0.0141
*T/T	44	17.6 (13.09–22.9)	27	12.44 (8.36–17.58)	0.1549
*C	277	55.4 (50.92–59.81)	238	54.84 (50.02–59.59)	0.8951
*T	223	44.6 (40.19–49.08)	196	45.16 (40.41–49.98)	
<i>CX3CR1</i> rs3732378 (T280M)					
*C/C	162	64.8 (58.53–70.71)	141	64.98 (58.23–71.31)	1
*C/T	80	32 (26.26–38.17)	67	30.88 (24.8–37.48)	0.8418
*T/T	8	3.2 (1.39–6.21)	9	4.15 (1.91–7.73)	0.6272
*C	404	80.8 (77.07–84.16)	349	80.41 (76.36–84.05)	0.9339
*T	96	19.2 (15.84–22.93)	85	19.59 (15.95–23.64)	
<i>CCL2</i> rs1024611 (–2518A>G)					
*A/A	151	60.4 (54.04–66.51)	126	58.06 (51.2–64.71)	0.6373
A/G	82	32.8 (27.02–39)	70	32.26 (26.09–38.92)	0.9213
*G/G	17	6.8 (4.01–10.66)	21	9.68 (6.09–14.41)	0.3092
*A	384	76.8 (72.85–80.43)	322	74.19 (69.81–78.25)	0.3605
*G	116	23.2 (19.57–27.15)	112	25.81 (21.75–30.19)	
<i>CCR2</i> rs1799864 (V64I)					
*G/G	181	72.4 (66.41–77.85)	157	72.35 (65.89–78.19)	1
*G/A	61	24.4 (19.21–30.21)	55	25.35 (19.7–31.68)	0.8306
*A/A	8	3.2 (1.39–6.21)	5	2.3 (0.75–5.29)	0.5884
*G	423	84.6 (81.13–87.65)	369	85.02 (81.31–88.25)	0.9272
*A	77	15.4 (12.35–18.87)	65	14.98 (11.75–18.69)	

The frequencies of the genotypes and alleles of polymorphic markers in the study groups were compared using two-tailed Fisher's exact test. Compliance of the observed genotype frequency distribution to the theoretically expected one under Hardy-Weinberg equilibrium was determined using an exact test implemented in the Arlequin 3.0 software. The search for combinations of alleles/genotypes associated with CHD was performed using APSampler 3.6.1 software available here: <https://code.google.com/p/apsampler>. The basic algorithm of this software is described elsewhere [10]. Permutation test was used as correction for multiple-comparisons, and $P_{perm} < 0.05$ was considered statistically significant.

RESULTS AND DISCUSSION

The results of the analysis of the genotype and allele frequency distribution for the studied polymorphic markers are shown in Table 2. The distribution of the genotype frequencies of polymorphic markers in the control group was in agreement with the theoretically expected ones according to the Hardy-Weinberg equilibrium. A comparative analysis of genotype frequency distribution demonstrated that *CRP**T/T ($P = 0.02$, OR = 1.74 95%CI 1.1–2.75) and *SAA1**T/C ($P = 0.014$, OR = 1.61 95%CI 1.11–2.34) genotype frequencies were increased in the group of patients with CHD.

A total of 743 combinations of genotypes and alleles associated with CHD were identified using the APSam-

Table 3. Combinations of the alleles/genotypes associated with a coronary heart disease obtained using the APSampler algorithm

Combination	Frequency, %		P_{perm}	OR	95%CI _{OR}
	Control	Cases			
<i>SAA1</i> *T/T+ <i>CRP</i> *C+ <i>CX3CR1</i> *G/A	6.00	0.46	0.0056	0.07	0.009–0.55
<i>SAA1</i> *T+ <i>CX3CR1</i> *G/A	7.30	0.92	0.0056	0.12	0.03–0.56
<i>SAA1</i> *T+ <i>CRP</i> *T+ <i>CCR2</i> *G/A+ <i>CX3CR1</i> *G	0.40	5.53	0.0063	14.58	1.88–113.04
<i>SAA1</i> *T/C+ <i>CCR2</i> *G+ <i>CCL2</i> *G	19.60	30.41	0.0348	1.79	1.17–2.74
<i>SAA1</i> *T+ <i>CCR2</i> *A+ <i>CCL2</i> *G/G	0.40	4.15	0.0351	10.77	1.35–85.74
<i>SAA1</i> *T+ <i>CRP</i> *T+ <i>CCR2</i> *A+ <i>CX3CR1</i> *A	1.20	5.53	0.039	4.82	1.34–17.31
<i>SAA1</i> *T+ <i>CRP</i> *T/T	12.40	21.20	0.0393	1.9	1.16–3.12
<i>CRP</i> *T/T+ <i>CCR2</i> *A+ <i>CCL2</i> *G	0.80	4.61	0.0425	5.99	1.3–27.65
<i>CRP</i> *T+ <i>CCR2</i> *G/A+ <i>CX3CR1</i> *A	2.40	7.37	0.0436	3.24	1.24–8.43
<i>SAA1</i> *T/T+ <i>CRP</i> *T+ <i>CCL2</i> *A	16.80	10.15	0.049	0.5	0.29–0.89
<i>CRP</i> *C+ <i>CCL2</i> *A	78.40	68.66	0.0492	0.6	0.4–0.92
<i>SAA1</i> *T/T+ <i>CX3CR1</i> *G+ <i>CCL2</i> *A	20.19	9.22	0.0492	0.5	0.29–0.89

pler algorithm; after the validation of the results, five combinations remained associated with a reduced risk of CHD, and seven combinations were associated with an increased risk of CHD (Table 3).

In the current study, we analyzed the frequency distribution of genotypes and alleles of polymorphic markers of *SAA1*, *CRP*, *CCL2*, *CCR2*, and *CX3CR1* genes in the ethnically homogeneous groups of men with CHD and control subjects. Combinations of polymorphic markers associated with the risk of disease development were identified using the APSampler software. It should be noted that while statistically significant results were obtained only for the *SAA1* and *CRP* genes when the studied polymorphic markers were analyzed individually, the identified patterns included all the studied polymorphic markers in various combinations.

Allele *SAA1**T (rs1136743) is present in the combinations associated with both an increased and reduced risk of CHD. As shown by other authors, homozygous carriers of rs1136743*T/rs1136747*C haplotype in a Moscow population of patients with rheumatoid arthritis and patients with Mediterranean fever in Turkey have an increased risk of amyloidosis [11, 12]. As mentioned earlier, SAA stimulates the expression of proinflammatory chemokines [8]. In addition, SAA is capable of replacing apolipoprotein A in high-density lipoproteins (HDL), resulting in a loss of antiatherogenic properties of HDL and its conversion into the proatherogenic form [13]. At the same time, there is evidence of the antiatherogenic effect of SAA. In particular,

SAA inhibits platelet activation and prevents their aggregation at sites of endothelial injury [14]; it has been reported that SAA promotes the removal of HDL from the cell [15].

According to the results of a multicenter study which included patients with myocardial infarction (MI) from six European cities, the carriers of *CRP* rs1205 *T/T genotype have a lower CRP plasma level compared to carriers of the *CRP**C allele [16]. Similar results were obtained for a Reykjavik population [17], European Americans, and African Americans [18]. At the same time, Hatzis G. *et al.* demonstrated the association of *CRP**T/T genotype with an increased risk of coronary atherosclerosis in a Greek population [19], the association of *CRP**T allele with an increased risk of vascular complications in patients with type 2 diabetes was also reported [20]. According to the results of several studies, CRP stimulates the expression of adhesion molecules (VCAM1, ICAM1 and selectin E) [6], *CCL2* chemokine [7], and inhibits the production of nitric oxide [21] in endothelial cells, while no evidence of proatherogenic properties of CRP was obtained from animal models. In *APOE* and *LDLR* knockout mice, the knockout of the *CRP* gene did not lead to a significant reduction in the size of atherosclerotic vascular lesions [22], and the introduction of human CRP in *LDLR*-/- mice had no significant effect [23]. Moreover, there is evidence of antiatherogenic properties for CRP: Lei Z.B. *et al.* demonstrated its ability to bind to oxidized low-density lipoproteins (LDL) [24], which, in turn, up-

regulate the expression of chemokines and adhesion molecules [25–27].

Our data on the role of rs1024611 (*CCL2* gene) and rs1799864 (*CCR2* gene) polymorphic markers in the formation of a genetic predisposition to CHD are consistent with the results of other studies. For example, the association of *CCL2**G allele with ischemic stroke has been demonstrated in the American population [28]. According to a meta-analysis of the results of 21 studies, carriage of *CCL2**G allele is associated with increased risk of CHD among Europeans [29]. The association of *CCR2**G/A genotype with abdominal aortic aneurysm has been shown in the Turkish population [30], while in the Czech Republic the same genotype is a marker of the risk of MI in women under the age of 50 [31]. A number of studies have established a correlation between the *CCL2**G/G genotype and higher plasma levels of CCL2 [32, 33], as well as with increased CCL2 expression compared to *CCL2**A allele carriers [34]. Furthermore, we have found an association of *CCL2**G/G genotype with an increased risk of MI, and an association of *CCL2**G/G+*CCR2**A combination with an increased risk of essential hypertension among the Tatars of Bashkortostan [35, 36].

The role of the rs3732378 (*CX3CR1* gene) polymorphic marker is controversial. McDermott *et al.* demonstrated association between *CX3CR1**M allele and lower rates of cell adhesion and leukocyte chemotax-

is, and decreased risk of CHD [37]. At the same time, *CX3CR1**M allele was found to be associated with type 2 diabetes among European Americans [38]. According to the results of meta-analysis of 49 studies, *CX3CR1**T/M genotype is associated with decreased risk of atherosclerosis and CHD, while *CX3CR1**M/M genotype is associated with increased risk of ischemic cerebrovascular disease [39], which is consistent with our data.

CONCLUSION

In conclusion, it should be noted that our results support the hypothesis of the influence of the *SAA1*, *CRP*, *CCL2*, *CCR2*, and *CX3CR1* gene polymorphisms on the processes that play an important role in CHD pathogenesis. We also demonstrated that allelic variants of the *SAA1* and *CRP* genes can have both a negative and positive effect on the development of the disease depending on the genetic environment, which illustrates the thesis of a complex nonlinear interaction of the studied factors and does not contradict the results obtained in other studies. ●

The study was performed with the equipment provided by USC “Complex equipment for the study of nucleic acids – KODINC” and Biomika (Department of biochemical research methods and nanobiotechnology RTSKP Agidel).

REFERENCES

- Ross R. // *Nature*. 1993. V. 362. P. 801–809.
- Han K.H., Tangirala R.K., Green S.R., Quehenberger O. // *Arteriosclerosis, Thrombosis, and Vascular Biology*. 1998. V. 18. № 12. P. 1983–1991.
- Zhang S., Wang X., Zhang L., Yang X., Pan J., Ren G. // *J. Atherosclerosis Thrombosis*. 2011. V. 18. № 10. P. 846–856.
- Haskell C.A., Cleary M.D., Charo I.F. // *J. Biol. Chem*. 2000. V. 275. № 44. P. 34183–34189.
- White G.E., Greaves D.R. // *Arteriosclerosis, Thrombosis and Vascular Biology*. 2012. V. 32. № 3. P. 589–594.
- Pasceri V., Willerson J.T., Yeh E.T. // *Circulation*. 2000. V. 102. № 18. P. 2165–2168.
- Pasceri V., Cheng J.S., Willerson J.T., Yeh E.T. // *Circulation*. 2011. V. 103. № 21. P. 2531–2534.
- Gouwy M., Buck M., Pörtner N., Opendakker G., Proost P., Struyf S., Damme J. // *Eur. J. Immunol*. 2015. V. 45. № 1. P. 101–112.
- Sambrook J., Fritsch E.F., Maniatis T. *Molecular Cloning*. N.Y.: Cold Spring Harbor Lab. Press, 1989. V. 2. P. 14–9.23.
- Favorov A.V., Andreewski T.V., Sudomoina M.A., Favorova O.O., Parmigiani G., Ochs M.F. // *Genetics*. 2005. V. 171. № 4. P. 2113–2121.
- Myakotkin V.A., Muravyev Yu.V., Alekseyeva A.V., Kadnikova V.A., Polyakov A. V. // *Nauchno-prakticheskaya revmatologiya*. 2012. V. 53. № 4. P. 40–43.
- Yilmaz E., Balci B., Kutlay S., Ozen S., Erturk S., Oner A., Besbas N., Bakkaloglu A. // *Turkish J. Pediatrics*. 2003. V. 45. № 3. P. 198–202.
- van Lenten B.J., Hama S.Y., de Beer F., Stafforini D.M., McIntyre T.M., Prescott S.M., La Du B.N., Fogelman A.M., Navab M. // *J. Clin. Invest*. 1995. V. 96. № 6. P. 2758–2767.
- Zimlichman S., Danon A., Nathan I., Mozes G., Shainkin-Kestenbaum R. // *J. Lab. Clin. Med*. 1990. V. 116. № 2. P. 180–186.
- Stonik J.A., Remaley A.T., Demosky S.J., Neufeld E.B., Bocharov A., Brewer H.B. // *Biochem. Biophys. Res. Commun*. 2004. V. 321. № 4. P. 936–941.
- Kolz M., Koenig W., Müller M., Andreani M., Greven S., Illig T., Khuseynova N., Panagiotakos D., Pershagen G., Salomaa V., et al. // *Eur. Heart J*. 2008. V. 29. № 10. P. 1250–1258.
- Eiriksdottir G., Smith A.V., Aspelund T., Hafsteinsdottir S.H., Olafsdottir E., Launer L.J., Harris T.B., Gudnason V. // *Int. J. Obes*. 2009. V. 33. № 2. P. 267–272.
- Lange L.A., Carlson C.S., Hindorff L.A., Lange E.M., Walston J., Durda J.P., Cushman M., Bis J.C., Zeng D., Lin D., et al. // *JAMA*. 2006. V. 296. № 22. P. 2703–2711.
- Hatzis G., Tousoulis D., Papageorgiou N., Miliou A., Bouras G., Tsioufis C., Sinetos A., Latsios G., Siasos G., Stefanadis C. // *J. Am. Coll. Cardiol*. 2012. V. 59. № 13. P. E1413.
- Papaoikonomou S., Tousoulis D., Tentolouris N., Papageorgiou N., Miliou A., Androulakis E., Antoniadis C., Stefanadis C. // *J. Diabetes Metab*. 2015. V. 6. № 4. P. 529.

21. Hein T. W., Singh U., Vasquez-Vivar J., Devaraj S., Kuo L., Jialal I. // *Atherosclerosis*. 2009. V. 206. № 1. P. 61–68.
22. Teupser D., Weber O., Rao T.N., Sass K., Thiery J., Fehling H.J. // *J. Biol. Chem.* 2011. V. 286. № 8. P. 6272–6279.
23. Torzewski M., Reifenberg K., Cheng F., Wiese E., Küpper I., Crain J., Lackner K.J., Bhakdi S. // *Thromb. Haemost.* 2008. V. 99. № 1. P. 196–201.
24. Tabuchi M., Inoue K., Usui-Kataoka H., Kobayashi K., Teramoto M., Takasugi K., Shikata K., Yamamura M., Ando K., Nishida K., et al. // *J. Lipid Res.* 2007. V. 48. № 4. P. 768–781.
25. Lei Z.B., Zhang Z., Jing Q., Qin Y.W., Pei G., Cao B.Z., Li X.Y. // *Cardiovascular Res.* 2002. V. 53. № 2. P. 524–532.
26. Amberger A., Maczek C., Jürgens G., Michaelis D., Schett G., Trieb K., Eberl T., Jindal S., Xu Q., Wick G. // *Cell Stress Chaperones*. 1997. V. 2. № 2. P. 94–103.
27. Barlic J., Zhang Y., Murphy P.M. // *J. Biol. Chem.* 2007. V. 282. № 26. P. 19167–19176.
28. Arakelyan A., Zakharyan R., Hambardzumyan M., Petrakova J., Olsson M.C., Petrek M., Boyajyan A. // *J. Interferon Cytokine Res.* 2014. V. 34. № 2. P. 100–105.
29. Bai X.Y., Li S., Wang M., Qu X., Hu G., Xu Z., Chen M., He G.-W., Wu H. // *Ann. Hum. Genet.* 2015. V. 79. № 3. P. 173–187.
30. Katrancioğlu N., Manduz S., Karahan O., Yılmaz M. B., Sezgin I., Bağcı G., Berkan O. // *Angiology*. 2011. V. 62. № 2. P. 140–143.
31. Petrakova J., Cermakova Z., Drabek J., Lukl J., Petrek M. // *Immunol. Lett.* 2003. V. 88. № 1. P. 53–55.
32. Zakharyan R., Boyajyan A., Arakelyan A., Melkumova M., Mrazek F., Petrek M. // *Cytokine*. 2012. V. 58. № 3. P. 351–354.
33. McDermott D.H., Yang Q., Kathiresan S., Cupples L.A., Massaro J.M., Keaney J.F., Larson M.G., Vasan R.S., Hirschhorn J.N., O'Donnell C.J., Murphy Ph.M., Benjamin E. J. // *Circulation* 2005. V. 112. № 8. P. 1113–1120.
34. Rovin B.H., Lu L., Saxena R. // *Biochem. Biophys. Res. Commun.* 1999. V. 259. № 2. P. 344–348.
35. Nasibullin T. R., Sadikova R. I., Timasheva Y. R., Tuktarova I. A., Erdman V. V., Khusainova L. N., Nikolaeva I. E., Mustafina O. E. // *Russian Journal of Genetics*. 2014. V. 50. № 2. P. 211–217.
36. Timasheva Y. R., Nasibullin T. R., Tuktarova I. A., Erdman V. V., Nikolaeva I. E., Mustafina O. E. // *Molecular medicine*. 2015. № 3. P. 62–64.
37. McDermott D.H., Fong A.M., Yang Q., Sechler J.M., Cupples L.A., Merrell M.N., Wilson P.W., D'Agostino R.B., O'Donnell C.J., Patel D.D., Murphy P.M. // *J. Clin. Invest.* 2003. V. 111. № 8. P. 1241–1250.
38. Shah R., Hinkle C.C., Ferguson J.F., Mehta N.N., Li M., Qu L., Lu Y., Putt M.E., Ahima R.S., Reilly M.P. // *Diabetes*. 2011. V. 60. № 5. P. 1512–1518.
39. Wu J., Yin R.X., Lin Q.Z., Guo T., Shi G.Y., Sun J.Q., Shen S.W., Li Q. // *Disease Markers*. 2014. V. 2014. P. 1–13.

Cloning and Characterization of a New Site-Specific Methyl-Directed *ElmI* Endonuclease Recognizing and Cleaving C5-methylated DNA Sequence 5'-G(5mC)[^]NG(5mC)-3'

V. A. Chernukhin*, D. A. Gonchar, M. A. Abdurashitov, O. A. Belichenko, V. S. Dedkov, N. A. Mikhnenkova, E. N. Lomakovskaya, S. G. Udal'yeva, S. Kh. Degtyarev

SibEnzyme, Timakova St., 2/12, 630117, Novosibirsk, Russia

*E-mail: valera@sibenzyme.ru

Received August 13, 2015

Copyright © 2016 Park-media, Ltd. This is an open access article distributed under the Creative Commons Attribution License, which permits unrestricted use, distribution, and reproduction in any medium, provided the original work is properly cited.

ABSTRACT Putative open reading frames of MD-endonucleases have been identified in Enterobacteria genomes as a result of the search for amino acid sequences homologous to MD-endonuclease *BisI*. A highly conserved DNA primary structure of these open reading frames in different genera of Enterobacteria (*Escherichia*, *Klebsiella* and *Cronobacter*) has allowed researchers to create primers for PCR screening, which was carried out on Enterobacteria DNA collected from natural sources. The DNA fragment, about 440 bp in length, was amplified by use of the genomic DNA of a wild *E.coli* LM N17 strain as a template and was inserted into the pMTL22 vector. Endonuclease activity was detected in an *E.coli* ER 2267 strain transformed with the obtained construction. A new enzyme named *ElmI* was purified by chromatographic techniques from the recombinant strain biomass. It was discovered that similarly to *BisI* this enzyme specifically cleaves the methylated DNA sequence 5'-GC-NGC-3' before the central nucleotide "N" if this sequence contains two 5-methylcytosines. However, unlike *BisI*, *ElmI* more efficiently cleaves this sequence if more than two cytosine residues are methylated.

KEYWORDS methyl-directed site specific endonuclease, MD-endonuclease, epigenetics, methylome analysis, DNA endonuclease gene cloning.

ABBREVIATIONS u.a. – unite activity of enzyme, MD-endonuclease – methyl-directed site specific endonuclease.

INTRODUCTION

Methyl-directed site specific endonucleases (MD-endonucleases) recognize and cleave DNA at specific methylated sequences, leaving unmethylated DNA untouched. In the last nine years, more than 10 prototypes of these enzymes have been described. They have different recognition sites, which are cleaved only when the cytosine residues within them are C5-methylated.

In contrast to restriction endonucleases, MD-endonucleases recognize not only a specific nucleotide sequence and relative hydrolysis position in this sequence, but also a specific pattern of methylation. Therefore, different MD-endonucleases, even those with similar recognition sites, may cleave DNA differently based on its methylation pattern. Enzymes that recognize the methylated 5'-GCNGC-3' sequence are a great example. Among the enzymes that recognize

this site and cleave DNA after the central nucleotide "N" *BisI* [1] cleaves this sequence if it contains at least two and *PkrI* [2] if it contains at least three 5-methylcytosine residues. Among the enzymes that cleave the sequence before the central nucleotide "N," MD-endonuclease *BisI* [3] cleaves the 5'-GCNGC-3' sequence if it contains two 5-methylcytosine residues (and much less efficiently, if there is only one), whereas *GluI* [4] needs four 5-methylcytosine residues.

We have described a new representative of this group of enzymes, MD-endonuclease *ElmI*, that recognizes the methylated 5'-GCNGC-3' sequence and cleaves it before the central nucleotide "N" (to form 5'-overhanging single-nucleotide ends) if the sequence contains at least two 5-methylcytosine residues; the enzyme activity increases by an order of magnitude if three or four cytosines in the recognition site are methylated.

MATERIALS AND METHODS

PCR screening of Enterobacteria DNA collected from natural sources and production of pElmI plasmid with the new MD-endonuclease gene

Coliform bacteria were isolated from natural sources (sewage water) on a selective Endo medium according to [5]. Eight to twenty strains with different morphological characteristics were collected from each sample inoculation (LM, LT, LP, and LV series).

Chromosomal DNA was isolated from these strains and screened by PCR using the primers listed below. The fragment amplified using DNA from one of the wild-type strains was inserted into the pMTL22 plasmid [6] at the BglII and FauNDI restriction sites.

After transformation of the *E. coli* ER2267 cells, the clones carrying the target plasmid (called pElmI) were plated on Petri dishes with an agarized LB medium supplemented with ampicillin (50 µg/ml). The clones were grown overnight at 37°C, subcultured to separate dishes with ampicillin (100 µg/ml), and allowed to grow overnight for further analysis.

Production of biomass of the recombinant ElmI producer strain and assay of the target activity

The recombinant clone of the *E. coli* ER2267 strain, which was transformed with pElmI plasmid, was transferred from Petri dishes to a bottle with 200 ml of a LB broth supplemented with ampicillin (100 µg/ml) using an inoculation loop. The inoculum was grown overnight using a thermostatted shaker (37°C, 120 rpm).

5 ml of inoculum were seeded into 20 bottles with 200 ml LB broth supplemented with ampicillin (100 µg/ml) and 0.5 mM isopropyl-β-D-thiogalactopyranoside (IPTG).

The culture was grown for 10 hours in a thermostatic shaker (120 rpm), and then an aliquot (1 ml) for the enzyme activity assay was withdrawn and transferred to a 1.5 ml Eppendorf tube. The cells were pelleted using a 5416 Eppendorf tabletop centrifuge (Eppendorf GmbH, Germany, 12,000 rpm, 2 min). The supernatant was removed, and the precipitate was resuspended in 0.2 ml of a lysis buffer (10 mM Tris-HCl, pH 8.5, 0.1 mg/ml lysozyme, 0.5 M NaCl, 1 mM EDTA, 0.1% Triton X-100).

The activity of the enzyme in the lysate was assayed in 20 µl of the reaction mixture, which contained pFsp4HI3 plasmid, pre-linearized with DriI restriction enzyme, as a DNA substrate [4]. The linearization was performed in a SE buffer "W" (10 mM Tris-HCl (pH 8.5 at 25°C), 10 mM MgCl₂, 100 mM NaCl, 1 mM dithiothreitol) for 2 hours at 37°C. The amount of ElmI enzyme sufficient for complete hydrolysis of 1 µg of pFsp4HI3 DNA (2 hours, 37°C, SE buffer "W") was taken as 1 unit

activity of the enzyme. The presence or absence of hydrolysis of the DNA substrate was determined by electrophoresis in 1% agarose gel.

The cells of all of the produced biomass were pelleted using a J2-21 centrifuge (30 min, 8,000 rpm, JA-10 rotor, Beckman, USA) and frozen.

Production of ElmI enzyme preparation

All procedures for isolation and purification of the enzyme preparation were performed at 4°C using the following solutions:

- Buffer A: 10 mM Tris-HCl, pH 7.5; 0.1 mM EDTA; 7 mM 2-mercaptoethanol;
- Buffer B: 10 mM K-phosphate buffer, pH 7.4; 0.1 mM EDTA; 7 mM 2-mercaptoethanol.

pFsp4HI3 in the SE buffer "W," digested for 15 min in 20 µl of the reaction mixture by adding aliquots (1 µl) of chromatographic fractions, was used as the DNA substrate [4] to determine the activity of the enzyme.

Isolation of the crude extract. The biomass (8 g) was suspended in 30 ml of buffer A containing 0.2 M NaCl, 1 mM phenylmethylsulfonyl fluoride (PMSF), 0.1% Triton X-100; and 0.1 mg /mL lysozyme. The cells were disrupted by sonication on a Soniprep 150 sonicator (MSE, UK, 2 cm adapter, amplitude of 20 µm), using four 1-minute periods followed by 1-minute intervals to cool the suspension in an ice bath.

Cell debris was removed by centrifugation at 15,000 rpm for 30 min (JA-20 rotor, J2-21 centrifuge, Beckman, USA).

Chromatography on phosphocellulose P-11. The crude extract was diluted twofold with buffer A and applied to a column with phosphocellulose P-11 (30 ml), pre-equilibrated with buffer A containing 0.1 M NaCl, and washed with 160 mL of the same buffer. The adsorbed material was eluted using a linear gradient of NaCl (0.1 to 1 M) in buffer A (total volume of 800 ml); 30 fractions were collected, and fractions 16 to 22 (0.35 to 0.47 M NaCl) exhibiting target activity were pooled together.

Chromatography on hydroxylapatite. The pooled fractions were applied to a column with hydroxylapatite (2 ml), pre-equilibrated with buffer B containing 0.05 M NaCl, and washed with 10 ml of the same buffer. The adsorbed material was eluted using a linear gradient of K-phosphate buffer (pH 7.4) containing 0.05 M NaCl (0.01 to 0.1 M, total volume of 30 ml). A gradient of 20 fractions was collected, and fractions 8 to 12 (0.044 to 0.056 M K-phosphate) exhibiting ElmI activity were pooled together. The pooled fractions were dialyzed for 1 h against 300 ml of buffer A.

Chromatography on heparin-agarose. The dialyzed fractions were applied to a column with heparin-agarose (2 ml), pre-equilibrated with buffer B containing 0.05 M NaCl, and washed with 4 ml of the same buffer. The adsorbed material was eluted using a linear gradient of NaCl (0.05 to 1 M) in buffer B (a total volume of 30 ml); 20 fractions were collected, and fractions 12 and 13 (0.62 to 0.67 M NaCl) exhibiting the target activity were pooled together.

Concentration, activity assays and storage. The pooled fractions were dialyzed for 20 hours against a 15-fold volume of buffer B with 50% glycerol and 0.2 M NaCl, and stored at -20°C.

The activity was assayed by adding eight consecutive two-fold dilutions of the enzyme preparation (2, 1, ½ µl, etc.) to 20 µl of the reaction mixture containing 0.5 µg of pFsp4HI3/DriI DNA in the SE buffer “W,” followed by 2 h incubation at 37°C. The SE buffer for enzyme dilution “B100” (10 mM Tris-HCl (pH 7.6 at 25°C), 50 mM KCl, 0.1 mM EDTA, 200 µg/ml BSA, 1 mM dithiothreitol, 50% glycerol) was used to dilute enzyme preparations. The reaction was stopped by adding 1 µl of a stop buffer (50% glycerol, 10 mM EDTA, 0.2% bromophenol blue) to each reaction mixture.

Sanger sequencing was used to **determine the DNA sequence** on a ABI 3130xI Genetic Analyzer automatic sequencer (Applied Biosystems, USA) according to the manufacturer’s instructions.

Preparations of enzymes, DNA, deoxynucleoside triphosphates, and synthetic oligonucleotides, as well as the molecular weight markers (1 kb Ladder and Lambda/StyI) used in this work, were produced by SibEnzyme (Russia).

RESULTS AND DISCUSSION

Cloning of the new MD-endonuclease *ElmI* gene and comparative analysis of nucleotide and amino acid sequences

Previously, we found MD-endonucleases in bacteria from different taxonomic groups, but mostly in representatives of the Microbacteriaceae and Bacillaceae families. The earlier screening of cell lysates did not allow us to identify similar site-specific enzymes in Enterobacteriaceae strains, which may indicate either the absence or the extremely low activity of MD-endonucleases in this group of bacteria. To resolve this issue, we decided to use bioinformatic rather than the biochemical method to search for homologous enterobacterial proteins.

The PSI-BLAST (<https://blast.ncbi.nlm.nih.gov>) software was used to screen the database of Enterobacteriaceae amino acid sequences for sequences homolo-

gous to the previously described MD-endonuclease *BisI* (GenBank AJW87312) [7]. Two search iterations revealed ~50 enterobacterial amino acid sequences which were homologous to the *BisI* sequence (32–48% similarity, 17–30% identity). The roles of all these homologous proteins have been unknown. The nucleotide sequences of the corresponding genes were extracted from the GenBank database and compared to each other. It has been shown that the sample contains two groups of highly homologous genes. The first group includes genes of four putative proteins with a length of 143–144 amino acid residues from the bacteria of genera *Escherichia* (GenBank accession numbers ACT43858 and AKN48098), *Cronobacter* (CCJ93299), and *Klebsiella* (KEG36084). A comparison of these genes to each other revealed a 93–99% identity. The second group contained enterobacterial genes which encode proteins with a length of 290 amino acid residues, whose N-terminal portion is homologous to the *BisI* protein (GenBank protein accession numbers: KFC97828, WP_000794335, WP_000794336, WP_000794337, WP_001655794, WP_004952390, WP_008806407, WP_021557167, WP_025912430, WP_032653240, WP_032671961, and WP_033070923). The degree of nucleotide sequence identity in this group is 83–99%.

Figure 1 shows multiple alignment of the amino acid sequences of the four highly homologous enterobacterial proteins from the first group, which have a *BisI* sequence. The sequence of endonuclease *ElmI*, which was detected by PCR screening, is also shown (see the description below).

Multiple alignment of the corresponding enterobacterial genes (*Fig. 2*) revealed that their nucleotide compositions also have a high degree of identity, even though the host organisms belong to different genera. The sequence of the *elmI* gene, established in this work, is added to the alignment.

The high degree of sequence identity for the genes from the two aforementioned groups, which holds true for their end sites, allowed us to select primers for PCR screening of wild-type strains for the presence of similar genes. To search for genes encoding proteins related to the first group of proteins, we used primers containing the recognition sites of *FauNDI* and *BamHI* restriction endonucleases for inserting PCR fragments into a plasmid vector:

Esp-1 5'-CCCCCATATGAGTGCACGT-GAAGCATATC-3'

Esp-2 5'-CGCGGATCCTTAGGGATTACACT-GACTGAAACTCTTC-3'

For PCR screening for genes similar to the second group of genes, the following primers were synthesized:

Esp-3 - 5'-TTGAAAATAATCATTTAACAT-CATATG-3'

		1		50
Bisl	(1)	MTVSLK	LDDELE	TLLYSS
ACT43858	(1)	MSAREAYRQYREAVTACKDI		FARGGNVTGDYGEHLVKQLYGG
AKN48098	(1)	MSAREAYRQYREAVTACKDI		FARGGNVTGDYGEHLVKQLYGG
KEG36084	(1)	MSAREAYRQYREAVTACKGI		FARGGNVTGDYGEHLVKQLYGG
CCJ93299	(1)	MHVKHIGSIEKRWLLAKAF		FARGGNVTGDYGEHLVKQLYGG
Elml	(1)	MSAREAYRQYREAVTACKDI		FARGGNVTGDYGEHLVKQLYGG
		51		100
Bisl	(51)	TKGLPKLQAAPTGTQNI	DALS	IKGDRYS
ACT43858	(43)	ELLPN	SHKSAD	VRLDDG
AKN48098	(43)	ELLPN	SHKSAD	VRLDDG
KEG36084	(43)	ELLPN	SHKSAD	VRLDGD
CCJ93299	(42)	ELLPN	SHKSAD	VRLSDG
Elml	(43)	ESL	PN	SHKSAD
		101		150
Bisl	(101)	PDIQK	FEYV	TI
ACT43858	(76)	IRSWDE	DYLI	GIQL
AKN48098	(76)	IRSWDE	DYLI	GIQL
KEG36084	(76)	IRSWDE	DYLI	GIQL
CCJ93299	(75)	IRSWDE	DYLI	GIQL
Elml	(76)	IRSWDE	DYLI	GIQL
		151		170
Bisl	(151)	AM	SDSE	IF
ACT43858	(126)	VIL	KTPG	VENV
AKN48098	(126)	VIL	KTPG	VENV
KEG36084	(126)	VIL	KTPG	VENV
CCJ93299	(125)	VIL	KTPG	VENV
Elml	(126)	VIL	KTPG	VENV

Fig. 1. Alignment of the amino acid sequences of Bisl and Elml with the most homologous proteins from enterobacteria. The designations of amino acid sequences correspond to GenBank numbers, as described in the text. Amino acids that are identical in all presented protein sequences are shown in white on a black background. Amino acids with similar physical and chemical properties are shown in black on a gray background.

Esp-4 – 5'-TCACTCCAGAACGCTGATA-AGTTT-3'.

Genomic DNA was isolated from 64 strains of coliforms bacteria detected in sewage waters and used as a template for PCR. Amplification with the Esp-3 and Esp-4 primers (the second group of genes) did not result in a fragment of the expected length (~870 bp) in any of the matrix DNA. The use of the Esp-1 and Esp-2 primers (the first group of genes) resulted in a PCR fragment of the expected length (~430 bp) in one DNA sample.

This amplified fragment was treated with the BamHI and FauNDI restriction enzymes and ligated into the pMTL22 vector, which had been previously digested with FauNDI and BglII. The resulting plasmid, named pElmI, was used to transform the *E. coli* ER2267 cells.

Taxonomic specificity of the original strain whose genomic DNA was amplified to obtain the fragment was determined using conventional biochemical and morphological criteria [8], and by analyzing the structure of the 16S rRNA fragment by BLAST [9]. The original natural producing strain was identified as *E.*

coli LM N17. The site-specific DNA endonuclease produced by the strain was named ElmI.

The PCR fragment inserted in the pElmI plasmid was sequenced. The nucleotide sequence of the fragment, 432 bp in length, was deposited in the GenBank with accession number LN869919. The sequence begins with a ATG start codon and ends with a TAA stop codon (the hypothetical reading frame has no other stop codons), and, therefore, it can be considered as an hypothetical reading frame of DNA endonuclease ElmI, and the gene encoding this protein, as *elmI*.

A comparative analysis of the sequenced fragment of the gene shows that *elmI* has essentially the same sequence as the genes encoding polypeptides of the closest homologues: *E. coli* strains BL21 (DE3) (ACT43858) and C41 (DE3) (AKN48098). The only identified substitution was the presence of cytosine at position 131 of the *elmI* gene instead of thymine in the homologous genes (Fig. 2).

Therefore, the derived amino acid sequence of ElmI endonuclease differs from the closest homologues

<i>elml</i>	(1)	<u>ATGAGTGCACGTGAAGCATATC</u> GGCAGTATCGAGAAGCGGTGACTGCTTGCAAAG
ACT43858	(1)	<u>ATGAGTGCACGTGAAGCATATC</u> GGCAGTATCGAGAAGCGGTGACTGCTTGCAAAG
KEG36084	(1)	<u>ATGAGTGCACGTGAAGCATATC</u> GGCAGTATCGAGAAGCGGTGACTGCTTGCAAGG
AKN48098	(1)	<u>ATGAGTGCACGTGAAGCATATC</u> GGCAGTATCGAGAAGCGGTGACTGCTTGCAAGG
CCJ93299	(1)	----GTGCACGTGAAGCATATCGGCAGTATCGAGAAGCGGTG <u>CT</u> GCTTGCAAAG
<i>elml</i>	(56)	<u>ACATTTTT</u> -GCCCCAGGTGGTAATGTCACTGGTGATTACGGTGAACATCTCGTAA
ACT43858	(56)	<u>ACATTTTT</u> -GCCCCAGGTGGTAATGTCACTGGTGATTACGGTGAACATCTCGTAA
KEG36084	(56)	<u>GCATTTTT</u> -GCCCCAGGTGGTAATGTCACTGGTGATTATGGTGAACATCTCGTAA
AKN48098	(56)	<u>GCATTTTT</u> -GCCCCAGGTGGTAATGTCACTGGTGATTATGGTGAACATCTCGTAA
CCJ93299	(52)	<u>GCATTTTTTT</u> GCCCCAGGTGGTAATGTCACTGGTGATTATGGTGAACATCTCGTAA
<i>elml</i>	(110)	AGCAACTTTTATGGTGGTGAAT <u>C</u> ATTGCCAAACTCCCATAAAAAGCGCCGATGT <u>CAG</u>
ACT43858	(110)	AGCAACTTTTATGGTGGTGAAT <u>T</u> ATTGCCAAACTCCCATAAAAAGCGCCGATGT <u>CAG</u>
KEG36084	(110)	AGCAACTTTTATGGCGGTGAAT <u>T</u> ATTGCCAAACTCCCATAAAAAGCGCCGATGT <u>TAAG</u>
AKN48098	(110)	AGCAACTTTTATGGCGGTGAAT <u>T</u> ATTGCCAAACTCCCATAAAAAGCGCCGATGT <u>TAAG</u>
CCJ93299	(107)	AGCAACTTTTATGGGGGTGAAT <u>T</u> ATTGCCAAACTCCCATAAAAAGCGCCGATGT <u>TAAG</u>
<i>elml</i>	(165)	ATTAG <u>AC</u> GATGGCAGCTGTTGCAGGTCAAACCAGAGTCAATAAAAACCCAGTTA
ACT43858	(165)	ATTAG <u>AC</u> GATGGCAGCTGTTGCAGGTCAAACCAGAGTCAATAAAAACCCAGTTA
KEG36084	(165)	ATTAGGCGATGGCAGCT <u>ATT</u> GCAGGTCAAACCAGAGTCAATAAAAACCCAGTTA
AKN48098	(165)	ATTAGGCGATGGCAGCT <u>ATT</u> GCAGGTCAAACCAGAGTCAATAAAAACCCAGTTG
CCJ93299	(162)	ATTA <u>AG</u> CGATGGGACGCTGTTGCAGGTCAAACCAGAGTCAATAAAAACCCAGTTA
<i>elml</i>	(220)	GGCGGAATTCGCTCCTGGGATTTTCGATTACCTGATCGGT <u>T</u> ATT <u>CAGCTTAATGACG</u>
ACT43858	(220)	GGCGGAATTCGCTCCTGGGATTTTCGATTACCTGATCGGT <u>T</u> ATT <u>CAGCTTAATGACG</u>
KEG36084	(220)	GGCGGAATTCGCTCCTGGGATTTTCGATTACCTGATCGGT <u>T</u> ATT <u>CAGCTTAATGACG</u>
AKN48098	(220)	GGCGGAATTCGCTCCTGGGATTTTCGATTACCTGATCGGT <u>T</u> ATT <u>CAGCTTAATGACG</u>
CCJ93299	(217)	GGCGGAATTCGCTCCTGGGATTTTCGATTACCTGATCGG <u>C</u> ATT <u>CAGCTTAATGAAG</u>
<i>elml</i>	(275)	ATGCCGAAGT <u>CATGTT</u> GGCAGTTCGTGTCCCTGTAGATGTTTGTGCGCCAAATTGC
ACT43858	(275)	ATGCCGAAGT <u>CATGTT</u> GGCAGTTCGTGTCCCTGTAGATGTTTGTGCGCCAAATTGC
KEG36084	(275)	ATGCCGAAGT <u>CATGTT</u> GGCAGTTCGTGTCCCTGTAGATGTTTGTGCGCCAAATTGC
AKN48098	(275)	ATGCCGAAGT <u>CATGTT</u> GGCAGTTCGTGTCCCTGTAGATGTTTGTGCGCCAAATTGC
CCJ93299	(272)	ATGCCGAAGT <u>AGTGAT</u> GGCAGTTCGTGTCCCTGT <u>GGT</u> ATTTGTGCGCCAAATTGC
<i>elml</i>	(330)	CGGATATGCCAGCCATGATAACAAATTTGTGATCCATCTTAATGGCGTGCTTCTT
ACT43858	(330)	CGGATATGCCAGCCATGATAACAAATTTGTGATCCATCTTAATGGCGTGCTTCTT
KEG36084	(330)	CGGATATGCCAGCCATGATAACAAATTTGTGATCCATCTTAATGGCGTGCTTCTT
AKN48098	(330)	CGGATATGCCAGCCATGATAACAAATTTGTGATCCATCTTAATAGCGTGCTTCTT
CCJ93299	(327)	CGGATATGCCAGCC <u>C</u> GATAACAAATTTGTGAT <u>TC</u> ATCTCAATGGCGTGCTTCTT
<i>elml</i>	(385)	AAAACGCCTGGCGTAGAAAACGTCAC <u>TGAAGAGTTTCAGTCAGTGTAATCCCTAA</u>
ACT43858	(385)	AAAACGCCTGGCGTAGAAAACGTCAC <u>TGAAGAGTTTCAGTCAGTGTAATCCCTAA</u>
KEG36084	(385)	AAAACGCCTGGCGTAGAAAACGTCAC <u>TGAAGAGTTTCAGTCAGTGTA</u> -----
AKN48098	(385)	AAAACGCCTGGCGTAGAAAACGTCAC <u>TGAAGAGTTTCAGTCAGTGTA</u> -----
CCJ93299	(382)	AAAACGCCTGGCGTAGAAAACGTCAC <u>TGAAGAGTTTC</u> -GTCAATGTAATCCTTAA

Fig. 2. Alignment of the nucleotide sequence of the putative gene encoding Elml (*elml* gene) with the most homologous DNA sequences. Nucleotide sequences are identified by GenBank accession numbers for the corresponding encoded proteins. Nucleotides identical for most, but not for all, of the analyzed sequences of 5 genes are shown on a gray background. Nucleotides that are not found in the majority of the sequences are shown in italics and underlined. The single nucleotide by which the *elml* gene differs from the nearest homologues from *Escherichia coli* BL21(DE3) and C41(DE3) is indicated by a frame. The sequences on the 5' and 3' ends corresponding to the primers by which the PCR screening for isolation of coliform bacteria genomic DNA from natural sources was performed are indicated by frames as well.

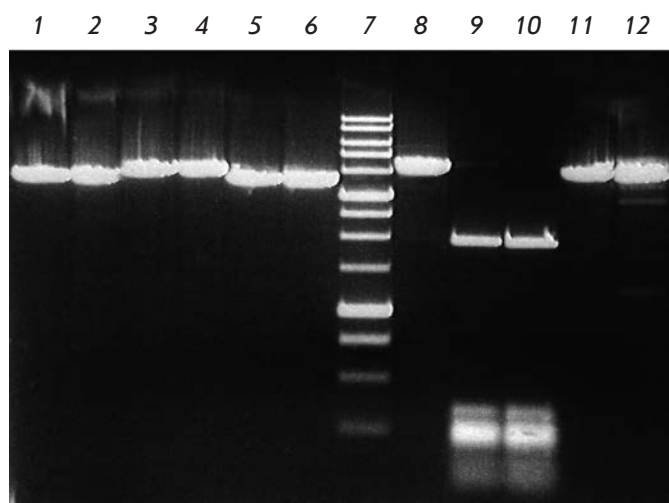


Fig. 3. ElmI site-specificity analysis with various C5-methylated DNA substrates. Electrophoresis in 1% agarose gel. Lanes: 1 – pMHpaII/Dril; 2 – pMHpaII/Dril + ElmI; 3 – pHspAI2/Dril; 4 – HspAI2/Dril + ElmI; 5 – pMHaeIII/Dril; 6 – pMHaeIII/Dril + ElmI; 7 – DNA molecular weight marker 1 kb; 8 – pFsp4HI3/Dril; 9 – pFsp4HI3/Dril + ElmI; 10 – pFsp4HI3/Dril + BisI. 11 – pHspAI4; 12 – pHspAI4 + ElmI.

from the *E. coli* strains BL21 (DE3) and C41 (DE3) by one amino acid residue: ElmI has serine at position 44, whereas the closest homologues (*E. coli* BL21 (DE3) and C41 (DE3)) have leucine at the same position (Fig. 1). At the same time, the amino acid sequence similarity between ElmI and BisI is ~50%, and the number of identical amino acids is 112%. Therefore, the cloned DNA fragment that was identified by PCR screening and represented by a putative gene of methyl-directed ElmI DNA endonuclease is highly homologous to portions of genomic DNA from well-known *E. coli* strains.

Determination of the new ElmI MD-endonuclease specificity

In contrast to the parental strain, the lysate of *E. coli* ER2267 clones carrying pElmI plasmid exhibited endonuclease activity and one of the *E. coli* pElmI clones was chosen for production of biomass and isolation of the enzyme.

A total of 8 g of *E. coli* pElmI biomass were produced as described in the Materials and Methods section. Chromatographic purification of the biomass resulted in 3 ml of the ElmI enzyme preparation with a concentration of 4 u.a./ μ l.

Various substrate DNAs were digested in pre-established optimum conditions (37°C, SE reaction buffer “W”, 20 μ l of the reaction mixture containing 0.5 μ g of substrate DNA, 2h) in order to determine the site-specificity of ElmI. DNA was cleaved by the BisI con-

trol enzyme under the same conditions, but using the SE reaction buffer “Y.”

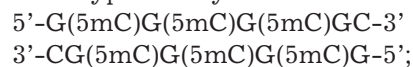
DNA of plasmids carrying genes of different DNA methyltransferases was used as substrates to determine the specificity of the ElmI enzyme. The activity of these genes in *E. coli* strains, from which the plasmids were isolated, resulted in modification of DNA substrates by the corresponding DNA methyltransferases, and, therefore, they had distinctive patterns of methylation.

The following plasmids were used as methylated DNA substrates:

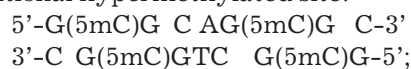
1) pMHpaII plasmid carrying the gene encoding DNA methyltransferase HpaII, which methylates the first cytosine residues in all 5'-CCGG-3' sequences in both strands of DNA [10];

2) pMHaeIII plasmid carrying the gene encoding DNA methyltransferase HaeIII, which methylates the first cytosine residues in all 5'-GGCC-3' sequences in both strands of DNA [11];

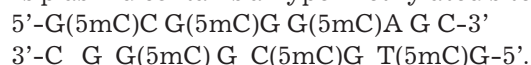
3) pHspAI2 plasmid carrying the gene encoding DNA methyltransferase HspAI, which methylates the first cytosine residues in all 5'-GCGC-3' sequences in both strands of DNA [12]. This plasmid contains an additional hypermethylated site:



4) pHspAI4 plasmid also carrying the gene encoding DNA methyltransferase HspAI, which methylates the first cytosine residues in all 5'-GCGC-3' sequences in both strands of DNA [12]. This plasmid contains an additional hypermethylated site:



5) pFsp4HI3 plasmid carrying the gene encoding DNA methyltransferase Fsp4HI, which methylates the first cytosine residues in all 5'-GCNGC-3' sequences [4]. This plasmid contains a hypermethylated site:



All plasmids were pre-linearized by DriI restriction endonuclease at the 5'-GACNNNNGTC-3' site (unique to each plasmid).

The results of the site-specificity analysis of the DNA substrates are shown in Fig. 3.

As can be seen from Fig. 3, ElmI does not cleave sequences methylated by DNA methyltransferases HpaII (lane 2), HspAI2 (lane 4), and HaeIII (lane 6), and, therefore, ElmI does not recognize the 5'-C(5mC)GG-3'/3'-GG(5mC)C-5', 5'-G(5mC)GC-3'/3'-CG(5mC)G-5', and 5'-GG(5mC)C-3'/3'-C(5mC)GG-5' sequences.

Figure 3 also shows that ElmI cleaves pFsp4HI3/DriI DNA (lane 9), producing DNA fragments of the same length as those from the treatment of the same

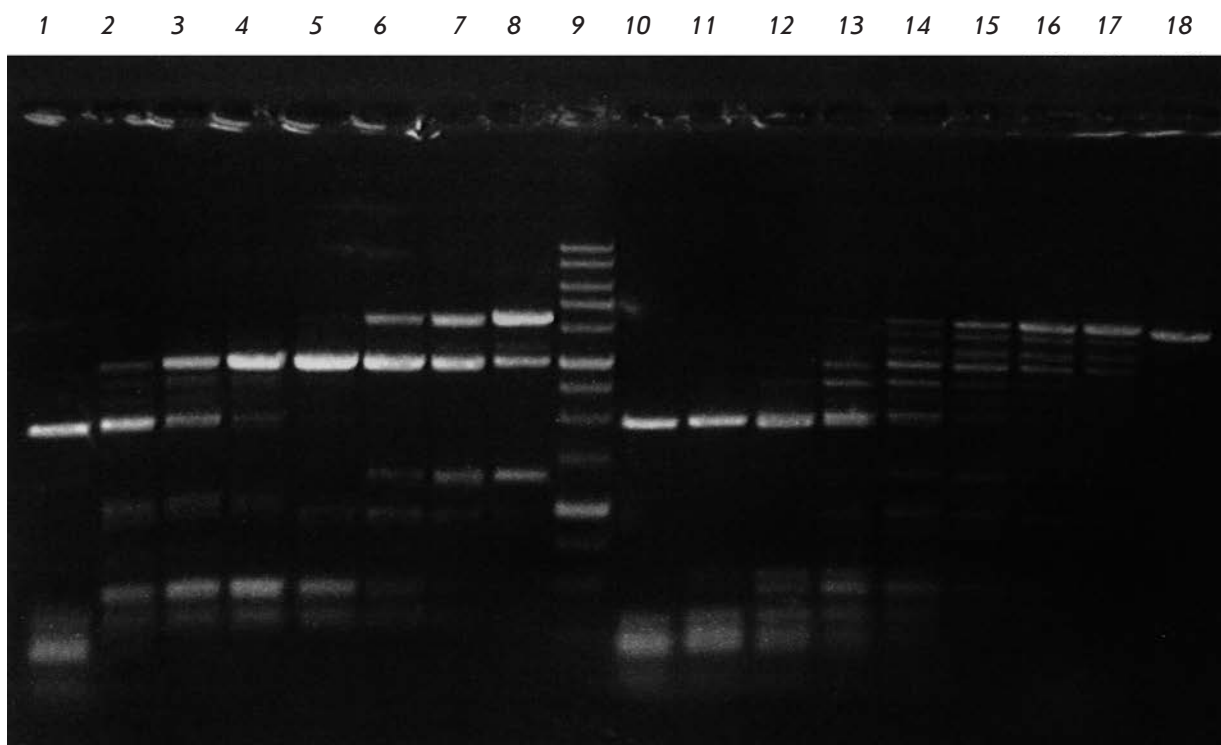


Fig. 4. Incomplete cleavage of pFsp4HI3/Dril showing higher ElmI activity in 5'-GCNGC-3' sequences with three or four 5-methylcytosines, compared with 5'-GCNGC-3' sequences with only two 5-methylcytosines that BisI cuts preferably. Electrophoresis in 1% agarose gel. Lanes: 1-8, pFsp4HI3/Dril, treated with serial 2-fold dilutions of ElmI (initial amount, added to the initial reaction mixture is 1 u.a.); 9, DNA molecular weight marker 1 kb; 10-17, pFsp4HI3/Dril, treated with serial 2-fold dilutions of BisI (initial amount, added to the reaction mixture is 1 u.a.); 18, pFsp4HI3/Dril.

substrate with BisI (lane 10). Since all first cytosines residues in the 5'-GCNGC-3' sequences of this plasmid are C5-methylated [4], and they are all digested by BisI MD-endonuclease, this suggests that ElmI recognizes and cleaves the same methylated sites. It is also important to point out that ElmI is substantially less efficient in cleaving pHspAI4 plasmid, forming two weak fragments (lane 12). This is attributed to the fact that in contrast to pFsp4HI3 plasmid, the hypermethylated portion of pHspAI4 plasmid (see above) includes the unique 5'-GCNGC-3' sequence in which the external (second), rather than the internal (first), cytosines in both strands are methylated.

The data obtained indicate that ElmI recognizes and cleaves the methylated 5'-GCNGC-3' sequence containing two 5-methylcytosine residues and is an order of magnitude more efficient if two internal, rather than external, cytosine residues in both strands are methylated.

In order to establish how effectively ElmI cleaves a 5'-GCNGC-3' sequence with a higher number of 5-methylcytosine residues, pFsp4HI3/Dril was treated with ElmI in an amount insufficient for complete hydrolysis and the result was compared with the result of its cleavage by BisI endonuclease (Fig. 4).

pFsp4HI3 plasmid contains two 5'-GCNGCNGC-3' and one 5'-GCNGCNGCNGC-3' sequences, which include, respectively, two and three intersecting Fsp4HI methylase recognition sites. Methylation of these sequences by Fsp4HIL methylase leads to a 5'-GCNGC-3' sequence with three 5-methylcytosines or, in the case of 5'-GCNGCNGCNGC-3', in a central 5'-GCNGC-3' site containing four such residues. Analysis of the nucleotide sequence of pFsp4HI3 plasmid using the Vector NTI Suite 7 software shows that the cleavage of pFsp4HI3/Dril at these sequences only, as well as at the recognition site of Dril endonuclease, which was used to linearize the plasmid, should result in fragments of ~ 3000, ~ 490 (double fragment), and ~ 340 bp in size. Figure 4 shows that these fragments are easily visualized for 2-6 dilutions of ElmI (lanes 2-5). Even the last enzyme dilution (lane 8) contains a fragment ~1300 bp in length, which should form by cleavage of the unique hypermethylated 5'-GCNGCNGCNGC-3' sequence, containing, among others, the 5'-GCNGC-3' site with four 5-methylcytosine residues.

These fragments are much less visible in the case of BisI. Even though the hydrolysis of pFsp4HI3/Dril plasmid by 2-4 dilutions is much more complete com-

pared to ElmI, the last (eighth) dilution of BisI hardly contains any ~1,300 bp fragment (Lane 17).

These data suggest that, in contrast to BisI, the new ElmI MD-endonuclease is an order of magnitude more efficient in cleaving the 5'-GCNGC-3' sequence in the presence of three or four 5-methylcytosine residues than in the presence of only two methylated residues. Therefore, the original DNA is completely absent after digestion with 1/16 u.a. of ElmI (lane 5) due to a more efficient cleavage of 5'-GCNGC-3' with three or four 5-methylcytosine residues. In contrast, BisI cleaves such hypermethylated variants less efficiently: therefore, the original DNA fragment remains visible if 1/16 u.a. is used (lane 14).

Determination of the position of the hydrolizable linkage in the ElmI recognition site

The position of the hydrolizable linkage was determined by comparing the lengths of the fragments generated during the cleavage of the oligonucleotide D1/D2 duplex, formed from oligonucleotides D1 and D2, using ElmI, PkrI, and GluI MD-endonucleases (the latter also recognizes the 5'-GCNGC-3' methylated sequence [4] and cleaves it similarly to BisI before the central nucleotide. The putative sequence recognized by ElmI is underlined):

D1: 5'-GAGTTTAG(5mC)GG(5mC)TATCGATCC-3'

D2: 5'-G G A T C G A T A G (5mC) C G (m5) C T A - A A C T C - 3'.

Figure 5 shows a autoradiograph of the electropherograms of the cleavage products of the radiolabelled D1*/D2 duplex in 20% polyacrylamide gel with 7M urea.

As can be seen from Fig. 5, the fragments derived from the hydrolysis of the D1*/D2 duplex with PkrI and ElmI (lanes 2 and 3, respectively) have different electrophoretic mobilities, indicating that these enzymes have different positions of hydrolizable linkage relative to the recognition site. At the same time, the electrophoretic mobilities of DNA fragments produced by ElmI and GluI are identical (lanes 3 and 4, respectively). Therefore, ElmI and GluI have the same position of hydrolizable linkage relative to the recognized 5'-GCNGC-3' sequence. Since GluI cleaves the 5'-GCNGC-3' sequence before the central nucleotide "N" [4], ElmI also cleaves it before the central nucleotide.

CONCLUSION

Thus, the first identified recombinant enterobacterial MD-endonuclease ElmI recognizes the 5'-GCNGC-3' nucleotide sequence and cleaves both strands of DNA before the central nucleotide "N," producing 5'-overhanging single-nucleotide ends.

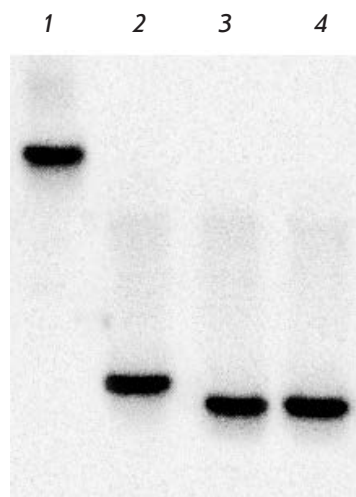


Fig. 5. Cleavage position determination for ElmI on the oligonucleotide duplexes D1/D2. The symbol "*" denotes the labeled chain. Electrophoresis in 20% polyacrylamide gel with 7M urea. Lanes: 1, D1*/D2; 2, D1*/D2 + PkrI; 3, D1*/D2 + ElmI; 4, D1*/D2 + GluI.

Our results indicate that enterobacterial genomes contain genes for MD-endonucleases whose amino acid sequences have only moderate homology to BisI and that only half of the amino acid residues may be regarded as similar in physical and chemical properties. Nevertheless, despite the only moderate homology of the primary structure BisI and ElmI have similar recognition sites and positions of hydrolizable linkages.

The use of the Esp-1 and Esp-2 primers and a laboratory *E. coli* BL21 (DE3) (ACT43858) strain results in amplification of an ~ 430 bp DNA fragment which is highly homologous to the *elmI* gene. According to GenBank, this fragment represents a reading frame that encodes a polypeptide of unknown function: Enterobact1 - WP_001276099.1 hypothetical protein Enterobact1 - WP_001276099.1 hypothetical protein [*Escherichia coli*] >ref|YP_003035796.1| hypothetical protein ECBD_1551 [*Escherichia coli* 'BL21]. However, according to our data, this reading frame is a gene encoding a methyl-directed DNA endonuclease. We have denoted the gene corresponding to this frame as *ecoBLI*, and the encoded protein as EcoBLI. Its properties will be discussed in a separate publication.

The site-specific ElmI endonuclease can be used in epigenetic studies, molecular biology, and genetic engineering for site-specific cleavage of methylated DNA: e.g., for the analysis of genomic DNA methylation in plants [13], where CNG-methylation is considered to be epigenetically important. ●

This work was financially supported by the Ministry of Education and Science of the Russian Federation according to Agreement № 14.576.21.0075 of 06.11.2014 (unique identifier RFMEFI57614X0075), signed within the framework of the Federal Target Program Research and development in priority areas of development of scientific-technological complex of the Russian Federation for the years 2014–2020.

REFERENCES

1. Chernukhin V.A., Tomilova Yu.E., Chmuzh E.V., Sokolova O.O., Dedkov V.S., Degtyarev S.Kh. // Bulletin of biotechnology and physico-chemical biology named by Yu.A.Ovchinnikov (Moscow). 2007. V.3. № 1. P. 28-33. (In Russian)
2. Chernukhin V.A., Nayakshina T.N., Gonchar D.A., Tomilova Ju.E., Tarasova M.V., Dedkov V.S., Mikhnenkova N.A., Degtyarev S.Kh. // Bulletin of biotechnology and physico-chemical biology named by Yu.A.Ovchinnikov (Moscow). 2011. V. 7. № 3. P. 35-42. (In Russian)
3. Chmuzh E.V., Kashirina J.G., Tomilova J.E., Mezentseva N.V., Dedkov V.S., Gonchar D.A., Abdurashitov M.A., Degtyarev S.Kh. // Biotechnology (Moscow). 2005. № 3. P. 22-26. (In Russian)
4. Chernukhin V.A., Chmuzh E.V., Tomilova Yu.E., Nayakshina T.N., Gonchar D.A., Dedkov V.S., Degtyarev S.Kh. // Bulletin of biotechnology and physico-chemical biology named by Yu.A.Ovchinnikov (Moscow). 2007. V. 3. № 2. P. 13-17. (In Russian)
5. Manual of methods for general bacteriology. Edited by Gerhard P. Washington, D.C.: American Society for Microbiology, 1981. 524 pages.
6. Chambers S.P., Prior S.E., Barstow D.A., Minton N.P. // Gene. 1988. V. 68. P. 139-149.
7. Xu S.-Y., Boitano M., Clark T.A., Vincze T., Fomenkov A., Kumar S., Too P.H.-M., Gonchar D., Degtyarev S.Kh, Roberts R.J. // Genome A. 2015. V. 3. Issue 3. e00395-159.
8. Bergey's manual of determinative bacteriology. Edited by Holt J.G. et al. 9th ed. Williams and Williams, Baltimore, 1993. 787 pages.
9. Madden T.L., Tatusov R.L., Zhang J. // Meth. Enzymol. 1996. V. 266. P. 131-141.
10. Chernukhin V.A., Kileva E.V., Tomilova Yu.E., Boltengagen A.A., Dedkov V.S., Mikhnenkova N.A., Gonchar D.A., Golikova L.N., Degtyarev S.Kh. // Bulletin of biotechnology and physico-chemical biology named by Yu.A.Ovchinnikov (Moscow). 2011. V. 7. № 1. P. 14-20. (In Russian)
11. Chernukhin V.A., Belichenko O.A., Tarasova G.V., Gonchar D.A., Akishev A.G., Dedkov V.S., Mikhnenkova N.A., Degtyarev S.Kh. Patent RU 2399663, Russia, C12N1/21, C12R1/06, 2009.
12. Chernukhin V.A., Gonchar D.A., Kileva E.V., Sokolova V.A., Golikova L.N., Dedkov V.S., Mikhnenkova N.A., Degtyarev S.Kh. // Bulletin of biotechnology and physico-chemical biology named by Yu.A.Ovchinnikov (Moscow). 2012. V. 8. № 1, P. 16-26 (In Russian).
13. Vanyushin B.F. // Curr. Top. Microbiol. Immunol. 2006. V. 301. P. 67-122.

GENERAL RULES

Acta Naturae publishes experimental articles and reviews, as well as articles on topical issues, short reviews, and reports on the subjects of basic and applied life sciences and biotechnology.

The journal is published by the Park Media publishing house in both Russian and English.

The journal *Acta Naturae* is on the list of the leading periodicals of the Higher Attestation Commission of the Russian Ministry of Education and Science. The journal *Acta Naturae* is indexed in PubMed, Web of Science, Scopus and RCSI databases.

The editors of *Acta Naturae* ask of the authors that they follow certain guidelines listed below. Articles which fail to conform to these guidelines will be rejected without review. The editors will not consider articles whose results have already been published or are being considered by other publications.

The maximum length of a review, together with tables and references, cannot exceed 60,000 characters with spaces (approximately 30 pages, A4 format, 1.5 spacing, Times New Roman font, size 12) and cannot contain more than 16 figures.

Experimental articles should not exceed 30,000 symbols (approximately 15 pages in A4 format, including tables and references). They should contain no more than ten figures.

A short report must include the study's rationale, experimental material, and conclusions. A short report should not exceed 12,000 symbols (8 pages in A4 format including no more than 12 references). It should contain no more than four figures.

The manuscript and the accompanying documents should be sent to the Editorial Board in electronic form:

- 1) text in Word 2003 for Windows format;
- 2) the figures in TIFF format;
- 3) the text of the article and figures in one pdf file;
- 4) the article's title, the names and initials of the authors, the full name of the organizations, the abstract, keywords, abbreviations, figure captions, and Russian references should be translated to English;
- 5) the cover letter stating that the submitted manuscript has not been published elsewhere and is not under consideration for publication;
- 6) the license agreement (the agreement form can be downloaded from the website www.actanaturae.ru).

MANUSCRIPT FORMATTING

The manuscript should be formatted in the following manner:

- Article title. Bold font. The title should not be too long or too short and must be informative. The title should not exceed 100 characters. It should reflect the major result, the essence, and uniqueness of the work, names and initials of the authors.
- The corresponding author, who will also be working with the proofs, should be marked with a footnote *.
- Full name of the scientific organization and its departmental affiliation. If there are two or more scientific organizations involved, they should be linked by digital superscripts with the authors' names. Ab-

stract. The structure of the abstract should be very clear and must reflect the following: it should introduce the reader to the main issue and describe the experimental approach, the possibility of practical use, and the possibility of further research in the field. The average length of an abstract is 20 lines (1,500 characters).

- Keywords (3 – 6). These should include the field of research, methods, experimental subject, and the specifics of the work. List of abbreviations.

• INTRODUCTION

• EXPERIMENTAL PROCEDURES

• RESULTS AND DISCUSSION

• CONCLUSION

The organizations that funded the work should be listed at the end of this section with grant numbers in parenthesis.

• REFERENCES

The in-text references should be in brackets, such as [1].

RECOMMENDATIONS ON THE TYPING AND FORMATTING OF THE TEXT

- We recommend the use of Microsoft Word 2003 for Windows text editing software.
- The Times New Roman font should be used. Standard font size is 12.
- The space between the lines is 1.5.
- Using more than one whole space between words is not recommended.
- We do not accept articles with automatic referencing; automatic word hyphenation; or automatic prohibition of hyphenation, listing, automatic indentation, etc.
- We recommend that tables be created using Word software options (Table → Insert Table) or MS Excel. Tables that were created manually (using lots of spaces without boxes) cannot be accepted.
- Initials and last names should always be separated by a whole space; for example, A. A. Ivanov.
- Throughout the text, all dates should appear in the “day.month.year” format, for example 02.05.1991, 26.12.1874, etc.
- There should be no periods after the title of the article, the authors' names, headings and subheadings, figure captions, units (s – second, g – gram, min – minute, h – hour, d – day, deg – degree).
- Periods should be used after footnotes (including those in tables), table comments, abstracts, and abbreviations (mon. – months, y. – years, m. temp. – melting temperature); however, they should not be used in subscripted indexes (T_m – melting temperature; T_{pt} – temperature of phase transition). One exception is mln – million, which should be used without a period.
- Decimal numbers should always contain a period and not a comma (0.25 and not 0,25).
- The hyphen (“-”) is surrounded by two whole spaces, while the “minus,” “interval,” or “chemical bond” symbols do not require a space.
- The only symbol used for multiplication is “×”; the “x” symbol can only be used if it has a number to its

right. The “.” symbol is used for denoting complex compounds in chemical formulas and also noncovalent complexes (such as DNA·RNA, etc.).

- Formulas must use the letter of the Latin and Greek alphabets.
- Latin genera and species' names should be in italics, while the taxa of higher orders should be in regular font.
- Gene names (except for yeast genes) should be italicized, while names of proteins should be in regular font.
- Names of nucleotides (A, T, G, C, U), amino acids (Arg, Ile, Val, etc.), and phosphonucleotides (ATP, AMP, etc.) should be written with Latin letters in regular font.
- Numeration of bases in nucleic acids and amino acid residues should not be hyphenated (T34, Ala89).
- When choosing units of measurement, SI units are to be used.
- Molecular mass should be in Daltons (Da, KDa, MDa).
- The number of nucleotide pairs should be abbreviated (bp, kbp).
- The number of amino acids should be abbreviated to aa.
- Biochemical terms, such as the names of enzymes, should conform to IUPAC standards.
- The number of term and name abbreviations in the text should be kept to a minimum.
- Repeating the same data in the text, tables, and graphs is not allowed.

GUIDENESS FOR ILLUSTRATIONS

- Figures should be supplied in separate files. Only TIFF is accepted.
- Figures should have a resolution of no less than 300 dpi for color and half-tone images and no less than 500 dpi.
- Files should not have any additional layers.

REVIEW AND PREPARATION OF THE MANUSCRIPT FOR PRINT AND PUBLICATION

Articles are published on a first-come, first-served basis. The members of the editorial board have the right to recommend the expedited publishing of articles which are deemed to be a priority and have received good reviews.

Articles which have been received by the editorial board are assessed by the board members and then sent for external review, if needed. The choice of reviewers is up to the editorial board. The manuscript is sent on to reviewers who are experts in this field of research, and the editorial board makes its decisions based on the reviews of these experts. The article may be accepted as is, sent back for improvements, or rejected.

The editorial board can decide to reject an article if it does not conform to the guidelines set above.

The return of an article to the authors for improvement does not mean that the article has been accept-

ed for publication. After the revised text has been received, a decision is made by the editorial board. The author must return the improved text, together with the responses to all comments. The date of acceptance is the day on which the final version of the article was received by the publisher.

A revised manuscript must be sent back to the publisher a week after the authors have received the comments; if not, the article is considered a resubmission.

E-mail is used at all the stages of communication between the author, editors, publishers, and reviewers, so it is of vital importance that the authors monitor the address that they list in the article and inform the publisher of any changes in due time.

After the layout for the relevant issue of the journal is ready, the publisher sends out PDF files to the authors for a final review.

Changes other than simple corrections in the text, figures, or tables are not allowed at the final review stage. If this is necessary, the issue is resolved by the editorial board.

FORMAT OF REFERENCES

The journal uses a numeric reference system, which means that references are denoted as numbers in the text (in brackets) which refer to the number in the reference list.

For books: the last name and initials of the author, full title of the book, location of publisher, publisher, year in which the work was published, and the volume or issue and the number of pages in the book.

For periodicals: the last name and initials of the author, title of the journal, year in which the work was published, volume, issue, first and last page of the article. Must specify the name of the first 10 authors. Ross M.T., Grafham D.V., Coffey A.J., Scherer S., McLay K., Muzny D., Platzer M., Howell G.R., Burrows C., Bird C.P., et al. // Nature. 2005. V. 434. № 7031. P. 325–337.

References to books which have Russian translations should be accompanied with references to the original material listing the required data.

References to doctoral thesis abstracts must include the last name and initials of the author, the title of the thesis, the location in which the work was performed, and the year of completion.

References to patents must include the last names and initials of the authors, the type of the patent document (the author's rights or patent), the patent number, the name of the country that issued the document, the international invention classification index, and the year of patent issue.

The list of references should be on a separate page. The tables should be on a separate page, and figure captions should also be on a separate page.

The following e-mail addresses can be used to contact the editorial staff: vera.knorre@gmail.com, actanaturae@gmail.com, tel.: (495) 727-38-60, (495) 930-87-07

NANOTECHNOLOGIES

in Russia

Peer-review scientific journal

Nanotechnologies in Russia
(*Rossiiskie Nanotekhnologii*)

focuses on self-organizing structures and nanoassemblages, nanostructures including nanotubes, functional nanomaterials, structural nanomaterials, devices and facilities on the basis of nanomaterials and nanotechnologies, metrology, standardization, and testing in nanotechnologies, nanophotonics, nanobiology.

→ **Russian edition:** <http://nanoru.ru>

→ **English edition:** <http://www.springer.com/materials/nanotechnology/journal/12201>

Issued with support from:



The Ministry of Education and Science of the Russian Federation

Science and Technologies in Russia – STRF.RU



40% of scientists agree that the publication of research results helps the enlightenment of the society, leads to the growth of authority of scientific work

34% believe that wide communicating of research results helps to rise the foundation

12% hope that media communications helps them to stand out in public opinion...
...but

17% never speak to journalists*

Open your work to the world!

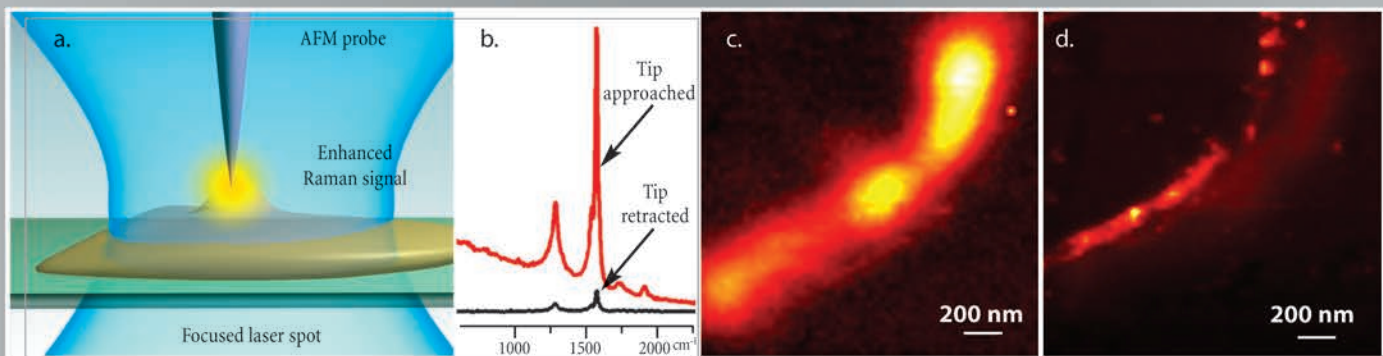
Colours do not play at nanometer scale

But you can colour molecules by their Raman spectra.



Raman mapping by TERS with ultra-high resolution

NTEGRA Spectra



a — a specially prepared AFM probe (metal coated cantilever or etched metal wire) is precisely positioned inside a tightly focused laser spot. b — intensity of carbon nanotube G- and D- Raman bands increases by several orders of magnitude when the special AFM probe is landed and positioned over a small (5 nm height) nanotube bundle - the effect of Tip enhanced Raman scattering (TERS). c — "conventional" confocal Raman image of the nanotube bundle, the observed width of the bundle is ~250 nm (diffraction limit of confocal microscopy, laser

wavelength - 633 nm). d — TERS image of the same bundle - now the observed width is ~70 nm.

Note, in this example, TERS provides more than 4-times better spatial resolution as compared to confocal microscopy. Resolution down to 10 nm and less is theoretically possible. Measurements are done with NTEGRA Spectra in Inverted configuration. Data courtesy of Dr. S. Kharintsev, Dr. J. Loos, Dr. G. Hoffmann, Prof. G. de With, TUE, the Netherlands and Dr. P. Dorozhkin, NT-MDT Co.

* Enter the Gift code at www.nt-mdt.com and get a present from NT-MDT Co. Attention: limited quantity! Be in time to get your gift!



NT-MDT Co., building 100, Zelenograd,
124482, Moscow, Russia
tel: +7 (499) 735-0305, +7 (495) 913-5736
fax: +7 (499) 735-6410, +7 (495) 913-5739
e-mail: spm@ntmdt.ru; www.ntmdt.com

NT-MDT Europe BV, High Tech Campus 83
5656 AG Eindhoven, the Netherlands
tel: +31(0) 88 338 99 99
fax: +31(0) 88 338 99 98
e-mail: info@ntmdt.eu, www.ntmdt.com